(Fig [illegible] stages, coincident with movement [illegible] ordia across the extracellular matrix [illegible] by elongation of the embryo in the anterior-posterior axis[11]. Stretching the ectodermal sheet to which the fibrils are attached could align the fibrils parallel to the axis of elongation. Second, there could be quantitative or qualitative differences from left to right either in extracellular matrix components or factors anchored to it which are eliminated by a perturbation of normal matrix deposition. In other systems, a number of growth factors are known to be sequestered in the extracellular matrix[23]. □

Received 15 November 1991; accepted 30 March 1992.

1. Oppenheimer, J. M. *Am. Zool.* **15**, 867–879 (1974).
2. Brown, N. A. & Wolpert, L. *Development* **109**, 1–9 (1990).
3. Wood, W. B. *Nature* **349**, 536–538 (1991).
4. Galloway, J. *Nature* **346**, 223–224 (1990).
5. Lee, G., Hynes, R. & Kirschner, M. *Cell* **36**, 729–740 (1984).
6. Keller, R. & Winklbauer, R. in *Seminars in Developmental Biology* Vol. 1 (ed. Bronner-Frasier, M. A.) 25–33 (Saunders, Philadelphia, 1990).
7. Spemann, H. *Verh. dt. zool. Ges.* **16**, 195–202 (1906).
8. von Woellwarth, C. *Roux Arch.* **144**, 178–256 (1950).
9. Takaya, H. *Annot. Zool. Japon.* **26**, 38–42 (1953).
10. Wehrmaker, A. *Roux Arch.* **163**, 1–32 (1969).
11. Keller, R. E. *Devl Biol.* **42**, 222–241 (1975).
12. Keller, R. E. *Devl Biol* **51**, 118–137 (1976).
13. Yost, H. J. *Development* **110**, 865–874 (1990).
14. Brickman, M. *J. Cell Biol.* **111**, 484 (1990).
15. Fey, J. & Hausen, P. *Differentiation* **42**, 144–152 (1990).
16. Clark, R. A. F. *Curr. Opin. Cell Biol.* **1**, 1000–1008 (1989).
17. Ruoslahti, E. & Pierschbacher, M. D. *Science* **238**, 491–497 (1987).
18. Boucat, J. C. *et al. J. Cell Biol.* **99**, 1822–1830 (1984).
19. Linask, K. K. & Lash, J. W. *Devl Biol.* **129**, 315–323 (1988).
20. Brueckner, M., D'Eustachio, P. & Horwich, A. L. *Proc. natn. Acad. Sci. U.S.A.* **86**, 5035–5038 (1989).
21. Yost, H. J. in *Biological Asymmetry and Handedness* (eds Bock, G. R. & Marsh, J.) 165–181 (Wiley, Chichester, 1991).
22. Winklbauer, R. & Nagel, M. *Devl Biol.* **148**, 573–589 (1991).
23. Flaumenhaft, R. & Rifkin, D. B. *Curr. Opin. Cell Biol.* **3**, 817–823 (1991).
24. Gerhart, J., *et al. Development* **105** (suppl.) 37–51 (1989).
25. Keller, R., Danilchik, M., Gimlich, R. & Shih, J. *J. Embryol. exp. Morph.* **89** (suppl.), 185–209 (1985).
26. Nieuwkoop, P. D. & Faber, J. *Normal table of* Xenopus laevis (*Daudin*) (North-Holland, Amsterdam, 1967).
27. Hemmati Brivanlou, A. & Harland, R. M. *Development* **106**, 611–617 (1989).
28. Schefler, W. C. *Statistics for the Biological Sciences* 1–231 (Addison-Wesley, Reading, Massachusetts, 1968).

ACKNOWLEDGEMENTS. I thank M. L. Condic, J. C. Gerhart, R. Keller and T. Doniach for discussions, advice and comments on the manuscript. This study was supported by a USPHS grant to J. C. Gerhart at U.C. Berkeley. H.J.Y. was supported in part by an American Cancer Society California Affiliate postdoctoral fellowship.

Profound block in thymocyte development in mice lacking p56^{lck}

T. J. Molina, K. Kishihara, D. P. Siderovski, W. van Ewijk*, A. Narendran, E. Timms, A. Wakeham, C. J. Paige, K.-U. Hartmann†, A. Veillette‡, D. Davidson‡ & T. W. Mak§

Ontario Cancer Institute and Departments of Immunology and Medical Biophysics, University of Toronto, 500 Sherbourne Street, Toronto, Ontario M4X 1K9, Canada
* Department of Cell Biology II and Immunology, Erasmus Universiteit, 3000 DR Rotterdam, The Netherlands
† Institut für Experimentelle Immunologie, Philipps-Universität, D-3550 Marburg, Germany
‡ McGill Cancer Centre, McGill University, Montréal, Québec H3G 1Y6, Canada

THE protein Lck (p56^{lck}) has a relative molecular mass of 56,000 and belongs to the Src family of tyrosine kinases[1–3]. It is expressed exclusively in lymphoid cells, predominantly in thymocytes and peripheral T cells[4,5]. Lck associates specifically with the cytoplasmic domains of both CD4 and CD8 T-cell surface glycoproteins[6,7] and interacts with the β-chain of the interleukin-2 receptor[8], which implicates Lck activity in signal transduction during thymocyte ontogeny[9–13] and activation of mature T cells[14–19]. Here we generate an *lck* null mutation by homologous recombination in embryonic stem cells to evaluate the role of p56^{lck} in T-cell development and activation. Lck-deficient mice show a pronounced thymic atrophy, with a dramatic reduction in the double-positive (CD4$^+$CD8$^+$) thymocyte population. Mature, single-positive thymocytes are not detectable in these mice and there are only very few peripheral T cells. These results illustrate the crucial role of this T-cell-specific tyrosine kinase in the thymocyte development.

For homologous recombination, a replacement-type vector (PmlckBSNeo2.3) was constructed (Fig. 1*a*) and introduced into D3 embryonic stem cells by electroporation. Six independently targeted embryonic stem cell lines were generated. The average frequency of homologous recombination was about 1 in 2×10^7 electroporated cells and 1 in 130 G418-resistant clones. Southern blot analysis confirmed the homologous recombination event (Fig. 1*b*). Germ-line transmission of the *lck* disruption was obtained with two embryonic stem cell lines. Heterozygous mice were inbred to obtain mice homozygous for the disrupted *lck* gene.

Although mice homozygous for the disrupted *lck* gene are expected to lack p56^{lck}, it was conceivable that part of the Lck protein to the amino-terminal side of the mutation could still have been expressed. Therefore for western blotting we used a rabbit antiserum directed against the N-terminal end of Lck, using either thymic (Fig. 2*a*) or lymph node cell lysates (data not shown). No Lck protein, either full-length or truncated, was detected in homozygous mutant mice. In addition, immune complex kinase was assayed using a different rabbit anti-Lck antiserum and there was no detectable p56^{lck} kinase activity in homozygous mutant mice (Fig. 2*b*).

Heterozygous mutant mice appeared healthy; their lymphoid organs and thymocyte and peripheral T cell populations were normal (data not shown). But CD4 staining of peripheral blood lymphocytes showed a consistent decrease in fluorescence intensity (Fig. 3*a*); this decrease was not seen on CD4$^+$ thymocytes, nor was there any downregulation of CD8 expression (data not shown).

Lck-deficient mice appeared healthy and fertile under specific pathogen-free conditions. Spleen and lymph nodes were normal in size but we observed considerable thymic atrophy; conventional histology showed a thymic cortex sparsely populated with lymphoid cells and a very tiny medulla (data not shown). Thus thymic atrophy is associated with a decrease in the thymocyte population (6×10^6–2×10^7 cells versus 2×10^8 for normal littermates), consisting of 20–40% double negative (CD4$^-$CD8$^-$) and 60–80% double positive (CD4$^+$CD8$^+$) thymocytes. The number of double negative thymocytes is similar to that of normal littermates (3×10^6–6×10^6), but there is a dramatic reduction in double-positive thymocytes (0.3×10^7–1.6×10^7 versus 1.8×10^8 for normal littermates), evident in mice from 10 days to 8 weeks old. Neither CD4$^+$CD8$^-$ nor CD4$^-$CD8$^+$ single-positive thymocytes were detectable in homozygous mutant mice (Fig. 3*b*).

The double-negative thymocyte population is Thy-1$^+$ CD3 (low-intermediate), with the presence of a J11d (high), interleukin-2(IL-2) receptor α-chain-positive subpopulation (40% of double-negative thymocytes). The double-positive thymocyte population does not contain CD3 (low) cells and there is, on average, increased CD3 expression at intermediate to high levels: 25% of the CD3$^+$ cells have an expression level similar to that of normal CD3 (high), single-positive thymocytes

§ To whom correspondence should be addressed.

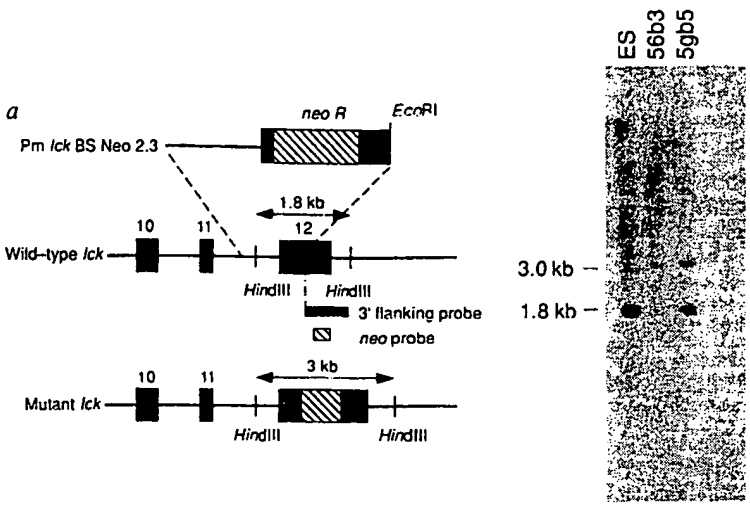

FIG. 1 Disruption of *lck* gene by homologous recombination. *a*, Schematic diagrams of the targeting vector (PmlckBSNeo2.3), the *lck* locus in parental D3 cells (wild-type *lck*), and the predicted structure of the disrupted *lck* locus (mutant *lck*). The neomycin-resistance gene (*neo R*) cassette contains 1.2 kilobases (kb) derived from the *XhoI–SalI* fragment of plasmid pMC1PolA (ref. 28) and was inserted into a *SalI* site created at a previous *BspMII* site in exon 12 of the *lck* gene, 110 base pairs (bp) upstream of the codon corresponding to Tyr 505. The 2.3 kb of genomic *lck* in the targeting vector was obtained by screening of a mouse (BALB/c) genomic library with a human *lck* complementary DNA probe[2]. Electroporation of the D3 embryonic stem cells and screening for homologous recombination were done as previously described[25,26]. A primer specific for the *neo* cassette in the neomycin-resistance coding sequence (5'-TATCAGGACATAGCGTTGGCTACCC-3'), and another antisense primer specific for exon 12 of *lck*, 3' of the targeting vector (5'-CTTAGACTCACGTGCTCCACAGGTA-3'), were used in the polymerase chain reaction (PCR) to detect homologous recombination; *lck* cDNA sequences spanning exon 12 were used as a probe in this PCR detection method (data not shown). *b*, Southern blot analysis of the structure of the *lck* locus in parental D3 cells (ES) and two targeted cell lines (56b3 and 5gb5). Genomic DNA was digested with *HindIII* and probed using the 3' flanking probe (600 bp *EcoRI–HindIII* fragment). In cases of homologous recombination, a 3-kb fragment is detected from the disrupted *lck* allele, instead of a 1.8-kb fragment from the wild-type allele. The same profile of hybridization was observed using the targeting vector as a probe, whereas probing with the neomycin-resistance gene showed only the single 3-kb fragment (data not shown).

(Fig. 3*b*). The drastic reduction of double-positive thymocytes may reflect an inability of this cell population to enter the cell cycle. However, propidium iodide staining[20] of thymocytes from 4-week-old homozygous mutant mice showed a cell-cycle profile similar to that of normal littermates (+/+; ref. 21): about 20% of thymocytes were in the S or G2+M phase of the cell cycle (data not shown).

Although the overall numbers of cells in lymph nodes and spleens are normal, a dramatic inversion in the B/T cell ratio was observed: 90 to 95% B cells and 5 to 10% T cells (Fig. 3*c*). Peripheral T cells are positive for Thy-1, CD3 and for the α- and β-chains of the T-cell antigen receptor (TCR$\alpha\beta^+$) and expression of CD4 or CD8 (Lyt2–Lyt3 heterodimer; Fig. 3*d*) is decreased. One per cent of the lymph node population are TCR$\gamma\delta^+$ T cells (data not shown).

Proliferative responses of peripheral T cells to mitogenic stimuli were identical for both normal and heterozygous mutant mice (data not shown). T cells from Lck-deficient mice exhibited

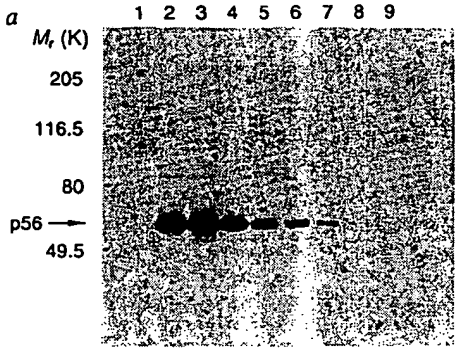

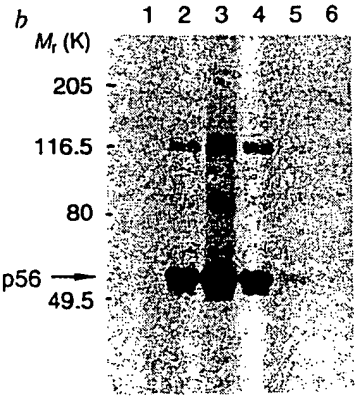

FIG. 2 Analysis of p56^{lck} expression and activity. *a*, Immunoblot quantitation of p56^{lck} protein. Thymocyte lysates (100 μg) are shown from homozygous mutant (−/−; lane 1), heterozygous mutant (+/−; lane 2), and wild-type mice (+/+; lane 3); lanes 4–9, titration of wild-type (+/+) thymocyte lysate (50, 25, 12.5, 6.25, 3.12 and 1.6 μg, respectively). Autoradiograph exposure time was 15 h. Quantitation of the bands revealed that the amount of p56^{lck} in the heterozygous mutant mouse cell lysate (lane 2) was roughly half of the amount in wild-type mouse lysate (lane 3). *b*, Immune complex kinase assay of p56^{lck} activity. The tyrosine kinase activity of p56^{lck} (autophosphorylation) was assessed using Lck immunoprecipitates from cell lysates: 150 μg thymocyte lysates from homozygous mutant (−/−; lane 1), heterozygous mutant (+/−; lane 2), and wild-type mice (+/+; lane 3); lanes 4–6, titration of the wild-type (+/+) thymocyte lysate (75, 37.5, and 18.8 μg, respectively). Autoradiograph exposure time was 15 h. Quantitation revealed that the kinase activity in the heterozygous mutant mouse cell lysate (lane 2) was roughly half of the wild-type activity (lane 3). Positions of markers of known molecular weight and the postion of p56^{lck} are indicated on the left of each figure.

METHODS. Immunoblot analysis: Thymic and lymph nodes cells of 3–4-week-old mice were washed in PBS and lysed in TNE buffer (50 mM Tris, pH 8.0, 1% NP40, 2 mM EDTA) supplemented with protease inhibitors and phosphatase inhibitors as before[14]. Defined amounts of proteins from cellular lysates were denatured in sample buffer, boiled and resolved by 8% SDS-PAGE. Proteins were electrophoretically transferred to nitrocellulose and analysed for p56^{lck} expression using a rabbit antiserum generated against a fusion protein containing amino acids 2–148 of the murine p56^{lck} sequence[16]. Bands were cut from the nitrocellulose blot and counted in a γ-counter. Immune complex kinase assay: p56^{lck} was recovered from cell lysates using a rabbit anti-Lck antiserum directed against amino acids 39–64. After collection on formalin-fixed *Staphylococcus aureus* (Pansorbin, CalBiochem), immune complexes were washed and resuspended in kinase buffer[14]. Kinase reactions were performed for 2 min at room temperature with constant shaking in 25 μl kinase buffer containing 1 μM in labelled ATP, 12.5 μCi [γ-^{32}P]-ATP (3,000 Ci mmol^{-1}; NEN). Reactions were stopped by addition of 1 ml lysis buffer, washed three times, and resuspended in sample buffer. Phosphorylated polypeptides were subsequently resolved on 8% SDS-PAGE gels.

a proliferative response, albeit reduced, to both CD3 and TCR$\alpha\beta$ crosslinking (Fig. 4*a*), demonstrating that Lck is not indispensable for the TCR-CD3 signalling pathway and may act as a signal amplifier[16]. In addition, the enhanced response to CD3 or TCR crosslinking in the presence of IL-2, as well as the response to IL-2 alone (Fig. 4*a*), suggests that p56^{lck} is not indispensable for the IL-2 signalling pathway[8]. The responses to phorbol ester and ionomycin treatment were identical in normal and Lck-deficient T cells.

Evaluation of serum immunoglobulin levels revealed an increase in IgM, a significant decrease in IgG_1, and a marginal increase in IgG_{2a} and IgG_3 isotypes in homozygous mutant mice (Fig. 4*b*), representing an immunoglobulin profile comparable to that seen in the absence of T-helper cell function (for example, major histocompatibility complex class II-deficient mice[22] and IL-4-deficient mice[23]). Splenic B cells responded normally to lipopolysaccharide (Fig. 4*b*), however, demonstrating that the lack of *lck* does not interfere with T-independent B-cell function.

The profound perturbation of thymocyte development in Lck-deficient mice underlines the crucial role of this kinase in T-cell ontogeny, because the other T-cell-specific tyrosine kinases, p59^{fynT} and p62^{yes}, are unable to compensate for the absence of p56^{lck}. This lack of functional redundancy is surprising in light of the paucity of abnormalities present in Src-deficient mice[24] and the observation of normal thymocyte development and peripheral immune responses in mice lacking *fyn* (P. Stein and P. Soriano, personal communication).

The interaction between p56^{lck} and the accessory molecules CD4 and CD8 in double-positive thymocytes[11], as well as the enhancement of Lck activity upon CD4 crosslinking[16], suggest that the impairment of thymocyte maturation in Lck-deficient mice reflects an inability of CD4 and/or CD8 to transduce their signal(s). But both CD4-deficient and CD8-deficient mice have normal thymic architectures and no decrease in the total number

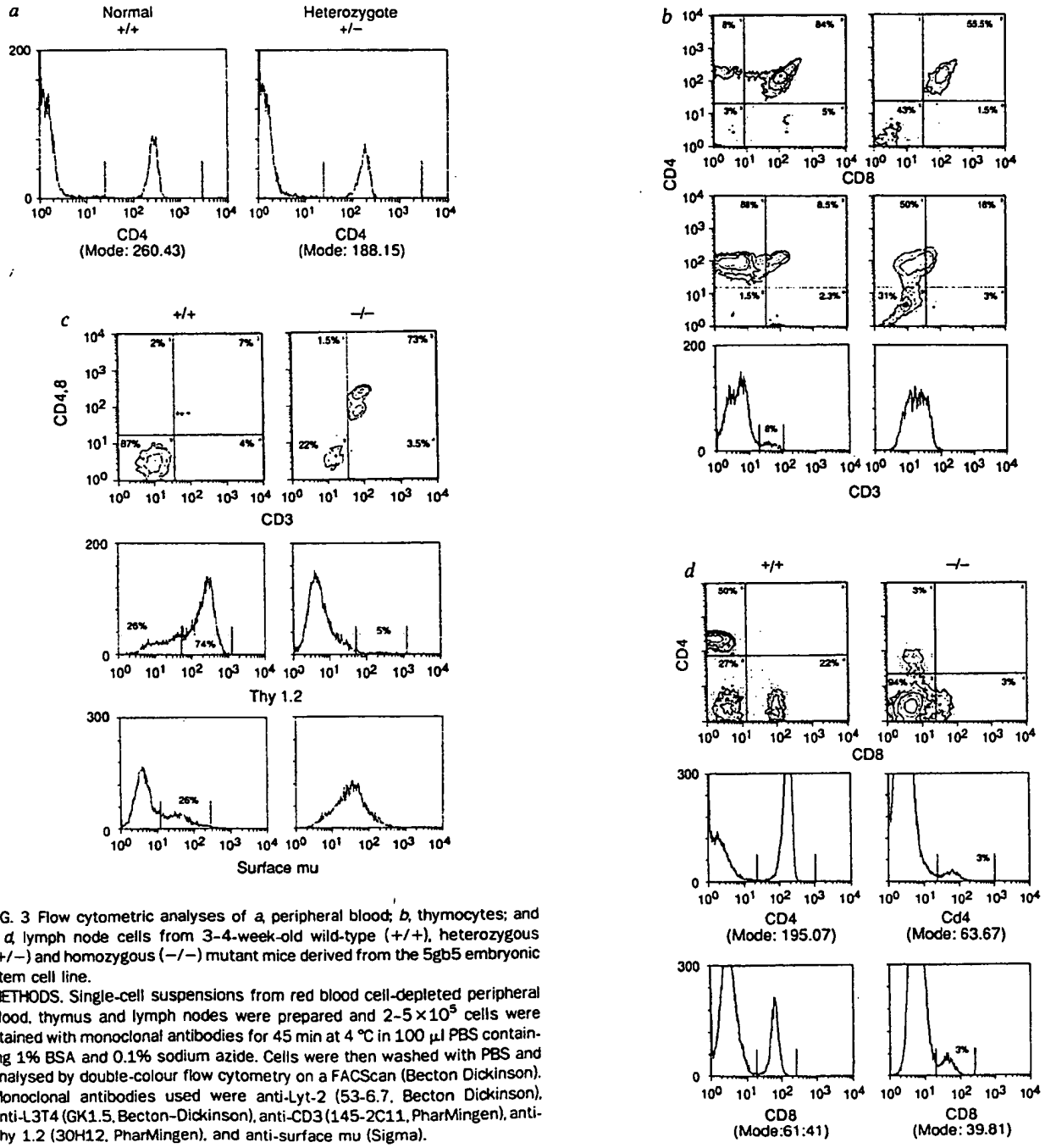

FIG. 3 Flow cytometric analyses of *a*, peripheral blood; *b*, thymocytes; and *c*, *d*, lymph node cells from 3–4-week-old wild-type (+/+), heterozygous (+/−) and homozygous (−/−) mutant mice derived from the 5gb5 embryonic stem cell line.

METHODS. Single-cell suspensions from red blood cell-depleted peripheral blood, thymus and lymph nodes were prepared and $2–5\times10^5$ cells were stained with monoclonal antibodies for 45 min at 4 °C in 100 μl PBS containing 1% BSA and 0.1% sodium azide. Cells were then washed with PBS and analysed by double-colour flow cytometry on a FACScan (Becton Dickinson). Monoclonal antibodies used were anti-Lyt-2 (53-6.7, Becton Dickinson), anti-L3T4 (GK1.5, Becton-Dickinson), anti-CD3 (145-2C11, PharMingen), anti-Thy 1.2 (30H12, PharMingen), and anti-surface mu (Sigma).

of thymocytes[25,26]. Therefore, an inability to signal through CD4 or CD8 cannot be considered as the main factor responsible for the thymocyte developmental defect in Lck-deficient mice.

Whereas CD4- and CD8-mediated signals are considered important during positive selection[12,13], the signalling pathway(s) involved in the prior phase of expansion of the double-positive thymocyte population are still unknown[27]. The drastic reduction in the number of double-positive thymocytes observed in Lck-deficient mice therefore implicates $p56^{lck}$ in the signalling pathway required for this expansion phase, but does not exclude the possibility that $p56^{lck}$-mediated signals are also important during thymic selection events. □

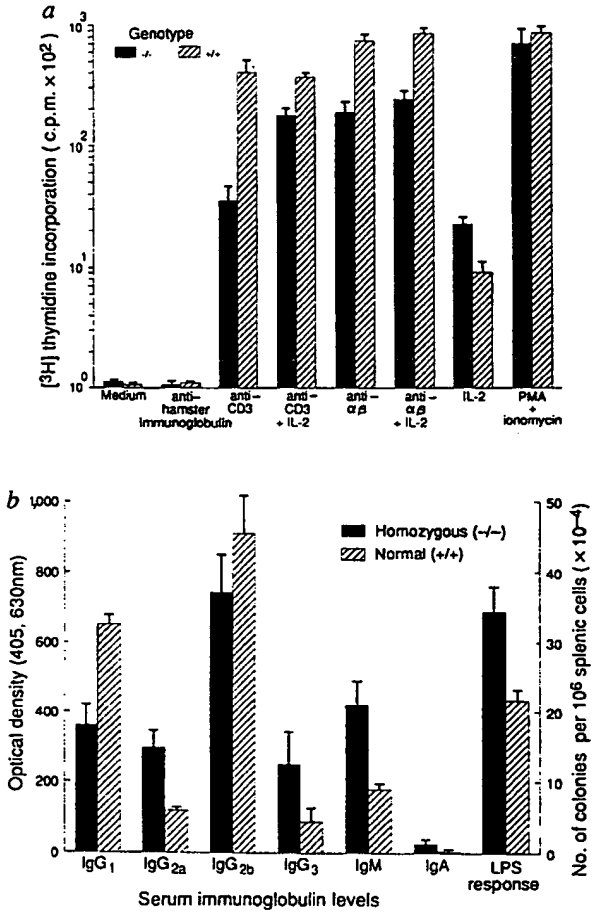

FIG. 4 Analyses of peripheral T-cell and B-cell function. *a*, Proliferative responses of peripheral T cells from normal (+/+) and Lck-deficient (−/−) mice. Values represent mean of triplicate cultures ± standard deviations. This experiment is representative of four different experiments. *b*, B-cell responses in normal (+/+) and Lck-deficient (−/−) mice. Serum immunoglobin levels and splenic cell lipopolysaccharide (LPS) responsiveness were analysed by a modified enzyme-linked immunosorbent assay and an agar colony assay, respectively.

METHODS. T cell proliferation: Lymph node and splenic T cells from normal, heterozygous (data not shown), and homozygous mutant mice were purified using nylon wool and cultured in flat-bottomed 96-well plates at a concentration of 5×10^4 T cells per well (as measured by Thy-1 and CD3 staining on FACScan). For crosslinking experiments plate-bound antibody stimulation was used and 10^6 irradiated (3,000 rads) spleen cells were added. Before stimulation with anti-CD3 (2C11) and anti-TCR$\alpha\beta$ (H57-597) antibodies, plates were coated overnight with purified rabbit anti-hamster IgG (10 μg mL^{-1}). Concentrations used were 20 units per ml recombinant interleukin-2 (Roche), 10 ng ml^{-1} phorbol 12-myristyl 13-acetate (PMA; Sigma) and 400 ng ml^{-1} ionomycin (CalBiochem). Cells were cultured for 3 days in IMDM medium with 10% FCS, pulsed with 1 μCi [^{3}H]thymidine on day 3 and collected 9 h later. B cell responses: The immunoglobulin isotypes in 5-week-old homozygous mutant (−/−) and age/sex-matched normal (+/+) mice were determined by a panel of mouse isotyping antibodies (Bio-Rad), according to the manufacturer's protocol, using sera diluted 100 times in PBS. The frequency of lipopolysaccharide-responsive splenic cells was determined by a double-layer agar culture assay[29]. Spleens of homozygous mutant mice contained, on average, ~30% more B cells (data not shown). Optical densities are given in arbitrary units.

Received 23 January; accepted 31 March 1992.

1. Marth, J. D., Peet, R., Krebs, E. G. & Perlmutter, R. M. *Cell* **43**, 393–404 (1985).
2. Koga, Y. *et al. Eur. J. Immun.* **16**, 1643–1646 (1986).
3. Voronova, A. F. & Sefton, B. M. *Nature* **319**, 682–686 (1986).
4. Perlmutter, R. M. *et al. J. cell Biochem.* **38**, 117–126 (1988).
5. Veillette, A., Abraham, N., Caron, L. & Davidson, D. *Semin. Immun.* **3**, 143–152 (1991).
6. Veillette, A., Bookman, M. A., Horak, E. M. & Bolen, J. B. *Cell* **55**, 301–308 (1988).
7. Shaw, A. S. *et al. Cell* **59**, 627–636 (1989).
8. Hatakeyama, M. *et al. Science* **252**, 1523–1528 (1991).
9. Abraham, K. M., Levin, S. D., Marth, J. D., Forbush, K. A. & Perlmutter, R. M. *J. exp. Med.* **173**, 1421–1432 (1991).
10. Reynolds, P. J. *et al. Molec. cell. Biol.* **10**, 4266–4270 (1990).
11. Veillette, A., Zúñiga-Pflücker, J. C., Bolen, J. B. & Kruisbeek, A. M. *J. exp. Med.* **170**, 1671–1680 (1989).
12. Ferrick, D. A., Ohashi, P. S., Wallace, V., Schilham, M. & Mak, T. W. *Immun. Today* **10**, 403–407 (1989).
13. von Beohmer, H. *A. Rev. Immun.* **8**, 531–556 (1990).
14. Veillette, A., Bookman, M. A., Horak, E. M., Samelson, L. E. & Bolen, J. B. *Nature* **338**, 257–259 (1989).
15. Miceli, M. C., von Hoegen, P. & Parnes, J. R. *Proc. natn. Acad. Sci. U.S.A.* **88**, 2623–2627 (1991).
16. Abraham, N., Miceli, M. C., Parnes, J. R. & Veillette, A. *Nature* **350**, 62–66 (1991).
17. Glaichenhaus, N., Shastri, N., Littman, D. R. & Turner, J. M. *Cell* **64**, 511–520 (1991).
18. June, C. H. *et al. Proc. natn. Acad. Sci. U.S.A.* **87**, 7722–7726 (1990).
19. Klausner, R. D. & Samelson, L. E. *Cell* **64**, 875–878 (1991).
20. Taylor, I. W. *J. Histochem. Cytochem.* **28**, 1021–1024 (1980).
21. Egerton, M., Scollay, R. & Shortman, K. *Proc. natn. Acad. Sci. U.S.A.* **87**, 2579–2582 (1990).
22. Cosgrove, D. *et al. Cell* **66**, 1051–1066 (1991).
23. Kühn, R., Rajewsky, K. & Müller, W. *Science* **254**, 707–710 (1991).
24. Soriano, P., Montgomery, C., Geske, R. & Bradley, A. *Cell* **64**, 693–702 (1991).
25. Rahemtulla, A. *et al. Nature* **353**, 180–184 (1991).
26. Fung-Leung, W.-P. *et al. Cell* **65**, 443–449 (1991).
27. Huesmann, M., Scott, B., Kisielow, P. & von Boehmer, J. *Cell* **66**, 533–540 (1991).
28. Thomas, K. R. & Capecchi, M. R. *Cell* **51**, 503–512 (1987).
29. Paige, C. J. & Skarvall, H. *J. immunol. Meth.* **52**, 51–61 (1982).

ACKNOWLEDGEMENTS. We thank A. Arabian, J. Potter, C. Quarrington and J. Voerman for technical help, and W.-P. Fung-Leung, J. Penninger, K. Pfeffer, A. Rahemtulla, M. Schilham, W. Slieker and V. Wallace for advice. This work was supported by INSERM (T.J.M.), the Medical Research Council of Canada (T.J.M., K.K. and D.P.S.), by the UCB Institute of Allergy (T.J.M.), by the Arthritis Society of Canada (A.N.), the Natural Science and Engineering Research Council of Canada, and the National Cancer Institute of Canada.

Tetrameric cell-surface MHC class I molecules

Sudhir Krishna, Philippe Benaroch & Shiv Pillai

Molecular Immunology Laboratory, Molecular Genetics Group, The Cancer Center of Massachusetts General Hospital and Harvard Medical School, Building 149, 13th Street, Boston, Massachusetts 02129, USA

PURIFIED major histocompatibility complex (MHC) class I molecules have been studied at high resolution by X-ray crystallography[1]; the structure is a complex of a single heavy chain, a β_2-microglobulin light chain and a tightly bound peptide moiety. We show here that complete MHC class I molecules are post-translationally assembled into tetramers (made up of four heavy chains and four β_2-microglobulin units) and that this tetrameric species is expressed on the cell surface. The multivalent tetrameric structure of class I molecules can be reconciled with models of T-cell activation that invoke antigen–receptor crosslinking, as opposed to models that depend on an allosteric change.

Lymphoid cell lines were metabolically labelled and lysed with 1% digitonin with or without a cleavable crosslinking reagent. MHC class I molecules were immunoprecipitated from control and crosslinked lysates and samples analysed on non-reducing, reducing and two-dimensional non-reducing/reducing polyacrylamide-sodium dodecyl sulphate gels. On non-reducing gels, in addition to a free heavy chain band migrating at a position corresponding to an M_r of 45,000 (45K), and a 60K heavy chain–$\beta_2$microglobulin complex, a species of 240K was seen (Fig. 1, lanes 3 and 5). This band was not observed

2-Phenylaminoimidazo[4,5-*h*]isoquinolin-9-ones: Orally Active Inhibitors of lck Kinase

Daniel R. Goldberg,*,† Tanja Butz,† Mario G. Cardozo,† Robert J. Eckner,§ Abdelhakim Hammach,† Jessica Huang,† Scott Jakes,§ Suresh Kapadia,‡ Mohammed Kashem,† Susan Lukas,§ Tina M. Morwick,† Maret Panzenbeck,⊥ Usha Patel,† Susan Pav,§ Gregory W. Peet,§ Jeffrey D. Peterson,⊥ Anthony S. Prokopowicz, III,† Roger J. Snow,† Rosemarie Sellati,⊥ Hidenori Takahashi,† Jonathan Tan,‡ Matt A. Tschantz,† Xiao-Jun Wang,‡ Yong Wang,† John Wolak,† Pla Xiong,† and Neil Moss†

Departments of Medicinal Chemistry, Biology, Chemical Development, and Pharmacology, Boehringer Ingelheim Pharmaceuticals, Inc., 900 Ridgebury Road, Ridgefield, Connecticut 06877

Received October 8, 2002

The tyrosine kinase p56lck (lck) is essential for T cell activation; thus, inhibitors of lck have potential utility as autoimmune agents. Our initial disclosure of a new class of lck inhibitors based on the phenylaminoimidazoisoquinolin-9-one showed reasonable cellular activity but did not work in vivo upon oral administration. Our current work highlights the further use of rational drug design and molecular modeling to produce a series of lck inhibitors that demonstrate cellular activity below 100 nM and are as efficacious as cyclosporin A in an in vivo mouse model of anti-CD3-induced IL-2 production.

Tyrosine kinases play an essential role in the regulation of cell signaling and cell proliferation by phosphorylating tyrosine residues of peptides and proteins.[1−3] We have been exploring a novel series of molecules that inhibit the catalytic activity of p56lck (lck), a member of the src family of protein tyrosine kinases (vide infra).[4]

The lck (−) Jurkat cell lines are unable to proliferate, produce cytokines, and generate increases in intracellular calcium, inositol phosphate, and tyrosine phosphorylation in response to T cell receptor (TCR) stimulation.[5,6] Therefore, an agent inhibiting lck would effectively block T cell function, act as an immunosuppressive agent, and have potential utility in autoimmune diseases, such as rheumatoid arthritis, multiple sclerosis, and lupus, as well as in the area of transplant rejection and allergic diseases.[7,8]

The TCR is the antigen-specific component of the T cell, which is activated upon presentation of antigenic peptides.[9] TCR activation initiates a series of enzyme-mediated signal transduction cascades that result in the production of proinflammatory cytokines such as interleukin-2 (IL-2).[10−12]

Our initial disclosure of phenylaminoimidazoisoquinolinones as a new class of lck inhibitors highlighted the use of a model of inhibitors bound to lck to advance our screening hit **1** with micromolar potency against lck, to a nanomolar inhibitor of lck, **2** (Figure 1).[4] Although quite potent in vitro, **2** only demonstrated in vivo efficacy when dosed at 100 mg/kg, ip. Our current work highlights modifications to **2** that improve in vitro potency to subnanomolar levels and also provide oral efficacy in a mouse model of IL-2 production.

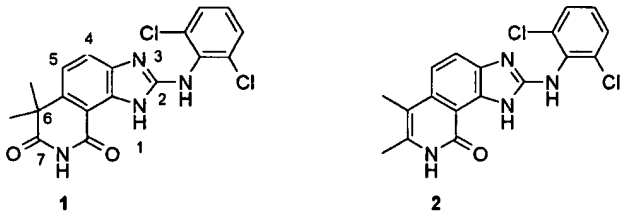

1 **2**

Figure 1. Initial lead **1** and optimized compound **2**.

Chemistry

Our previously reported synthetic route to the phenylaminoimidazoisoquinolinone inhibitor **2** involved a 12-step linear sequence.[4] We therefore looked for opportunities to shorten our synthesis and allow for flexibility to introduce a variety of functionality. We could accomplish our first goal through the use of a selective S_NAr reaction starting with 2,6-dichloro-3-nitrobenzonitrile **3** as the key building block (Scheme 1).[13] Treatment of **3** with ammonia or an alkylamine provided benzonitrile **4** or **5**, respectively. This ultimately allowed access to products alkylated at the N-1 position, e.g., methylamine **12**, which were not accessible via our previous synthetic route. A subsequent S_NAr reaction with ethyl 2-methylacetoacetate to form **6** allowed ready introduction of the atoms necessary for formation of the isoquinoline core.[14] Formation of the benzimidazole **11** was best accomplished by reacting diamine **7**, 2,6-dichlorophenyl isocyanate, and HgO in refluxing THF. The isoquinolone was then formed by treatment of **11** with a mixture of concentrated sulfuric acid, water, and acetic acid to provide **2** or **12**. The last step in the reaction included the hydrolysis of the nitrile, condensation with the ketone, and hydrolysis and decarboxylation of the ester functionality in one step.

Reacting **5** with methyl acetoacetate to provide intermediate **13** accomplished introduction of a methyl ester directly attached to C-6 (Scheme 2). Isoquinolone formation as for **12** and **2** provided a mixture of C-6

* To whom correspondence should be addressed. Phone: 203-778-7828. Fax: 203-791-6072. E-mail: dgoldber@rdg.boehringer-ingelheim.com.
† Department of Medicinal Chemistry.
§ Department of Biology.
‡ Department of Chemical Development.
⊥ Department of Pharmacology.

10.1021/jm0204461 CCC: $25.00
Published on Web 03/18/2003

Scheme 1. Improved Synthesis of **2**[a]

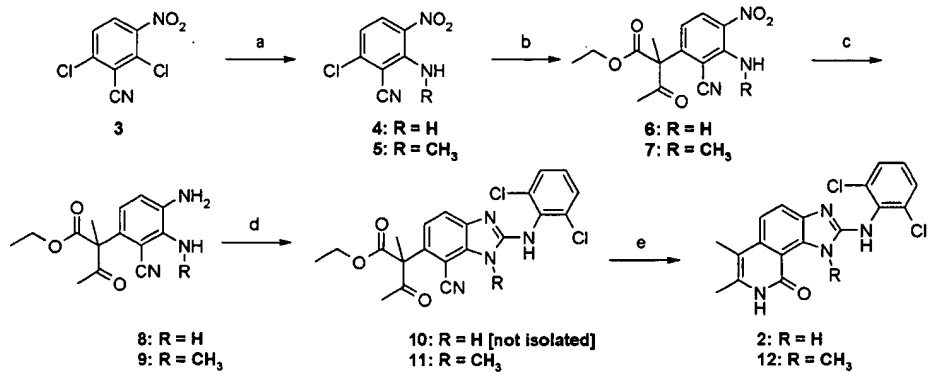

[a] Reagents: (a) H_2NR, MeOH, 80 °C; (b) ethyl 2-methylacetoacetate, K_2CO_3, DMF; (c) H_2, 10% Pd/C, MeOH; (d) 2,6-$Cl_2C_6H_3NCS$, EtOAc, or 2,6-$Cl_2C_6H_3NCS$, HgO, THF, 80 °C; (e) concentrated H_2SO_4, H_2O, HOAc, 100 °C.

Scheme 2. β-Keto Ester Additions[a]

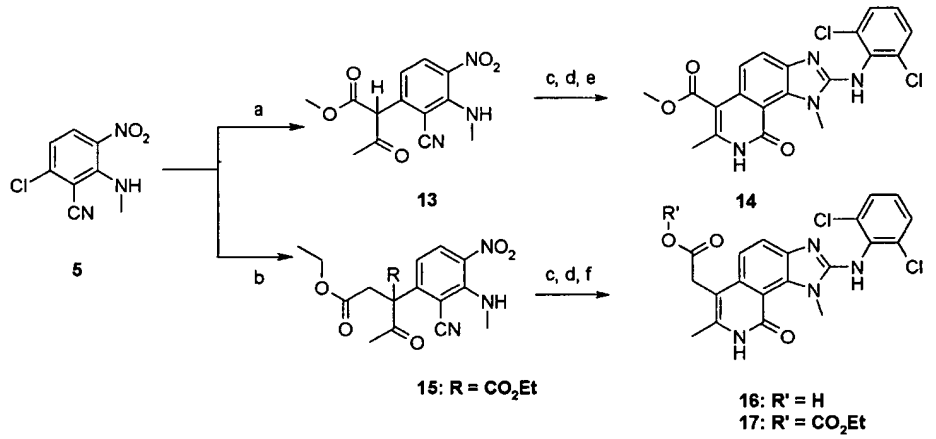

[a] Reagents: (a) 3-oxobutyric acid methyl ester, K_2CO_3, DMF; (b) 2-acetylmalonic acid diethyl ester, $CsCO_3$, DMF; (c) H_2, 10% Pd/C, MeOH; (d) 2,6-$Cl_2C_6H_3NCS$, EtOAc; (e) concentrated H_2SO_4; (f) (1) concentrated H_2SO_4 H_2O, HOAc, 100 °C, (2) EtOH, H_2SO_4.

Scheme 3. Amide and Amine Synthesis at C-6[a]

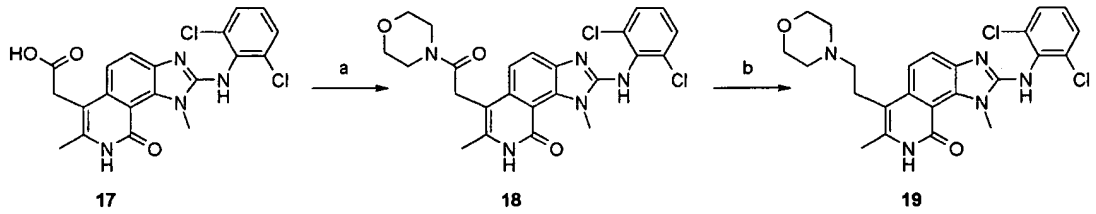

[a] Reagents: (a) morpholine, TBTU, DMF; (b) BH_3, SMe_2, THF.

ester and decarboxylated material that could not be separated easily. However, performing the reaction at room temperature with concentrated sulfuric acid solved this issue and provided **14** in good yield. The homologous ester, **15**, was prepared in a similar manner with diethylacetyl succinate. Isoquinolone formation under the standard acidic conditions resulted in ester hydrolysis of the final product to provide **16**. Consequently, reesterification with ethanol and sulfuric acid was required to obtain **17**.

Ester **14** proved to be resistant to further manipulation perhaps because of steric congestion around the ester carbonyl caused by the C-7 methyl group and the isoquinoline phenyl. The homologated analogue **16** did not suffer from this liability and could be transformed, via hydrolysis to the acid, into amide derivatives, e.g., **18** (Scheme 3). The resulting amides could be reduced to the corresponding amines, e.g., **19**, with BH_3–dimethyl sulfide in THF, without affecting the isoquinolone amide.

Functionalization of the C-4 position of the isoquinolone was accomplished via a bromine atom as a functional handle. Of all the potential precursors for introduction of the bromine atom at C-4, diamine **9** was the only intermediate that was readily brominated in the desired manner (Scheme 4). The sequence progressed as described above to provide benzimidazole **21**. The bromine in compound **21** was further manipulated before isoquinolone formation via palladium cross-coupling with vinyl- or aryltin reagents to provide **22** and **23**. Conversion to the corresponding isoquinolone derivative occurred as described above. Vinyl compound **22** could be converted to aldehyde **25** that could undergo reductive aminations, e.g., **26** and **27** (Scheme 4).

Attempts to introduce a functional handle at the C-7 position through the use of substituted β-keto esters had

Scheme 4. Introduction of C-4 Bromine and Cross-Coupling Reactions[a]

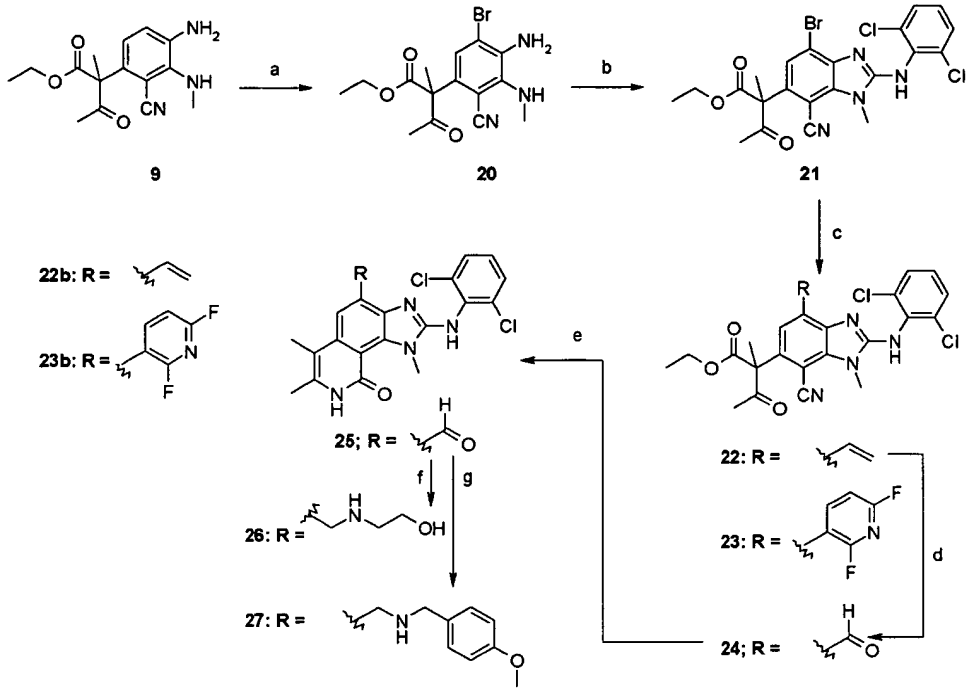

[a] Reagents: (a) Br_2, $CHCl_3$; (b) ArNCS, HgO, THF, 80 °C; (c) $RSnBu_3$, $(PPh_3)_2PdCl_2$; (d) $NaIO_4$, OsO_4, THF; (e) H_2SO_4,100 °C; (f) $NaBH_4$, MeOH; (g) *p*-methoxybenzylamine, $NaCNBH_3$, MeOH.

limited success either because of poor yields of the S_NAr reaction or difficulties in obtaining appropriately substituted keto esters. Literature precedent demonstrated that 3-methyl-1*H*-quinolin-2-one undergoes oxidation with selenium dioxide to the corresponding aldehyde.[15] Reaction of **12** with SeO_2 in dioxane resulted in selective oxidation at the C-7 methyl to provide the corresponding aldehyde **28** exclusively with no sign of oxidation at the C6 methyl group (Scheme 5). The 2D NMR experiments with NOESY (nuclear Overhauser effect spectroscopy) confirmed the site of oxidation. The predicted greater acidity of the C-7 methyl hydrogens due to conjugation with the isoquinolone carbonyl could explain the observed selectivity.

Aldehyde **28** constitutes an intermediate for a wide range of functionality at C-7 (Scheme 5). **28** can be reduced directly to alcohol **29**, converted to an amine through reductive amination, e.g. **30**, or converted to secondary alcohol **31** by addition of vinylmagnesium chloride. Although Wittig olefination procedures with unstabilized ylides were not successful, Horner–Wadsworth–Emmons olefination with trimethyl phosphonoacetate and lithium hydroxide provided α,β-unsaturated ester **36**.[16] Alternatively, **28** could be transformed to the simple vinyl analogue **32** via a Peterson olefination.[17] α,β-unsaturated ester **36** underwent 1,4-reduction to the corresponding alkyl ester **37** upon hydrogenation over PtO_2 in methanol. Reduction of **36** to the corresponding allylic alcohol **38** was more troublesome than initially expected. Hydride reducing agents such as $LiAlH_4$ had no effect on the ester, and returned only un-reacted starting material. We found that if the amide NH of the isoquinolone was deprotonated initially with sodium bis(trimethylsilyl)amide, followed by addition of $LiAlH_4$, the desired alcohol could be obtained successfully.

Secondary alcohol **31** provides another functional handle when transformed into allylic acetate **33**. Palladium-catalyzed allylic transposition of **33** worked well with secondary amines to provide compounds such as **34**.[18] However, primary amines failed to react in the allylic transposition reaction. To obtain secondary amines, **33** was treated with NaN_3 as a nucleophile followed by a Staudinger reaction to provide **35**. Reductive amination with acetaldehyde provided amine **39**.

Results and Discussion

The two issues we felt were most important in obtaining inhibitors with oral efficacy in our mouse model of IL-2 production were to improve in vitro potency and to improve physicochemical properties, most notably aqueous solubility. One of the benefits of our improved synthetic route was the ready access it allowed for providing N-1 alkylated products. We found that the corresponding N-1 methyl analogue **12** shows a 5-fold increase in potency over **2** (Table 1). The methyl appears to be optimal because the corresponding ethyl analogue **40** is over 100-fold less potent.

This important result also helped to further validate our previously developed binding model, which predicted the 2,6-dichlorophenyl group to be pointing toward the N-3 nitrogen of the benzimidazole (conformer **A**, Figure 2).[19] Because the introduction of a methyl group on either nitrogen would be expected to strongly favor a conformation in which the dichlorophenyl group is oriented away from the methyl, the favorable potency of **12** strongly supports conformer **A** (Figure 2) as representing the bioactive conformation of the 2,6-dichlorophenyl group. Previous SAR studies showed that the N-3 methylated compound **41** is over 20-fold less potent than compound **2**.[4] However, the improved in vitro potency is likely due to a

Scheme 5. C-7 Oxidation and Functionalization[a]

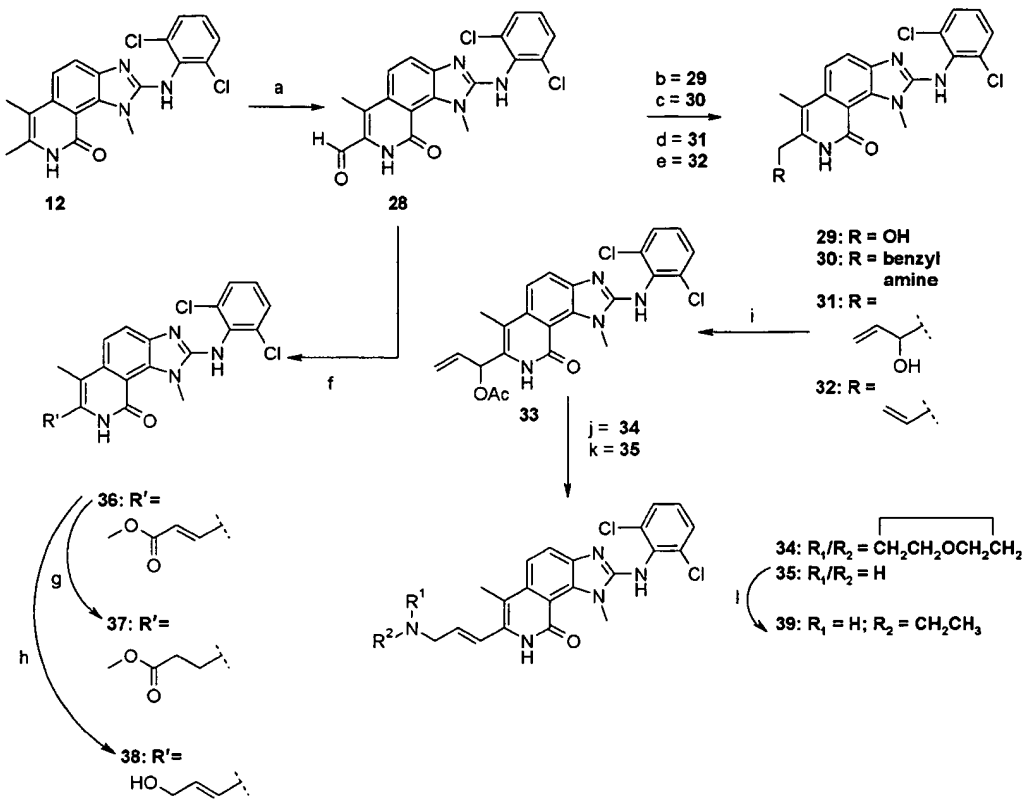

[a] Reagents: (a) SeO_2, dioxane, 100 °C; (b) $LiAlH_4$, THF; (c) (1) benzylamine, THF, (2) $NaBH_4$, MeOH; (d) vinylmagnesium bromide, THF, 0 °C to room temp; (e) (1) $TMSCH_2MgCl$, THF, −78 °C to room temp, (2) $BF_3(OEt)_2$, CH_2Cl_2, 0 °C to room temp; (f) $(MeO_2)P(O)CH_2CO_2Me$, LiOH, THF, H_2O; (g) H_2, PtO_2, HOAc, EtOAH; (h) (1) $NaN[Si(CH_3)_3]_2$, (2) $LiALH_4$, THF, 0 °C to room temp; (i) Ac_2O, Et_3N; (j) morpholine, $Pd_2(dba)_3$, PPh_3, THF; (k) NaN_3, $Pd_2(dba)_3$, PPh_3, THF, (2) PPh_3, THF; (l) acetaldehyde, $Na(OAc)_3BH$, MeOH.

Table 1. Methylation Studies on Benzimidazole Core[c]

Compound Code	Structure	Enzyme IC_{50} (μM)[a]	Calcium assay EC_{50} (μM)[b]
2	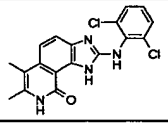	0.11	0.18±0.02
12	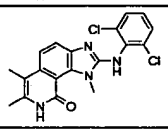	0.023	0.13±0.02
40	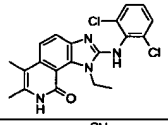	> 2.5	NT
41	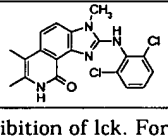	> 2.0	NT

[a] IC_{50} values for inhibition of lck. For active compounds, they are the mean values of two or more separate determinations, in duplicate. [b] EC_{50} values for inhibition of Ca release in Jurkat cells. Values are the mean of two or more separate experiments in duplicate ± SD. [c] NT = not tested.

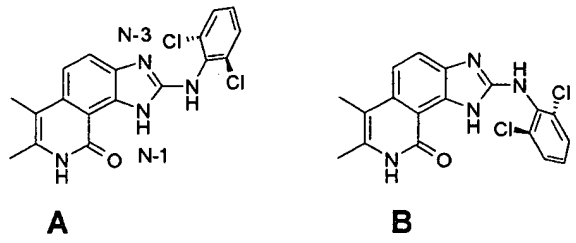

Figure 2. Bioactive conformer of **2**.

combination of locking the dichlorophenyl group into the bioactive conformation, increasing hydrophobic interactions with lck, and reducing desolvation factors.

On the basis of our model highlighted in Figure 3, we had little expectation of improving potency through further modification of the *N*-phenyl ring. SAR at this position tracked with our previous reported work with no noticeable improvement in potency. Thus, we concentrated on functionalizing the isoquinoline core. We had previously shown the requirement for 2,6-disubstitution on the phenyl ring with either chlorine atoms or methyl groups.

The spine of the isoquinolone core (Figure 3, C-4 through C-7) points out toward the cleft between the N and C lobes of lck. We therefore reasoned that substitution along this side of the molecule would be tolerated and could provide an opportunity to improve the potency and physicochemical properties of this inhibitor class.

We were able to introduce a wide range of functionality at both C-4 and C-6 that improved solubility; however, most modifications provided less potent compounds compared to **12** (Tables 2 and 3).

Although we were successful in introducing amine and alcohol functionality at the C-7 position, the initial SAR was also discouraging (Table 4). However, on

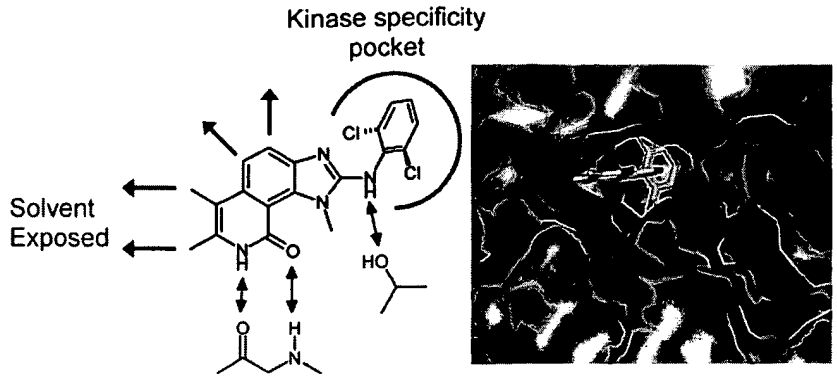

Figure 3. Opportunities suggested by the binding model of **12**.

Table 2. Effects of Substitution at C-6

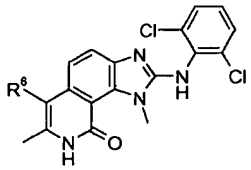

Compound Code	R^6	Enzyme IC_{50} (μM)[a]	Calcium assay EC_{50} (μM)[b]
12		0. 023	0.13±0.02
14		0.087	0.09±0.01
16	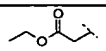	0.70	0.14±0.04
18	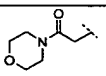	0.12	0.66±0.01
19	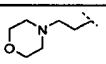	0.03	0.27±0.05
49	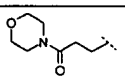	0.12	0.27±0.03
50	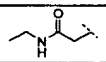	0.46	0.60±0.10
51	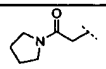	0.74	0.27±0.10
52	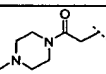	0.44	1.2±0.21
53	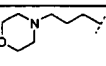	0.11	0.30±0.04
54		0.027	0.09±0.01

[a] IC_{50} values for inhibition of lck. For active compounds, they are the mean values of two or more separate determinations, in duplicate. [b] EC_{50} values for inhibition of Ca release in Jurkat cells. Values are the mean of two or more separate experiments in duplicate ± SD.

conversion of **28** to the α,β-unsaturated ester **36**, we observed our first signs, albeit modest, of improved cellular potency. This prompted a deeper investigation of the newly introduced ester and olefin functionality. While the saturated ester **37** showed a 16-fold loss in molecular potency and nearly a 2-fold loss in cellular potency compared to **12**, remarkably, the simple vinyl group **32** maintained molecular potency and improved cell potency nearly 10-fold when compared to **12**. The relatively poor potency of the ethyl analogue **42** further demonstrated the importance of an olefin substituent at C-7.

Table 3. Effects of Substitution at the C-4 Position

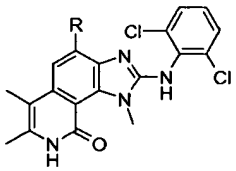

Compound Code	R	Enzyme IC_{50} (μM)[a]	Calcium assay EC_{50} (μM)[b]
12		0. 023	0.13±0.02
23		0.05	0.37±0.01
26		0.026	0.12±0.01
27		0.18	0.50±0.01

[a] IC_{50} values for inhibition of lck. For active compounds, they are the mean values of two or more separate determinations, in duplicate. [b] EC_{50} values for inhibition of Ca release in Jurkat cells. Values are the mean of two or more separate experiments in duplicate ± SD.

The loss in activity on going from an sp^2 to an sp^3 group at C-7 can be rationalized on the basis of our lck inhibitor binding model. As shown in Figure 4, the protein is very close above and below the plane of the molecule at the C-7 position. Therefore, planar substituents at the C-7 position fit well in this narrow cleft. Compounds that contain functionality attached to an sp^3 atom adopt a conformation that would position the attached group out of the plane of the molecule toward the protein, thereby lowering binding affinity. These results parallel our initial discovery of **2** from **1** in which removing the *gem*-dimethyl groups at C-6 and creating a planar system resulted in a significant boost in potency.[4]

By maintainance of the olefin substituent and introduction of polar functionality, further enhancements in cellular and molecular potency were achieved. Furthermore, compounds of this nature also resulted in an increase in aqueous solubility. Allylic alcohol **38** showed a small improvement in molecular potency but a significant boost in cellular potency. Furthermore, introduction of an allylic amine substituent provided an enhancement in both molecular and cellular potency. Although the polar allylic group does not appear to

Table 4. Effect of C-7 sp^2 Substitution[d]

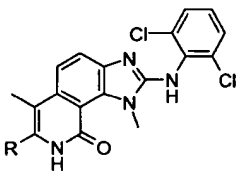

Compound Code	R	Enzyme IC_{50} (μM)[a]	Calcium assay EC_{50} (μM)[b]	EC_{50} SEB IL-2 Whole Blood (μM)[c]	EC_{50} Human Whole Blood IL-2(μM)[c]
12		0. 023	0.13±0.01	NT	1.1±0.8
28		0.17	0.45±0.05	NT	NT
29		0.77	0.24±0.02	NT	NT
30		2.0	4.2±0.01	NT	NT
31		0.570	1.3±0.10	NT	NT
32		0.045	0.02±0.04	0.90±0.8	12.0±0.04
36		0.086	0.07±0.01	NT	NT
37		0.36	0.23±0.04	NT	NT
42		0.78	0.08±0.01	NT	NT
38		0.009	0.008±0.01	0.22±0.1	3.0±0.05
34		0.004	0.030±0.01	0.170±0.1	NT
35		0.002	0.021±0.01	0.92±0.1	3.3±0.05
39		0.002	0.009±0.05	NT	NT
43		0.0007	0.007±0.01	0.13±0.02	1.8±0.5
44		0.002	0.005±0.01	0.15±0.1	0.30±0.1
45		0.01	0.20±0.01	NT	NT
46	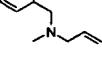	0.003	0.01±0.01	0.56±0.01	0.68±0.2

[a] IC_{50} values for inhibition of lck. For active compounds, they are the mean values of two or more separate determinations, in duplicate. [b] EC_{50} values for inhibition of Ca release in Jurkat cells. Values are the mean of two or more separate experiments in duplicate ± SD. [c] EC_{50} values for SEB IL2 and human whole blood IL2 values are the mean of two or more separate experiments in duplicate ± SD. [d] NT = not tested.

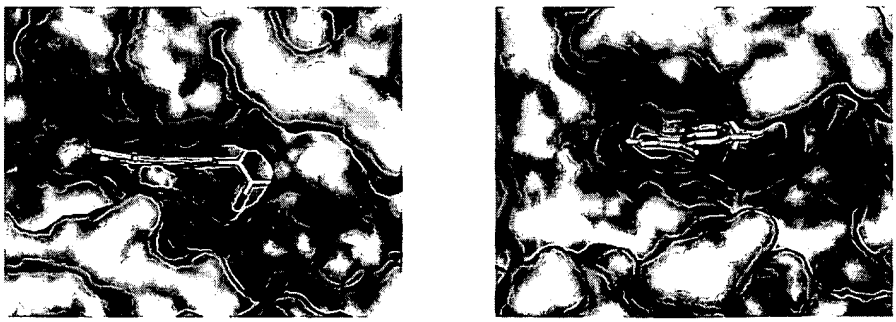

Figure 4. Views of **12** in relationship to C-7 and the enzyme cleft.

interact with the protein directly (vide infra), overall improvements in the physicochemical properties likely contribute to enhanced cellular potency. Further profiling this series of compounds showed them to be effica-

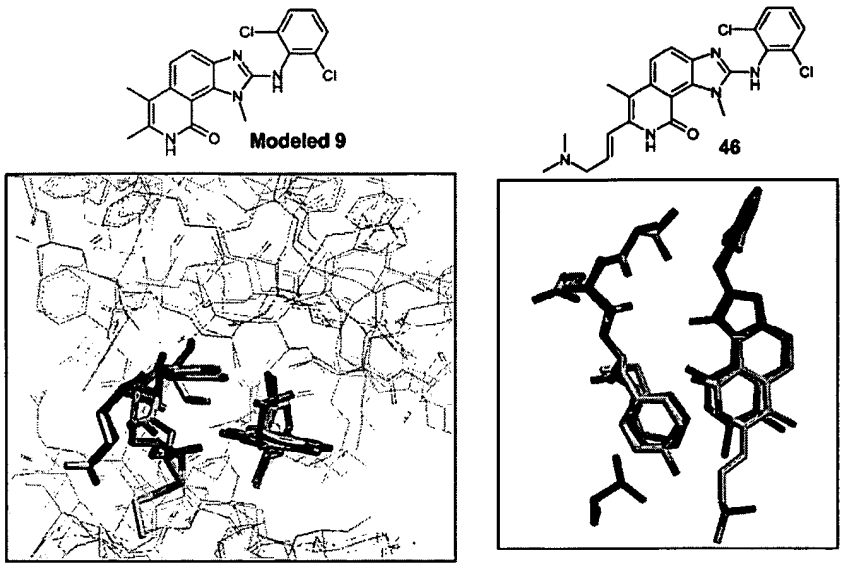

Figure 5. Overlay of X-ray of **46** with homology model of **12**.

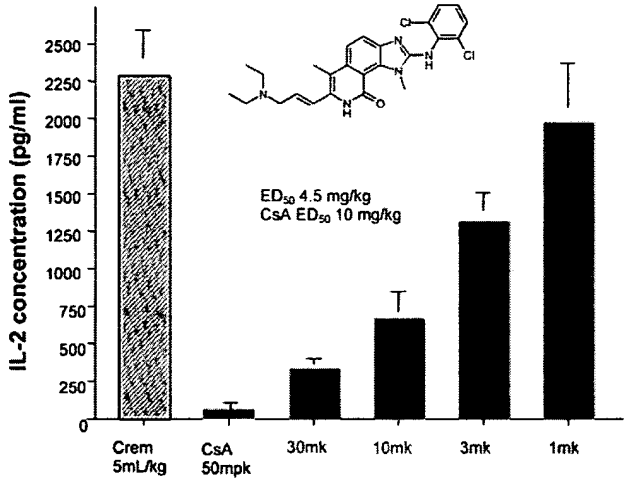

Figure 6. IL-2 inhibition by **43** when dosed orally.

cious in both the Jurkat IL-2 and human whole blood IL-2 assay.

X-ray. Through the course of this work, our binding model proved to be very useful in guiding the SAR studies. After compound **43** was profiled, we obtained an inhibitor–lck cocrystal structure, which confirmed the accuracy of this model with one of our more potent allylic amines, **46**. As shown (Figure 5), our model structure and the X-ray structure essentially overlap identically. Although the vinyl group is clearly resolved, the amine functionality is disordered and was therefore modeled into the crystal structure.

In Vivo Activity. Compounds were tested for in vivo efficacy in mice by measuring inhibition of IL-2 production following stimulation with anti-CD3. In this model, **2** was only moderately active when dosed ip as reported previously.[4] However, **43** demonstrated an ED_{50} of 4.5 mg/kg, which was comparable with that of cyclosporin A (ED_{50} = 10 mg/kg, Figure 6). Tertiary amines **34**, **44**, and **46** gave similar results in this model (data not shown). Interestingly, allylic alcohol **38**, which has in vitro potency comparable to that of **43**, proved to be ineffective when tested in this model. The lack of adequate oral exposure of **38** (~0 μM at 100 and 30 mg/kg) might simply be due to its poor solubility compared to **43** (0.25 vs 195 μg/mL at pH 7.4, respectively).

Table 5. Selectivity Profile of **43**

kinase	enzyme IC_{50} (μM)[a]	kinase	enzyme IC_{50} (μM)[a]
lck	0.0005	EGFR	>10
lyn	0.002	PDGFR	0.008
src	0.0002	HER2	>10
zap70	0.40	insulinRK	>100
syk	>40	IKKα & β	50
PKC	>300	IGFR	>100
PKA	>100	VEGFR	>100
p38	0.15	HGFR	>100
Btk	0.0004	Erk	>30
Itk	>10		

[a] IC_{50} values for inhibition of listed kinases. For active compounds, they are the mean of two or more separate determinations, in duplicate. ATP concentrations are at or below k_m of the listed kinases.

Table 6. Selectivity Profile of **43**

kinase	enzyme IC_{50} (μM)[a]	kinase	enzyme IC_{50} (μM)[a]
CDK4	>100	P70S6K	>1.0
CaMK	>100	GSK3β	>1.0
JNK	>1.0	ROCK–II	>1.0
MAPKAP-1b&2	>1.0	AMPK	>1.0
MSK-1	>1.0	CHK1	>1.0
PRAK	>1.0	CK2	>1.0
PDK1	>1.0	PHK	>1.0
PKBα	>1.0	CDK2	>1.0
SGK	>1.0	CSK	87% inh @ 1.0

[a] IC_{50} values for inhibition of listed kinases. ATP concentrations are run at 100 μM through the Dundee consortium.

Selectivity Profile. Selectivity over other kinases will be an important consideration for developing a chronically administered therapeutic agent. **43** demonstrates high selectivity when compared to a variety of both tyrosine and serine/threonine kinases (Tables 5 and 6). As expected, **43** shows no significant selectivity over two other members of the src family. Two kinases that demonstrated significant activity were PDGFR and Btk, both of which have a high homology in the ATP binding site, although less so in the whole kinase domain.

Conclusions

We have improved our class of phenylaminoimidazoisoquinolinones as potent inhibitors of lck kinase by 1000-fold over our screening hit. Our ability to accomplish this was aided through the use of a binding model, whose high level of accuracy has been confirmed by an X-ray structure of one of our inhibitors. Two key discoveries that led to significant improvements of this novel series were the N-1 alkylation of the benzimidazole and the conversion of the C-7 methyl group to a planar, sp^2 vinyl group that provided an increase in both molecular and cellular potency. Furthermore, introduction of an allylic polar substituent at the C-7 position, in particular an allylic amine, not only provided picomolar inhibitors of lck and improved aqueous solubility but also provided in vivo oral efficacy with activity comparable to that of cyclosporin A.

Experimental Section

Melting points were determined with an electrothermal capillary melting point apparatus or a Fisher-Johns apparatus and are uncorrected. Proton NMR (^{1}H NMR) spectra were recorded on Bruker Avance 400, Varian Gemini 2300, and Bruker AF270 spectrometers operating at 400, 300, and 270 MHz, respectively. Chemical shifts are reported as δ values in ppm downfield from TMS, using the solvent peak as an internal reference. Electron impact mass spectra (EIMS) were run on a Finnigan SSQ7000 instrument at 70 eV. Chemical ionization mass spectra (CIMS) were run on the same machine, with NH_3 as reagent gas. Electrospray mass spectra (ESMS) were run on a MicroMass Platform LCZ instrument, at a cone voltage of 30 V. Flash column chromatography was carried out on silica gel (230–400 mesh). Organic solutions that had been in contact with water were dried over $MgSO_4$ prior to concentration in a rotary evaporator.

2-Amino-6-chloro-3-nitrobenzonitrile (4). To 2,6-dichloro-3-nitrobenzonitrile (30 g, 139 mmol) was added a solution (200 mL, 5.15 M) of freshly prepared ammonia in ethanol. The flask was sealed and then placed in a preheated oil bath at 80 °C for 1.5 h. After the mixture was cooled, the resulting precipitate was taken up in ethyl acetate, washed with water and brine, dried over $MgSO_4$, and concentrated to afford 18.4 g (68%) of the title compound. ^{1}H NMR ($CDCl_3$, 270 MHz): δ 6.80 (d, 1H, J = 8.0 Hz), 8.33 (d, 1H, J = 8.0 Hz), 8.69 (bs, 2H).

6-Chloro-2-methylamino-3-nitrobenzonitrile (5). A solution of 2,6-dichloro-3-nitrobenzonitrile (98.7 g, 455 mmol) in EtOAc (910 mL) was cooled to 5 °C. A 40% aqueous methylamine (79.5 mL, 1.14 mol) solution was added with vigorous mechanical stirring, keeping the temperature at 10–15 °C. After addition was complete, stirring was continued for 3 h at the same temperature. More methylamine (16 mL, 230 mmol) was added, and the mixture was stirred for a further 1.5 h at room temperature. Water (300 mL) was added, followed by hexane (450 mL). The mixture was stirred for 15 min and filtered and the solid was washed with water and MeOH to provide 80.3 g (83%) of the title compound. Mp 168–171 °C. ^{1}H NMR (DMSO-d_6, 300 MHz): δ 3.45–3.50 (m, 3H), 6.80 (d, 1H, J = 9.0 Hz), 8.31 (d, 1H, J = 9.0 Hz), 8.69 (bs, 1H).

2-(3-Amino-2-cyano-4-nitrophenyl)-3-oxobutyric Acid Ethyl Ester (6). To a solution of 2-amino-6-chloro-3-nitrobenzonitrile (1.97 g, 10 mmol) in DMF was added ethyl 2-methylacetoacetate (3.60 g, 25 mmol) and potassium carbonate (1.50 g, 11 mmol). The reaction was stirred for 24 h at room temperature. The reaction mixture was diluted with EtOAc, then washed with 1 M HCl, water, and brine, and dried over $MgSO_4$. Column chromatography using hexanes/EtOAc (2:1) afforded 1.78 g (58%) of the title compound. ^{1}H NMR (DMSO-d_6, 400 MHz): δ 1.13 (t, 3H, J = 4.0 Hz), 1.72 (s, 3H), 2.26 (s, 3H), 4.14–4.17 (m, 2H), 6.55 (d, 1H, J = 8.0 Hz), 7.45 (bs, 2H), 8.23 (d, 1H, J = 8.0 Hz).

2-(2-Cyano-3-methylamino-4-nitrophenyl)-2-methyl-3-oxobutyric Acid Ethyl Ester (7). To a stirred solution of potassium *tert*-butoxide (24.3 g, 206 mmol) in DMSO (500 mL) was added ethyl 2-methylacetoacetate (34.3 g, 233 mmol) dropwise over 5 min. The temperature rose to 30 °C. 6-Chloro-2-methylamino-3-nitrobenzonitrile (43.6 g, 190 mmol) was added in portions over 15 min. The temperature rose to 40 °C. The solution was stirred for 1 h with no external heating or cooling. The mixture was poured into 10% aqueous NH_4Cl (500 mL) and was extracted with EtOAc. The combined extracts were washed with water and brine and were evaporated. MeOH (200 mL) was added to the residue, and the mixture was stirred for 1.5 h. The yellow solid was filtered, washed with cold MeOH (25 mL), and dried to provide 36.2 g (60%) of the title compound. Mp 84–87 °C. ^{1}H NMR (DMSO-d_6, 300 MHz): δ 1.22 (t, 3H, J = 7 Hz), 1.81 (s, 3H), 2.36 (s, 3H), 3.55 (bs, 3H), 4.18–4.30 (bs, 2H), 6.64 (d, 1H, J = 9 Hz), 8.06 (bs, 1H), 8.24 (d, 1H, J = 9 Hz).

2-(3,4-Diamino-2-cyanophenyl)-3-oxobutyric Acid Ethyl Ester (8). To a solution of 2-(3-amino-2-cyano-4-nitrophenyl)-3-oxobutyric acid ethyl ester (850 mg, 2.79 mmol) in methanol (50 mL) was added 10% palladium on carbon (85 mg). The flask was pressurized with hydrogen to 50 psi and hydrogenated until no loss of H_2 could be detected. The reaction mixture was filtered over Celite and concentrated to afford the title compound. ^{1}H NMR (DMSO-d_6, 400 MHz): δ 1.3 (t, 3H, J = 4.0 Hz), 1.80 (s, 3H), 2.30 (s, 3H), 4.25–4.35 (m, 2H), 6.42 (d, 1H, J = 8.0 Hz), 6.77 (d, 1H, J = 8.0 Hz), 8.10 (bs, 2H), 8.69 (bs, 2H).

2-(4-Amino-2-cyano-3-methylaminophenyl)-2-methyl-3-oxobutyric Acid Ethyl Ester (9). A solution of **7** (10.5 g, 32.5 mmol) in EtOAc (130 mL) was hydrogenated over 10% palladium on carbon (0.5 g) at 50 psi for 24 h. The catalyst was removed by filtration through diatomaceous earth, and the filtrate was evaporated. A mixture of EtOAc/hexane (1:1, 10 mL) was added to the residue, and the resulting mixture was stirred for 0.5 h. The crystals were filtered and washed with hexane to provide 7.74 g (81%) of the title compound. Mp 130–131.5 °C. ^{1}H NMR (DMSO-d_6, 300 MHz): δ 1.21 (t, 3H, J = 7.0 Hz), 1.67 (s, 3H), 2.23 (s, 3H), 2.96–3.0 (m, 3H), 4.18–4.21 (m, 2H), 4.89–4.91 (m, 1H), 5.17 (s, 2H), 6.35 (d, 1H, J = 8 Hz), 6.72 (d, 1H, J = 8 Hz). CIMS *m/z*: 290 (MH^+). Anal. ($C_{15}H_{19}N_3O_3$) C, H, N.

2-(2,6-Dichlorophenylamino)-6,7-dimethyl-1,8-dihydroimidazo[4,5-*h*]isoquinolin-9-one (2). To a solution of **8** (767 mg, 2.79 mmol) in ethyl acetate (30 mL) was added 2,6-dichlorophenyl isothiocyanate (626 mg, 3.07 mmol). The reaction mixture was stirred at room temperature overnight. The reaction mixture was diluted with ethyl acetate (20 mL), washed with water (3 × 20 mL), dried ($MgSO_4$), and concentrated. The crude residue was chromatographed using hexanes/EtOAc (1:1) to afford the thiourea. To the intermediate thiourea (1.30 g, 2.72 mmol) was added DCC (600 mg, 2.91 mmol) and THF. The reaction mixture was heated at 80 °C for 3 h. After the mixture was cooled, solvent was concentrated and crude residue was taken back up in ethyl acetate. Insoluble material was filtered off. The filtrate was concentrated to afford 600 mg (50%) of the title compound. The ^{1}H NMR results were identical to the results reported in ref 4.

2-[4-Cyano-2-(2,6-dichlorophenylamino)-3-methyl-3*H*-benzimiazol-5-yl]-2-methyl-3-oxobutyric Acid Ethyl Ester (11). A solution of **9** (7.7 g, 26.6 mmol) and 2,6-dichlorophenyl isothiocyanate (5.43 g, 26.6 mmol) in THF (150 mL) was stirred at room temperature for 5 h. Mercuric oxide (6.34 g, 29.3 mmol) was then added in one portion, and stirring continued overnight. The mixture was filtered through diatomaceous earth, washing well with THF. The filtrate was evaporated and the residue was triturated with ether to provide 7.7 g (63%) of the title compound. ^{1}H NMR (DMSO-d_6, 400 MHz): δ 1.17 (t, 3H, J = 8.0 Hz), 1.82 (s, 3H), 2.30 (s, 3H), 4.08 (s, 3H), 4.16–4.25 (m, 2H), 7.16 (d, 1 H, J = 8 Hz), 7.48 (t, 1 H, J = 8 Hz), 7.50 (d, 1 H, J = 8 Hz), 7.67 (d, 2 H, J = 8 Hz).

2-(2,6-Dichlorophenylamino)-6,7-dimethyl-1,8-dihydroimidazo[4,5-*h*]isoquinoline-9-one (12). To a stirred mixture of concentrated H_2SO_4 (40 mL), HOAc (40 mL), and water (40 mL) at 60 °C was added **11** (7.4 g, 16 mmol) in one portion. The solution was heated at 100 °C for 2.5 h and then stirred overnight at room temperature. The reaction mixture was poured onto ice and neutralized with concentrated NH_4OH, with ice-cooling. The precipitate was filtered and washed well with water. The solid was slurried in MeOH, stirred well, filtered, washed with MeOH until the washings were colorless, and dried to provide 5.5 g (88%) of the title compound. Mp >300 °C. ^{1}H NMR (DMSO-d_6, TFA, 400 MHz): δ 2.22 (s, 3H), 2.32 (s, 3H), 4.28 (s, 3H), 7.60 (t, 1H, J = 8 Hz), 7.70 (d, 1H, J = 9 Hz), 7.73 (d, 1H, J = 9 Hz), 7.77 (d, 2H, J = 8 Hz). CIMS *m/z*: 387 (MH^+). Anal. ($C_{19}H_{16}Cl_2N_4O$) C, H, N.

2-(2,6-Dichlorophenylamino)-1-ethyl-6,7-dimethyl-1,8-dihydroimidazo[4,5-*h*]isoquinolin-9-one (40). 40 was prepared as described for compound **12** with ethylamine. ^{1}H NMR (DMSO-d_6, TFA, 400 MHz): δ 2.25 (t, 3H, J = 7.0 Hz), 2.16 (s, 3H), 2.25 (s, 3H), 5.23 (q, 2H, J = 7, 8 Hz), 7.54 (dd, 1H, J = 1, 8 Hz), 7.64 (dd, 2H, J = 1, 8 Hz), 7.70 (d, 2H, J = 8 Hz), 11.44 (s, 1H). ESMS *m/z*: 431 (MH^+).

2-(2-Cyano-3-methylamino-4-nitrophenyl)-3-oxobutyric Acid Methyl Ester (13). 13 was prepared as described for **6** and **7**. ^{1}H NMR ($CDCl_3$, 400 MHz): δ 1.95 (s, 3H), 3.48 (s, 3H), 3.91 (s, 3H), 6.52 (d, 1H, J = 8 Hz), 8.37 (d, 1H, J = 8 Hz), 8.61 (bs, 1H).

1,7-Dimethyl-2-dichlorphenylamino-9-oxo-8,9-dihydro-1*H*-imidazo[4,5-*h*]isoquinoline-6-carboxylic Acid Methyl Ester (14). 14 was prepared as described above for **12**. ^{1}H NMR (TFA-*d*, 400 MHz): δ 2.62 (s, 3H), 4.19 (s, 3H), 4.42 (s, 3H), 7.46–7.50 (m, 1H), 7.51 (d, 2H, J = 8 Hz), 7.87 (d, 1H, J = 9 Hz), 7.93 (d, 1H, J = 9 Hz). ESMS *m/z*: 431 (MH^+).

2-Acetyl-2-(2-cyano-3-methylamino-4-nitrophenyl)succinic Acid Dimethyl Ester (15). 15 was prepared as described for **6** and **7**. ^{1}H NMR ($CDCl_3$, 400 MHz): δ 1.25–1.29 (m, 5H), 1.37 (t, 3H, J = 8 Hz), 2.08 (s, 3H), 2.43 (s, 3H), 3.41–3.45 (m, 2H), 4.15 (apt t, 2H, J = 8 Hz), 4.39 (apt t, 2H, J = 8 Hz), 6.72 (d, 1H, J = 8 Hz), 8.33 (d, 1H, J = 8 Hz), 8.39 (bs, 1H).

2-(2,6-Dichlorophenylamino)-1,7-dimethyl-9-oxo-1,8-dihydroimidazo[4,5-*h*]isoquinolin-6-ylacetic Acid (16). 16 was prepared as described for compounds **2** and **12**. ^{1}H NMR (TFA-*d*, 400 MHz): δ 2.92 (s, 3H), 4.37 (s, 2H), 4.61 (s, 3H), 7.59 (t, 1H, J = 7 Hz), 7.72 (d, 2H, J = 7 Hz), 8.06 (s, 2H), 7.98 (d, 1H, J = 8 Hz). ESMS *m/z*: 431.

2-(2,6-Dichlorophenylamino)-1,7-dimethyl-9-oxo-1,8-dihydroimidazo[4,5-*h*]isoquinolin-6-ylacetic Acid Ethyl Ester (17). 17 was prepared from **16** by refluxing in ethanol and H_2SO_4. Mp 280–285 °C. ^{1}H NMR (TFA-*d*, 400 MHz): δ 1.45 (bs, 3H), 2.75 (s, 3H), 4.20 (s, 2H), 4.50 (s, 3H), 7.35–7.40 (m, 1H), 7.75 (s, 1H), 7.95–8.0 (m, 2H), 8.37–8.39 (m, 1H), δ 8.97 (s, 1H), 11.08 (s, 1H). ESMS *m/z*: 500 (MH^+). MSCI *m/z*: 459, 461 (MH^+). Anal. ($C_{22}H_{20}Cl_2N_4O_3 \cdot 1H_2O$) C, H, N.

2-(2,6-Dichlorophenylamino)-1,7-dimethyl-6-(2-morpholin-4-yl-2-oxoethyl)-1,8-dihydroimidazo[4,5-*h*]isoquinoline-9-one (18). To a solution of **17** (1.0 g, 2.3 mmol) in DMF (7 mL) was added *O*-benzotriazol-1-yl-*N*,*N*,*N*′,*N*′-tetramethyluronium tetrafluoroborate (TBTU) (0.82 g, 2.6 mmol) and morpholine (0.24 mL, 2.8 mmol), and the mixture was stirred for 18 h at room temperature. Ice/water was added and the precipitate was collected, washed with water, and dried to give 0.97 g (84%) of the title compound. Mp >300 °C. ^{1}H NMR (TFA-*d*, 400 MHz): δ 2.58 (s, 3H), 3.89–3.99 (m, 2H), 4.03–4.14 (m, 4H), 4.15–4.23 (m, 2H), 4.28 (s, 2H), 4.44 (s, 3H), 7.51 (t, 1H, J = 8 Hz), 7.63 (d, 2H, J = 8 Hz), 7.70 (d, 1H, J = 9 Hz), 7.90 (d, 1H, J = 9 Hz). ESMS *m/z*: 500, 502 (MH^+). Anal. ($C_{24}H_{23}Cl_2N_5O_3 \cdot 0.3H_2O$) C, H, N.

2-(2,6-Dichlorophenylamino)-1,7-dimethyl-6-(2-(ethylamino)-2-oxoethyl)-1,8-dihydroimidazo[4,5-*h*]isoquinoline-9-one (50). 50 was prepared as described above. Mp >300 °C. ^{1}H NMR (TFA-*d*, 400 MHz): δ 1.26 (t, 3H, J = 8 Hz), 2.67 (s, 3H), 3.45–3.61 (m, 2H), 4.32 (s, 2H), 4.49 (s, 3H), 7.55 (t, 1H, J = 8 Hz), 7.67 (d, 2H, J = 8 Hz), 7.88 (d, 1H, J = 8 Hz), 7.98 (d, 1H, J = 8 Hz). ESMS *m/z*: 458, 460 (MH^+).

2-(2,6-Dichlorophenylamino)-1,7-dimethyl-6-(2-pyrrolidin-1-yl-2-oxoethyl)-1,8-dihydroimidazo[4,5-*h*]isoquinoline-9-one (51). 51 was prepared as described above. Mp >300 °C. ^{1}H NMR (TFA-*d*, 400 MHz): δ 2.12–2.20 (m, 2H), 2.25–2.30 (m, 2H), 2.60 (s, 3H), 3.70–3.88 (m, 2H), 3.92–4.16 (m, 2H), 4.32 (s, 2H), 4.44 (s, 3H), 7.51 (t, 1H, J = 8 Hz), 7.62 (d, 2H, J = 8 Hz), 7.67 (d, 1H, J = 9 Hz), 7.89 (d, 1H, J = 9 Hz). ESMS *m/z*: 484, 486 (MH^+).

2-(2,6-Dichlorophenylamino)-1,7-dimethyl-6-[2-(4-methylpiperazin-1-yl)-2-oxoethyl]-1,8-dihydroimidazo[4,5-*h*]isoquinoline-9-one (52). 52 was prepared as described as above. Mp >300 °C. ^{1}H NMR (TFA-*d*, 400 MHz): δ 2.66 (s, 3H), 3.30 (s, 3H), 3.41 (t, 1H, J = 7 Hz), 3.50–3.66 (m, 2H), 3.94 (d, 1H, J = 12 Hz), 4.07 (d, 1H, J = 12 Hz), 4.14–4.26 (m, 1H), 4.36 (d, 1H, J = 17 Hz), 4.46 (d, 1H, J = 17 Hz), 4.55 (s, 3H), 4.77 (d, 1H, J = 14 Hz), 5.08 (1H, d, J = 14 Hz), 7.61 (1H, t, J = 8 Hz), 7.63 (2H, d, J = 8 Hz), 7.75 (d, 1H, J = 8 Hz), 7.98 (d, 1H, J = 9 Hz). ESMS *m/z*: 513, 515 (MH^+).

2-(2,6-Dichlorophenylamino)-1,7-dimethyl-6-(2-morpholin-4-ylethyl)-1,8-dihydroimidazo[4,5-*h*]isoquinoline-9-one (19). A stirred suspension of **18** (85 mg, 0.17 mmol) in THF (9 mL) was heated to reflux, and borane methyl sulfide (0.09 mL, 0.9 mmol) added. Stirring was continued for 3.5 h at reflux and overnight at room temperature. Then 6 M HCl was added and the solution was stirred for 2 h. The solution was applied to a Varian SCX column and was washed with $MeOH/CH_2Cl_2$, 50:50. Then the product was eluted with $MeOH/CH_2Cl_2/NH_4OH$, 50:50:1. The product was further purified on a silica column, eluting with CH_2Cl_2/MeOH, 98:2, to provide 32 mg (39%) of the title compound. Mp 285–290 °C. ^{1}H NMR (TFA-*d*, 400 MHz): δ 2.65 (s, 3H), 3.46–3.65 (m, 6H), 4.01 (d, 2H, J = 12 Hz), 4.20 (t, 2H J = 12 Hz), 4.38–4.50 (m, 2H), 4.43 (s, 3H), 7.51 (t, 1H, J = 8 Hz), 7.63 (d, 1H, J = 8 Hz), 7.98 (d, 1H, J = 8 Hz), 7.97–8.0 (m, 2H). ESMS *m/z*: 486, 488 (MH^+).

2-(2,6-Dichlorophenylamino)-1,7-dimethyl-6-(3-morpholin-4-yl-3-oxopropyl)-1,8-dihydroimidazo[4,5-*h*]isoquinoline-9-one (49). 49 was prepared as described as above. Mp 277–282 °C. ^{1}H NMR (TFA-*d*, 400 MHz): δ 2.20–2.36 (m, 2H), 2.67 (s, 3H), 3.18 (t, 2H, J = 9 Hz), 3.43 (d, H, J = 9 Hz), 3.54–3.62 (m, 2H), 3.80 (d, 2H, J = 12 Hz), 4.05–4.15 (m, 2H), 4.38 (d, 2H, J = 12 Hz), 4.45 (s, 3H), 7.54 (t, 1H, J = 8 Hz), 7.65 (d, 2H, J = 8 Hz), 8.00 (s, 2H). ESMS *m/z*: 500, 502 (MH^+). Anal. ($C_{25}H_{27}Cl_2N_5O_2 \cdot 0.2H_2O$) C, H, N.

2-(2,6-Dichlorophenylamino)-1,7-dimethyl-6-(3-morpholin-4-ylpropyl)-1,8-dihydroimidazo[4,5-*h*]isoquinolin-9-one (53). 53 was prepared as described above. Mp 277–282 °C. ^{1}H NMR (TFA-*d*, 400 MHz): δ 2.18 (br, 2H), 2.67 (s, 3H), 3.17 (t, 2H, J = 8 Hz), 3.42 (t, 2H, J = 8 Hz), 3.3–3.6 (m, 2H), 3.81 (d, 2H, J = 12 Hz), 4.11 (t, 2H, J = 6 Hz), 4.39 (d, 2H, J = 12 Hz), 4.45 (s, 3H), 7.53 (t, 1H, J = 8 Hz), 7.65 (d, 2H, J = 8 Hz), 8.00 (s, 2 H). CIMS *m/z*: 500 (MH^+).

2-(4-Amino-5-bromo-2-cyano-3-methylaminophenyl)-2-methyl-3-oxobutyric Acid Ethyl Ester (20). To a solution of **9** (9.02 g, 31.2 mmol) in $CHCl_3$ (90 mL) was added bromine (4.98 g, 31.2 mmol) dropwise at ambient temperature. After the addition of bromine, the reaction mixture was diluted with EtOAc (800 mL). This solution was washed successively with saturated $NaHCO_3$ solution and brine and dried. The residue after evaporation was purified by flash chromatography in hexanes/EtOAc, 2:1, to provide 6.1 g (53%) of the title compound. ^{1}H NMR ($CDCl_3$, 400 MHz): δ 1.3 (t, 3H, J = 16 Hz), 1.89 (s, 3H), 2.45 (s, 3H), 2.95 (s, 3H), 4.30–4.40 (m, 2H), 7.01 (s, 1 H), 8.40 (bs, 2H), 8.6 (bs, 1H).

2-[8-Bromo-4-cyano-2-(2,6-dichlorophenylamino)-3-methyl-3*H*-benzimidazol-5-yl]-2-methyl-3-oxobutyric Acid Ethyl Ester (21). To **20** (3.32 g, 9.0 mmol) in 1,4-dioxane (45 mL) was added 2,6-dichlorophenyl isothiocyanate (2.02 g, 9.9 mmol) and mercuric oxide (2.54 g, 11.7 mmol) under nitrogen atmosphere. The resulting mixture was stirred and heated at 95 °C overnight. The reaction mixture was cooled to room temperature and filtered though a short pad of diatomaceous

earth and SiO_2. The filtrate was concentrated and the residue was purified by flash chromatography in hexanes/EtOAc, 2:1, to provide 3.44 g (71%) of the title compound. ^{1}H NMR (DMSO-d_6, 400 MHz): δ 1.36 (t, 3H, J = 4.0 Hz), 1.96 (s, 3H), 2.39 (s, 3H), 4.14 (s, 3H), 4.36−4.40 (m, 2H), 7.23 (s, 1 H), 7.55 (t, 1H, J = 8.0 Hz), 7.77 (d, 2H, J = 8.0 Hz), 9.62 (s, 1H).

2-[4-Cyano-2-(2,6-dichlorophenylamino)-3-methyl-8-vinyl-3*H*-benzimiazol-5-yl]-2-methyl-3-oxobutyric Acid Ethyl Ester (22). A mixture of 2-[8-bromo-4-cyano-2-(2,6-dichlorophenylamino)-3-methyl-3*H*-benzimiazol-5-yl]-2-methyl-3-oxobutyric acid ethyl ester (600 mg, 1.11 mmol), $(PPh_3)_2PdCl_2$ (78 mg, 0.11 mmol), and tributyl(vinyl)tin (0.49 mL, 1.67 mmol) in NMP (4 mL) was degassed and heated at 100 °C for 3 days under argon. The mixture was concentrated, and the residue was purified by flash chromatography in hexanes/EtOAc, 3:1, to provide 530 mg (98%) of the title compound. ^{1}H NMR ($CDCl_3$, 400 MHz): δ 1.38 (t, 3H, J = 8 Hz), 1.97 (s, 3H), 2.45 (s, 3H), 4.05 (s, 3H), 4.37−4.40 (m, 2H), 5.50 (d, 1H, J = 8 Hz), 6.10−6.30 (m, 1H), 6.97 (s, 2H), 7.10 (d, H, J = 8 Hz), 7.39 (d, H, J = 8 Hz).

2-(2,6-Dichlorophenylamino)-1,6,7-trimethyl-4-vinyl-1,8-dihydroimidazo-[4,5-*h*]isoquinoline-9-one (22b). 22 (66 mg, 0.14 mmol) in a mixture of H_2SO_4 (0.6 mL), acetic acid (0.6 mL), and water (0.6 mL) was heated at 100 °C for 2 h. The resulting mixture was cooled to room temperature and diluted with water (10 mL). The solution was adjusted to pH 8 with 10% NaOH solution. The precipitated brown solid was filtered and purified by flash chromatography in CH_2Cl_2/MeOH, 30:1, to provide 15 mg (27%) of the title compound. Mp >250 °C (dec). ^{1}H NMR (TFA-*d*, 400 MHz): δ 2.11 (s, 3H), 2.22 (s, 3H), 4.13 (s, 3H), 5.49 (d, 1H, J = 11 Hz), 6.35 (d, 1H, J = 16 Hz), 7.05 (dd, 1H, J = 11, 16 Hz), 7.31 (t, 1H, J = 8 Hz), 7.45 (d, 1H, J = 8 Hz), 7.68−7.71 (m, 1H), 8.86 (s, 1H), 10.9 (s, 1H). CIMS *m/z*: 413(MH$^+$).

2-[4-Cyano-2-(2,6-dichlorophenylamino)-7-formyl-3-methyl-3*H*-benzoimidazol-5-yl]-2-methyl-3-oxobutyric Acid Ethyl Ester (24). To a solution of **22** (0.58 g, 1.20 mmol) in THF (30 mL) was added osmium tetroxide (3 mL), followed by sodium periodate (0.77 g, 3.59 mmol) and water (3.0 mL). The mixture was stirred at room temperature for 30 min before dilution with water and extraction of the product with ethyl acetate. The organic layer was then diluted with an aqueous $NaHCO_3$ solution. The organic layer was then dried with $MgSO_4$ filtered, and concentrated to an oil. This was then loaded onto a silica gel column (2:1 hexanes/ethyl acetate) to provide 0.46 g (100% g) of the title compound. ^{1}H NMR ($CDCl_3$, 400 MHz): δ 1.40 (t, 3H, J = 16 Hz), 1.60 (s, 3H), 1.97 (s, 3H), 2.45 (s, 3H), 4.01 (s, 3H), 4.05 (s, 3H), 4.31−4.45 (m, 2H), 7.01 (d, 1H, J = 8 Hz), 7.19 (bs,1H), 7.45 (d, 1H, J = 8 Hz), 8.95 (bs, 1H), 10.01 (bs, 1H).

2-(2,6-Dichlorophenylamino)-1,6,7-trimethyl-9-oxo-1,8-dihydroimidazo[4,5-*h*]isoquinoline-4-carbaldehyde (25). 24 (35 mg, 0.07 mmol) in a mixture of H_2SO_4 (0.6 mL), acetic acid (0.6 mL), and water (0.6 mL) was heated at 100 °C for 1.5 h and cooled to room temperature. The resulting mixture was diluted with water (10 mL), and the pH was adjusted to 7 with ammonium hydroxide solution. The precipitated orange powder was filtered to provide 18 mg (60%) of the title compound. ^{1}H NMR (TFA-*d*, 400 MHz): δ 2.34 (s, 3H), 2.38 (s, 3H), 4.14 (s, 3H), 7.25 (t, 1H, J = 8 Hz), 7.60 (d, 2H, J = 8 Hz), 8.10 (s, 1H), 10.1 (s, 1H).

2-(2,6-Dichlorophenylamino)-4-(2-hydroxyethylaminomethyl)-1,6,7-trimethyl-1,8-dihydroimidazo[4,5-*h*]isoquinolin-9-one (26). A suspension of **25** (30 mg, 0.07 mmol) in methanol (5 mL) was treated with ethanolamine (44 μL, 0.72 mmol) and sodium cyanoborohydride (14 mg, 0.22 mmol) and stirred at room temperature for 16 h. The resulting mixture was concentrated, and the residue was diluted with water. The precipitated solid was filtered and dried to give 12 mg (36%) of the title compound. Mp >300 °C. ^{1}H NMR (MeOH-d_4, 400 MHz): δ 2.36 (s, 3H), 2.38 (s, 3H), 2.71 (t, 2H, J = 6.0 Hz), 3.62 (t, 2H, J = 6.0 Hz), 4.14 (s, 2H), 4.20 (s, 3H), 7.25 (s, 1H), 7.49−7.52 (m, 3H). ESMS *m/z*: 460, 462 (MH$^+$).

2-(2,6-Dichlorophenylamino)-4-[(4-methoxybenzylamino)methyl]-1,6,7-trimethyl-1,8-dihydroimidazo[4,5-*h*]isoquinolin-9-one (27). A suspension of **25** (30 mg, 0.07 mmol) in methanol (5 mL) was treated with 4-methoxybenzylamine (94 μL, 0.72 mmol) and sodium cyanoborohydride (14 mg, 0.22 mmol) and stirred at room temperature for 16 h. The resulting mixture was concentrated and preparative TLC (silica gel/5% MeOH in CH_2Cl_2) purified the residue to give 7 mg (18%) of the title compound. Mp 247−250 °C. ^{1}H NMR (MeOH-d_4, 400 MHz): δ 2.34 (s, 3H), 2.38 (s, 3H), 3.76 (s, 2H), 3.79 (s, 3H), 3.82 (s, 2H), 4.24 (s, 3H), 6.85 (d, 2H, J = 8 Hz), 7.13 (d, 2H, J = 8 Hz), 7.24 (t, 1H, J = 8 Hz), 7.45−7.47 (m, 3H). ESMS *m/z*: 536, 538 (MH$^+$).

2-(2,6-Dichlorophenylamino)-1,6,7-trimethyl-4-(2,6-difluoropyridin-3-yl)-1,8-dihydroimidazo[4,5-*h*]isoquinoline-9-one (23b). To 2-[8-bromo-4-cyano-2-(2,6-dichlorophenylamino)-3-methyl-3*H*-benzimidazol-5-yl]-2-methyl-3-oxobutyric acid ethyl ester (100 mg, 0.186 mmol) in dry NMP (3 mL) was added 2,6-difluoro-3-tributylstannanylpyridine (113 mg, 0.28 mmol) and dichlorobis(triphenylphosphine)palladium(II) (10 mg). The reaction mixture was heated in a sealed tube at 100 °C overnight. The reaction mixture was cooled to room temperature and extracted with EtOAc (25 mL). The organic fraction was washed with water, dried over anhydrous sodium sulfate, filtered, and evaporated. Column chromatography (1:1 EtOAc/hexanes) followed by preparative TLC (silica gel, 40% ethyl acetate/hexanes) provided 28 mg (26%) of the title compound. ESMS *m/z*: 572 (MH$^+$).

To the coupled product (25 mg, 0.044 mmol) was added 1:1 concentrated sulfuric acid/water (3 mL). The reaction mixture was heated at 100 °C for 2 h. The reaction mixture was cooled to room temperature, ice/water (2 mL) was added, and the reaction was made basic by addition of aqueous NH_4OH. The solid was filtered off and purified by preparative TLC (silica gel/5% CH_3OH/CH_2Cl_2) to provide 7 mg (32%) of the title compound. Mp >300 °C. ^{1}H NMR (DMSO-d_6, TFA, 400 MHz): δ 2.21 (s, 3H), 2.29 (s, 3H), 4.13 (s, 3H), 7.23−7.30 (m, 2H), 7.48 (s, 1H), 7.53−7.55 (m, 2H), δ 8.37−8.39 (m, 1H), 8.97 (s, 1H), 11.08 (s, 1H). ESMS *m/z*: 500 (MH$^+$).

2-(2,6-Dichlorophenylamino)-1,6-dimethyl-9-oxo-8,9-dihydro-1*H*-imidazo[4,5-*h*]isoquinoline-7-carbaldehyde (28). To a suspension of **12** (521 mg, 1.3 mmol) in dioxane (30 mL) was added selenium dioxide (430 mg, 3.9 mmol), and the mixture was heated at 100 °C for 5 h. The reaction mixture was then cooled to room temperature, filtered through diatomaceous earth with 10% MeOH/CH_2Cl_2, and then concentrated in vacuo. The crude material was triturated with CH_2Cl_2 to provide 476 mg (92%) of the title compound. Mp >300 °C. ^{1}H NMR (DMSO-d_6, TFA, 400 MHz): δ 2.27 (s, 3H), 4.30 (s, 3H), 7.38 (t, 1H, J = 8 Hz), 7.60 (d, 2H, J = 8 Hz), 7.69 (s, 2H), 8.68 (bs, 1H), 10.21 (s, 1H), 10.51 (bs, 1H), 11.72 (bs, 1H). NOSEY (DMSO-d_6, TFA): correlation between C5−H and C6−CH_3 and between C6−CH_3 and C7−CHO. CIMS *m/z*: 401, 403 (MH$^+$).

2-(2,6-Dichlorophenylamino)-1,6-dimethyl-7-(1-hydroxyprop-2-en-1-yl)-1,8-dihydroimidazo[4,5-*h*]isoquinolin-9-one (31). A suspension of **28** (100 mg, 0.25 mmol) in THF (3 mL) was cooled to −78 °C. Vinylmagnesium bromide (1 M in THF, 2.0 mmol) was added dropwise, and the brown suspension was warmed gradually to −10 °C over 2 h. The solution was quenched with saturated NH_4Cl, extracted with EtOAc, and concentrated in vacuo to provide the title compound, which was used in the next step without purification. Mp 235−236 °C. ^{1}H NMR (MeOH-d_4, 400 MHz): δ 2.35 (s, 3H), 4.24 (s, 3H), 5.26 (d, 1H, J = 10 Hz), 5.40 (d, 1H, J = 17 Hz), 5.56 (d, 1H, J = 5 Hz), 6.03 (ddd, 1H, J = 5, 10, 17 Hz), 7.32 (t, 1H, J = 8 Hz), 7.53 (d, 2H, J = 8 Hz), 7.61 (d, 1H, J = 9 Hz), 7.72 (d, 1H, J = 9 Hz). ESMS *m/z*: 429 (MH$^+$). Anal. ($C_{21}H_{18}Cl_2N_4O_3$) C, H, N.

3-[2-(2,6-Dichlorophenylamino)-1,6-dimethyl-9-oxo-8,9-dihydro-1*H*-imidazo[4,5-*h*]isoquinolin-7-yl]acrylic Acid Methyl Ester (36). To a suspension of **28** (329 mg, 0.82 mmol) in THF (5 mL) was added sequentially trimethyl phosphonoacetate (164 mg, 0.90 mmol), lithium hydroxide monohy-

drate (76 mg, 1.8 mmol), and water (0.9 mL). The blood-red solution was stirred for 2 h and quenched with water, and the resulting solid was collected and dried in vacuo. Column chromatography (5% MeOH/CH_2Cl_2) provided 300 mg (80%) of the title compound. Mp >300 °C. ^{1}H NMR (DMSO-d_6, TFA, 400 MHz): δ 2.45 (s, 3H), 3.76 (s, 3H), 4.20 (s, 3H), 6.89 (d, 1H, J = 16 Hz), 7.56 (t, 1H, J = 8 Hz), 7.73–7.77 (m, 3H), 7.81 (d, 1H, J = 16 Hz), 7.87 (d, 1H, J = 9 Hz), 11.29 (s, 1H). ESMS m/z 457, 459 (MH^+). Anal. ($C_{22}H_{18}Cl_2N_4O_3 \cdot 1.5H_2O$) C, H, N.

3-[2-(2,6-Dichlorophenylamino)-1,6-dimethyl-9-oxo-8,9-dihydro-1*H*-imidazo[4,5-*h*]isoquinolin-7-yl]propionic Acid Methyl Ester (37). To a solution of **36** (30 mg, 0.06 mmol) in EtOH (3 mL) and AcOH (4 mL) in a Parr reactor was added PtO_2 (2 mg, 0.007 mmol). The Parr reactor was charged with 50 psi of H_2 and shaken for 12 h. The crude reaction mixture was filtered through diatomaceous earth with EtOH and concentrated in vacuo. Column chromatography (2% MeOH/CH_2Cl_2) provided 9 mg (30%) of the title compound. Mp 268 °C (dec). ^{1}H NMR (DMSO-d_6, TFA, 400 MHz): δ 2.24 (s, 3H), 2.66 (t, 2H, J = 8 Hz), 2.90 (t, 2H, J = 8 Hz), 3.75 (s, 3H), 4.24 (s, 3H), 7.54 (t, 1H, J = 8 Hz), 7.70–7.76 (m, 4H), 11.37 (s, 1H). ESMS m/z 458 (MH^+).

2-(2,6-Dichlorophenylamino)-1,6-dimethyl-7-vinyl-1,8-dihydroimidazo[4,5-*h*]isoquinoline-9-one (32). To a suspension of **28** (100 mg, 0.25 mmol) in THF (5 mL) was added trimethylsilylmethylmagnesium chloride (2 mL, 2 mmol) at −78 °C. The reaction mixture was warmed to room temperature for 1 h, cooled to 0 °C, quenched with water, and extracted with EtOAc to provide the silyl alcohol (85 mg, 70%). The crude silyl alcohol was suspended in CH_2Cl_2 and cooled to 0 °C. Boron trifluoride etherate (42 μL, 0.32 mmol) was added, and the slurry was warmed to room temperature for 1 h. The reaction mixture was quenched with water, and the CH_2Cl_2 was removed in vacuo. Collection of the resulting solid followed by CH_2Cl_2 trituration provided 17 mg (61%) of the title compound. Mp >300 °C. ^{1}H NMR (DMSO-d_6, TFA, 400 MHz): δ 2.34 (s, 3H), 4.14 (s, 3H), 5.52 (1H, J = 8 Hz), 6.13 (d, 1H, J = 8 Hz), 7.69 (d, 1H, J = 8 Hz), 7.9 (bs, 1H), 7.67 (bs, 4H), 11.1 (s, 1H). ESMS m/z 399, 401 (MH^+).

2-(2,6-Dichlorophenylamino)-1,6-dimethyl-7-ethyl-1,8-dihydroimidazo[4,5-*h*]isoquinoline-9-one (42). 32 (50 mg, 0.13 mmol) was suspended in 3 mL of acetic acid and 3 mL of EtOH. PtO_2 (6 mg, 0.03 mmol) was added, and the reaction mixture was stirred under 1 atm of H_2(g) for 1 h. The reaction mixture was filtered, concentrated, and extracted with EtOAc. Column chromatography (0–10% MeOH/CH_2Cl_2) provided 25 mg (52%) of the title compound. Mp >300 °C. ^{1}H NMR (DMSO-d_6, TFA, 400 MHz): δ 1.14 (t, 3H, J = 6 Hz), 2.27 (s, 3H), 2.61 (q, 2H, J = 6 Hz), 4.24 (s, 3H), 7.75 (t, 1H, J = 8 Hz), 7.70 (s, 2H), 7.76 (d, 2H, J = 8 Hz), 11.42 (s, 1H). ESMS m/z 401 (MH^+). Anal. ($C_{20}H_{18}Cl_2N_4O \cdot 1.5H_2O$) C, H, N.

2-(2,6-Dichlorophenylamino)-1,6-dimethyl-7-(3-hydroxypropen-1-yl)-1,8-dihydroimidazo[4,5-*h*]isoquinolin-9-one (38). A suspension of **36** (100 mg, 0.22 mmol) in THF (7 mL) was cooled to −78 °C. Sodium bis(trimethylsilyl)amide (1 M in THF, 0.44 mmol) was added dropwise. The bright-red solution was warmed to 0 °C for 15 min. Then lithium aluminum hydride (1 M in THF, 2.6 mmol) was added, and the orange solution was then warmed to room temperature for 0.5 h. The mixture was cooled to 0 °C, quenched with saturated ammonium chloride, and extracted with EtOAc. Column chromatography (3–6% MeOH/CH_2Cl_2) provided 32 mg (34%) of the title compound. Mp 298–300 °C. ^{1}H NMR (DMSO-d_6, TFA, 400 MHz): δ 2.32 (s, 3H), 4.16 (s, 2H), 4.19 (s, 3H), 6.63 (d, 1H, J = 8 Hz), 6.82 (d, 1H, J = 8 Hz), 7.42 (bs, 1H), 7.64–7.68 (m, 4H), 10.92 (s, 1H). ESMS m/z 429, 431 (MH^+).

2-(2,6-Dichlorophenylamino)-7-(1-acetoxyprop-3-en-1-yl)-1,6-dimethyl-1,8-dihydroimidazo[4,5-*h*]isoquinolin-9-one (33). To a solution of **31** (106 mg, 0.25 mmol) in THF (1 mL) was added acetic anhydride (1 mL). Triethylamine (35 μL, 0.25 mmol) was added, and the reaction mixture was stirred for 14 h and then concentrated in vacuo. Column chromatography (2% MeOH/CH_2Cl_2) provided 85 mg (79%) of the title compound. Mp 169–171 °C. ^{1}H NMR (MeOH-d_4, 400 MHz): δ 2.16 (s, 3H), 2.40 (s, 3H), 4.18 (s, 3H), 5.34–5.48 (m, 2H), 6.08–6.16 (m, 1H), 6.55 (s, 1H), 7.27 (bs, 1H), 7.58 (d, 2H, J = 8 Hz), 7.59 (d, 1H, J = 8 Hz), 7.68 (bs, 1H). ESMS m/z 471 (MH^+).

2-(2,6-Dichlorophenylamino)-1,6-dimethyl-7-(3-morpholin-4-yl-propen-1-yl)-1,8-dihydroimidazo[4,5-*h*]isoquinolin-9-one (34). Tris(dibenzylideneacetone)dipalladium-(0) (1.8 mg, 0.002 mmol) and triphenylphosphine (1.6 mg, 0.006 mmol) were stirred in THF (0.5 mL) for 20 min under inert atmosphere until the red solution turned yellow. To this solution was added sequentially **33** (20 mg, 0.04 mmol) in THF (0.5 mL), triethylamine (17 μL, 0.12 mmol), and morpholine (11 μL, 0.12 mmol). The solution was stirred for 14 h and then concentrated to an oil. Column chromatography (10% MeOH/CH_2Cl_2) provided 10 mg (50%) of the title compound. Mp 175–177 °C. ^{1}H NMR (DMSO-d_6, TFA, 400 MHz): δ 2.35 (s, 3H), 3.16 (t, 2H, J = 12 Hz), 3.48 (d, 2H, J = 12 Hz), 3.66 (t, 2H, J = 12 Hz), 4.02 (d, 4H, J = 7 Hz), 4.24 (s, 3H), 6.47 (dt, 1H, J = 8, 16 Hz), 7.15 (d, 1H, J = 16 Hz), 7.58 (dd, 1H, J = 8, 9 Hz), 7.74–7.77 (m, 3H), 7.82 (d, 1H, J = 9 Hz). ESMS m/z 498 (MH^+).

7-(3-Aminopropen-1-yl)-2-(2,6-dichlorophenylamino)-1,6-dimethyl-1,8-dihydroimidazo[4,5-*h*]isoquinolin-9-one (35). A suspension of tris(dibenzylideneacetone)dipalladium(0) (185 mg, 0.25 mmol) and triphenylphosphine (320 mg, 1.2 mmol) in THF (40 mL) was stirred for 20 min under N_2. A solution of **33** (1.88 g, 4.0 mmol) in THF (5 mL) was added, and the mixture was stirred for 20 min. Sodium azide (280 mg, 4.4 mmol) and water (4.0 mL) were added, and the reaction mixture was heated at 60 °C for 3 h. The solution was cooled to room temperature, and triphenylphosphine (1.0 g, 3.8 mmol) was added. After the mixture was stirred for 45 min, ammonium hydroxide (4 mL) was added and stirring continued overnight. The resulting solution was dried over $MgSO_4$ and then concentrated to an oil. Column chromatography on silica eluting with CH_2Cl_2/MeOH (90:10 increasing to 50:50) provided 1.2 g (70%) of the title compound. Mp >300 °C. ^{1}H NMR (DMSO-d_6, TFA, 400 MHz): δ 2.35 (s, 3H), 3.68 (bs, 2H), 4.23 (s, 3H), 6.45–6.60 (m, 1H), 6.90–7.00 (m, 1H), 7.55–7.65 (m, 1H), 7.70–7.85 (m, 4H), 8.05–8.20 (m, 1H). ESMS m/z 428 (MH^+).

2-(2,6-Dichlorophenylamino)-1,6-dimethyl-7-(3-(ethylamino)propenyl)-1,8-dihydroimidazo[4,5-*h*]isoquinolin-9-one (39). A solution of **35** (100 mg, 0.234 mmol) in acetic acid (1 mL) was cooled to −10 °C. Sodium triacetoxyborohydride (87 mg, 0.410 mmol) was added, and the mixture was stirred for 20 min at −10 °C. Acetaldehyde (10 mg, 0.234 mmol) was taken up in THF (3 mL) and added dropwise to the reaction mixture (at −10 °C). Once all the aldehyde had been added, the reaction mixture was warmed to room temperature and was stirred overnight. The crude reaction mixture was diluted with EtOAc (10 mL), washed with water (5 mL), dried ($MgSO_4$), and concentrated under reduced pressure. Chromatography [CH_2Cl_2/MeOH/NH_4OH (9:1:0.1)] afforded 28 mg (26%) of the title compound. Mp 218–221 °C. ^{1}H NMR ($CDCl_3$, 400 MHz): δ 1.15–1.25 (m, 3H), 2.33 (s, 3H), 3.03–3.13 (m, 2H), 3.80 (bs, 2H), 4.21 (s, 3H), 6.45–6.60 (m, 1H), 7.09 (d, 1H, J = 15 Hz), 7.55 (t, 1H, J = 8 Hz), 7.7–7.9 (m, 4H).

2-(2,6-Dichlorophenylamino)-7-(3-diethylaminopropenyl)-1,6-dimethyl-1,8-dihydroimidazo[4,5-*h*]isoquinolin-9-one (43). 43 was prepared as described above. ^{1}H NMR (DMSO-d_6, TFA, 400 MHz): δ 1.27 (t, 6H, J = 7.0 Hz), 2.38 (s, 3H), 3.04–3.40 (m, 4H), 4.01 (d, 2H, J = 7 Hz), 4.26 (s, 3H), 6.54 (dt, 1H, J = 7, 16 Hz), 7.26 (d, 1H, J = 16 Hz), 7.60 (t, 1H, J = 8 Hz), 7.78 (d, 3H, J = 8 Hz), 7.84 (d, 1H, J = 9 Hz).

2-(2,6-Dichlorophenylamino)-1,6-dimethyl-7-(3-pyrrolidin-1-ylpropenyl)-1,8-dihydroimidazo[4,5-*h*]isoquinolin-9-one (44). 44 was prepared as described above. ^{1}H NMR (DMSO-d_6, TFA, 400 MHz): δ 1.91 (br, 2H), 2.06 (br, 2H), 2.38 (s, 3H), 3.11 (br, 2H), 3.59 (br, 2H), 4.04 (d, 2H, J = 7 Hz), 4.26 (s, 3H), 6.55 (dt, 1H, J = 7, 15 Hz), 7.16 (d, 1H, J = 15

Hz), 7.60 (dd, 1H, J = 8, 8 Hz), 7.78 (d, 3H, J = 8 Hz), 7.84 (d, 1H, J = 8 Hz). Anal. ($C_{25}H_{25}Cl_2N_5O_1 \cdot 0.2H_2O$) C, H, N.

2-(2,6-Dichlorophenylamino)-1,6-dimethyl-7-[3-(benzylmethylamino)propenyl]-1,8-dihydroimidazo[4,5-*h*]isoquinolin-9-one (45). **45** was prepared as described above. ^{1}H NMR (DMSO-d_6, TFA, 400 MHz): δ 2.38 (s, 3H), 2.76 (s, 3H), 3.81−4.10 (m, 2H), 4.27 (s, 3H), 4.31 (d, 1H, J = 13 Hz), 4.51 (d, 1H, J = 15 Hz), 6.62 (dt, 1H, J = 7, 15 Hz), 7.20 (d, 1H, J = 16 Hz), 7.40−7.67 (m, 6H), 7.71−7.92 (m, 3H), 7.85 (d, 1H, J = 8 Hz). Anal. ($C_{29}H_{27}Cl_2N_5O_1 \cdot 0.1H_2O$) C, H, N.

2-(2,6-Dichlorophenylamino)-1,6-dimethyl-7-(3-dimethylaminopropenyl]-1,8-dihydroimidazo[4,5-*h*]isoquinolin-9-one (46). **46** was prepared as described above. ^{1}H NMR (DMSO-d_6, TFA, 400 MHz): δ 2.37 (s, 3H), 2.85 (s, 6H), 3.96 (d, 2H, J = 7 Hz), 4.26 (s, 3H), 6.52 (dt, 1H, J = 7, 15 Hz), 7.16 (d, 1H, J = 15 Hz), 7.60 (t, 1H, J = 8 Hz), 7.77 (d, 3H, J = 8 Hz), 7.84 (d, 1H, J = 9.0 Hz). Anal. ($C_{23}H_{23}Cl_2N_5O_1 \cdot 0.2H_2O$) C, H, N.

2-(2,6-Dichlorophenylamino)-1,7-dimethyl-6-(2-hydroxyethyl)-1,8-dihydroimidazo[4,5-*h*]isoquinoline-9-one (54). To a stirred solution of 2-(2,6-dichlorophenylamino)-1,7-dimethyl-9-oxo-1,8-dihydroimidazo[4,5-*h*]isoquinolin-6-ylacetic acid ethyl ester (25 mg, 0.05 mmol) in THF (2 mL) was added a solution of lithium aluminum hydride (1 M in THF, 0.25 mL, 0.25 mmol). The mixture was stirred for 30 min at room temperature. EtOAc was added, followed by water, and then the mixture was acidified with 1 N HCl. The crude product was applied to a Varian SCX cartridge and washed in turn with 1 N HCl, water, acetone, MeOH, and MeOH/CH_2Cl_2 (1:1). The product was then eluted with MeOH/CH_2Cl_2/NH_4OH (49:49:2). Evaporation of the eluent provided 15 mg (72%) of the title compound. Mp >300 °C. ^{1}H NMR (TFA-d_6, 400 MHz): δ 2.76 (s, 3H), 3.49 (br, 2H), 4.22 (br, 2H), 4.45 (s, 3H), 7.55 (t, 1H, J = 8 Hz), 7.68 (d, 2H, J = 8 Hz), 8.04 (d, 1H, J = 9 Hz), 8.19 (d, 1H, J = 9 Hz). ESMS m/z 417, 419 (MH^+). Anal. ($C_{20}H_{18}Cl_2N_4O_3 \cdot 1.5H_2O$) C, H, N.

Tyrosine Kinase Inhibition Assay. The kinase activity is measured using DELFIA (dissociation enhanced lanthanide fluoroimmunoassay), which utilizes europium chelate-labeled anti-phosphotyrosine antibodies to detect phosphate transfer to a random polymer, poly-Glu_4-Tyr_1 (PGTYR). The kinase assay is performed in a neutravidin-coated 96-well white plate (PIERCE) in kinase assay buffer (50 mM HEPES, pH 7.0, 25 mM $MgCl_2$, 5 mM $MnCl_2$, 50 mM KCl, 100 μM Na_3VO_4, 0.2% BSA, 0.01% CHAPS). Test samples initially dissolved in DMSO at 1 mg/mL are prediluted for dose response (10 doses with starting final concentration of 1 μg/mL, 1−3.5 serial dilutions) with the assay buffer. A 25 μL aliquot of this diluted sample and a 25 μL aliquot of diluted enzyme (0.8 nM final concentration) are sequentially added to each well. The reaction is started with a 50 μL/well of a mixture of substrates containing 2 μM ATP (final ATP concentration is 1 μM) and 7.2 ng/μL PGTYR-biotin (CIS Biointernational) in kinase buffer. Background wells are incubated with buffer and substrates only. Following 45 min of incubation at room temperature, the assay plate is washed three times with 300 μL/well DELFIA wash buffer. A 100 μL/well aliquot of europium-labeled anti-phosphotyrosine (Eu^{3+}-PT66, 1 nM, Wallac CR04-100) diluted in DELFIA assay buffer is added to each well and incubated for 30 min at room temperature. Upon completion of the incubation, the plate is washed four times with 300 μL/well of wash buffer and 100 μL/well of DELFIA wash buffer. Enhancement solution (Wallac) is added to each well. After 15 min, time-resolved fluorescence is measured on the LJL's analyst (excitation at 360 nm, emission at 620 nm, EU 400 dichroic mirror) after a delay time of 250 μs.

Calcium Release in Jurkat Cells. 1. Loading of Jurkat Cells with Fluo-3. Jurkat cells were pelleted, washed 2 times with RPMI, 10 mM HEPES, and 10% fetal bovine serum (complete media), and then resuspended at 2 × 10^7 cells/mL in the above. Fluo-3 solution was prepared from 40 μL of Fluo-3 stock AM (Molecular Probes catalog no. F-1242) (4 μM), 180 μL of pluronic F127 detergent (Molecular Probes catalog no. P-3000), and 9.8 mL of complete media. An equal volume of Fluo-3 solution was added to give a 1 × 10^7 cells/mL solution and 2 μM Fluo-3. The tube was wrapped in foil and incubated at room temperature with very gentle rocking for 45 min. Additional media to fill a 50 mL tube was added, and it was incubated another 15 min at room temperature.

Cells were pelleted and washed three times with Hanks' balanced salt solution (HBSS) (GibcoBRL no. 14175-095), containing 1 mM $CaCl_2$, 1 mM $MgCl_2$, 10 mM HEPES, 2 mM probenecid, and 1% fetal bovine serum (FBS), pH 7.4. Finally, cells were resuspended at 2 × 10^7 cells/mL and kept on ice and in the dark until ready for use.

Compounds were made up as 5 mg/mL stocks in DMSO and diluted as appropriate with the following diluent: HBSS, 1 mM $CaCl_2$, 1 mM $MgCl_2$, 10 mM HEPES, pH 7.4, 2 mM probenecid, 1% FBS. A 96-well V-bottom plate is used for the compound dilutions.

2. Stimulus Plate. Anti-CD3 (Immunotech, clone X35, catalog no. 0178) was prepared by taking 69 μL of a 200 μg/mL stock into 11 mL of diluent to give a 5× stock for a final test concentration of 0.25 μg/mL. Then 100 μL was added per well of V-bottom 96-well plate.

3. Cell Plate Preparation. An amount of 2 mL of loaded cell suspension was mixed with 18 mL of diluent, and 150 μL of this mixture was then added per well of a 96-well Black Packard viewplate for a final cell number of 3 × 10^5/mL. The plate was then centrifuged at 1500 rpm for 5 min at room temperature and immediately placed in the center position in the drawer of an FLIPR (fluorometric imaging plate reader).

4. Assay. The assay was performed on the FLIPR system (Molecular Devices). All experiments were run at room temperature. The cell plate was placed in the center position in the drawer. The compound dilution plate was placed in the left position and the stimulus plate in the right. An amount of 50 μL of compound was added to the cells, and this was incubated at room temperature for 15 min. An amount of 50 μL of anti-CD3 was added to the cell plate, and fluorescence intensity was monitored for an additional 13 min.

5. Analysis. Calcium release was measured by fluorescence intensity via a SAS program that measures the difference between baseline values and peak height. These values are plotted versus compound concentration to obtain an EC_{50} value. A decrease in fluorescence intensity indicated inhibition of the release of calcium by the compound being tested.

Inhibition of IL-2 Production. The 96-well flat bottom plates were coated with anti-CD3 and clone UCHT1 (Immunotech catalog no. 1304) at 4 μg/mL in phosphate-buffered saline (PBS), 100 μL/well. The solution was prepared by taking 200 μL of 200 μg/mL anti-CD3 stock/10 mL PBS. The plate was then incubated at 37 °C for 2 h. Jurkat cells were pelleted and counted. The cells were resuspended at 2.5 × 10^6 cells/mL in RPMI and 10% FBS (complete media). Test compounds were diluted from a 5 mg/mL DMSO stock directly into complete media.

An amount of 10 μL of 20 X compound per well was added to a separate plate, followed by 100 μL of cell suspension in triplicate, and this plate was preincubated at 37 °C for 30 min. The 96-well plate containing anti-CD3 was aspirated, and the cells and compound were transferred to this plate. An amount of 100 μL of PMA (phorbol 12-myristate 13-acetate, Sigma catalog no. P-8139) at 20 ng/mL was added, and the plate was incubated overnight at 37 °C. (PMA stock at 1 mg/mL in ethanol, diluted 10 μL/mL in complete media, then 20 μL/10 mL in complete media; 100 μL/well = 10 ng/mL, final concentration). The next day, the plate was centrifuged at 1500 rpm for 5 min at room temperature and the supernatants were removed. The supernatants were tested using R&D Systems Quantikine Human IL-2 Kit (catalog no. 2050). Samples were diluted 1:5 in RPMI 1640, and 100 μL/well was used in the ELISA. The optical density of each well was determined using a microplate reader set to 450 nm. EC_{50} values were determined using Origin (nonlinear regression) or SAS by plotting absorbance vs concentration of compound.

Inhibition of IL-2 Production in Human Whole Blood. Human whole blood was obtained from in-house donors by venipuncture collected into 25 mL heparinized Vacu-tainer tubes.

Test compounds were dissolved in DMSO to yield 5 mg/mL stock solutions. Stock solutions were freshly diluted in RPMI 1640 and 10% fetal bovine serum (complete media) to yield solutions that were 10 times the final assay concentration. Compounds were diluted serially into complete media.

SEB Solution. Staphylococcal enterotoxin B was dissolved in PBS to yield a 2.5 mg/mL stock. This is further diluted in complete media to yield a 3000 ng/mL solution (10 times the final assay concentration). SEB stock solution is stored at 4 °C.

Assay Procedure. Add 20 μL of 10× compound dilutions, in triplicate, to wells of a U bottom 96-well plate. For "no compound" samples, add 20 μL of complete media. Also, dilute DMSO to the highest concentration used in the assay and use 20 μL/well as controls. Add 160 μL of whole human blood to each well and incubate plate for 20−30 min at 37 °C. Add 20 μL of 10x SEB solution to all test wells and to stimulated control wells. Add 20 μL of complete media to nonstimulated wells as controls. Incubate plate overnight at 37 °C. The next day, centrifuge plate at 2000 rpm for 10 min at room temperature and transfer supernatants to a fresh plate. Dilute supernatants 1:5 in RPMI 1640 and then use 100 μL/well in R&D Systems Quantikine Human IL-2 Kit.

Follow the ELISA procedure as outlined in the section "Inhibition of IL-2 Production" in Jurkat cells protocol.

1. Analysis. EC_{50} values are determined using Origin (nonlinear regression) or SAS (Secondary Screening Program, EC_{50} calculation) by plotting absorbance vs actual concentration of the compound.

2. In Vivo Anti-CD3 Assay. Female BALB/c mice (Charles River, The Jackson Laboratories) were used for anti-CD3 studies. Animals were numbered by tail tattoo and were 6−8 weeks old at the initiation of experiments. For the induction of IL-2 in vivo by anti-CD3, 1 μg of anti-CD3 (monoclonal hamster−antimouse 145-2C11, lot M03283) in 200 μL of PBS was injected intraperitoneally (ip) into experimental mice to stimulate the polyclonal activation of T cells. Upon activation, these T cells produced the T cell cytokine IL-2 that was detected in the plasma.

For the measurement of plasma cytokine levels, 3 h after anti-CD3 injection, each mouse was anesthetized with isoflurane, and approximately 0.5 mL of whole blood was collected in heparinized tubes following cardiac puncture. Plasma IL-2 levels were determined by ELISA (R&D Systems, Minneapolis MN) of 1:10 dilutions of samples. Levels were quantitated by linear regression analysis of samples in comparison to a recombinant cytokine IL-2 curve, and plasma levels in vehicle-treated groups were 1900−2800 pg/mL in each experiment.

3. Treatment Groups. All doses of compounds and controls are represented as milligram of compound per kilogram of body mass and were administered orally in 100 μL of vehicle, 30% Cremophor. The compound was administered to mice ($n = 8$ per group) 1 h prior to anti-CD3 injection. Control mice received either 100 μL of vehicle alone (negative control) or 30 mg/kg cyclosporin A (positive control).

References

(1) Levitzki, A. Protein tyrosine kinase inhibitors as therapeutic agents. *Top. Curr. Chem.* **2001**, *211*, 1−15.

(2) Longati, P.; Comoglio, P. M.; Bardelli, A. Receptor tyrosine kinases as therapeutic targets: the model of the MET oncogene. *Curr. Drug Targets* **2001**, *2*, 41−55.

(3) Qian, D.; Weiss, A. T cell antigen receptor signal transduction. *Curr. Opin. Cell Biol.* **1997**, *9*, 205−211.

(4) Snow, R. J.; Cardozo, M. G.; Morwick, T. M.; Busacca, C. A.; Dong, Y.; Eckner, R. J.; Jakes, S.; Kapadia, S.; Lukas, S.; Moss, N.; Panzenbeck, M.; Peet, G. W.; Peterson, J. D.; Prokopowicz, A. P.; Sellati, R.; Tschantz, M. A. The Discovery of 2-Phenylamino-imidazo[4,5-*h*]isoquinolin-9-ones, a New Class of Inhibitors of Lck Kinase. *J. Med. Chem.* **2002**, *45*, 3394−3405.

(5) Straus, D. B.; Weiss, A. Genetic Evidence for the Involvement of the Lck Tyrosine Kinase in Signal Transduction through the Cell Antigen Receptor. *Cell* **1992**, *70*, 585−593.

(6) Yamasaki, S.; Masako, T.; Iwashima, M. The kinase, SH3, and SH2 domains of Lck play critical roles in T-cell activation after ZAP-70 membrane localization. *Mol. Cell. Biol.* **1996**, *16*, 7151−7160.

(7) Hanke, J. H.; Pollok, B. A.; Changelian, P. S. Role of tyrosine kinases in lymphocyte activation: targets for drug intervention. *Inflammation Res.* **1995**, *44*, 357−371.

(8) Compounds that have been shown to inhibit lck are described in ref 4. Additionally, see the following. (a) Burchat, A. F.; Calderwood, D. J.; Friedman, M. M.; Hirst, G. C.; Li, B.; Rafferty, P.; Ritter, K.; Skinner, B. S. Pyrazolo[3,4-*d*]pyrimidines containing an extended 3-substituent as potent inhibitors of lck-a selectivity insight. *Bioorg. Med. Chem. Lett.* **2002**, *12*, 1687−1690 and references within. (b) Chen, P.; Iwanowicz, E. J.; Norris, D.; Gu, H. H.; Lin, J.; Moquin, R. V.; Das, J.; Wityak, J.; Spergel, S. H.; de Fex, H.; Pang, S.; Pitt, S.; Ren Shen, D.; Schieven, G. L.; Barrish, J. C. Synthesis and SAR of novel imidazoquinoxaline based lck inhibitors: improvement of cell potency. *Bioorg. Med. Chem. Lett.* **2002**, *12*, 3153−3156 and references within.

(9) Weiss, A.; Littman, D. R. Signal transduction by lymphocyte antigen receptors. *Cell* **1994**, *76*, 263−274.

(10) Makni, H.; Malter, J. S.; Reed, J. C.; Nobuhiko, S.; Lang, G.; Kioussis, D.; Trinchieri, G.; Kamoun, M. Reconstitution of an active surface CD2 by DNA transfer in CD2−CD3+ Jurkat cells facilitates CD3-T cell receptor-mediated IL-2 production. *J. Immunol.* **1991**, *146*, 2522−2529.

(11) August, A. Association between mitogen-activated protein kinase and the ζ chain of the T cell receptor (TCR) with the SH2,3 domain of p56lck. Differential regulation by TCR crosslinking. *J. Biol. Chem.* **1996**, *271*, 10054−10059.

(12) Molina, T. J.; Kishihara, K. I.; Siderovski, D. P.; van Ewijk, W.; Narendran, A.; Timms, E.; Wakeham, A.; Paige, C. J.; Hartmann, K.-U.; Veillette, A.; Davidson, D.; Mak, T. W. Profound block in thymocyte development in mice lacking p56lck. *Nature* **1992**, *357*, 161−164.

(13) Sommer, M. B.; Begtrup, M.; Bogeso, K. P. Displacement of halogen of 2-halogeno-substituted benzonitriles with carbanions. Preparation of (2-cyanoaryl)arylacetonitriles. *J. Org. Chem.* **1990**, *55*, 4817−4821.

(14) Snow, R. J.; Butz, T.; Hammach, A.; Kapadia, S.; Morwick, T. M.; Prokopowicz, A. S.; Takahashi, H.; Tan, J. D.; Tschantz, M. A.; Wang, X.-J. Synthesis of isoquinolones by S_NAr reaction: a versatile route to imidazo[4,5-*h*]isoquinolin-9-ones, a new class of kinase inhibitor. *Tetrahedron Lett.* **2002**, *43*, 7553−7556.

(15) Modi, A. R.; Nadkarni, D. R.; Usgaonkar, R. N. Isocoumarins. Part XVIII. Isoquinolones. Part III. 3-Formylisocoumarins, 3-formylisoquinolones, 3-(isocoumarin-3′-yl)- and 3-(isoquinolon-3′-yl)-acrylic acids and related compounds. *Indian J. Chem.* **1979**, *17B*, 624.

(16) Finch, N.; Fitt, J. J.; Hsu, H. S. Total synthesis of DL-9-deoxyprostaglandin E1. *J. Org. Chem.* **1975**, *40*, 206−215.

(17) Furstner, A.; Kollegger, G.; Weidmann, H. Selective formation of alkenes from trimethylsilyl ketones and from acylsilanes. *J. Organomet. Chem.* **1991**, *414*, 295−305.

(18) (a) Overman, L. E.; Knowll, F. M. Palladium(II)-catalyzed rearrangement of allylic acetates. *Tetrahedron Lett.* **1979**, *4*, 321−324. (b) Nikaido, M.; Aslanian, R.; Scavo, F.; Helquist, P.; Akermark, B.; Backvall, J. E. Direct preparation of 5-amino-1,3-pentadienes through use of palladium-promoted reactions. *J. Org. Chem.* **1984**, *49*, 4738−4740.

(19) During the course of our work, two crystal structures of the catalytic domain of lck in its active state were published. The results did not change any of the conclusions drawn from our initial model with hck. (a) Yamaguchi, H.; Hendrickson, W. A. Structural basis for activation of human lymphocyte kinase Lck upon tyrosine phosphorylation. *Nature* **1996**, *384*, 484−489. (b) Zhu, X.; Kim, J. L.; Newcomb, J. R.; Rose, P. E.; Stover, D. R.; Toledo, L. M.; Zhao, H.; Morgenstern, K. A. Structural analysis of the lymphocyte-specific kinase Lck in complex with non-selective and Src family selective kinase inhibitors. *Structure* **1999**, *7*, 651−661.

JM020446L

Lck inhibitors as a therapeutic approach to autoimmune disease and transplant rejection

Joanne S Kamens*, Sheldon E Ratnofsky & Gavin C Hirst

Address
Abbott Bioresearch Center
100 Research Drive
Worcester
MA 01605
USA
*Email: joanne.niewood@abbott.com

*To whom correspondence should be addressed

Current Opinion in Investigational Drugs 2001 2(9):1213-1219
 ISSN 1472-4472

T-cells play an important role in the pathogenesis of many diseases. These include diseases with large commercial markets and also with significant unmet medical needs, such as rheumatoid arthritis and asthma in addition to those with smaller markets such as organ transplantation, multiple sclerosis, inflammatory bowel diseases, type 1 diabetes, systemic lupus erythematosus and psoriasis. The use of currently available immunomodulatory agents is often limited by the appearance of dose-limiting side effects that result from the actions of these agents on non-lymphoid tissues. LSTRA cell kinase (lck), one of eight known members of the human src family of non-transmembrane protein tyrosine kinases, has a pivotal role in T-cell signaling. Lck expression is restricted to lymphoid cells, so an lck-selective inhibitor would be expected to have a significantly improved safety profile for the treatment of T-cell-driven diseases.

Keywords Autoimmune disease, cyclosporin A, immunosuppression, lck inhibitor, src kinase, T-cell signaling, transplantation, tyrosine kinase

Role of lck in T-cell signaling

Six of the src family kinases have a role in signal transduction pathways in lymphocytes, monocytes or granulocytes (lck, lyn, fyn, hck, fgr and blk). Lck expression is restricted to T-cells and NK cells, but some family members (src, yes and fyn) have widespread expression patterns [1]. Src family kinases all consist of a unique N_t domain followed by SH3, SH2, catalytic, and C_t tail regulatory domains [2]. Myristoylation and palmitoylation of the unique region directs lck to the plasma membrane and a cysteine-containing motif in this region enables association with the CD4 or CD8 co-receptors. The SH3 and SH2 protein-protein interaction modules facilitate binding of lck to proline-rich sequences (SH3) or phosphotyrosine-containing motifs (SH2). Lck catalytic activity is regulated by tyrosine phosphorylation at two sites: phosphorylation of a tyrosine in the activation loop of the catalytic domain promotes activation of lck. Phosphorylation of a C_t tyrosine promotes a downregulatory, intramolecular interaction between the C_t tail and the SH2 domain [3]. Studies with cell lines that lack expression of lck or express mutant forms of the protein have demonstrated the crucial role of lck at a proximal point in the T-cell receptor (TCR) signaling pathway [4•]. Productive T-cell activation is characterized by the appearance of a hyperphosphorylated ζ-chain and by phosphorylation and catalytic activation of the syk family ZAP-70 kinase by lck (Figure 1) [5,6].

Initial efforts to elucidate the biology of lck in primary tissue involved the targeted disruption of the *lck* gene to generate a lck knockout mouse [7•]. Mice lacking lck have diminished thymic cellularity (5 to 10% of wild-type), with most resultant thymocytes failing to make the transition to the CD4, CD8 double positive state and few of these are able to make the next transition to the single positive state. NK cell function appears to be unaffected. The block in T-cell development observed in these mice precluded evaluation of mature peripheral T-cell function in the absence of lck. To circumvent this, a tetracycline-based system was developed which allows for positive and negative regulation of lck expression in T-cells in the presence or absence of doxycycline [8,9]. In these transgenic mice, thymic atrophy was observed due to downregulation of lck expression after removal of doxycycline from the drinking water. In contrast to the thymus, the cellularity of lymph nodes does not decrease in the absence of lck expression. Long-term survival of the T-cells is not impaired in the absence of lck, but these cells are incapable of proliferating when transferred into lethally irradiated hosts. Consistent with this observation, the peripheral T-cells from these animals were also defective in their ability to propagate TCR proximal signaling events when lck expression was turned off. Thus, lck was shown to be necessary for T-cell signaling and homeostasis but not cell survival in the periphery, supporting the validity of lck as a target for immunosuppressive therapy. Corroborating the murine studies, there has been one report of an infant with a severe combined immunodeficiency demonstrated to be the result of profoundly diminished, but not totally deficient lck expression [10].

T-cell inhibitors in the prevention of transplant rejection

During the past 25 years, organ transplantation has become a widespread remedy for life-threatening situations involving diseased organs. Graft rejection following transplant surgery results from the recognition of allogeneic or xenogeneic histocompatibility antigens expressed on the graft by the host immune system. T-cells are the key mediators of these immune system assaults [11]. Cyclosporin A (CsA), currently the leading clinical agent for the treatment of graft rejection, binds to cyclophilin in the cytosol and this complex inhibits the catalytic function of calcineurin, a phosphatase that plays a key role in signal transduction from the TCR to the nucleus [12]. Calcineurin is ubiquitously expressed and is involved in the transduction of signals in tissues other than the T-cell. As a result, CsA suffers from a propensity to cause dose-limiting kidney failure, liver damage and neuropathy and has a small therapeutic index. Other agents currently approved for use in these indications also have significant side effects associated with chronic use. These include nephrotoxicity and hyperlipidemia with sirolimus (Wyeth-Ayerst Laboratories), bone marrow suppression with mycophenolate mofetil (Roche Holding AG) and azathioprine, hepatotoxicity with methotrexate and leflunomide (Aventis

Figure 1. The role of lck in TCR signal transduction.

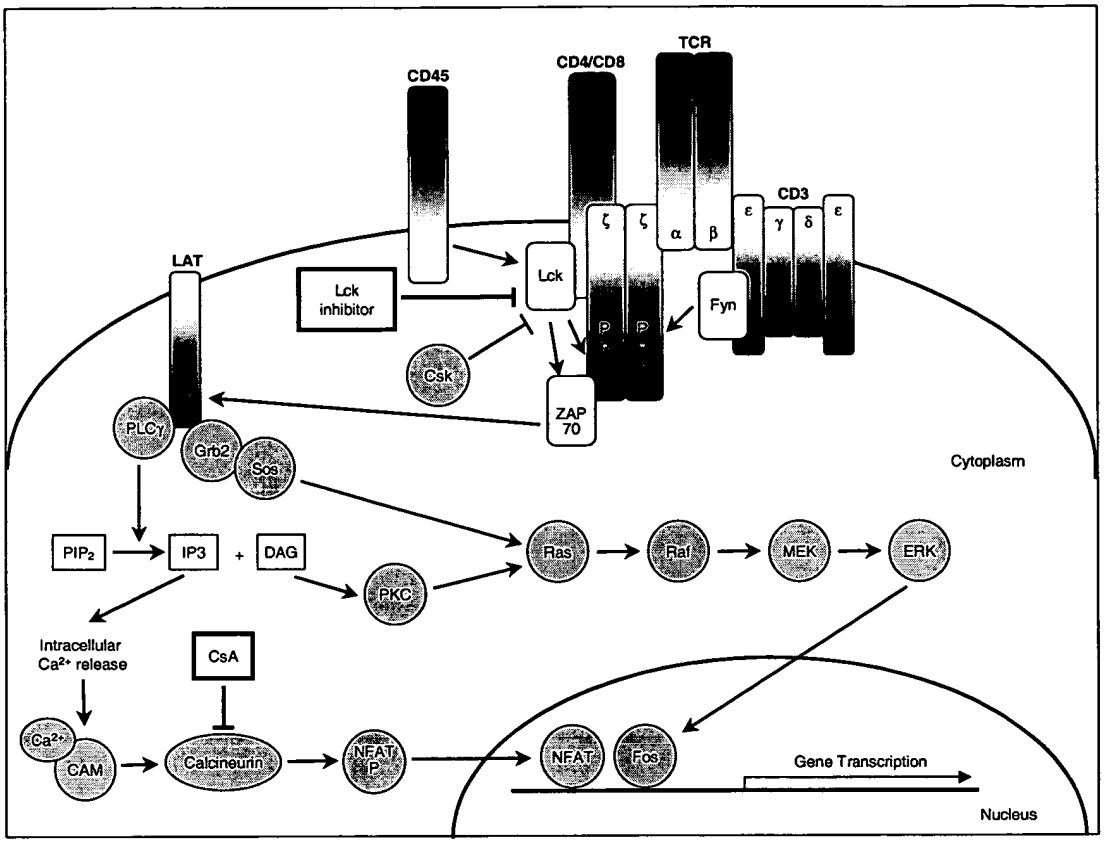

Lck associates non-covalently with the CD4 and CD8 co-receptors. The src family kinase, fyn associates with the TCR/CD3 complex and plays a subordinate role to lck in this signaling pathway. Lck and fyn are regulated positively by the dephosphorylation of a C_t tyrosine by the CD45 phosphatase and negatively by the phosphorylation of that tyrosine by csk. Association of the T-cell and the antigen-presenting cell leads to juxtaposition of lck with its substrates, the TCR/CD3 complex and the ζ-chain. These phosphorylation events generate docking sites for ZAP-70 which itself must be phosphorylated by lck in order to be catalytically competent. ZAP-70 kinases multiple substrates, generating second messengers and the assembly of multimolecular complexes that activate several pathways. Activation of ras triggers the MAP kinase cascade resulting in increased transcription of fos, a component of the transcription factor AP-1. Translocation of PLCγ1 to phosphorylated LAT brings it into proximity with PIP_2 leading to the generation of IP_3 and DAG. IP_3 signals the release of calcium from intracellular stores and DAG is an essential factor for the activation of PKC. The rise in intracellular calcium levels activates both PKC and the calcium/calmodulin (CAM)-dependent phosphatase calcineurin. These pathways result in the activation of transcription factors and increased transcription of the genes regulated by these factors. The action of CsA is downstream of lck opening the possibility for combination therapy with lck inhibitors in protocols that would spare the concentration of either drug.

Pharma AG), and osteoporosis and metabolic side effects with glucocorticoids. The molecular targets of these agents are also broadly distributed, and the major adverse effects are due to their actions on non-T-cells. Although a high level of immunosuppression is required immediately following organ transplantation to prevent acute organ rejection, patients require life-long immunosuppressive therapy with lower 'maintenance' doses of drugs to prevent chronic organ rejection. There is a constant need to balance the beneficial effects with the threat of toxic side effects, infections and malignancies. An lck inhibitor would target only lymphoid cells since the molecular target expression is restricted to these cells.

T-cell inhibitors and autoimmune disease

A breakdown in self-tolerance can result in the immune system raising an attack against 'self' leading to autoimmune disease. T-cell inhibitors that have been used to treat graft rejection are also efficacious in the treatment of chronic autoimmune inflammatory diseases that are thought to be T-cell-dependent. Of the prevalent autoimmune diseases, development and progression of autoimmune skin diseases, psoriasis in particular, are most clearly dependent on activated T-cells. Psoriasis is a skin disease in which keratinocyte proliferation is initiated by T-cell infiltration and activation [13]. Although CsA has been used successfully in the treatment of psoriasis, in most cases the physician must weigh the risk of side effects with the need for treatment based on the severity of the disease. Similarly, while CsA was efficacious in controlled trials for the treatment of systemic lupus erythematosus (SLE) and inflammatory bowel diseases (IBDs), its use is frequently associated with side effects of which nephropathy and hypertension are the most common [14-16,17•]. These results suggest that an lck-selective inhibitor with improved safety characteristics could offer an effective treatment for psoriasis, IBDs and SLE.

Evidence for a causal role for T-cells in the pathophysiology of other immune diseases is less conclusive. Disease induction in murine experimental autoimmune encephalomyelitis, a model of multiple sclerosis (MS) requires activated T-cells and can be induced in naive animals by the transfer of T-cell clones specific for encephalitogenic antigens [18]. In humans, the increased relative risk of individuals who are HLADR2 positive implies a role for T-cells in the initiation of the disease [19]. Additionally, the presence of T-cells in the inflammatory infiltrate in the white matter of MS patients and the exacerbation of disease by Th1 cytokines in murine models suggests a prominent role for T-cells in the inflammatory process that is a hallmark of the disease [20]. Animal models and human studies strongly suggest that T-cells are a necessary driver in the onset of type I diabetes, although there is no evidence that T-cell inhibitors will be advantageous once islet cell destruction is complete. It has been observed that peripheral T-cell activation in response to TCR stimulation is actually reduced in type 1 diabetic patients [21,22]. One study demonstrates a correlation between T-cell hyporesponsiveness and reduced levels of lck in a cohort of patients with type 1 diabetes, supporting the hypothesis that an inhibitor leading to reduced lck activity might not be useful for the treatment of active diabetes [23].

The role of T-cells in the pathogenesis of rheumatoid arthritis (RA) and in related diseases, such as spondyloarthropathies, continues to be controversial [24•,25•]. The response of RA patients to T-cell directed approaches such as CsA, antibodies to CD4 or IL-2 receptor/diphtheria toxin fusion proteins was modest compared to, for example, anti-tumor necrosis factor (TNF) therapies. While large numbers of T-cells are detected in synovial tissue and fluid of RA patients, there are only low levels of T-cell-derived cytokines - especially in comparison to the high levels of monokines derived from other immune cells in the synovium [26]. Perhaps the best evidence for a pivotal role for T-cell involvement is the fact that RA susceptibility and severity are associated with specific class II MHC alleles. Studies in a TCR transgenic mouse that spontaneously develops a disease with most of the features of human RA suggest that T-cells may be required for disease initiation, but not for maintenance of the condition [27]. On the other hand, it was reported that T-cells may function as regulators of bone physiology via regulation of osteoprotegerin-ligand and this mechanism might offer an explanation for bone loss associated with immune disease [28]. It has been suggested that the evidence as a whole still points to a role for T-cells in both the induction and maintenance of RA and that the role of T-cells in disease maintenance might be obscured by the presence of inhibitory Th2 cytokines [29].

Current development of lck inhibitors

Pfizer's pyrazolopyrimidine derivatives such as PP1 (Figure 2) and PP2 were some of the first src family-selective inhibitors described in the literature. PP1 was reported to have an IC_{50} value of approximately 5 nM and to have micromolar activity in cellular assays [30]. Subsequently, there has been a rich patent literature claiming src family kinase inhibitors (Figure 3), particularly inhibitors of lck, for treatment of immune diseases, and inhibitors of src for treatment of cancer and modulation of bone metabolism [31]. Sequence alignments and modeling studies of the catalytic domains of the src family kinases show that similarity between any two members is > 70%, can be as high as 90% and that the key residues for ATP and substrate binding are highly conserved [32]. Even when comparing src kinase catalytic domains to distantly related kinases there is a very high level of homology, but there are now numerous examples of compounds with good selectivity against non-src kinases. Obtaining inhibitor selectivity within the src family presents a daunting challenge and few examples of significant selectivity have been reported. Recent efforts to overcome this significant selectivity barrier include structural studies of lck in complex with non-selective and src family-selective inhibitors, as well as src kinase mutagenesis studies [33•,34•].

As more is understood about the structural elements and regulatory mechanisms of an increasing number of kinases, another significant hurdle to the identification of potent, selective lck kinase inhibitors (or selective inhibitors of other kinases) has become apparent. While few groups report the activation status of the enzymes used in their *in vitro* assays for establishment of inhibitor activities and selectivity profiles, src family kinases are known to have distinct structures depending on the phosphorylation state of the activation loop [35]. The activation status of an enzyme can have a major effect on potency measurements for some inhibitor series and testing with uncharacterized enzymes can lead to misinterpretation of the compound selectivity profiles. Based on a co-crystal structure of lck in complex with PP1, it was suggested that there may be greater opportunity for obtaining selectivity by targeting compounds to the autoinhibited form of kinases in the src family [32,36]. These structural studies highlight the importance of precise characterizations of screening enzymes. Evaluation of the kinase inhibitor literature is also complicated by the fact that few groups share similar assay conditions especially with regard to concentration of ATP, and this information is often not reported. Since the majority of kinase inhibitors are ATP competitive, variation in this condition can have dramatic effects on IC_{50} values. Additionally, discrepancies between *in vitro* assay activity and cellular activity data would certainly occur if the ATP concentration used for assays with isolated enzymes is not reflective of the concentration of ATP in the target cell. There is evidence that the concentration of ATP in human cells is in the millimolar range [37].

Examples of both of these issues, ie, enzyme activation state and assay conditions, were presented for a series of potent pyrrolopyrimidines (BSF1, BSF2, Figure 2) [38,39•]. Compounds in this series showed lower IC_{50} values (up to 100-fold) when tested *in vitro* with an autoinhibited form of lck, compared to a version of the protein that was phosphorylated on the activation loop and thereby activated. In addition, biological data were presented for assays at two concentrations of ATP. Increasing the ATP concentration from 5 μM to 1 mM has the expected effect of increasing the IC_{50} values of the compounds tested. The *in vitro* potency of representatives from this pyrrolopyrimidine series is reflected both in the nanomolar activity observed in cell-based assays and the activity *in vivo* after oral administration in a murine model of interleukin (IL)-2 production (ED_{50} = 25 mg/kg).

Figure 2. Structures of lck inhibitors from the primary literature.

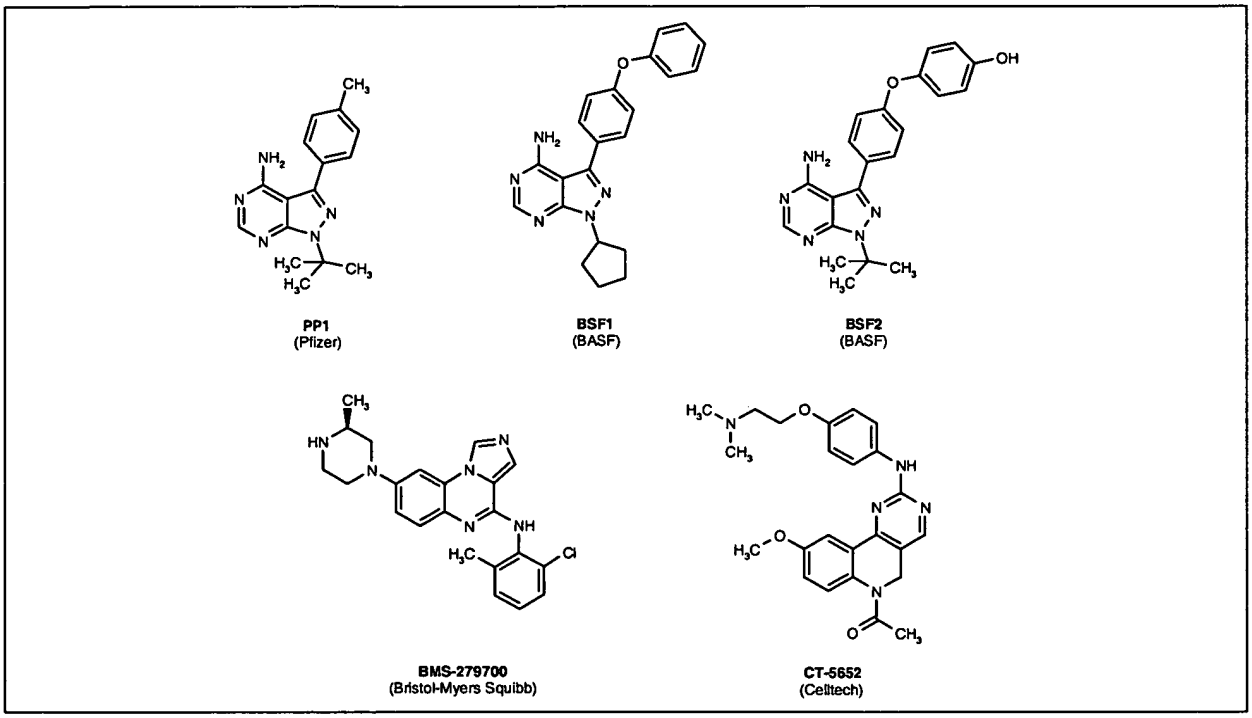

Numerous publications report src family kinase inhibitors with selectivity against representative kinases from other families. In 1998, RW Johnson described an indandione derivative which inhibited lck with an IC_{50} of 32 nM at 50 µM ATP and had > 50-fold less activity against protein kinase (PK) A and 14-fold less activity against c-src [40]. At a recent meeting, Celltech reported benzo[*h*]-5,6-dihydroquinazoline-2-amine-derived lck inhibitors exemplified by CT-5652 (Figure 2) with the most potent compound having an IC_{50} of 1.1 nM against lck [41] and selectivity against PKC, epidermal growth factor receptor (EGFR), csk and cdc2. Celltech has also filed a number of patents claiming other inhibitor series that potently inhibit lck and have selectivity against other kinases (Figure 3), but few biological data are disclosed [101-103]. Additionally, research groups at both Merck and Bristol-Myers Squibb have patents describing src family inhibitors (Figure 3) [104-108]. All contain claims for inhibition of lck in particular and for use in treatment of immune disorders, but no biological data are included. However, Bristol-Myers Squibb did disclose biological data for BMS-279700 (Figure 2) from a 1,5-imidazoquinoxaline series at a recent meeting. This src family-selective kinase inhibitor is reported to have sub-micromolar activity in cellular assays as well as significant activity in murine models of T-cell- and monocyte-mediated responses when administered topically, sc or po [42•].

AstraZeneca claims quinoline- and quinazoline-derived tyrosine kinase inhibitors for use in T-cell-mediated diseases (Figure 3) [109,110]. One quinoline has an IC_{50} value of 30 nM against lck *in vitro*, an IC_{50} of 700 nM in a cellular assay of TCR-stimulated proliferation, and selectivity against EGFR and/or vascular endothelial growth factor receptor (VEGFR). Novartis has a series of publications describing a number of pyrrolo[2,3-*d*]-pyrimidine with sub-micromolar activity on c-src [43,44]. Additionally, compounds with a pyrrolo or pyrazolo pyrimidine core structure have been reported by Knoll/BASF to be potent inhibitors of lck [111-115]. Parke-Davis [45], Wyeth-Ayerst [46,47] and SUGEN [116, 117] have all reported inhibitors of src (Figure 3), many of which are likely to have activity on all members of the src family and thus may be good leads for lck inhibitor development.

In addition to the reversible src family inhibitors described above, Abbott has described an irreversible isothiazolone inhibitor of lck kinase activity that leads to modification of cysteine SH groups in the catalytic domain [48]. Finally, there have been attempts to develop compounds that bind to the lck SH2 protein-protein interaction domain, serving to prevent the adaptor function of this domain and thereby block downstream signaling [49,50]. This approach may prove to be less fruitful as current SH2 inhibitors appear to lack 'drug-like' properties.

Conclusions

The evidence presented above and in the referenced sources supports the hypothesis that a safe and efficacious T-cell inhibitor should be an effective treatment for transplant rejection and for some autoimmune diseases. The lck protein tyrosine kinase continues to be an attractive small molecule target for the treatment of such disorders. Recent advances in the structural biology of the src family kinases may accelerate discovery of selective compounds for use as lck inhibitors. Optimization of even the current leads may allow discovery of appropriate compounds with *in vivo* activity in immune-mediated disease models to determine the real usefulness of T-cell inhibitors.

Figure 3. Structures of tyrosine kinase inhibitors from the patent literature.

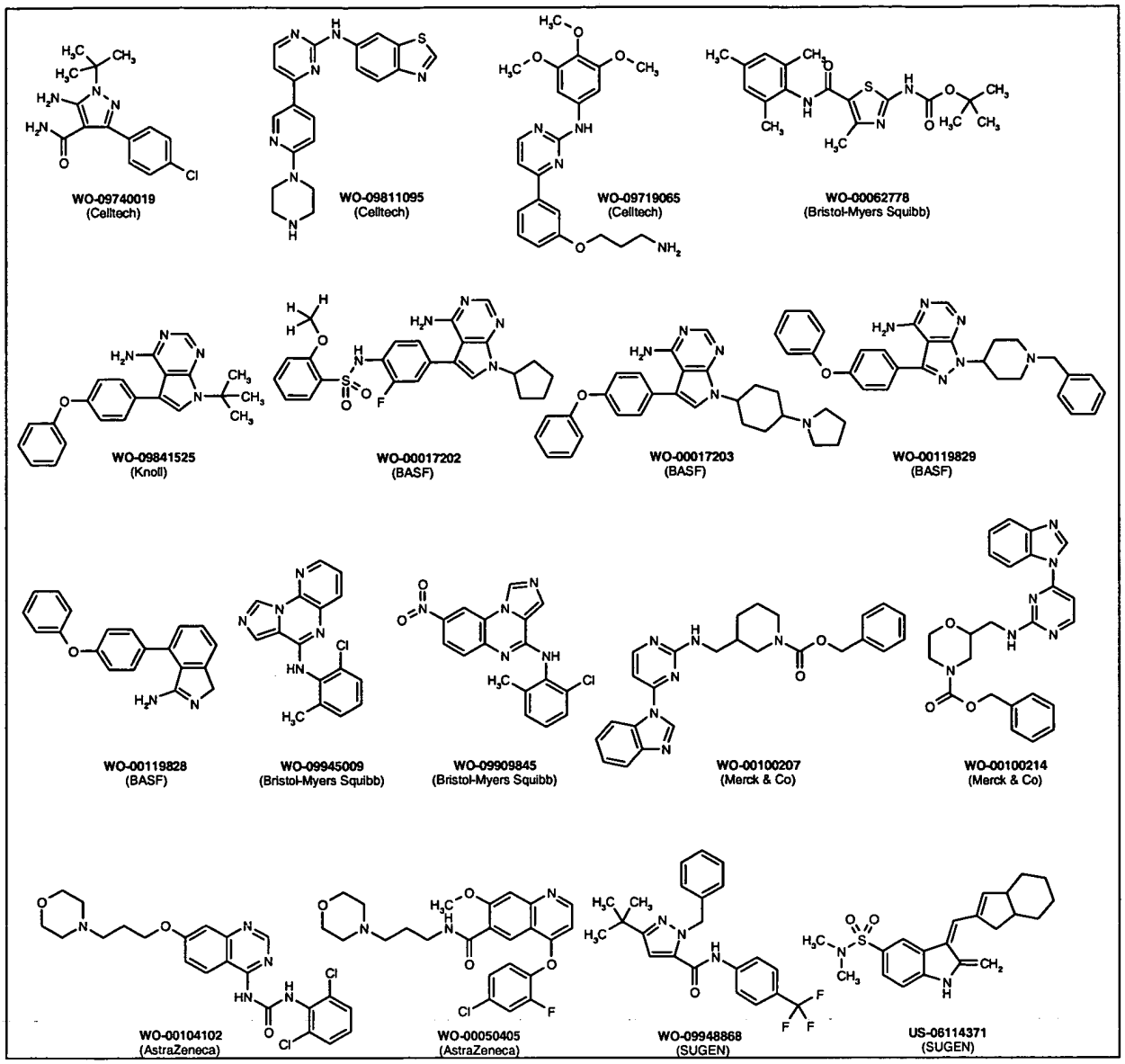

References to primary literature

1. Bolen JB, Brugge JS: **Leukocyte protein tyrosine kinases: potential targets for drug discovery.** *Annu Rev Immunol* (1997) **15**:371-404.

2. Mayer BJ: **Signal transduction: clamping down on Src activity.** *Curr Biol* (1997) **7**(5):R295-R298.

3. Johnson LN, Noble ME, Owen DJ: **Active and inactive protein kinases: structural basis for regulation.** *Cell* (1996) **85**(2):149-158.

4. Straus DB, Weiss A: **Genetic evidence for the involvement of the lck tyrosine kinase in signal transduction through the T cell antigen receptor.** *Cell* (1992) **70**(4):585-593.
• *Demonstrates that lck is required for TCR signaling using an lck-deficient cell line.*

5. Neumeister EN, Zhu Y, Richard S, Terhorst C, Chan AC, Shaw AS: **Binding of ZAP-70 to phosphorylated T-cell receptor ζ and η enhances its autophosphorylation and generates specific binding sites for SH2 domain-containing proteins.** *Mol Cell Biol* (1995) **15**(6):3171-3178.

6. Chan AC, Dalton M, Johnson R, Kong GH, Wang T, Thoma R, Kurosaki T: **Activation of ZAP-70 kinase activity by phosphorylation of tyrosine 493 is required for lymphocyte antigen receptor function.** *EMBO J* (1995) **14**(11):2499-2508.

7. Molina TJ, Kishihara K, Siderovski DP, Van Ewijk W, Narendran A, Timms E, Wakeham A, Paige CJ, Hartmann KU, Veillette A, Davidson D, Mak TW: **Profound block in thymocyte development in mice lacking p56lck.** *Nature* (1992) **357**(6374):161-164.
• *Describes the phenotype of the lck-deficient mouse demonstrating the role of lck in thymocyte development.*

8. Legname G, Seddon B, Lovatt M, Tomlinson P, Sarner N, Tolaini M, Williams K, Norton T, Kioussis D, Zamoyska R: **Inducible expression of a p56Lck transgene reveals a central role for Lck in the differentiation of CD4 SP thymocytes.** *Immunity* (2000) **12**(5):537-546.

9. Seddon B, Legname G, Tomlinson P, Zamoyska R: **Long-term survival but impaired homeostatic proliferation of naïve T cells in the absence of p56lck.** *Science* (2000) **290**(5489):127-131.

10. Goldman FD, Ballas ZK, Schutte BC, Kemp J, Hollenback C, Noraz N, Taylor N: **Defective expression of p56lck in an infant with severe combined immunodeficiency.** *J Clin Invest* (1998) **102**(2):421-429.

11. Dumont FJ: **Immunosuppressive strategies for prevention of transplant rejection.** *Exp Opin Ther Pat* (2001) **11**(3):377-404.

12. Elliott JF, Lin Y, Mizel SB, Bleackley RC, Harnish DG, Paetkau V: **Induction of interleukin 2 messenger RNA inhibited by cyclosporin A.** *Science* (1984) **226**(4681):1439-1441.

13. Robert C, Kupper TS: **Inflammatory skin diseases, T cells, and immune surveillance.** *New Engl J Med* (1999) **341**(24):1817-1828.

14. Meijssen MAC: **Cyclosporine and inflammatory bowel disease: buying time.** *Mediators Inflamm* (1998) **7**(3):145-147.

15. Ruiz-Irastorza G, Khamashta MA, Hughes GRV: **Therapy of systemic lupus erythematosus: new agents and new evidence.** *Exp Opin Invest Drugs* (2000) **9**(7):1581-1593.

16. Rutgeerts P, Baert F: **Novel therapies for Crohn's disease.** *Drugs Today* (2000) **36**(Suppl G, Doctor in Focus):59-68.

17. Haslam N, Hearing SD, Probert CS: **Audit of cyclosporin use in inflammatory bowel disease: limited benefits, numerous side-effects.** *Eur J Gastroenterol Hepatol* (2000) **12**(6):657-660.
• *Good summary of CsA side effects when used for treatment of IBD.*

18. Zamvil S, Nelson P, Trotter J, Mitchell D, Knobler R, Fritz R, Steinman L: **T-cell clones specific for myelin basic protein induce chronic relapsing paralysis and demyelination.** *Nature* (1985) **317**(6035):355-358.

19. Altmann DM, Sansom D, Marsh SG: **What is the basis for HLA-DQ associations with autoimmune disease?** *Immunol Today* (1991) **12**(8):267-270.

20. Sharief MK, Hentges R: **Association between tumor necrosis factor-alpha and disease progression in patients with multiple sclerosis.** *New Engl J Med* (1991) **325**(7):467-472.

21. Nervi S, Atlan-Gepner C, Fossat C, Vialettes B: **Constitutive impaired TCR/CD3-mediated activation of T cells in IDDM patients co-exist with normal co-stimulation pathways.** *J Autoimmun* (1999) **13**(2):247-255.

22. De Maria R, Todaro M, Stassi G, Di Blasi F, Giordano M, Galluzzo A, Giordano C: **Defective T cell receptor/CD3 complex signaling in human type I diabetes.** *Eur J Immunol* (1994) **24**(4):999-1002.

23. Nervi S, Atlan-Gepner C, Kahn-Perles B, Lecine P, Vialettes B, Imbert J, Naquet P: **Specific deficiency of p56lck expression in T lymphocytes from type 1 diabetic patients.** *J Immunol* (2000) **165**(10):5874-5883.

24. Fox DA: **The role of T cells in the immunopathogenesis of rheumatoid arthritis: new perspectives.** *Arthritis Rheum* (1997) **40**(4):598-609.
• *Reviews the role of T-cells in RA progression and suggests that a T-cell centered paradigm is outdated.*

25. Falta MT, Kotzin BL: **T cells as primary players in rheumatoid arthritis.** In: *T Cells in Arthritis.* Miossec P, van den Berg WB, Firestein GS (Eds), Birkhauser Verlag, Basel, Switzerland (1998):201-231.
• *Presents evidence supporting a central role for T-cells in the immunopathogenesis of RA.*

26. Smeets TJM, Dolhain RJEM, Miltenburg AMM, De Kuiper R, Breedveld F, Tak PP: **Poor expression of T cell-derived cytokines and activation and proliferation markers in early rheumatoid synovial tissue.** *Clin Immunol Immunopathol* (1998) **88**(1):84-90.

27. Korganow A-S, Ji H, Mangialaio S, Duchatelle V, Pelanda R, Martin T, Degott C, Kikutani H, Rajewsky K, Pasquali J-L, Benoist C, Mathis D: **From systemic T cell self-reactivity to organ-specific autoimmune disease via immunoglobulins.** *Immunity* (1999) **10**(4):451-461.

28. Kong Y-Y, Feige U, Sarosi L, Bolon B, Tafuri A, Morony S, Capparelli C, Li J, Elliott R, McCabe S, Wong T, Campagnuolo G, Moran E, Bogoch ER, Van G, Nguyen LT, Ohashi PS, Lacey DL, Fish E, Boyle WJ, Penninger JM: **Activated T cells regulate bone loss and joint destruction in adjuvant arthritis through osteoprotegerin ligand.** *Nature* (1999) **402**(6759):304-309.

29. Feldmann M, Brennan FM, Maini RN: **Rheumatoid arthritis.** *Cell* (1996) **85**(3):307-310.

30. Hanke JH, Gardner JP, Dow RL, Changelian PS, Brissette WH, Weringer EJ, Pollok BA, Connelly PA: **Discovery of a novel, potent, and Src family-selective tyrosine kinase inhibitor. Study of Lck- and FynT-dependent T cell activation.** *J Biol Chem* (1996) **271**(2):695-701.

31. Susa M, Teti A: **Tyrosine kinase Src inhibitors: Potential therapeutic applications.** *Drug News Perspect* (2000) **13**(3):169-175.

32. Sicheri F, Kuriyan J: **Structures of Src-family tyrosine kinases.** *Curr Opin Struct Biol* (1997) **7**(6):777-785.

33. Zhu X, Kim JL, Newcomb JR, Rose PE, Stover DR, Toledo LM, Zhao H, Morgenstern KA: **Structural analysis of the lymphocyte-specific kinase Lck in complex with non-selective and Src family selective kinase inhibitors.** *Structure* (1999) **7**(6):651-661.
• *Demonstrates a structural basis for src family selectivity.*

34. Bishop AC, Ubersax JA, Petsch DT, Matheos DP, Gray NS, Blethrow J, Shimizu E, Tsien JZ, Schultz PG, Rose MD, Wood JL, Morgan DO, Shokat KM: **A chemical switch for inhibitor-sensitive alleles of any protein kinase.** *Nature* (2000) **407**(6802):395-401.
• *Describes an interesting approach for obtaining src family kinase selectivity primarily useful for proof-of-concept studies.*

35. Yamaguchi H, Hendrickson WA: **Structural basis for activation of human lymphocyte kinase Lck upon tyrosine phosphorylation.** *Nature* (1996) **384**(6608):484-489.

36. Schindler T, Sicheri F, Pico A, Gazit A, Levitzki A, Kuriyan J: **Crystal structure of Hck in complex with a Src family-selective tyrosine kinase inhibitor.** *Molecular Cell* (1999) **3**(5):639-648.

37. Gribble FM, Loussouarn G, Tucker SJ, Zhao C, Nichols CG, Ashcroft FM: **A novel method for measurement of submembrane ATP concentration.** *J Biol Chem* (2000) **275**(39):30046-30049.

38. Arnold LD, Calderwood DJ, Dixon RW, Johnston DN, Kamens JS, Munschauer R, Rafferty P, Ratnofsky SE: **Pyrrolo[2,3-*d*]pyrimidines containing an extended 5-substituent as potent and selective inhibitors of lck I.** *Bioorg Med Chem Lett* (2000) **10**(19):2167-2170.

39. Burchat AF, Calderwood DJ, Hirst GC, Holman NJ, Johnston DN, Munschauer R, Rafferty P, Tometzki GB: **Pyrrolo[2,3-*d*]pyrimidines containing an extended 5-substituent as potent and selective inhibitors of lck II.** *Bioorg Med Chem Lett* (2000) **10**(19):2171-2174.
• *Describes potent src family-selective inhibitors with descriptions of in vivo activity after oral dosing.*

40. Bullington JL, Cameron JC, Davis JE, Dodd JH, Harris CA, Henry JR, Pellegrino-Gensey JL, Rupert KC, Siekierka JJ: **The development of novel and selective p56lck tyrosine kinase inhibitors.** *Bioorg Med Chem Lett* (1998) **8**(18):2489-2494.

41. Davis JM, Batchelor M, Berg DA, Davis PD, Hutchings MC, Johnson J, Moffat D, Parry DM: **Benzo[*h*]-5,6-dihydroquinazoline-2-amines as potent and selective inhibitors of p56lck.** *Eur Med Chem Symposium* (1998) Edinburgh, UK.

42. Schieven G, Tramposch K, Stanley P, McIntyre K, Kanner S, Pang S, de Fex H, Pitt S, Shuster D, Pattoli M, Chen P, Norris D, Wityak J, Spergel S, Gu H, Iwanowicz E, Shen Z, Lin J, Barrish J: **Identification of anti-inflammatory Lck inhibitors that block T cell activation *in vitro* and *in vivo*.** *FASEB J* (2001) **15**:A1043
• *Describes a potent src family-selective inhibitor with activity in multiple in vivo models.*

43. Missbach M, Altmann E, Widler L, Susa M, Buchdunger E, Mett H, Meyer T, Green J: **Substituted 5,7-diphenylpyrrolo[2,3-*d*]pyrimidines: potent inhibitors of the tyrosine kinase c-Src.** *Bioorg Med Chem Lett* (2000) **10**(9):945-949.

44. Altmann E, Missbach M, Green J, Susa M, Wagenknecht HA, Widler L: **7-Pyrrolidinyl- and 7-piperidinyl-5-aryl-pyrrolo[2,3-*d*]pyrimidines-potent inhibitors of the tyrosine kinase c-Src.** *Bioorg Med Chem Lett* (2001) **11**(6):853-856.

45. Kraker AJ, Hartl BG, Amar AM, Barvian MR, Showalter HDH, Moore CW: **Biochemical and cellular effects of c-Src kinase-selective pyrido[2,3-*d*]pyrimidine tyrosine kinase inhibitors.** *Biochem Pharmacol* (2000) **60**(7):885-898.

46. Boschelli DH, Wang YD, Ye F, Wu B, Zhang N, Dutia M, Powell DW, Wissner A, Arndt K, Weber JM, Boschelli F: **Synthesis and Src kinase inhibitory activity of a series of 4-phenylamino-3-quinolinecarbonitriles.** *J Med Chem* (2001) **44**(5):822-833.

47. Wang YD, Miller K, Boschelli DH, Ye F, Wu B, Floyd MB, Powell DW, Wissner A, Weber JM, Boschelli F: **Inhibitors of src tyrosine kinase: the preparation and structure-activity relationship of 4-anilino-3-cyanoquinolines and 4-anilinoquinazolines.** *Bioorg Med Chem Lett* (2000) **10**(21):2477-2480.

48. Trevillyan JM, Chiou XG, Ballaron SJ, Tang QM, Buko A, Sheets MP, Smith ML, Putman CB, Wiedeman P, Tu N, Madar D, Smith HT, Gubbins EJ, Warrior UP, Chen YW, Mollison KW, Faltynek CR, Djuric SW: **Inhibition of p56(lck) tyrosine kinase by isothiazolones.** *Arch Biochem Biophys* (1999) **364**(1):19-29.

49. Llinàs- Brunet M, Beaulieu PL, Cameron DR, Ferland JM, Gauthier J, Ghiro E, Gillard J, Gorys V, Poirier M, Rancourt J, Wernic D, Betageri R, Cardozo M, Jakes S, Lukas S, Patel U, Proudfoot J, Moss N: **Phosphotyrosine-containing dipeptides as high-affinity ligands for the p56lck SH2 domain.** *J Med Chem* (1999) **42**(4):722-729.

50. Hajduk PJ, Zhou M-M, Fesik SW: **NMR-based discovery of phosphotyrosine mimetics that bind to the Lck SH2 domain.** *Bioorg Med Chem Lett* (1999) **9**(16):2403-2406.

References to patent literature

101. CELLTECH THERAPEUTICS LTD (Davis PD, Davis JM, Moffat DFC): **Preparation of 5-aminopyrazoles as selective inhibitors of the protein tyrosine kinase p56lck.** WO-09740019 (1997).

102. CELLTECH THERAPEUTICS LTD (Davis PD, Moffat DFC, Batchelor MJ): **Preparation of substituted 2-pyrimidineamines as protein kinase inhibitors.** WO-09811095 (1998).

103. CELLTECH THERAPEUTICS LTD (Davis PD, Moffat DFC, Davis JM, Hutchings MC): **Preparation of substituted 2-anilinopyrimidines as protein kinase inhibitors.** WO-09719065 (1997).

104. BRISTOL-MYERS SQUIBB CO (Das J, Padmanabha R, Chen P, Norris DJ, Doweyko AMP, Barrish JC, Wityak J): **Preparation of cyclic protein tyrosine kinase inhibitors.** WO-00062778 (2000).

105. BRISTOL-MYERS SQUIBB CO (Chen P, Norris DJ, Barrish JC, Iwanowicz EJ, Gu HH, Schieven GL): **Preparation of heterocyclo-substituted imidazopyridopyrazine as protein tyrosine kinase inhibitors.** WO-09945009 (1999).

106. BRISTOL-MYERS SQUIBB CO (Barrish JC, Chen P, Das J, Iwanowicz EJ, Norris DJ, Padmanabha R, Roberge JY, Schieven GL): **Preparation of imidazoquinoxaline protein tyrosine kinase inhibitors.** WO-09909845 (1999).

107. MERCK & CO INC (Hunt JA, Mills SG, Sinclair PJ, Zaller DM): **Preparation of pyrimidine derivatives as Src-family protein tyrosine kinase inhibitor compounds.** WO-00100214 (2001).

108. MERCK & CO INC (Goulet JL, Holmes MA, Hunt JA, Mills SG, Parsons WH, Sinclair PJ, Zaller DM): **Preparation and effect of benzimidazolylpyrimidine derivatives as SRC kinase inhibitors.** WO-00100207 (2001).

109. ASTRAZENECA AB (Crawley GC): **Preparation of quinoline-6-carboxamides as tyrosine kinase inhibitors.** WO-00050405 (2000).

110. ASTRAZENECA UK LTD; ZENECA PHARMA SA (Crawley GC, McKerrecher D, Poyser JP, Hennequin LFA, Ple P, Lambert CM): **Preparation of quinazolinyl ureas, thioureas and guanidines for use in the prevention or treatment of T cell mediated diseases or medical conditions.** WO-00104102 (2001).

111. BASF AG (Calderwood D, Arnold LD, Mazdiyasni H, Hirst G, Deng BB): **Preparation of 4-aminopyrrolopyrimidines as protein kinase inhibitors.** WO-0017202 (2000).

112. KNOLL AG (Calderwood DJ, Johnston DJ, Rafferty P, Twigger HL, Munschauer R, Arnold LD): **Preparation of 4-aminopyrrolopyrimidines as protein kinase inhibitors.** WO-9841525 (1998).

113. BASF AG (Hirst G): **Kinase inhibitors as therapeutic agents.** WO-0119828 (2001).

114. BASF AG (Hirst GC, Calderwood D, Wishart N, Ritter K, Arnold LD): **Preparation of pyrrolopyrimidines as protein kinase inhibitors.** WO-0017203 (2000).

115. BASF AG (Hirst GC, Calderwood D, Wishart N, Rafferty P, Ritter K, Arnold LD, Friedman MM): **Preparation of pyrazolopyrimidines as protein kinase inhibitors.** WO-0119829 (2001).

116. SUGEN INC; NEW YORK UNIVERSITY; MAX-PLANCK INSTITUT FÜR BIOCHEMIE (Fong A, Hannah A, Harris DG, Hirth P, Hubbard SR, Langecker P, Liang C, McMahon G, Mohammadi M, Schlessinger J, Shawver LK, Sun L, Tang PC, Ullrich A): **Heterocyclic families of compounds [tricyclic-based indolinones and pyrazolecarboxylic acid amides] for the modulation of tyrosine protein kinase.** WO-09948868 (1999).

117. SUGEN INC (Tang PC, Sun L, McMahon G, Blake RA): **3-(Cyclohexanoheteroarylidenyl)-2-indolinone protein tyrosine kinase inhibitors, and their therapeutic use.** US-06114371 (2000).

RY
Biochemistry and Molecular Biology, Inc.

Vol. 273, No. 50, Issue of December 11, pp. 33714–33721, 1998
Printed in U.S.A.

c-Src Kinase Activity Is Required for Hepatocyte Growth Factor-induced Motility and Anchorage-independent Growth of Mammary Carcinoma Cells*

(Received for publication, July 23, 1998, and in revised form, August 18, 1998)

Nader Rahimi‡§, Wesley Hung‡¶, Eric Tremblay, Ron Saulnier‖, and Bruce Elliott**

From the Department of Pathology, Cancer Research Laboratories, Queen's University, Kingston, Ontario K7L 3N6, Canada

Overexpression and amplification of hepatocyte growth factor (HGF) receptor (Met) have been detected in many types of human cancers, suggesting a critical role for Met in growth and development of malignant cells. However, the molecular mechanism by which Met contributes to tumorigenesis is not well known. The tyrosine kinase c-Src has been implicated as a modulator of cell proliferation, spreading, and migration; these functions are also regulated by Met. To explore whether c-Src kinase is involved in HGF-induced cell growth, a mouse mammary carcinoma cell line (SP1) that co-expresses HGF and Met and a nonmalignant epithelial cell line (Mv1Lu) that expresses Met but not HGF were used. In this study, we have shown that c-Src kinase activity is constitutively elevated in SP1 cells and is induced in response to HGF in Mv1Lu cells. In addition, c-Src kinase associates with Met following stimulation with HGF. The enhanced activity of c-Src kinase also correlates with its ability to associate with Met. Expression of a dominant negative double mutant of c-Src (SRC-RF), lacking both kinase activity (K295R) and a regulatory tyrosine residue (Y527F), in SP1 cells significantly reduced c-Src kinase activity and strongly blocked HGF-induced motility and colony growth in soft agar. In contrast, expression of the dominant negative c-Src mutant had no effect on HGF-induced cell proliferation on plastic. Taken together, our data strongly suggest that HGF-induced association of c-Src with Met and c-Src activation play a critical role in HGF-induced cell motility and anchorage-independent growth of mammary carcinomas and further support the notion that the presence of paracrine and autocrine HGF loops contributes significantly to the transformed phenotype of carcinoma cells.

Evidence supports a role of hepatocyte growth factor (HGF)[1] and its receptor, the product of the *met* protooncogene, in both normal (1, 2) and malignant (3–5) epithelial cell development. In addition, a majority of human breast cancers show increased expression of HGF and Met (6–8), and this high level of HGF expression correlates with recurrence and poor patient survival (9). Met is also overexpressed in several other human cancers, including ovarian (10), melanoma (11), colon carcinomas (12), and osteosarcomas (13). Collectively, these observations suggest that activation of Met by overexpression, gene amplification, or establishment of an HGF autocrine loop may contribute to growth and development of mammary carcinomas. Previous studies demonstrated that co-expression of HGF and Met (4, 14), as well as expression of a constitutively active Met (Tpr-Met) in NIH-3T3 fibroblasts (15, 16) directly leads to cell transformation and tumorigenicity. However, the molecular mechanism by which HGF binding to its receptor elicits cell transformation is not fully understood.

A number of cytoplasmic signaling proteins, such as phosphatidylinositol (PI) 3-kinase, Grb2, Shc, Ras, and c-Src, have been shown to be involved in Met-dependent signal transduction pathways (17, 18). It is important to establish which of these signaling proteins regulate Met-dependent steps in tumor progression, because different signaling proteins may regulate various HGF-induced cellular functions, including mitogenic, motogenic, and morphogenic signals in target cells (18–22). The HGF-mediated signaling pathway is further complicated by the observation that the majority of SH2-containing cytoplasmic effectors bind to a single multifunctional docking site on the cytoplasmic domain of Met, whereas a second site is required for Grb2 binding (17, 18). Recent findings using a mutational approach demonstrated that different HGF-induced effects are regulated by these separate Met binding sites for cytoplasmic transducers (23–25) and that complementation in *trans* between these two binding sites is required for the invasive-metastatic phenotype (25). However, to study the role of specific SH2-containing cytoplasmic effectors in HGF receptor function, approaches to target individual cytoplasmic effectors are required. Recently, we (26) and others (27) have demonstrated that PI 3-kinase activity is required for HGF-induced mitogenic (26) and motogenic functions (27). These findings strongly argue that PI 3-kinase may play an important role in HGF-mediated growth of mammary carcinomas.

The tyrosine kinase c-Src is activated in response to HGF (17, 18) and other growth factors such as platelet-derived growth factor (PDGF) (28–30), fibroblast growth factor (31),

* This work was supported by Grant DAMD17-96-I-6251 from the U.S. Army Medical Research and Material Command (to B. E.) and by funds from the Canadian Breast Cancer Foundation. The costs of publication of this article were defrayed in part by the payment of page charges. This article must therefore be hereby marked "*advertisement*" in accordance with 18 U.S.C. Section 1734 solely to indicate this fact.

‡ These authors contributed equally to this work.

§ Present address: Schepens Eye Research Inst., Harvard Medical School, 20 Staniford St., Boston, MA 02114.

¶ Recipient of a postdoctoral fellowship from Cancer Care Ontario and Fellowship DAMD17-98-I-8330 from the U.S. Army Medical Research and Material Command.

‖ Recipient of the U.S. Army Medical Research and Material Command Studentship DAMD17-94-J-4127. Present address: Dept. of Biochemistry, Health Sciences Center, University of Western Ontario, London, ON N6A 5C1, Canada.

** To whom correspondence should be addressed. Tel.: 613-545-2825; Fax: 613-545-6830; E-mail: elliottb@post.queensu.ca.

[1] The abbreviations used are: HGF, hepatocyte growth factor; PI, phosphatidylinositol; FBS, fetal bovine serum; PAGE, polyacrylamide gel electrophoresis; PIPES, 1,4-piperazinediethanesulfonic acid; PDGF, platelet-derived growth factor.

and epidermal growth factor (32). c-Src kinase activity is known to modulate cell proliferation (33, 34), spreading (35, 36), and migration (36–38) in many cell types; these functions are also regulated by HGF (19–23). c-Src kinase activity is increased 4-fold in human breast cancer (39, 40) and is also elevated in Neu-induced mouse mammary carcinomas in transgenic mice (41, 42). Activation of c-Src tyrosine kinase in transgenic mice induces mammary epithelial hyperplasias and is required, but is not sufficient, for induction of mammary tumors in polyoma virus middle T-transgenic mice (42, 43). Altogether, these observations support the notion that increased c-Src kinase activity in mammary carcinomas plays an important role in mammary tumor growth and development. However, the role of c-Src kinase in HGF-induced functions in mammary carcinoma cells is not clearly known.

To analyze whether c-Src kinase is involved in HGF-induced mammary carcinoma cell growth, we used a mouse mammary carcinoma cell line, SP1, which expresses HGF and tyrosine-phosphorylated Met, thereby generating an autocrine HGF loop in these cells (44). Our current results demonstrate that c-Src kinase activity is elevated in SP1 cells, compared with nonmalignant Mv1Lu epithelial cells. The increased activity of c-Src kinase correlates with its ability to associate with tyrosine-phosphorylated Met. We therefore examined the effect of expressing a dominant negative mutant form of c-Src on c-Src kinase activity and HGF-induced cell motility and anchorage-independent growth of SP1 carcinoma cells. Taken together, our findings show that c-Src kinase activation plays a significant role in HGF-induced cell motility and anchorage-independent growth, characteristics of the transformed phenotype.

EXPERIMENTAL PROCEDURES

Antibodies—Rabbit anti-sheep IgG conjugated to horseradish peroxidase was from Jackson ImmunoResearch Laboratories (Westgrove, PN). Mouse anti-phosphotyrosine (PY20) monoclonal antibody was purchased from Transduction Laboratories (Lexington, KT). Rabbit anti-c-Src IgG, anti-Met (mouse) IgG, and anti-PLC-γ1 IgG were obtained from Santa Cruz Biotechnology (San Diego, CA).

Tissue Culture and Cell Lines—Mv1Lu cells are members of a mink lung epithelial cell line obtained from ATCC (Rockville, MA). Maintenance medium for Mv1Lu cells was Dulbecco's modified Eagle's medium (Life Technologies, Inc.) supplemented with 10% FBS. The SP1 tumor cell line is derived from a spontaneous poorly metastatic murine mammary intraductal adenocarcinoma and expresses HGF and Met. The characteristics of the SP1 cell line have been described elsewhere (45, 46). Maintenance medium for SP1 cells was RPMI 1640 (Life Technologies, Inc.) supplemented with 7% FBS (Life Technologies, Inc.).

Cell Transfection—cDNAs encoding wild type *c-src* (SRC) and a dominant negative double mutant of *c-src* (SRC-RF) with loss-of-function mutations in the kinase domain (K295R) and a regulatory tyrosine residue (Y527F) ligated into the pRc/CMV plasmid (Invitrogen, San Diego, CA) carrying the neomycin resistance marker were obtained from Dr. J. Brugge (47). SP1 cells expressing the mutant c-Src and wild type c-Src were established using the stable transfection LipofectAMINE (Life Technologies, Inc.) method (48). Briefly, SP1 cells were grown to 80% confluence. The DNA (1 μg) was mixed with LipofectAMINE reagent (9 μl) in 200 μl of serum-free medium and was incubated for 15 min at room temperature. Before transfection, cells were washed once with 2 ml of serum-free medium. For each transfection, the mixed DNA and LipofectAMINE were combined with 0.8 ml of serum-free RPMI 1640 medium, and the cells were incubated with this transfection mixture. After 5 h of incubation, an equal volume of RPMI/14% FBS was added to the transfection medium, and incubation proceeded for an additional 24 h. For most experiments, pooled transfected cells selected with G418 (450 μg/ml) were used. In one experiment, SP1 cells were transfected with SRC-RF or SRC, and clones were isolated and tested for Src kinase activity and colony forming efficiency.

Cell Proliferation and Colony Growth Assay—Cell proliferation was carried out as described elsewhere (45). Briefly, SP1 carcinoma cells and Mv1Lu cells were plated at 10^4 cells/well in 24-well plates under the various conditions indicated. DNA synthesis was measured by adding 0.2 μCi of [^{3}H]thymidine (Amersham Pharmacia Biotech, Oakville, ON, Canada) at 24 h. After an additional 24 h, cells were harvested with trypsin/EDTA. Aliquots of cells were placed in 96-well microtiter plates and transferred to filters using a Titertek cell harvester (ICN, Costa Mesa, CA), and [^{3}H]thymidine incorporation was measured in a scintillation counter (Beckman, Mississauga, ON, Canada). Results are expressed as the mean cpm/well ± S.D. of triplicates.

Colony growth assays were performed as described previously (49). Briefly, a solution of 1.2% Bactoagar (Difco Lab) was mixed (1:1) with 2× RPMI 1640, supplemented with FBS at final concentrations of 7 or 1% alone or with HGF as indicated, and layered onto 60 × 15-mm tissue culture plates. SP1 cells (10^3/2.5 ml) were mixed in a 0.36% Bactoagar solution prepared in a similar way and layered (2.5 ml/plate) on top of the 0.6% Bactoagar layer. Plates were incubated at 37 °C in 5% CO_2 for 8–10 days. Colonies were fixed with methanol, stained with Giemsa, and counted manually. Results are expressed as mean number of colonies per dish ± S.D. of quadruplicates.

Cell Motility Assay—To measure cell motility, Transwell culture inserts (8-μm pore size) (Costar, Toronto, ON, Canada) were coated uniformly with gelatin (0.25% w/v, Sigma, Oakville, ON, Canada) on both sides for 2 min at room temperature (50). Membranes were washed twice with serum-free RPMI 1640 medium and inserted into a 24-well culture plate (Costar, Toronto, ON, Canada) with 1 ml of RPMI 1640 containing 0.5 mg/ml bovine serum albumin (Life Technologies, Inc.). Cells were grown to 50% confluence, serum-starved overnight, and harvested in 5 mM EDTA. Cells (2×10^4/100 μl) were plated in the insert and incubated for 6–8 h at 37 °C. Following the incubation, excess medium was removed, and cells were fixed in 1% paraformaldehyde (Sigma) for 15 min and stained with hematoxylin (Fisher, Oakville, ON, Canada). Cells on the upper side of the membrane were removed by wiping with cotton. Cells on the under side of the membrane were counted using an inverted microscope with phase contrast illumination. Cell motility is expressed as the number of migrating cells per well. In a parallel study, a wounding assay was performed, as described previously (36). Briefly, monolayers of each cell type were "wounded" by scraping with an Eppendorf yellow tip, washed, and incubated alone or with HGF for varying times. Migration was assessed visually by the ability of cells to close the wounded area.

Immunoprecipitation and Western Blotting—Cells were grown to confluence and serum-starved for 24 h. Cells were rinsed with cold phosphate-buffered saline three times and lysed in a lysis buffer containing 50 mM Tris-HCl, pH 7.5, 150 mM NaCl, 1% Nonidet P-40, 1 mM Na_3VO_4, 50 mM NaF, 2 mM EGTA, 2 μg/ml aprotinin, 2 μg/ml leupeptin, and 1 mM phenylmethylsulfonyl fluoride. Lysates were centrifuged for 10 min at 14,000 rpm in an IEC/Micromax centrifuge at 4 °C. Protein concentration of supernatants was determined using a bicinchoninic acid protein assay (Pierce). Equal protein amounts from each cell lysate were incubated with the indicated antibodies at 4 °C for 2 h or overnight. Immunoprecipitates were collected on protein A-Sepharose (Amersham Pharmacia Biotech), washed three times with lysis buffer, separated by SDS-PAGE, and transferred to a nitrocellulose membrane. The membrane was blocked for 15 min with 3% skimmed milk in TBST (10 mM Tris-HCl, pH 8.0, 150 mM NaCl, 0.1% Tween 20), and probed for 1 h with the indicated antibodies. The membrane was washed three times for 5 min each with TBST buffer, incubated with horseradish peroxidase-labeled secondary anti-rabbit or anti-mouse antibodies for 15 min, and washed three times with TBST for 10 min each time. Immune complexes were detected using ECL (Amersham).

In Vitro c-Src Kinase Assay—In most experiments, an *in vitro* c-Src kinase assay using enolase as a substrate was performed as described previously (51). Briefly, lysates from SP1 and Mv1Lu cells were prepared, and equal protein amounts from each cell lysate were immunoprecipitated with anti-c-Src IgG (Santa Cruz Biotechnology) as described above. The amount of anti-c-Src IgG was pre-determined to be in excess over c-Src protein, indicating that the majority of c-Src protein in cell lysates is immunoprecipitated (data not shown). One-half of each immunoprecipitate was subjected to SDS-PAGE under nonreducing conditions and Western blot analysis to confirm the amount of c-Src protein present. The other half of each immunoprecipitate was assayed for c-Src kinase activity, by incubating with 10 μl of reaction buffer (20 mM PIPES, pH 7.0, 10 mM $MnCl_2$, 10 μM Na_3VO_4), 1 μl of freshly prepared acid-denatured enolase (Sigma) (5 μg of enolase + 1 μl of 50 mM HCl incubated at 30 °C for 10 min then neutralized with 1 μl of 1 M PIPES, pH 7.0), and 10 μCi of [γ-^{32}P]ATP. After 10 min of incubation at 30 °C, reactions were terminated by the addition of 2× SDS sample buffer, and samples were subjected to 8% SDS-PAGE. Serine and threonine phosphorylations were hydrolyzed by incubating the acrylamide gel in 1 M KOH at 45 °C for 30 min, followed by fixing in 45% MeOH and 10% acetic acid for 30 min at room temperature and drying for 2 h at

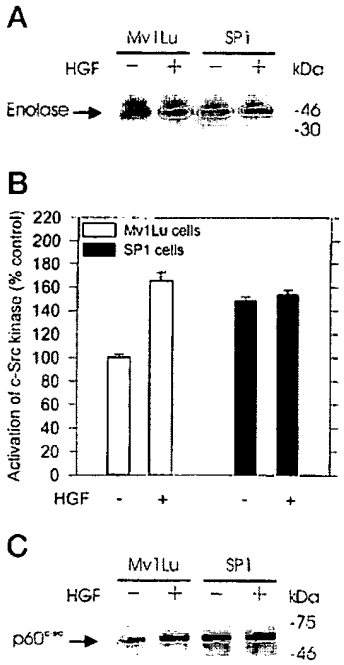

FIG. 1. **c-Src kinase activity is elevated in SP1 carcinoma cells compared with Mv1Lu epithelial cells.** Cell lysates were prepared from serum-starved Mv1Lu and SP1 cells treated without (−) or with (+) HGF (40 ng/ml) for 10 min and were immunoprecipitated with anti-c-Src IgG. Immunoprecipitates were subjected to an *in vitro* kinase assay using enolase as a substrate, and kinase activity was measured as described under "Experimental Procedures." *A*, autoradiogram showing ^{32}P-labeled enolase. *B*, quantitation of autoradiogram using PhosphorImager. Results are expressed as the percentage of cpm in untreated Mv1Lu cells (100%), normalized to the amount of c-Src protein in *C*. The means ± range of two experiments are shown. Similar results were obtained using the c-Src kinase family-specific cdc2 peptide as substrate (data not shown). *C*, Western blot analysis of immmunoprecipitates in *A*, probed with anti-c-Src IgG.

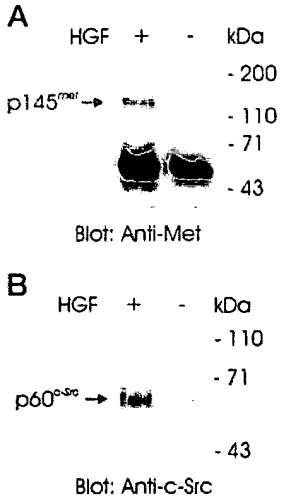

FIG. 2. **c-Src kinase binds to tyrosine-phosphorylated Met.** Cell lysates derived from serum-starved Mv1Lu cells treated without (−) or with (+) HGF (40 ng/ml) for 15 min were immunoprecipitated with anti-c-Src IgG (*A*) or anti-Met IgG (*B*). The immune complexes were separated by 8% SDS-PAGE and immunoblotted with anti-Met IgG (*A*) or anti-c-Src IgG (*B*). Protein molecular mass standards are shown on the *right*. This experiment was done twice with similar results.

80 °C under a vacuum. Autoradiograms were produced and quantitated using a Storm PhosphorImager (Molecular Dynamics, Sunnyvale, CA).

In some experiments (see Fig. 3), c-Src kinase activity was assayed according to Cheng *et al.* (52) using the c-Src tyrosine kinase family-

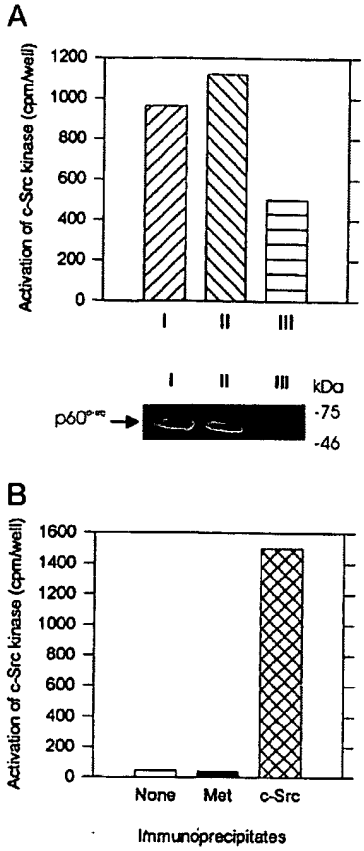

FIG. 3. **Detection of c-Src kinase activity in Met immunoprecipitates.** *A*, equal amounts of cell lysates derived from serum-starved SP1 cells were immunoprecipitated with anti-c-Src antibody (*bar I*) or anti-Met antibody (*bar II*). The supernatant from immunoprecipitates of anti-Met antibody was subsequently immunoprecipitated with anti-c-Src antibody (*bar III*). *In vitro* c-Src kinase activity was determined as described under "Experimental Procedures" using the c-Src kinase family-specific cdc2 peptide substrate. The amount of radiolabeled cdc2 substrate was determined and plotted as c-Src kinase activity (cpm/well) (*top panel*). Half of each immunoprecipitate in the *top panel* was subjected to SDS-PAGE, and p60$^{c\text{-}src}$ protein in each sample was identified by immunoblotting with anti-c-Src antibody (*bottom panel*). *B*, equal amounts of cell lysates derived from serum-starved SP1 cells were immunoprecipitated with anti-Met antibody or anti-c-Src antibody under more stringent conditions with RIPA buffer to prevent co-precipitation of other proteins (see "Experimental Procedures"). The immunoprecipitates were used in an *in vitro* c-Src kinase assay with the c-Src kinase family-specific cdc2 substrate. As a control, a reaction containing no protein (*None*) was carried out concurrently. Results are plotted as c-Src kinase activity (cpm/well) as in *A*. Anti-Met immunoprecipitates under these more stringent conditions showed no significant phosphorylation of the cdc2 substrate.

specific cdc2 peptide substrate. Anti-c-Src or anti-Met immunoprecipitates prepared as above were incubated with 40 μl of a reaction buffer (100 mM Tris-HCl, pH 7.0, 0.4 mM EGTA, 0.4 mM Na_3VO_4, 40 mM $Mg(OAc)_2$), 5 μl of cdc2 peptide (Life Technologies, Inc., 250 μM/assay), 5 μl of cold ATP (25 μM), and 2.5 μCi of [γ-^{32}P]ATP. A control consisting of immunoprecipitation with anti-Met IgG under more stringent conditions with RIPA buffer (150 mM NaCl, 1.0% Nonidet P-40, 0.5% deoxycholate, 0.1% SDS, 50 mM Tris, pH 8.0) where c-Src would not be co-precipitated was also carried out. After 15 min of incubation at 37 °C, reactions were terminated by the addition of 20 μl of 40% trichloroacetic acid and incubated for an additional 5 min. Aliquots subsequently were blotted on to p81 paper (Whatman, Fisher, Ottawa, ON, Canada). The p81 paper was washed three times (5 min/wash) with 0.75% phosphoric acid and once with acetone at room temperature, and the radiolabeled c-Src kinase substrate was counted in a liquid scintillation counter.

In Vitro Met Kinase Assay—Cell lysates from SP1 and Mv1Lu cells were prepared, and equal protein amounts of each lysate were immunoprecipitated with anti-Met IgG as described above. Immunoprecipitates were washed twice with cold lysis buffer and once with cold kinase

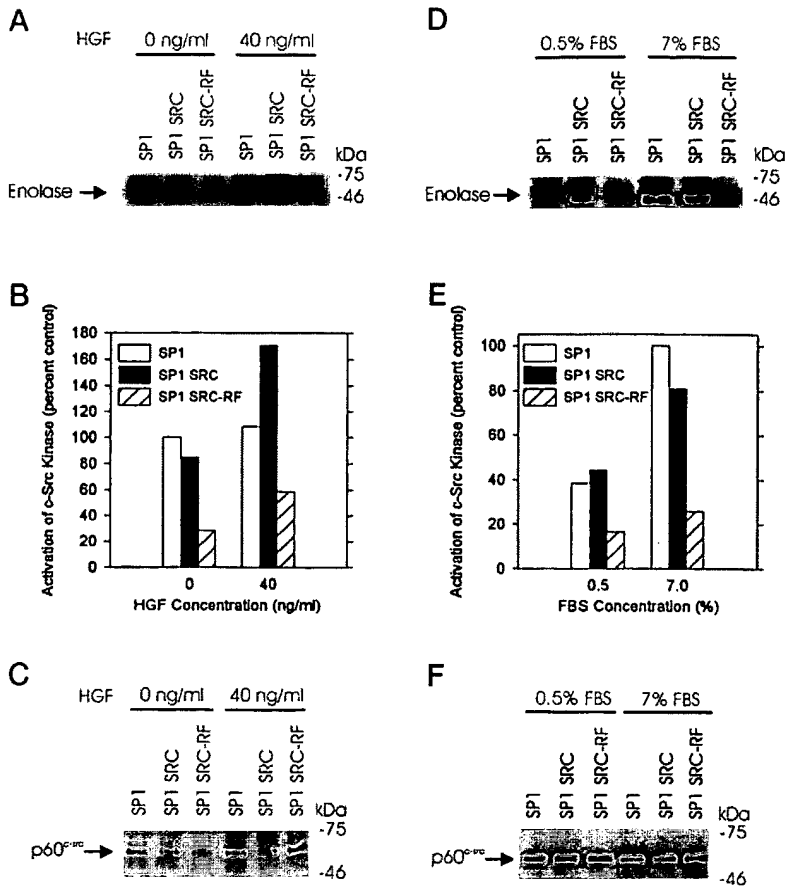

FIG. 4. **Effect of transfected dominant negative SRC-RF on Src kinase activity in SP1 cells.** Pooled SP1 cells transfected with SRC-RF or SRC or untreated SP1 cells were plated at 70% confluence and prestarved overnight. Cells in each group were then cultured alone, with HGF (40 ng/ml), or with 0.5 or 7% FBS, and an *in vitro* c-Src kinase assay using enolase as a substrate was performed as described under "Experimental Procedures." *A* and *D*, autoradiograms showing ^{32}P-labeled enolase. *B*, and *E*, quantitation of autoradiogram using densitometry. Results are normalized to amount of c-Src protein in *C* and *F*. *C*, and *F*, Western blot analysis of immmunoprecipitates in *A* and *D*, probed with anti-c-Src IgG. This result is representative of five experiments.

buffer (20 mM PIPES, pH 7.0, 10 mM $MnCl_2$, 10 μM Na_3VO_4). *In vitro* Met kinase activity was determined by incubating immunoprecipitates with 20 μl of kinase buffer containing 10 μCi of [γ-^{32}P]ATP at 30 °C for 10 min. The reaction was stopped by addition of 2× SDS sample buffer containing 5% β-mercaptoethanol. Samples were boiled for 3 min and subjected to 7% SDS-PAGE. Serine and threonine phosphorylations were hydrolyzed by incubating the acrylamide gel in 1 M KOH at 45 °C for 30 min, followed by fixing and drying as described above. Autoradiograms were produced and quantitated using a Storm PhosphorImager (Molecular Dynamics).

RESULTS

Detection of Elevated c-Src Tyrosine Kinase Activity in SP1 Carcinoma Cells—SP1 carcinoma cells express HGF and tyrosine-phosphorylated Met, consistent with an HGF autocrine loop in these cells (44). To test the possibility that activation of c-Src kinase may be involved in Met-induced signaling pathways, we measured the kinase activity of c-Src in SP1 carcinoma cells and an HGF-sensitive epithelial cell line, Mv1Lu. c-Src kinase activity was measured by the capacity of c-Src immunoprecipitates from these cells to tyrosine phosphorylate the substrate, enolase. c-Src immunoprecipitates from serum-starved SP1 cells showed a pronounced elevated kinase activity, which increased only slightly following treatment with exogenous HGF (Fig. 1). In contrast, c-Src kinase activity in Mv1Lu cells was highly dependent on stimulation of cells with exogenous HGF (Fig. 1). The levels of c-Src kinase activity observed correlated with the constitutive tyrosine phosphorylation of Met (44) and *in vitro* Met kinase activity (data not shown) in SP1 cells, and the HGF-induced tyrosine phosphorylation of Met in Mv1Lu cells (Ref. 26 and data not shown).

Association of c-Src Kinase Protein and Activity with Activated Met—It is conceivable that the high level of c-Src kinase activity in SP1 cells, could have resulted from interaction of c-Src with activated Met due to an autocrine HGF loop in these cells (44). To test for interaction of c-Src kinase family proteins with activated *versus* nonactivated Met, we first examined the association of c-Src with Met in Mv1Lu cells that express Met but not HGF. Serum-starved Mv1Lu cells were incubated alone or with HGF, and cell lysates were immunoprecipitated with anti-Met IgG or anti-c-Src IgG. Protein precipitates were electrophoresed and subjected to Western blotting with anti-c-Src IgG or anti-Met IgG, respectively. As shown in Fig. 2 (*A* and *B*), an increased amount of c-Src protein was recovered from anti-Met immunoprecipitates and *vice versa* in cell lysates from HGF-treated Mv1Lu cells compared with untreated Mv1Lu cells. We also showed that association of c-Src kinase with Met occurred via the SH2 domain of c-Src and correlated with tyrosine phosphorylation of Met (data not shown). It should be noted that a trace amount of c-Src protein was detected in lysates of unstimulated cells immunoprecipitated with anti-Met IgG and blotted with anti-c-Src IgG, possibly due to incomplete starvation of these cells before HGF stimulation (Fig. 2*B*). Thus, stimulation with HGF causes increased association of c-Src protein with Met.

To determine whether elevated activity of c-Src kinase in SP1 cells correlates with its ability to associate with Met, serum-starved SP1 cells were immunoprecipitated with anti-Met IgG or anti-c-Src IgG, and immunoprecipitates were tested for the ability to tyrosine phosphorylate the c-Src kinase family-specific cdc2 peptide substrate (52). As shown in Fig. 3*A* (*bars I* and *II*), similar amounts of c-Src kinase protein and activity were recovered from immunoprecipitates of both anti-Met and anti-c-Src antibodies. In contrast, immunoprecipitates from anti-Met IgG under more stringent conditions with RIPA buffer where c-Src is not co-precipitated resulted in no signifi-

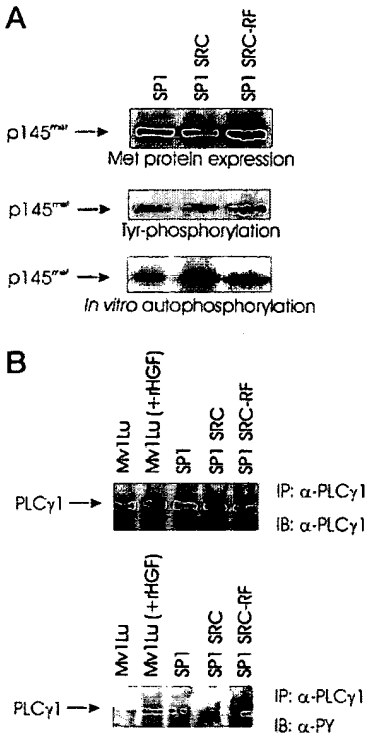

FIG. 5. **Expression of dominant negative mutant SRC-RF does not alter Met protein levels or activity and downstream signaling.** *A*, SP1 cells transfected with SRC-RF or SRC or untreated SP1 cells were prestarved overnight and lysed as described in the legend to Fig. 1. Equal amounts of protein from each lysate were concentrated on Microcon 10 filters (Amicon Inc., Beverly, MA) and analyzed by Western blotting with anti-Met IgG (*top panel*). The blot was stripped and reprobed with anti-phosphotyrosine antibody (*middle panel*). Cell lysates were also immunoprecipitated with anti-Met IgG, and immunoprecipitates were subjected to an *in vitro* Met kinase assay as described under "Experimental Procedures." The autoradiogram depicting ^{32}P-labeling of Met is shown (*bottom panel*). Relative band intensities and amount of ^{32}P labeling was determined using a Storm PhosphorImager. The relative amount of Met tyrosine phosphorylation (1.0, 1.0, or 1.0) or of *in vitro* Met autophosphorylation (1.0, 1.1, or 1.0) was not significantly different among the three cell lines. *B*, serum-starved SP1 cells transfected with SRC-RF or SRC and untreated SP1 cells were lysed as described in the legend to Fig. 1. Prestarved Mv1Lu cells untreated or treated with HGF (40 ng/ml) for 10 min were used as negative and positive controls, respectively. Equal amounts of protein from each lysate were immunoprecipitated with anti-PCL-γ1 IgG. Immunoprecipitates were subjected to 7% SDS-PAGE and transferred to nitrocellulose. The blot was probed with anti-PCL-γ1 IgG (*top panel*) before being stripped and reprobed with anti-phosphotyrosine antibody (*bottom panel*). This experiment was done twice with similar results. *IP*, immunoprecipitation; *IB*, immunoblot.

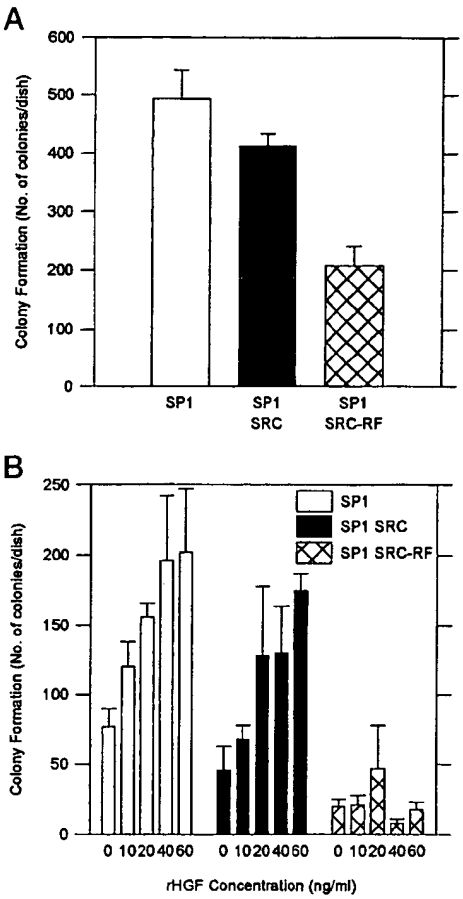

FIG. 6. **Effect of transfected dominant negative SRC-RF on growth of SP1 cells in agar.** Pooled SP1 cells transfected with SRC-RF or SRC or untreated SP1 cells were cultured (10^3 cells/dish) in 60-mm tissue culture plates in soft agar (0.36%) with RPMI 1640 medium supplemented with 7% FBS (*A*) or 1% FBS plus HGF at the concentrations indicated (*B*) as described previously (49). After 8 days, colonies were stained with Giemsa and counted visually. Results are expressed as the mean colony numbers ± S.D. of quadruplicate cultures. This experiment was done three times with similar results.

cant phosphorylation of cdc2 peptide (Fig. 3*B*), confirming the specificity of the cdc2 peptide as a substrate for c-Src (52). Thus a significant portion of c-Src kinase activity is associated with activated Met in SP1 cells. To further evaluate the contribution of c-Src association with Met, the supernatant from the immunoprecipitate of anti-Met IgG was immunoprecipitated for a second time with anti-c-Src IgG and subjected to the *in vitro* c-Src kinase assay. As shown in Fig. 3*A* (*bar III*), some c-Src kinase activity was detected in the Met-depleted SP1 cell lysate; however, it was with much lower activity, corresponding to the reduced amount of c-Src protein present. Immunoprecipitation of SP1 cell lysates with higher concentrations of anti-Met IgG and subsequently with anti-c-Src IgG showed a similar result (data not shown). These results demonstrate that the majority of c-Src kinase activity correlates with its ability to associate with Met in SP1 cells.

c-Src Kinase Activity Is Required for Colony Growth in Agar, but Not Cell Proliferation on Plastic—SP1 cells exhibit paracrine stimulation by HGF of colony growth in agar and proliferation on plastic (45, 49). To determine whether c-Src kinase activity is required for HGF-induced proliferation or colony growth in agar, an expression vector (SRC-RF) containing cDNA encoding a dominant negative double mutant of *c-src* with loss-of-function mutations in the kinase domain (K295R) and a regulatory tyrosine residue (Y527F) (47) was stably transfected into SP1 cells. A control consisted of cells transfected with the same vector expressing wild type *c-src* (SRC). Uncloned (pooled) transfected cells were selected in G418-containing medium and assessed for c-Src kinase activity and HGF-induced functions. For *in vitro* c-Src kinase assays, immunoprecipitation with anti-c-Src IgG was carried out at antibody excess, indicating that the majority of wild type c-Src protein was present in immunoprecipitates. The results showed that c-Src kinase activity was strongly reduced in SRC-RF transfected SP1 cells compared with SRC transfected or untransfected cells incubated alone, or following stimulation with 40 ng/ml HGF or 7% FBS (Fig. 4). However, tyrosine phosphorylation of Met or an unrelated signaling molecule PLC-γ1 and *in vitro* autophosphorylation of Met remained unaffected in SRC-RF- or SRC-transfected SP1 cells, compared with untransfected cells (Fig. 5). These results demonstrate

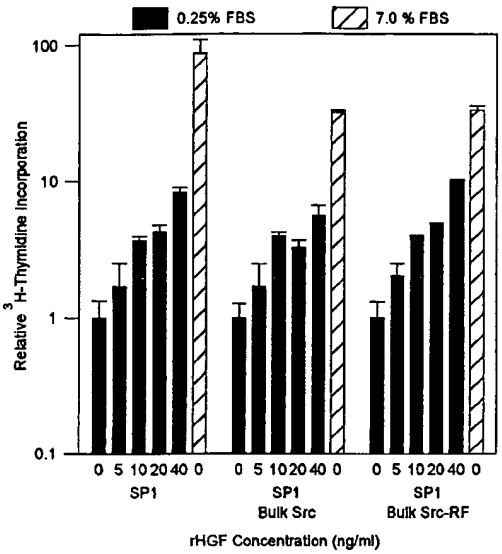

FIG. 7. **Effect of transfected dominant negative mutant SRC-RF on HGF-induced proliferation of SP1 cells on plastic.** Pooled SP1 cells transfected with SRC-RF or SRC or untreated SP1 cells were prestarved overnight, and each cell line was plated at 10^4 cells/well in 24-well plates in 0.25% FBS without or with HGF at the concentrations indicated. Controls consisted of cultures with 7% FBS. DNA synthesis was measured as described under "Experimental Procedures." Results are expressed as relative mean [^{3}H]thymidine incorporation compared with control (no HGF) (mean cpm/well ± S.D. of triplicates). This result is representative of four experiments.

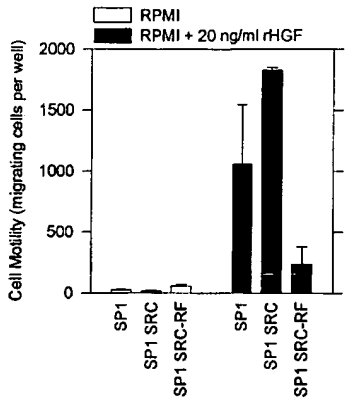

FIG. 8. **Effect of transfected dominant negative SRC-RF on HGF-induced cell motility.** SP1 cells transfected with SRC-RF or SRC or untreated SP1 cells were serum-starved overnight, and each cell line (2×10^4 cells) was plated into Transwell inserts (8-μm pore size) in 24-well plates in 0.5 mg/ml bovine serum albumin in RPMI without (*open bars*) or with (*closed bars*) HGF (20 ng/ml) as described under "Experimental Procedures." After 6–8 h of incubation at 37 °C, cells were fixed in 1% paraformaldehyde and stained with hematoxylin. Cells on the upper side of the membrane were removed by wiping with cotton. Cells on the underside were counted using an inverted microscope with phase contrast illumination. The results are expressed as the relative number of migrating cells/well (means ± range of two wells/point). This experiment was done twice with similar results. Similar results were obtained using a wound healing assay (data not shown).

specificity of the inhibitory effect of SRC-RF on c-Src kinase activity.

Expression of the dominant negative SRC-RF mutant in SP1 cells significantly inhibited FBS- and HGF-induced colony formation in soft agar, compared with SRC-transfected or untransfected SP1 cells (Fig. 6). Similarly, a subclone of SP1 cells expressing SRC-RF showed a marked reduction in colony formation, compared with a wild type SRC-transfected subclone or untransfected SP1 cells (data not shown). In contrast, SRC-RF-transfected SP1 cells showed no difference in HGF-induced or serum-induced proliferation on plastic, compared with SRC-transfected or untransfected SP1 cells (Fig. 7). Thus reduction of c-Src kinase activity in SRC-RF-transfected cells abrogated HGF- or serum-induced colony growth in soft agar but had no effect on cell proliferation on plastic.

c-Src Kinase Activity Is Required for HGF-induced Cell Motility—Because c-Src kinase activity has been shown to modulate cell motility in several cell types (36–38), we examined the role of c-Src kinase in HGF-induced cell motility in SP1 cells. Our results showed that HGF strongly stimulated motility of SP1 cells through collagen-coated porous membranes in a paracrine manner. HGF-induced motility was significantly reduced in SP1 cells transfected with dominant negative mutant SRC-RF, compared with SRC-transfected or untransfected cells (Figs. 8 and 9). Similar results were obtained using a wounding assay (data not shown). These results are consistent with a role of c-Src kinase in HGF-induced cell motility.

DISCUSSION

We (6) and others (7, 8) have previously shown that HGF and Met mRNA are strongly co-expressed in invasive carcinomas in human breast cancer. These findings suggest that signals transduced by activated Met confer survival and growth advantage to carcinoma cells during progression to metastasis. This concept is further supported by the observation that cells transfected with an activated version of *met* (*tpr-met*) acquire invasive and metastatic properties (15, 16). Unlike most other receptor tyrosine kinases, Met shows one high affinity binding site for the majority of SH2-containing cytoplasmic effectors, suggesting that these proteins bind Met in a competitive manner (23–25). Therefore, to study the role of specific SH2-containing cytoplasmic effectors in HGF receptor function, approaches to target individual cytoplasmic effectors are required.

To analyze downstream effector molecules in HGF-induced tumorigenic properties of mammary carcinoma cells, we have studied a mouse mammary carcinoma, SP1, which co-expresses HGF and Met (44). However, depending on culture conditions, both paracrine and autocrine effects of HGF have been observed in SP1 cells (44, 45, 49). In monolayer cultures, autocrine phosphorylation of Met at tyrosine in SP1 cells without addition of exogenous HGF was observed (44). In contrast, tyrosine phosphorylation of Met was reduced in suspended SP1 cells and can be restored by addition of exogenous HGF.[2] These observations suggest that the base level of Met activation may be influenced by extracellular environmental conditions, such as cell adhesion to various substrata (53), cell density effects on HGF expression and secretion (54), or proteolytic processing of pro-HGF to the biologically active form (55). In the present report, paracrine stimulation with exogenous HGF was required for optimal cell proliferation, motility, and colony growth in agar under serum-starved conditions. Previous studies showed that PI 3-kinase activity is elevated in SP1 cells and that its activity is required for HGF-induced proliferation in monolayer culture. Treatment of SP1 cells with wortmannin, a potent inhibitor of PI 3-kinase (56), or transfection of a dominant negative mutant of the p85 subunit of PI 3-kinase into these cells (26) inhibited HGF-induced cell proliferation in monolayer culture.

In the present report, we show that c-Src kinase activity is elevated in SP1 mammary carcinoma cells compared with nonmalignant Mv1Lu epithelial cells and is associated with Met. The elevated level of c-Src kinase activity in SP1 cells and its association with Met strongly suggest that this signaling mol-

[2] R. Saulnier and H. Qiao, unpublished observation.

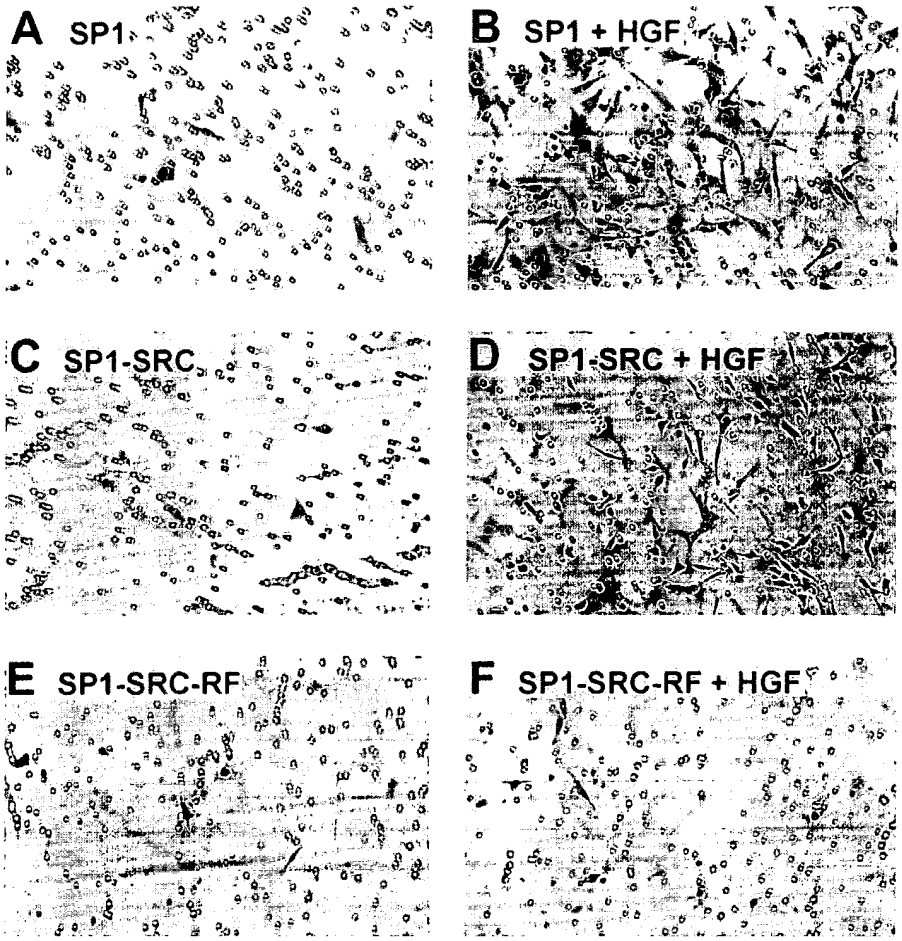

FIG. 9. **Photomicrographs of migrating SP1 cells transfected with SRC or SRC-RF or untransfected SP1 cells following HGF stimulation.** SP1 cells untransfected (*A* and *B*) and transfected with SRC (*C* and *D*) or SRC-RF (*E* and *F*) were serum-starved overnight and assessed for cell motility without (−) or with (+) HGF (20 ng/ml) as described in the legend to Fig. 8. After removing nonmigrating cells on the upper side of the membrane, membranes were mounted onto glass slides, and migrating cells were photographed using a Leitz microscope with phase contrast illumination. Photographs correspond to the groups shown in Fig. 8. Original magnification, 250×.

ecule may be involved in intracellular events triggered by HGF. This observation prompted us to test whether expression of a dominant negative mutant form of c-Src influences growth of SP1 cells. Expression of a dominant negative form of c-Src (SRC-RF) in SP1 cells showed no significant effect on HGF-induced cell proliferation on plastic but markedly inhibited HGF- or serum-induced colony growth in soft agar. Thus activation of c-Src kinase is essential for colony formation in agar by SP1 cells but appears not to be required for cell proliferation on plastic.

Other laboratories have reported variable effects of c-Src kinase on cell growth. In support of our observations, Demali and Kazlauskas (57) have shown that a mutant form of PDGF β-receptor that cannot bind or activate, c-Src, retains the ability to stimulate growth of fibroblasts on plastic or in agar in response to PDGF. In contrast, Courtneidge and co-workers (33, 58) have shown that microinjection of a kinase dead mutant c-Src or neutralizing antibodies that inhibit basal and stimulated c-Src kinase activity inhibited PDGF-dependent DNA synthesis in fibroblasts. Similarly, constitutive expression of c-Src mutants inhibited PDGF and epidermal growth factor-induced mitogenesis of mouse embryonal fibroblasts lacking c-Src (34). The apparent differences in the role of c-Src kinase in the above systems could be due to different levels of residual basal activity of c-Src kinase or the developmental and malignant status of the cells used. Our observation that anchorage-independent growth but not proliferation on plastic is inhibited in cells expressing dominant negative SRC-RF suggests that the reduced level of c-Src kinase activity in SRC-RF expressing SP1 cells is insufficient to support anchorage-independent growth, whereas proliferation on plastic remains unaffected. c-Src-independent signaling mechanisms may also promote HGF-induced proliferation of SP1 cells on plastic.

We have also shown that SP1 cells transfected with the dominant negative SRC-RF mutant showed reduced cell motility in response to HGF compared with SRC-transfected or untransfected SP1 cells. Thus c-Src kinase activity is required for HGF-induced cell motility in SP1 carcinoma cells, although complementary signaling molecules may also be involved. This observation reflects recent reports that c-Src kinase activity is required for epithelial cell scattering (38–40, 50) and organization of the cortical cytoskeleton (50). In addition, Richardson *et al.* (59) have shown that co-expression of c-Src in cells expressing the dominant negative C-terminal domain of focal adhesion kinase can reconstitute cell spreading and motility and induces tyrosine phosphorylation of paxillin. Together, these observations raise the possibility that HGF-induced c-Src kinase activity may regulate cell motility through the cytoskeletal complex. This possibility is currently being investigated.

There is now growing evidence that the c-Src family protein-tyrosine kinases are involved in signal transduction pathways that result in cell growth, adhesion, and differentiation. c-Src kinase activity is required for cell proliferation induced by platelet-derived growth factor, colony stimulating factor-1, and epidermal growth factor (51, 60), and increased c-Src kinase activity is associated with many cancers. These observations support the notion that increased c-Src kinase activity in mammary carcinomas may play an important role in mammary tumor growth and development. Our findings involving transfection of a dominant negative c-Src kinase-defective mutant into SP1 cells represent the first direct demonstration of a requirement for c-Src kinase activity in HGF-induced cell mo-

tility and anchorage-independent growth of carcinoma cells, although interactions with other signaling molecules may also be involved. These data strongly suggest that HGF-induced association of c-Src kinase with Met and its activation are important in growth and transformation of mammary carcinomas and further argue that paracrine and autocrine HGF loops play a significant role in the transformed phenotype of some mammary carcinomas.

Acknowledgment—Dr. J. Brugge kindly provided SRC and SRC-RF plasmids.

REFERENCES

1. Brinkmann, V., Foroutan, H., Sachs, M., Weidner, K. M., and Birchmeier, W. (1995) *J. Cell Biol.* **131,** 1573–1586
2. Niranjan, B., Buluwela, L., Yant, J., Perusinghe, N., Atherton, A., Phippard, D., Dale, T., Gusterson, B., and Kamalati, T. (1995) *Development* **121,** 2897–2908
3. Fixman, E. D., Naujokas, M. A., Rodrigues, G. A., Moran, M. F., and Park, M. (1995) *Oncogene* **10,** 237–249
4. Bellusci, S., Moens, G., Gaudino, G., Comoglio, P., Nakamura, T., Thiery, J. P., and Jouanneau, J. (1994) *Oncogene* **9,** 1091–1099
5. Maggiora, P., Gambarotta, G., Olivero, M., Giordano, S., Di Renzo, M. F., and Comoglio, P. M. (1997) *J. Cell. Physiol.* **173,** 183–186
6. Tuck, A. B., Park, M., Sterns, E. E., Boag, A., and Elliott, B. E. (1996) *Am. J. Pathol.* **148,** 225–232
7. Wang, Y., Selden, A. C., Morgan, N., Stamp, G. W., and Hodgson, H. J. (1994) *Am. J. Pathol.* **144,** 675–682
8. Jin, L., Fuchs, A., Schnitt, S., Yao, Y., Joseph, A., Lamszus, K., Park, M., Goldberg, I., and Rosen, E. (1997) *Cancer* **79,** 749–760
9. Yamashita, J., Ogawa, M., Yamashita, S., Nomura, K., Kuramoto, M., Saishoji, T., and Shin, S. (1994) *Cancer Res.* **54,** 1630–1633
10. Di Renzo, M. F., Olivero, M., Katsaros, D., Crepaldi, T., Gaglia, P., Zola, P., Sismondi, P., and Comoglio, P. M. (1994) *Int. J. Cancer* **58,** 658–662
11. Natali, P. G., Nicotra, M. R., Di Renzo, M. F., Prat, M., Bigotti, A., Cavaliere, R., and Comoglio, P. M. (1993) *Br. J. Cancer* **68,** 746–750
12. Di Renzo, M. F., Olivero, M., Giacomini, A., Porte, H., Chastre, E., Mirossay, L., Nordlinger, B., Bretti, S., Bottardi, S., Giordano, S., Plebani, M., Gespach, C., and Comoglio, P. M. (1995) *Clin. Cancer Res.* **1,** 147–154
13. Ferracini, R., Di Renzo, M. F., Scotlandi, K., Baldini, N., Olivero, M., Lollini, P., Cremona, O., Campanacci, M., and Comoglio, P. M. (1995) *Oncogene* **10,** 739–749
14. Rong, S., Bodescot, M., Blair, D., Dunn, J., Nakamura, T., Mizuno, K., Park, M., Chan, A., Aaronson, S., and Vande Woude, G. F. (1992) *Mol. Cell. Biol.* **12,** 5152–5158
15. Rong, S., Segal, S., Anver, M., Resau, J. H., and Vande Woude, G. F. (1994) *Proc. Natl. Acad. Sci. U. S. A.* **91,** 4731–4735
16. Cooper, C. S., Park, M., Blair, D., Tainsky, M. A., Huebner, K., Croce, C. M., and Vande Woude, G. F. (1994) *Nature* **311,** 29–33
17. Zhu, H., Naujokas, M. A., Fixman, E. D., Torossian, K., and Park, M. (1994) *J. Biol. Chem.* **269,** 29943–29948
18. Ponzetto, C., Bardelli, A., Zhen, Z., Maina, F., dalla Zonca, P., Giordano, S. A. U., Panayotou, G., and Comoglio, P. M. (1994) *Cell* **77,** 261–271
19. Tajima, H., Matsumoto, K., and Nakamura, T. (1991) *FEBS Lett.* **291,** 229–232
20. Rubin, J. S., Chan, A. M., Bottaro, D. P., Burgess, W. H., Taylor, W. G., Cech, A. C., Hirschfield, D. W., Wong, J., Miki, T., Finch, P. W., and Aaronson, S. A. (1991) *Proc. Natl. Acad. Sci. U. S. A.* **88,** 415–419
21. Rosen, E. M., Knesel, J., Goldberg, I. D., Jin, L., Bhargava, M., Joseph, A., Zitnik, R., Wines, J., Kelley, M., and Rockwell, S. (1994) *Int. J. Cancer* **57,** 706–714
22. Schmidt, C., Bladt, F., Goedecke, S., Brinkmann, V., Zschiesche, W., Sharpe, M., Gherardi, E., and Birchmeier, C. (1995) *Nature* **373,** 699–702
23. Ponzetto, C., Zhen, Z., Audero, E., Maina, F., Bardelli, A., Basile, M. L., Giordano, S., Narsimhan, R., and Comoglio, P. (1996) *J. Biol. Chem.* **271,** 14119–14123
24. Fixman, E. D., Fournier, T. M., Kamikura, D. M., Naujokas, M. A., and Park, M. (1996) *J. Biol. Chem.* **271,** 13116–13122
25. Giordano, S., Bardelli, A., Zhen, Z., Menard, S., Ponzetto, C., and Comoglio, P. M. (1997) *Proc. Natl. Acad. Sci. U. S. A.* **94,** 13868–13872
26. Rahimi, N., Tremblay, E., and Elliott, B. (1996) *J. Biol. Chem.* **271,** 24850–24855
27. Royal, I., and Park, M. (1995) *J. Biol. Chem.* **270,** 27780–27787
28. Oude Weernink, P. A., and Rijksen, G. (1995) *J. Biol. Chem.* **270,** 2264–2267
29. Courtneidge, S. A., Kypta, R. M., Cooper, J. A., and Kazlauskas, A. (1991) *Cell Growth Differ.* **2,** 483–486
30. Kypta, R. M., Goldberg, Y., Ulug, E. T., and Courtneidge, S. A. (1990) *Cell* **62,** 481–492
31. Zhan, X., Plourde, C., Hu, X., Friesel, R., and Maciag, T. (1994) *J. Biol. Chem.* **269,** 20221–20224
32. Muthuswamy, S. K., and Muller, W. J. (1995) *Oncogene* **11,** 271–279
33. Barone, M. V., and Courtneidge, S. A. (1995) *Nature* **378,** 509–512
34. Broome, M. A., and Hunter, T. (1996) *J. Biol. Chem.* **271,** 16798–16806
35. Kaplan, K. B., Swedlow, J. R., Morgan, D. O., and Varmus, H. E. (1995) *Genes Dev.* **9,** 1505–1517
36. Rodier, J-M., Vallés, A. M., Denoyelle, M., Thiery, J. P., and Boyer, B. (1995) *J. Cell Biol.* **131,** 761–773
37. Hansen, K., Johnell, M., Siegbahn, A., Rorsman, C., Engstrom, U., Wernstedt, C., Heldin, C. H., and Ronnstrand, L. (1996) *EMBO J.* **15,** 5299–5313
38. Hall, C. L., Lange, L. A., Prober, D. A., Zhang, S., and Turley, E. A. (1996) *Oncogene* **13,** 2213–2224
39. Rosen, N., Bolen, J. B., Schwartz, A. M., Cohen, P., DeSeau, V., and Israel, M. A. (1986) *J. Biol. Chem.* **261,** 13754–13759
40. Ottenhoff-Kalff, A. E., Rijksen, G. A. U., Hennipman, A., Michels, A. A., and Staal, G. E. (1992) *Cancer Res.* **52,** 4773–4778
41. Muthuswamy, S. K., Siegel, P. M., Dankort, D. L., Webster, M. A., and Muller, W. J. (1994) *Mol. Cell. Biol.* **14,** 735–743
42. Guy, C. T., Muthuswamy, S. K., Cardiff, R. D., Soriano, P., and Muller, W. J. (1994) *Genes Dev.* **8,** 23–32
43. Webster, M. A., Cardiff, R. D., and Muller, W. J. (1995) *Proc. Natl. Acad. Sci. U. S. A.* **92,** 7849–7853
44. Rahimi, N., Tremblay, E., McAdam, L., Park, M., Schwall, R., and Elliott, B. (1996) *Cell Growth & Differ.* **7,** 263–270
45. Rahimi, N., Saulnier, R., Nakamura, T., Park, M., and Elliott, B. (1994) *DNA Cell Biol.* **13,** 1189–1197
46. Elliott, B. E., Tam, S. P., Dexter, D., and Chen, Z. Q. (1992) *Int. J. Cancer* **51,** 416–424
47. Mukhoupadhyay, D., Tsiokas, L., Zhou, X. M., Foster, D., Brugge, J. S., and Sukhatme, V. P. (1995) *Nature* **375,** 577–581
48. Seth, P., Brinkmann, U., Schwartz, G. N., Katayose, D., Gress, R., Pastan I., and Cowan, K. (1996) *Cancer Res.* **56,** 1346–1351
49. Saulnier, R., Bhardwaj, B., Klassen, J., Leopold, D., Rahimi, N., Tremblay, E., Mosher, D., and Elliott, B. (1996) *Exp. Cell Res.* **222,** 360–369
50. Boyer, B., Roche, S., Denoyelle, M., and Thiery, J. P. (1997) *EMBO J.* **16,** 5904–5913
51. Atfi, A., Drobetsky, E., Boissonneault, M., Chapdelaine, A., and Chevalier, S. (1994) *J. Biol. Chem.* **269,** 30688–30693
52. Cheng, H., Nishio, H., Hatase, O., Ralph, S., and Wang, J. (1992) *J. Biol. Chem.* **267,** 9248–9256
53. Wang, R., Kobayashi, R., and Bishop, J. M. (1996) *Proc. Natl. Acad. Sci. U. S. A.* **93,** 8425–8430
54. Mizuno, K., Higuchi, O., Tajima, H., Yonemasu, T., and Nakamura, T. (1993) *J. Biochem.* **114,** 96–102
55. Naldini, L., Vigna, E., Bardelli, A., Follenzi, A., Galimi, F., Comoglio, P. M. (1995) *J. Biol. Chem.* **270,** 603–611
56. Okada, T., Sakuma, L., Fukui, Y., Hazeki, O., and Ui, M. (1994) *J. Biol. Chem.* **269,** 3563–3567
57. Demali, K., and Kazlauskas, A. (1998) *Mol. Cell. Biol.* **18,** 2014–2022
58. Roche, S., Koegl, M., Barone, M. V., Roussel, M. F., and Courtneidge, S. A. (1995) *Mol. Cell. Biol.* **15,** 1102–1109
59. Richardson, A., Malik, R. K., Hildebrand, J. D., and Parsons, J. T. (1997) *Mol. Cell. Biol.* **17,** 6906–6914
60. Sasaoka, T., Rose, D. W., Jhun, B. H., Saltiel, A. R., Draznin, B., and Olefsky, J. M. (1994) *J. Biol. Chem.* **269,** 13689–13694

ESEARCH COMMUNICATIONS 243, 503–508 (1998)

Overexpression and Activation of the Tyrosine Kinase Src in Human Pancreatic Carcinoma

Manfred P. Lutz,* I. B. Silke Eßer,* Berenike B. M. Flossmann-Kast,* Roger Vogelmann,* Hardi Lührs,* Helmut Friess,† Markus W. Büchler,† and Guido Adler*

*Department of Internal Medicine I, University of Ulm, 89070 Ulm, Germany; and †Department of Visceral and Transplantation Surgery, University of Bern, 3010 Bern, Switzerland

Received December 19, 1997

Src family tyrosine kinases participate in the regulation of cell adhesion, cell growth and differentiation. Here, we examine for the first time the potential role of Src for growth regulation of human pancreatic carcinoma cells. By immunohistochemical analysis, Src was overexpressed in 13/13 pancreatic carcinoma tissue but not in 6 normal pancreatic tissue specimen. In Western blots of total cellular extracts, Src protein expression was elevated in 14/17 carcinoma cell lines as compared to normal pancreas or cultured human pancreatic duct cells. Kinase activity was only detectable in cancer cells and did not correlate with the amount of kinase protein or with the expression of the regulatory kinase Csk, indicating that Src is not regulated through protein expression or through expression of Csk. The Src-specific tyrosine kinase inhibitor herbimycin A decreased cell growth in a dose-dependent manner. We suggest that Src family kinases participate in growth regulation of pancreatic cancer cells. © 1998 Academic Press

Knowledge of pancreatic cancer growth control is still limited although many molecular changes have been reported which partly explain the aggressive nature of this tumor. These changes include loss of function of the tumor suppressor genes p53, DCC and DPC4, and activating mutations of the proto-oncogene K-ras in at least 70% of pancreatic tumors (1-5). In addition, most of pancreatic cancers examined overexpress a number of tyrosine kinase growth factor receptors (6-8). In analogy to colon cancer or to breast cancer, it has been speculated that some of these changes contribute to rapid tumor growth, invasion or metastasis (9).

Reversible phosphorylation of signal transducing proteins on tyrosine residues is a well recognized mechanism of cellular growth control. Tyrosine phosphorylation events are catalyzed by two major groups of protein tyrosine kinases. One group are transmembrane kinases which act as receptors for various growth factors and directly modulate substrate proteins by phosphorylation through their catalytic intracellular domain (10). A second group of tyrosine kinases is located within the cytosol and acts as intermediate intracellular signal transducing proteins. Representatives of this latter category are the Src family tyrosine kinases, which are enzymes with high structural similarity coupling to and transducing signals from growth factor receptors, G protein-coupled receptors and adhesion molecules. At least nine members of this kinase family are known to date and most of them are expressed predominantly in hemopoetic cells. Only the four members Src, Yes, Fyn, and Lyn could be demonstrated in other tissues so far (11). In fibroblasts, kinase-activated Src-mutants are able to act as transforming oncogene, indicating the potential of Src for growth regulation (12). In addition, infection of rat colon with retroviral *v-src* induces dysplasia, and cotransfection with *v-myc* induces carcinoma (13). Based in part on this evidence, it has been speculated, that upregulation of the Src kinase is important for growth and transformation of intestinal epithelial cells (14). The potential role of Src in pancreatic cancer has not been examined.

Therefore, the purpose of this study was to determine whether the tyrosine kinase Src might play a role in pancreatic tumor growth regulation. We now report, that Src is overexpressed in human pancreatic carcinoma tissue as compared to normal pancreas. In addition, Src is activated in many cultured pancreatic carcinoma cells and cell growth is inhibited by herbimycin A, a Src kinase inhibitor, demonstrating the potential role of Src in regulation of pancreatic cancer cell proliferation.

MATERIAL AND METHODS

Tissue and cell lines. Human pancreatic cancer tissue samples were obtained from thirteen patients undergoing surgical resection for pancreatic adenocarcinoma after written informed consent. Nor-

0006-291X/98 $25.00

mal pancreatic tissue samples were taken from 2 previously healthy multi organ donors in which no recipient for pancreatic transplantation was present at the time of explantation or from normal tissue adjacent to the tumor (n=4). The studies were approved by the human ethics comittees of the Universities of Ulm, Germany, and Bern, Switzerland. Short term cultivated human pancreatic cells, IMIM-PC-2, MS40-II, Sk-PC-2, and Hs766t cells were a gift of F.X.Real (Barcelona, Spain) (15). PC-2, PC-3 cells were a gift of H. P. Elsässer (Marburg, Germany). The human pancreatic carcinoma cell lines PaTu 8988s, PaTu 8988t and PaTu 8902 as well as the colon carcinoma cell line Colo 320 were from the 'Deutsche Sammlung für Mikroorganismen' (Braunschweig, Germany). The cell lines HPAF and AsPC 1 were from the American Type Culture Collection (Rockville, MD). DanG, Capan-1, Capan-2, and the colon carcinoma cell line CaCo 2 were from the 'Deutsches Krebsforschungszentrum' (Heidelberg, Germany), and MIA Paca 2 and PANC-1 cells were from the European Collection of Animal Cell Cultures (Salisbury, U.K.). Cells were maintained under standard culture conditions in Dulbecco's modified eagle medium with high glucose and with 10% fetal calf serum.

Immunohistochemistry. Paraffin-embedded tissue sections (3-4 μm) of human pancreatic tumor tissue and normal pancreas were deparaffinized and endogenous peroxidase activity was quenched using 0.2% hydrogen peroxide in methanol. After rehydration, unspecific binding was blocked with 1% bovine serum albumine. Polyclonal sheep Src antiserum (1:100, Affiniti, Exeter, UK) in phosphate-buffered saline containing 0.5% bovine serum albumine was added for 60 min. Rabbit anti sheep peroxidase-coupled secondary antibody and the diaminobenzidine reaction (1 mg/ml diaminobenzidine in 0.02% hydrogen peroxide) were used to detect antibody binding. Three washing steps in phosphate buffered saline containing 0.05% Tween 20 were performed between primary and secondary antibody incubations. Counterstaining was performed by incubation with hematoxylin for 5 min.

Protein extraction, immunoprecipitation, and in vitro kinase assay. Cell cultures in the logarithmic phase of cell growth were rinsed twice with ice-cold phosphate-buffered saline, and were harvested mechanically by scraping into phosphate-buffered saline. The immunoprecipitation and kinase assay were performed following the procedure described by Bolen et al. (16). Briefly, pelleted cells were lysed in 50 mM Tris-HCL, pH 8.0, 150 mM sodium chloride, 2 mM EDTA, 1% NP40, 1 mM sodium orthovanadate, 10 μg/ml aprotinin, 10 μg/ml leupeptin, 0.5 μg/ml pepstatin A, 5 mM sodium fluoride, 1 mM phenylmethylsulfonyl fluoride and 10 μg/ml soybean trypsin inhibitor. Lysates were cleared by centrifugation at 13.000 × g for 3 min. Protein determinations were performed using the Bradford method (BioRad, München, Germany) with bovine serum albumin as standard. Lysate containing 200 μg of protein was incubated with excess of monoclonal anti-Src antibody (Clone 327, Dianova, Hamburg, Germany) for 1 hour at 4°C and with rabbit anti-mouse preincubated protein G-plus agarose. The immunoprecipitates were washed three times with ice-cold lysis buffer, and once with ice-cold kinase reaction buffer (20 mM MOPS, pH 7.0, 15 mM magnesium chloride). The phosphorylation was initiated by adding 5 μM [γ-^{32}P]ATP (10 μCi per reaction) in 25 μl reaction buffer with 1 μg acid-denatured rabbit muscle enolase (Boehringer, Mannheim, Germany) for 15 min. The reaction was stopped by adding sodium dodecylsulfate-containing sample buffer and proteins were resolved by gel electrophoresis in 8.75 % sodium dodecylsulfate polyacrylamide gels. The gels were stained with Coomassie brilliant blue to ensure that equal amounts of enolase were present, and labeled proteins were detected autoradiographically on KODAK X-OMAT AR Films. Under these conditions, the amount of kinase activity measured was linearly related to the amount of protein extract used for immunoprecipitation.

Western blotting. Lysates were separated in 8.75 % sodium dodecylsulfate polyacrylamide gels. Separated proteins were transferred to PVDF Membranes (Immobilon P, Sigma, Deisenhofen, Germany) by semi dry blotting. Membranes were blocked over night at room temperature in blocking buffer (10 mM Tris-HCl, pH 7.2, 150 mM sodium chloride, containing 2% bovine serum albumin and 0.1% Tween 20). After three washes for 10 min with 10 mM Tris-HCl, pH 7.2, 150 mM sodium chloride, 0.2% Tween 20, membranes were incubated with clone 327 (1:1000) or with anti-Csk monoclonal antibody (1:500, Transduction Laboratories, Lexington, KY) in blocking buffer. After three washing steps, horse radish peroxidase-coupled secondary antibody was added for one hour in blocking buffer. Antibodies were visualized after three additional washing steps using the ECL technique (Amersham, Buckinghamshire, England).

Growth inhibition assays. Cells were plated in 96-well plates at a density of 10,000 cells per well. After culture in standard medium for 24 hours, herbimycin A was added as indicated. Control cells were incubated with the appropriate concentrations of the carrier DMSO. After 72 hours, cell number was estimated using the tetrazolium salt (MTT) assay (17). Briefly, cells were incubated for 150 min in phosphate buffered saline containing 5 mg/ml MTT. After three washes in phosphate-buffered saline, the precipitated formazan was solubilized over night in 50% dimethylformamide containing 1% acetic acid, 1% hydrochloric acid, and 10% sodium dodecylsulfate. The absorption was measured at 570 nm and results were calculated relative to control cells which had been grown without inhibitor or carrier substance. For comparison, cell numbers were counted in several experiments and did yield similar results.

RESULTS

Immunostaining of Src in Pancreatic Tumor Tissue

Src protein expression was examined in 13 ductal adenocarcinomas, in 2 normal pancreatic tissue specimens and in normal tissue adjacent to the tumor mass of patients 8, 9, 12 and 13. As demonstrated in Fig. 1A, faint cytoplasmic staining for Src was observed in a normal tissue specimen and in normal tissue of patient # 9, 12 and 13 in less than 2 % of the acinar cells and Src positive cells were located mainly around ductular structures. Src was not detectable in another normal tissue specimen and in normal tissue of patient # 8. As illustrated in Fig. 1, all of the examined tumors did show strong cytoplasmic staining of more than 10 % of the tumor cells (Table 1) with only occasional staining of non-tumor cells. Src expression did not correlate with tumor stage or with differentiation.

Protein Expression and Kinase Activity of Src Pancreatic Tumor Cell Lines

To examine the regulation of Src, protein expression and kinase activity was examined in a panel of 17 human pancreatic cancer cell lines with ductular cell morphology. Primary cultures of pancreatic cells from human organ grafts which develop a ductal phenotype after various time periods and two colon carcinoma cell lines known to express the activated Src kinase were used as controls (15; 18).

Src protein expression was detected in 14 of the 17 tumor cell lines tested, and kinase activity was elevated in 12 of them (Fig. 2). Kinase protein was undetectable in the normal pancreatic tissue extracts, and a minor amount was expressed only in one of the three

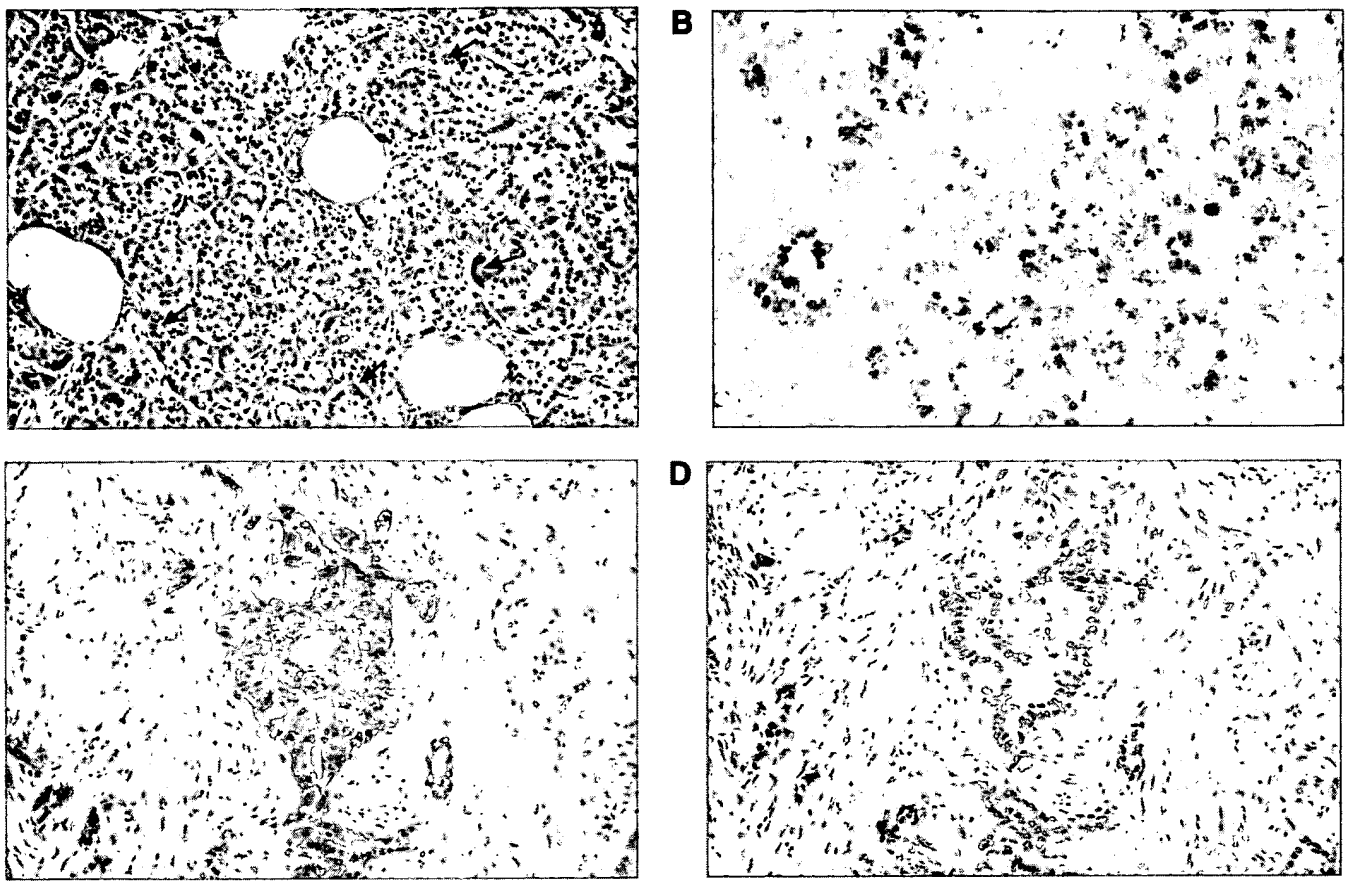

FIG. 1. Expression of Src in pancreatic tissue. Immunohistochemical staining of paraffin embedded normal pancreas demonstrating faint cytoplasmatic staining of less than 1% of the exocrine cells is shown in panel A. Pancreatic carcinoma specimen of patients 11 (B) and 1 (C) demonstrate +++ (patient 11) or ++++ (patient 1) expression of Src. Panel D demonstrated background staining using secondary antibody alone. Magnification was × 200 (A, C, D) or × 400 (B).

short term cultures of epithelial pancreatic cells. Significant kinase activity could be detected in none of them. Kinase activity and protein expression were regulated in a parallel fashion in both colon cancer cell lines as well as in PaTu 8988s and t, PC-2, MIA Paca-2, PANC-1, HPAF and in Hs766t cells, whereas in the remaining 10 cell lines kinase activity was independent from protein levels. Src protein expression and kinase activities were quantified densitometrically to calculate correlation coefficients. Src activity levels did not correlate with protein expression (correlation coefficient = 0.2). The C-terminal Src kinase Csk is a major regulatory protein for Src activity. Therefore, expression of Csk was determined in Western blots (Fig. 2C) and quantified densitometrically. We did not find significant correlation of Csk expression and relative Src activity (correlation coefficient = −0.2).

Inhibition of Cell Growth by Herbimycin A

Herbimycin A inhibits Src kinase activity *in vitro* as well as *in vivo*. The effect of herbimycin A on cell proliferation is demonstrated in Fig. 3. Exposure of cells to herbimycin A decreased cell numbers with similar efficacy in all four cell lines tested. The effect of growth inhibition was significant after 2 days of incubation and reached 56% ± 3.5% for PaTu 8988s cells, 60% ± 5.6% for PaTu 8988t cells, 79% ± 1.4% for PC 2 cells, and 76% ± 0.7 % for PC 3 cells after three days of exposure to the drug. The potency of growth inhibition was dependent on the level of activity of the Src kinase. In PaTu 8988s, PC 2, and PC 3 cells, which do express relevant kinase activity, growth was inhibited with IC_{50}'s of 60 ng/ml, 20 ng/ml, and 50 ng/ml, respectively. In contrast, growth of the cell line PaTu 8988t which has barely detectable levels of Src kinase was inhibited at halfmaximal concentrations of above 350 ng/ml and maximal inhibition was not reached at 2,000 ng/ml. After incubation with concentrations of up to 2000 ng/ml of the inhibitor for four days, more than 95% of the cells were viable and did exclude trypan blue. The effects of herbimycin A were reversible, i.e. cells could be trypsinized and subcultured after removal of the inhibitor and addition of standard culture medium for 24 hours.

TABLE 1

Src Kinase Expression Levels in Pancreatic Tumor Tissue

Patient #	Age (years)	TNM stage	Tumor grading	Src expression (positive tumor cells)
1	55	T2 N1 M1	2	+++
2	71	T2 N0 M0	2	+++
3	53	T2 N1 M0	2	++++
4	64	T3 N1 M0	3	++++
5	70	T2 N0 M0	2	++++
6	53	T2 N1 M1	2	++++
7	55	T3 N0 M0	2	+
8	61	T1 N0 M0	1	+
9	55	T2 N1 M0	2	++
10	58	T3 N1 M0	2	+++
11	62	T2 N1 M0	3	++++
12	53	T2 N1 M0	2	+
13	74	T3 N1 M0	2	++
normal tissue (n = 6)				less than 2% positive acinar cells

Paraffin-embedded exocrine pancreatic carcinoma tissue sections were stained immunohistochemically for Src. The percentage of Src-positive tumor cells is indicated as + (10–20% positive cells), ++ (21–40%), +++ (41–60%), and ++++ (61–80%). Tumors were graded according to standard pathological criteria with well differentiated tumor graded 1, and undifferentiated tumors graded 3. TNM stage was established from surgical specimen using UICC criteria. Controls were normal pancreatic tissue specimen (n = 2) or normal pancreatic tissue adjacent to tumor tissue of patients 8, 9, 12 and 13.

DISCUSSION

Members of the Src-kinase family participate in the control of a variety of cellular functions, including the response to various polypeptide growth factors or the regulation of the cellular cytoskeleton. Activated Src stimulates cell growth and may act as transforming oncogene (11). Our results indicate, that the tyrosine kinase Src is overexpressed in malignant pancreatic tissue as compared to adjacent normal tissue. In addition, expression of Src is increased in neoplastic cell lines as compared to primary cultures of normal human pancreatic cells with ductular differentiation and the kinase is activated in neoplastic cells only. Therefore, pancreatic tumor cells seem to possess a specific mechanism of kinase regulation.

Src kinase activity may be regulated either by changing protein expression or by specific regulation of kinase activity (11). A parallel increase or decrease in Src expression and activity was observed only in 6/17 cell lines. Overall, levels of kinase activity did not correlate with the abundance of the kinase protein and activation of Src in pancreatic carcinoma cells therefore was not regulated by protein expression. Regulation of Src has been extensively studied and a mechanism of inactivation by phosphorylation and by phosphorylation-dependent folding of the protein was suggested (19). According to this model, phosphorylation of Src on Tyr-527 by Csk or Csk-like kinases results in intramolecular binding of this residue to the SH2 domain. Folding is further stabilized by interaction of the SH3 domain with an unidentified region of the protein and the folded kinase is thought to be unable to couple to downstream signaling proteins. Repression of Src family kinase activity is critically dependent on phosphorylation by Csk. Deletion of Csk results in markedly increased Src kinase activity (20), whereas overexpression inhibits Src kinase activity (21). In the present study, Csk expression and relative Src activity did not correlate. A role of Csk for the regulation of Src in pancreatic carcinoma therefore seems unlikely and the mechanisms of Src activation remain to be determined. Other regulating factors which could account for the upregulation of Src acitivity are overexpression of receptor tyrosine kinases like HER-2 or the epidermal growth factor receptor which are able to activate Src in mammary tumor cells or in fibroblasts (22; 23), or the activation of Ras which induces accumulation and increased activity of Src in transformed fibroblasts (24).

To investigate the role of Src for pancreatic tumor cell growth control, we examined the effects of the tyrosine kinase inhibitor herbimycin A, which is known to inhibit Src and Src-related kinases *in vivo* and *in vitro* by binding to their SH2 domains (25). Growth inhibition by herbimycin A correlated with the level of Src kinase activation. Cell lines with elevated kinase activity were inhibited with higher potency than the cell line PaTu 8988t, which expresses low levels of Src and barely detectable kinase activities. Similar observations have been made in colonic tumor cell lines, where herbimycin A decreased growth and Src kinase activities by over 40% at concentrations of 125 ng/ml, but was ineffective in cell lines derived from normal colonic tissue (26). Taken together with the observation that

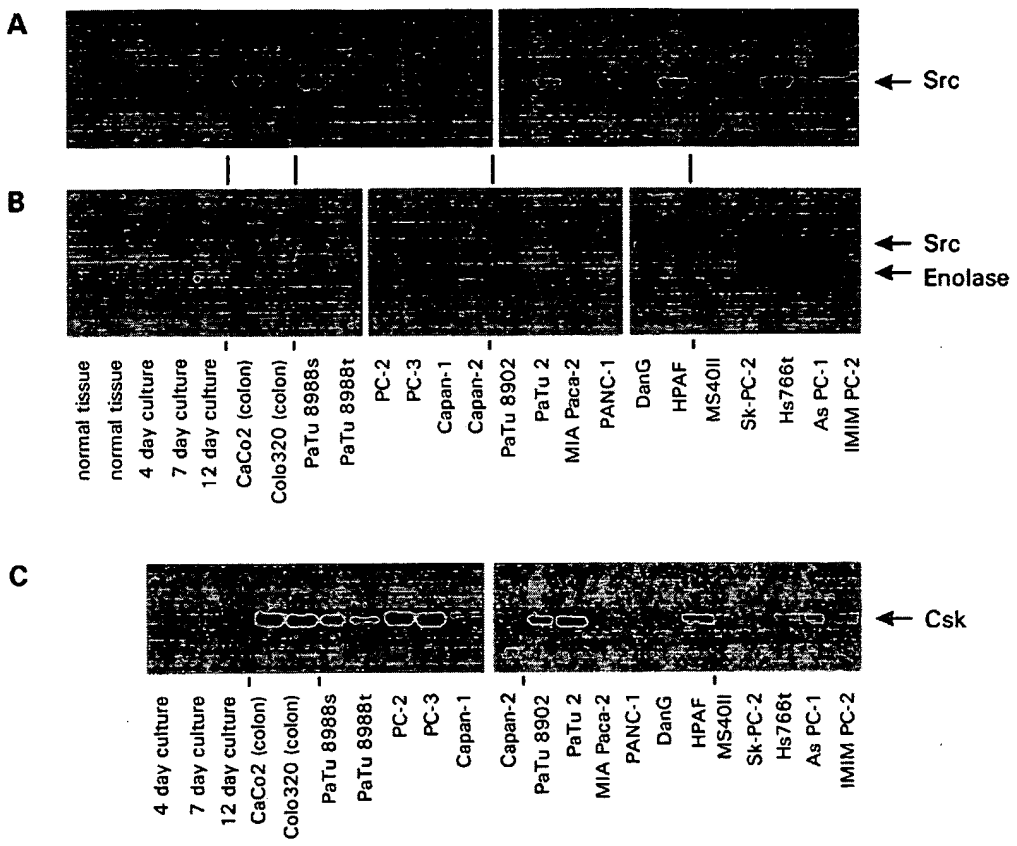

FIG. 2. Expression and activity of the tyrosine kinase Src (Panels A and B) and Expression of Csk (Panel C) in human pancreatic tissue, in short term cultures of human pancreatic cells with ductular morphology, in colon carcinoma cell lines, and in pancreatic tumor cell lines. Shown are representative Western blots of Src in total cellular extracts (A), autoradiograms of Src immunoprecipitation kinase assays demonstrating autophosphorylation of the kinase protein as well as phosphorylation of the substrate protein enolase (B), or Western blots of Csk in total cellular extracts (C).

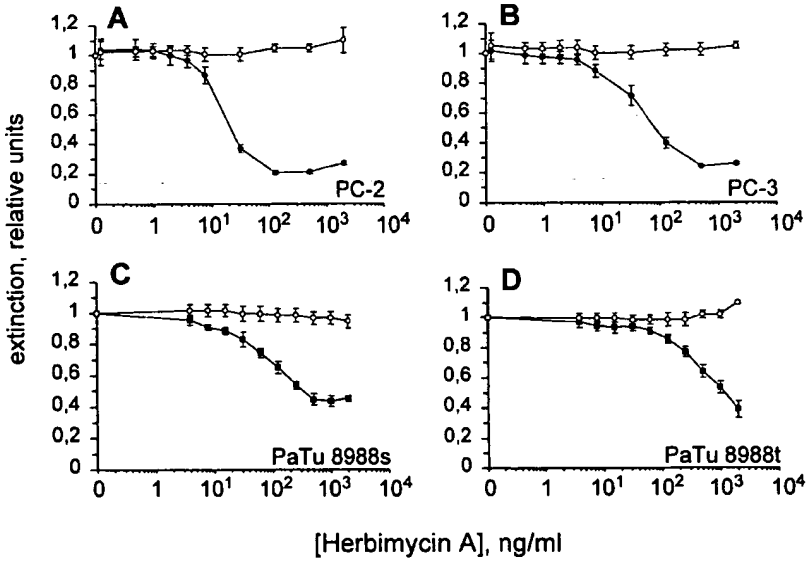

FIG. 3. Inhibition of Src kinase activity and cell growth by herbimycin A in the pancreatic carcinoma cell lines PC-2 (A), PC-3 (B), PaTu 8988s (C), and PaTu 8988t (D). Cell growth was measured using the tetrazolium salt method after three days of incubation with the inhibitor. Results are representative of at least three independent experiments.

Src is activated in malignant pancreatic cells and the ability of the activated kinase to function as transforming oncogenes, it seems likely that Src family kinases participate in growth control of pancreatic tumor cells. In addition, Src kinase activity is elevated in preneoplastic and in neoplastic lesions in a rat model of azaserin-induced pancreatic acinar cell tumors (27). Even though this model is not well suited for comparison since 95 % of human pancreatic carcinoma are of ductal phenotype, it supports similar observations in human colon tissue. During the progression of adenomatous lesions to colon cancer, Src and Yes kinase activities are elevated in large dysplastic adenoma with a high risk for cancer (28-30), and Src kinase activity is elevated in preneoplastic lesions in ulcerative colitis (31). These data indicate that Src likely participates in one of the early steps of intestinal carcinogenesis.

ACKNOWLEDGMENTS

We thank Tanja Wissling, Elke Wolff-Hieber, and Eliana Schacher for their excellent technical assistance. We thank F. X. Real for generously providing cultured human pancreatic cells. This work was supported by the Deutsche Forschungsgemeinschaft (Lu 441/2-1).

REFERENCES

1. Hahn, S. A., Schutte, M., Hoque, A. T., Moskaluk, C. A., da Costa, L. T., Rozenblum, E., Weinstein, C. L., Fischer, A., Yeo, C. J., Hruban, R. H., and Kern, S. E. (1996) *Science* **271**, 350–353.
2. Berrozpe, G., Schaeffer, J., Peinado, M. A., Real, F. X., and Perucho, M. (1994) *Int. J. Cancer* **58**, 185–191.
3. Simon, B., Weinel, R., Höhne, M., Watz, J., Schmidt, J., Kortner, G., and Arnold, R. (1994) *Gastroenterology* **106**, 1645–1651.
4. Kalthoff, H., Schmiegel, W., Roeder, C., Kasche, D., Schmidt, A., Lauer, G., Thiele, H. G., Honold, G., Pantel, K., Riethmuller, G., and et al (1993) *Oncogene* **8**, 289–298.
5. Rozenblum, E., Schutte, M., Goggins, M., Hahn, S. A., Panzer, S., Zahurak, M., Goodman, S. N., Sohn, T. A., Hruban, R. H., Yeo, C. J., and Kern, S. E. (1997) *Cancer Res.* **57**, 1731–1734.
6. Barton, C. M., Hall, P. A., Hughes, C. M., Gullick, W. J., and Lemoine, N. R. (1991) *J. Pathol.* **163**, 111–116.
7. Lemoine, N. R., Lobresco, M., Leung, H., Barton, C., Hughes, C. M., Prigent, S. A., Gullick, W. J., and Kloppel, G. (1992) *J. Pathol.* **168**, 269–273.
8. Bergmann, U., Funatomi, H., Yokoyama, M., Beger, H. G., and Korc, M. (1995) *Cancer Res.* **55**, 2007–2011.
9. Friess, H., Büchler, M., and Korc, M. (1996) *in* Pancreatic cancer : Molecular and clinical advances (Neoptolemos, J., and Lemoine, N. R., Eds.), pp. 51–60.
10. Schlessinger, J., and Ullrich, A. (1992) *Neuron* **9**, 383–391.
11. Brown, M. T. and Cooper, J. A. (1996) *Biochim. Biophys. Acta* **1287**, 121–149.
12. Cooper, J. A., Gould, K. L., Cartwright, C. A., and Hunter, T. (1986) *Science* **231**, 1431–1434.
13. D'Emilia, J. C., Mathey-Prevot, B., Jaros, K., Wolf, B., Steele, G., Jr., and Summerhayes, I. C. (1991) *Oncogene* **6**, 303–309.
14. Park, J., and Cartwright, C. A. (1995) *Mol. Cell. Biol.* **15**, 2374–2382.
15. Vila, M. R., Lloreta, J., and Real, F. X. (1994) *Lab. Invest.* **71**, 423–431.
16. Bolen, J. B., Thompson, P. A., Eiseman, E., and Harak, I. D. (1991) *Adv. Cancer Research* **72**, 103–149.
17. Hansen, M. B., Nielsen, S. E., and Berg, K. (1989) *J. Immunol. Meth.* **119**, 203–210.
18. Bolen, J. B., Veillette, A., Schwartz, A. M., DeSeau, V., and Rosen, N. (1987) *Proc. Natl. Acad. Sci. U.S.A.* **84**, 2251–2255.
19. Roussel, R. R., Brodeur, S. R., Shalloway, D., and Laudano, A. P. (1991) *Proc. Natl. Acad. Sci. U.S.A.* **88**, 10696–10700.
20. Imamoto, A., and Soriano, P. (1993) *Cell* **73**, 1117–1124.
21. Della, R. G., van, B. T., Daaka, Y., Luttrell, D. K., Luttrell, L. M., and Lefkowitz, R. J. (1997) *J. Biol. Chem.* **272**, 19125–19132.
22. Muthuswamy, S. K., Siegel, P. M., Dankort, D. L., Webster, M. A., and Muller, W. J. (1994) *Mol. Cell. Biol.* **14**, 735–743.
23. Osherov, N., and Levitzki, A. (1994) *Eur. J. Biochem.* **225**, 1047–1053.
24. Topol, L. Z., Kisseljova, N. P., Gutierrez, M. L., Deichman, G. I., Musatkina, E. A., Shtutman, M. S., Zakamaldina, T. Z., Blair, D. G., and Tatosyan, A. G. (1993) *Mol. Çarcinog.* **8**, 167–176.
25. Fukazawa, H., Li, P. M., Yamamoto, C., Murakami, Y., Mizuno, S., and Uehara, Y. (1991) *Biochem. Pharmacol.* **42**, 1661–1671.
26. Garcia, R., Parikh, N. U., Saya, H., and Gallick, G. E. (1991) *Oncogene* **6**, 1983–1989.
27. Visser, C. J., Rijksen, G., Woutersen, R. A., and De Weger, R. A. (1996) *Lab. Invest.* **74**, 2–11.
28. Pena, S. V., Melhem, M. F., Meisler, A. I., and Cartwright, C. A. (1995) *Gastroenterology* **108**, 117–124.
29. Cartwright, C. A., Meisler, A. I., and Eckhart, W. (1990) *Proc. Natl. Acad. Sci. U.S.A.* **87**, 558–562.
30. Talamonti, M. S., Roh, M. S., Curley, S. A., and Gallick, G. E. (1993) *J. Clin. Invest.* **91**, 53–60.
31. Cartwright, C. A., Coad, C. A., and Egbert, B. M. (1994) *J. Clin. Invest.* **93**, 509–515.

pp60$^{c\text{-}src}$ Activation in Hepatocellular Carcinoma of Humans and LEC Rats

TSUTOMU MASAKI,[1,4] MASATO OKADA,[2] YASUSHI SHIRATORI,[1] WILLIAM RENGIFO,[1] KOZOU MATSUMOTO,[3] SHINN MAEDA,[1] NAOYA KATO,[1] FUMIHIKO KANAI,[1] YUTAKA KOMATSU,[1] MIKIO NISHIOKA,[4] AND MASAO OMATA[1]

For the related Src kinases, a close correlation exists between elevated tyrosine kinase activity and cell transformation. However, the involvement of pp60$^{c\text{-}src}$ in hepatocellular carcinoma (HCC) remains obscure. The aim of this study was to evaluate whether pp60$^{c\text{-}src}$ tyrosine kinase activity is elevated in HCC. We analyzed the kinase activity of pp60$^{c\text{-}src}$ in normal liver tissue, chronic hepatitis liver tissue, and tumorous and adjacent nontumorous portions of HCC tissue from patients and Long–Evans cinnamon (LEC) rats that are known to develop liver cancer spontaneously. The kinase activity of pp60$^{c\text{-}src}$ was rarely detected in the normal human liver tissue and chronic hepatitis liver tissue, but it was elevated in tumorous and nontumorous portions of HCC tissue. Furthermore, the kinase activity of pp60$^{c\text{-}src}$ was significantly elevated in tumorous tissues compared with nontumorous tissues. The kinase activity of pp60$^{c\text{-}src}$ was also higher in poorly differentiated HCC. In addition, the kinase activity of pp60$^{c\text{-}src}$ increased proportionately with the development of HCC of LEC rats. Our results suggest that activation of the protooncogene product pp60$^{c\text{-}src}$ may play an important role in the malignant transformation of hepatocytes in human and LEC rats, and that it may be closely related to the histopathological grading of human HCC. (HEPATOLOGY 1998;27:1257-1264.)

Hepatocellular carcinoma (HCC) is thought to develop through a multistep process.[1] A long history of viral hepatitis or prolonged exposure to environmental toxins predisposes liver cells to mutations of genes critical in the control of hepatocyte growth. In fact, both activation of cellular oncogenes and inactivation of tumor-suppressor genes are involved in HCC. Activation of oncogenes by hepatitis virus integration has been shown in the woodchuck animal model,[2,3] although its significance in hepatocarcinogenesis in humans and in Long–Evans cinnamon (LEC) rats is still under investigation. A large number of cellular protein tyrosine kinase (PTK) genes have been cloned and sequenced. These kinases are classified into two major groups: the first comprises growth factor receptor tyrosine kinases; the second includes retroviral protein PTKs and their cellular homologues.[4] The main representatives of the latter group are non–receptor-linked and –membrane-associated *src*-related tyrosine kinases.[5] At least nine *src*-related tyrosine kinases have been identified. These include c-*src*, c-*yes*, c-*lck*, c-*fyn*, c-*hck*, c-*lyn*, c-*blk*, c-*fgr*, and c-*yrk* protooncogene products.[6] All members of the PTK *src* family have a molecular weight ranging between 55 and 62 kd and myristoylated glycine residues at the amino termini.[7,8] Among these PTKs, the protooncogene pp60$^{c\text{-}src}$ is the cellular homologue of the Rous sarcoma transforming gene, v-*src*.[9] Both c-*src* and v-*src* encode 60-kd, membrane-associated PTKs. For pp60$^{c\text{-}src}$, a close correlation exists between elevated activity of tyrosine kinase and cell transformation.[10-17] Bolen et al.[10-12] reported high kinase activity of pp60$^{c\text{-}src}$ in several types of human malignancies including colon carcinoma, breast adenocarcinomas, rhabdomyosarcomas, and neuroblastoma. We know that pp60$^{c\text{-}src}$ expression and activity are increased in a limited number of cases in human tumors. However, the role of pp60$^{c\text{-}src}$ in hepatocarcinogenesis in humans and LEC rats has not been investigated. In the present study, we determined the activity of pp60$^{c\text{-}src}$ in human HCC by measuring the *in vitro* protein kinase activity of pp60$^{c\text{-}src}$ using liver tissues of normal liver (NL) and chronic hepatitis (CH), tumorous (T), and adjacent nontumorous (N) cirrhotic liver tissue samples. We also investigated the relationship between pp60$^{c\text{-}src}$ kinase activity and histological grade of human HCC. Furthermore, we investigated the role of kinase activity of pp60$^{c\text{-}src}$ in the development of HCC in LEC rats, an animal model of HCC.[18-25]

MATERIALS AND METHODS

Materials

Human Tissues. Tissue samples, including T and the surrounding N cirrhotic tissue, were obtained during surgery from 20 patients with HCC. Three NL tissues were obtained from surgical cases of liver metastases of colon cancer. Liver tissue samples from 5 patients with CH were obtained during surgery or by liver biopsy. Tissues were frozen immediately at −70°C. The experimental protocol was

Abbreviations: HCC, hepatocellular carcinoma; LEC rats, Long–Evans cinnamon rats; PTK, protein tyrosine kinase; NL, normal liver; CH, chronic hepatitis; T, tumorous; N, nontumorous; mAb 327, monoclonal antibody to pp60$^{c\text{-}src}$; sc-19, rabbit polyclonal antibody specific for *src*-related tyrosine kinases; TNE buffer, 10 mmol/L Tris HCl (pH 7.5), 1 mmol/L ethylene glycol-bis(β-aminoethyl ether)*N,N,N ,N* ,tetraacetic acid, 150 mmol/L NaCl, 1 mmol/L Na_3VO_4, 50 mmol/L Na_2MoO_4, 1% Nonidet P-40, and 100 U/mL aprotinin; SDS, sodium dodecyl sulfate; PAGE, polyacrylamide gel electrophoresis; LC, liver cirrhosis; Csk, C-terminal Src kinase.

From the [1]Second Department of Internal Medicine, Faculty of Medicine, University of Tokyo, Tokyo, Japan; [2]Division of Protein Metabolism, Institute for Protein Research, Osaka University, Suita, Osaka, Japan; [3]Institute for Animal Experimentation of University of Tokushima School of Medicine, Kuramoto, Tokushima, Japan; and [4]Third Department of Internal Medicine, Ikenobe Miki-cho, Kagawa, Japan.

Received July 7, 1998; accepted January 1, 1998.

Supported by a Grant-in-Aid for Scientific Research from the Ministry of Education, Science and Culture of Japan.

Address reprint requests to: Yasushi Shiratori, M.D., Ph.D., Second Department of Internal Medicine, Faculty of Medicine, The University of Tokyo, 7-3-1 Hongo, Bunkyo-ku, Tokyo 113, Japan. Fax: 81-3-3814-0021.

0270-9139/98/2705-0011$3.00/0

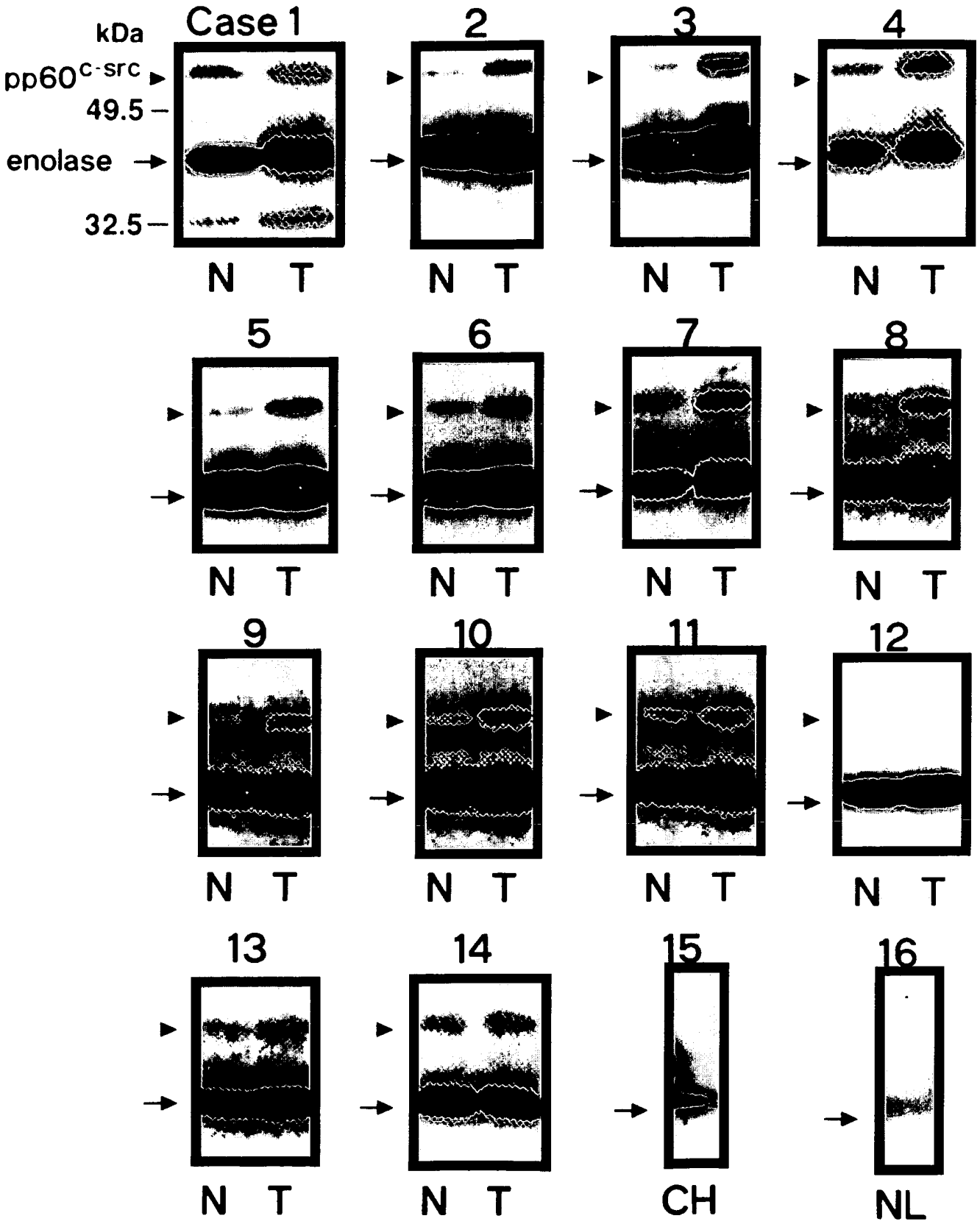

FIG. 1. Protein kinase activity of pp60$^{c\text{-}src}$ in NL, CH, N, and T portions of human HCC. Samples of N and T tissues of each patient are shown. Lysates containing 100 g of total cellular protein were prepared as described in Materials and Methods. The protein was precipitated with excess pp60$^{c\text{-}src}$ antibody, incubated for 10 minutes at 30°C with [γ-^{32}P]-adenosine triphosphate and acid-denatured rabbit muscle enolase; the protein was then resolved on 10% SDS-polyacrylamide gels. *Arrowheads* indicate bands corresponding to pp60$^{c\text{-}src}$ tyrosine phosphorylation; *arrows* indicate bands corresponding to enolase.

approved by the Human Subjects Committee of Kagawa Medical School.

Animal Tissue. Inbred LEC and Wistar rats were bred under specific pathogen-free conditions in the Institute for Animal Experimentation at the University of Tokushima School of Medicine. Wistar rats were used as controls. The experimental protocol was approved by the Animal Care Committee at our institution.

Chemicals. The monoclonal antibody to pp60$^{c\text{-}src}$ (mAb 327) and rabbit polyclonal antibody specific for src-related tyrosine kinases (clone, sc-19) were purchased from Oncogene Science Co., Ltd. (Tokyo, Japan) and Santa Cruz Biotechnology, Inc. (Tokyo, Japan), respectively. These antibodies react with pp60$^{c\text{-}src}$ of mouse, rat, and human origin by Western blot and immunoprecipitation analysis; they are not cross-reactive with other tyrosine kinases.[10-17,26,27] Chemicals were purchased from Sigma Chemical Co. (Tokyo, Japan) or Wako Pure Chemical Co. (Tokyo).

Tissue Lysates. The tissue samples were frozen on dry ice within 20 minutes of collection. The samples were homogenized in TNE buffer (10 mmol/L Tris HCl [pH 7.5], 1 mmol/L ethylene glycol-bis[β-aminoethyl ether]*N,N,N′,N′*,tetraacetic acid, 150 mmol/L NaCl, 1 mmol/L Na_3VO_4, 50 mmol/L Na_2MoO_4, 1% Nonidet P-40, and 100 U/mL aprotinin) and centrifuged at 29,000*g* for 60 minutes at 4°C. The protein concentration was measured in tissue lysates by the bicin choninic acid protein assay.

Gel Electrophoresis and Western Blot Analysis. Sodium dodecyl sulfate (SDS)–polyacrylamide gel electrophoresis (PAGE) was performed according to the method of Laemmli.[28] Western blot analysis was performed according to the method of Towbin et al.,[29] using horseradish peroxidase–linked secondary antibody. Immunoreactive proteins were visualized with an enhanced chemiluminescence detection system (Amersham) on radiographic film. The exposure times in the enhanced chemiluminescence method were 30 seconds at room temperature in all samples.

Immune Complex Protein and Tyrosine Kinase Assay of pp60$^{c\text{-}src}$. Aliquots of lysate containing 100 μg of cellular protein were incubated with mAb 327,[26] or with sc-19, with pp60$^{c\text{-}src}$, and then with 5 μg of affinity-purified rabbit antibody to mouse immunoglobulin G as described.[30-33] After adsorbing to pansorbin, the immunoprecipitates were washed five times with TNE buffer and twice with a kinase assay buffer (in mmol/L, 50 Tris HCl [pH 7.4], 3 $MnCl_2$, and 0.1 Na_3VO_4). In kinase assay, immunoprecipitate gained from 100 μg of total proteins, 1.0 μg of acid-treated enolase, and 4 nmol/0.74 MBq of [γ-^{32}P]adenosine triphosphate were included in 25 L of kinase assay buffer. Phosphorylation was allowed to proceed at 30°C for 10 minutes, and phosphoproteins were resolved by SDS-PAGE (10% polyacrylamide gel) followed by autoradiography or image analysis by a BAS 2000 system (Fuji film). The kinase activity of pp60$^{c\text{-}src}$ in each sample was obtained by averaging three measurements for each sample.

Histological Grade of HCC. Tumors were classified into three grades—well, moderately, and poorly differentiated—according to the grading system of The Liver Cancer Study Group of Japan.[34] These grades correspond with Edmondson I, Edmondson II or Edmondson III with a trabecular pattern, and Edmondson III without a trabecular pattern, respectively, of the criteria established by Edmondson and Steiner.[35] The selected grade was based on the predominant histopathological features.

Statistical Analysis. Data were expressed as means ± SEM. The significance of the differences between observations in Figs. 2 and 5 was determined with the Student's *t* test and Scheffé's Multiple Comparison Test, respectively. Statistical significance was set at $P < .05$.

RESULTS

Protein Kinase Activity of pp60$^{c\text{-}src}$ in the N and T Portions of Human HCC and CH Liver Tissues. To study protein kinase activity of pp60$^{c\text{-}src}$ in the N and T portions of HCC, we prepared lysates of tissue samples, precipitated protein with a monoclonal antibody specific for pp60$^{c\text{-}src}$, and measured the phosphorylation of pp60$^{c\text{-}src}$ and exogenous substrate, enolase, using an *in vitro* protein kinase assay. Activity of pp60$^{c\text{-}src}$ in representative HCC (patients 1-14), CH (patient 15), and NL (patient 16) tissue is shown in Fig. 1. In Fig. 1, considering the electrophoretic mobility and the previous studies,[10-17,36] the upper and lower bands can be thought to represent pp60$^{c\text{-}src}$ (mol wt 60 kd) and enolase (mol wt 42 kd), respectively. The mean of pp60$^{c\text{-}src}$ activity in the T tissues of these patients was 5.3 ± 4.2 or 1.7 ± 0.37 times higher than the activity level in the N tissue, as measured by autophosphorylation ($P < .001$) or enolase phosphorylation ($P < .01$), respectively (Fig. 2). Patients 1 to 4 and 5 to 11 were classified as poorly and moderately differentiated HCC, respectively, whereas the remaining patients (12 to 14) were classified as well-differentiated HCC. In addition, the pp60$^{c\text{-}src}$ activity in NL tissue (Fig. 1, patient 16) and CH (Fig. 1, patient 15) was very low as measured by autophosphorylation or enolase phosphorylation (Fig. 1). Thus, pp60$^{c\text{-}src}$ activity was high in human liver tissue with malignancy. In cases 1, 8, and 10 of Fig. 1, the faint phosphorylated bands other than the bands of 60-kd pp60$^{c\text{-}src}$ and 42-kd enolase probably represent ^{32}P uptake of the degradation products.

Amount of pp60$^{c\text{-}src}$ in N and T Portions of Human HCC, CH, and NL Tissues. Protein levels of pp60$^{c\text{-}src}$ were determined by immunoblot analysis. Antibody to pp60$^{c\text{-}src}$ immunoprecipitates, performed on lysates used for protein kinase assays, were resolved by SDS-PAGE before transfer to nitrocellulose membrane. Results from patients 1 to 16 are shown in Fig. 3. Three proteins were detected in each lane. The upper protein was pp60$^{c\text{-}src}$, the middle was mAb 327 heavy-chain immunoglobulin, and the lower protein was mAb 327 light-chain immunoglobulin.[14-17] We have also performed an additional experiment using the samples obtained from case 2 to confirm that the upper band obtained by Western blot analysis represented pp60$^{c\text{-}src}$ and that the two lower bands

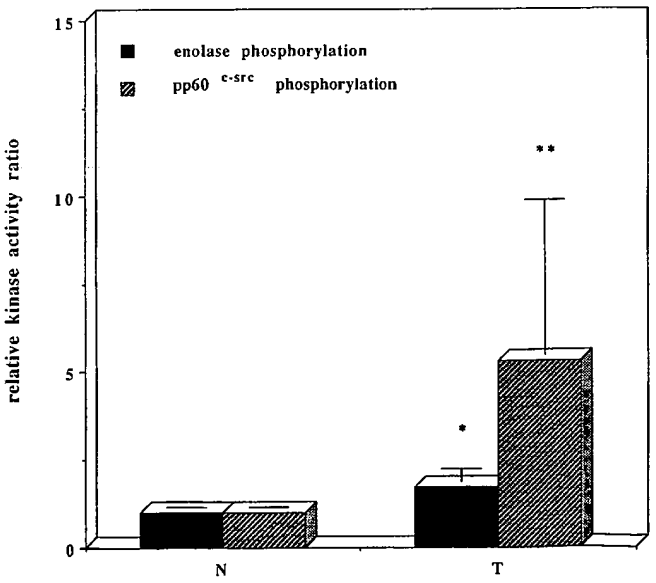

FIG. 2. The relative levels of total activity of pp60$^{c\text{-}src}$ tyrosine kinase. The total activity of pp60$^{c\text{-}src}$ in the T tissues was significantly higher than that in the N tissue (n = 20) when measured by enolase phosphorylation (■) and autophosphorylation (▨). Values represent the mean ± SEM of pp60$^{c\text{-}src}$ activity for each group. *$P < .01$; and **$P < .001$.

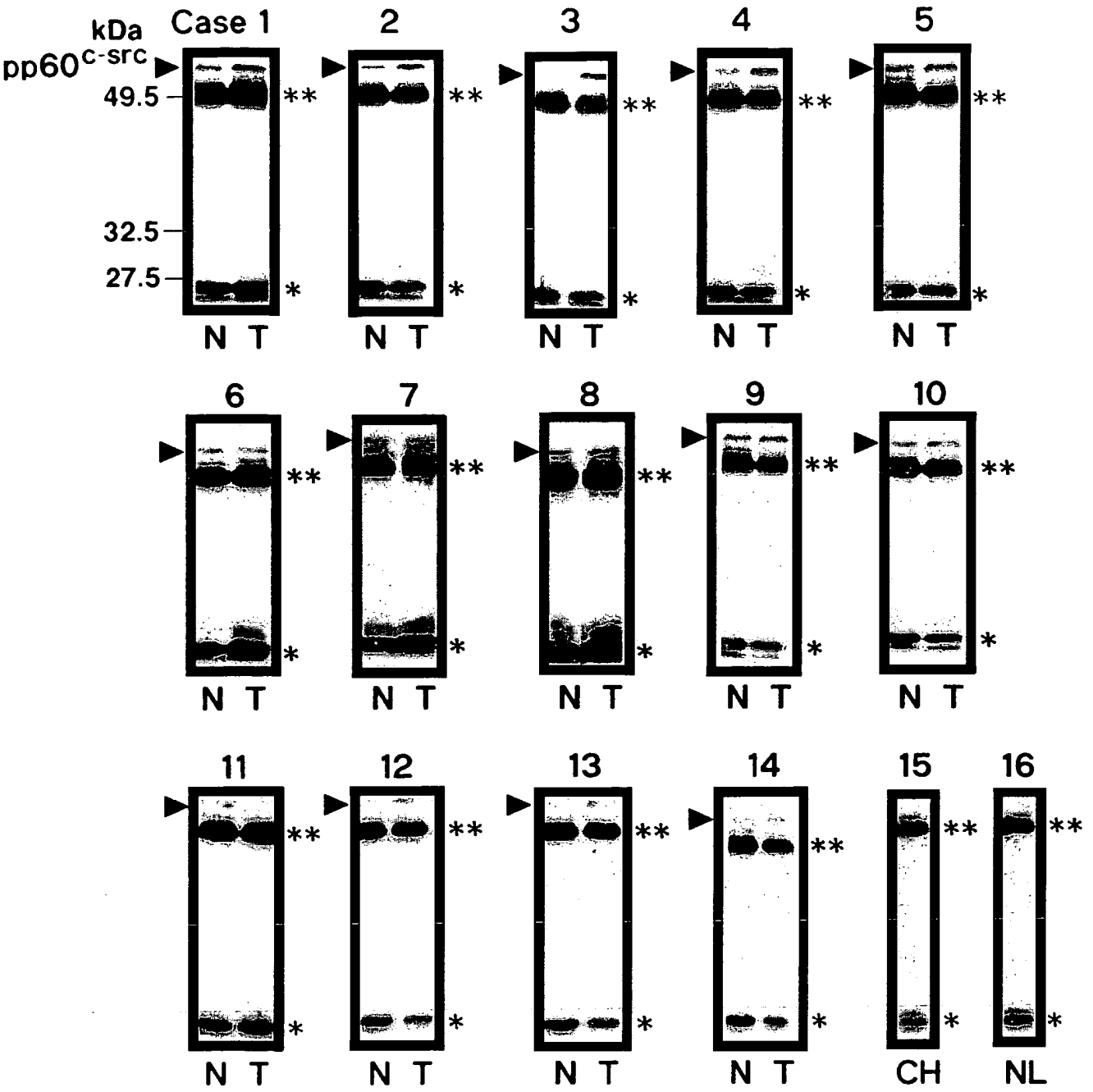

FIG. 3. Protein levels of pp60$^{c\text{-}src}$ in NL, CH, N, and T portions of human HCC. For Western blot analysis, precipitates of antibody to pp60$^{c\text{-}src}$ prepared from the same lysates as those used for the kinase assays shown in Fig. 1 were resolved by SDS-PAGE and transferred to nitrocellulose. The membranes were incubated with excess mAb 327 and washed; then immunoreactive proteins were visualized using an enhanced chemiluminescence detection system on radiographic film. Lysates containing 100 g of total cellular protein were prepared as described in Materials and Methods.

represented heavy and light chains, respectively. Figure 4A shows the results of Western blot analysis using mAb 327 as in the main experiments. One hundred micrograms of the tissue lysate of T and N regions of HCC tissue (case 2) were subjected to SDS-PAGE and analyzed as described in Materials and Methods. A 60-kd single band was obtained, indicating the specificity of this antibody. Figure 4B also shows the results of Western blot analysis using mAb 327. One hundred micrograms of the immunoprecipitate product of T and N regions of HCC tissue (case 2) were subjected to SDS-PAGE and analyzed described in Materials and Methods. In Fig. 4B, the control samples are the immunoprecipitate product of TNE buffer without tissues using monoclonal antibody. As shown in Fig. 4B, we could also detect 25- and 50-kd bands in control samples, probably representing light and heavy chains of the antibody, respectively. In addition, previous studies[14-17] have also indicated that these two bands represented immunoglobulins. Considering these previous reports[14-17] and an additional result in the present study, these two bands corresponded to immunoglobulins.

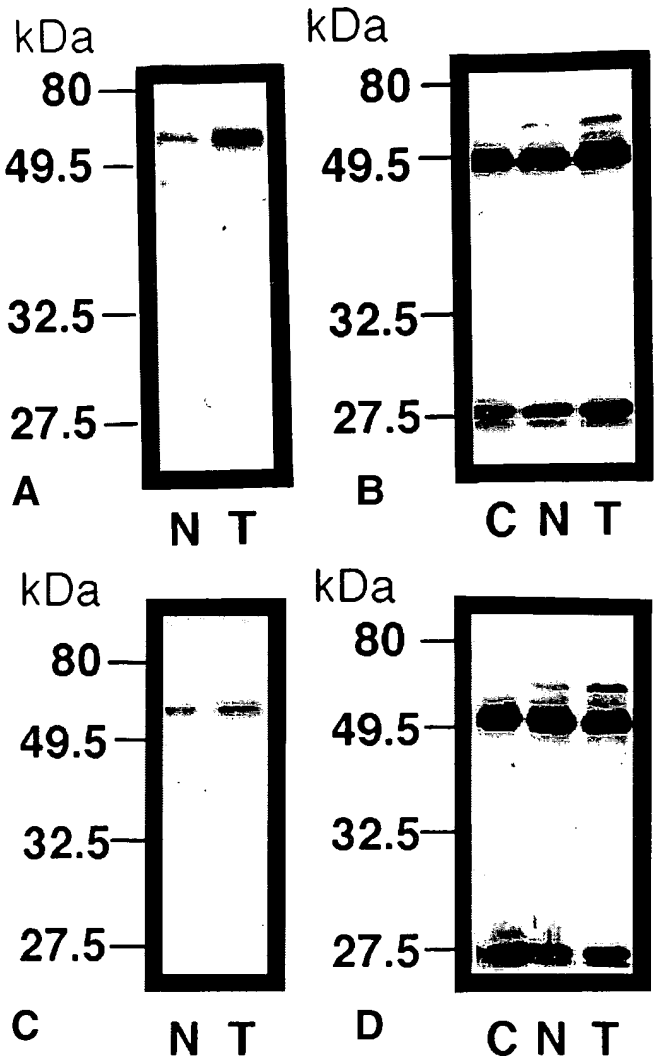

FIG. 4. Western blots of tissue lysate using (A) pp60$^{c\text{-}src}$ monoclonal (mAb 327) and (C) polyclonal (clone, N-16) antibodies, respectively, as probes. Twenty micrograms of tissue lysate of N and T regions of HCC in case 2 were subjected to SDS-PAGE and analyzed as described in Materials and Methods. Western blot of pp60$^{c\text{-}src}$ after immunoprecipitation using (B) pp60$^{c\text{-}src}$ monoclonal (clone, 317) and (D) polyclonal (clone, N-16) antibodies, respectively, as probes. The pp60$^{c\text{-}src}$ immunoprecipitate product of TNE buffer without tissues was used as control [C]. The bands at molecular size of 25 and 50 kd were also observed in the control sample. [C]: control sample.

We also studied a polyclonal antibody (clone, sc-19) other than that determined by Western blot analysis mAb 327. A 60-kd band was also shown in Fig. 4A and 4C. The 25-, 50-, and 60-kd bands were shown in Fig. 4B and 4D. These results suggest that the upper band shown in Figs. 3 and 4 represents pp60$^{c\text{-}src}$, and that the two lower bands represent heavy and light chains of the antibody, respectively. The kinase activity of pp60$^{c\text{-}src}$ correlated with its protein levels in cases 2, 3, 4, 12, and 13, and activity levels were elevated in the T tissues (Fig. 1). The other cases appear to show identical levels of pp60$^{c\text{-}src}$ protein. However, the kinase activity was also elevated in the T tissues of these cases. Estimates of pp60$^{c\text{-}src}$ specific activity (a ratio of total kinase activity to the amount of protein) also seemed to be elevated in T tissues. Thus, the high total pp60$^{c\text{-}src}$ kinase activity in the T tissues relative to that in N tissues was probably caused by an increase in the amount of pp60$^{c\text{-}src}$ protein as well as the specific activity of the enzyme. In addition, the low activity of total pp60$^{c\text{-}src}$ kinase in CH and NL seemed to be caused by a diminished amount of pp60$^{c\text{-}src}$.

Relationship between pp60$^{c\text{-}src}$ Kinase Activity and Histopathological Grade of Human Hepatocellular Carcinoma. As shown in Fig. 5, the total protein kinase activity of pp60$^{c\text{-}src}$ in the moderately differentiated tumor tissues (n = 10) was not significantly different from that in well-differentiated tissues (n = 5). The pp60$^{c\text{-}src}$ activity level in the poorly differentiated HCC tissue (n = 5) was 4.7 ± 2.7 and 1.6 ± 0.24 times higher than that in the well-differentiated tissues, as measured by autophosphorylation ($P < .001$) and enolase phosphorylation ($P < .05$), respectively. In addition, in the poorly differentiated HCC tissues, the level of pp60$^{c\text{-}src}$ activity was also 1.8 ± 0.41 and 1.2 ± 0.12 times higher than that in moderately differentiated HCC tissue, as measured by autophosphorylation ($P < .001$) and enolase phosphorylation ($P < .01$), respectively.

pp60$^{c\text{-}src}$ Protein Kinase Activity During Development of HCC in LEC Rats. We also compared the *in vitro* protein kinase activity of pp60$^{c\text{-}src}$ in liver tissue samples from LEC rats and Wistar rats. The histopathological findings in liver tissue from 2-, 6-, and 12-month-old LEC rats were those of NL (Fig. 6A), CH (Fig. 6B), and HCC (Fig. 6D), respectively. The histological finding in the N tissue of 12-month-old LEC rats was CH (Fig. 6C). The protein kinase autoradiograms in the liver tissues of 2-, 6-, and 12-month-old LEC rats and 12-month-old Wistar rat are shown in Fig. 7. The kinase activity level in liver tissues of 2- and 6-month-old LEC rats and in the N and T portions of tissues of 12-month-old LEC rats was 1.0, 1.9, 3.8, and 12.1 times higher, as measured by enolase phosphorylation, or 1.1, 2.0, 4.1, and 19.2 times

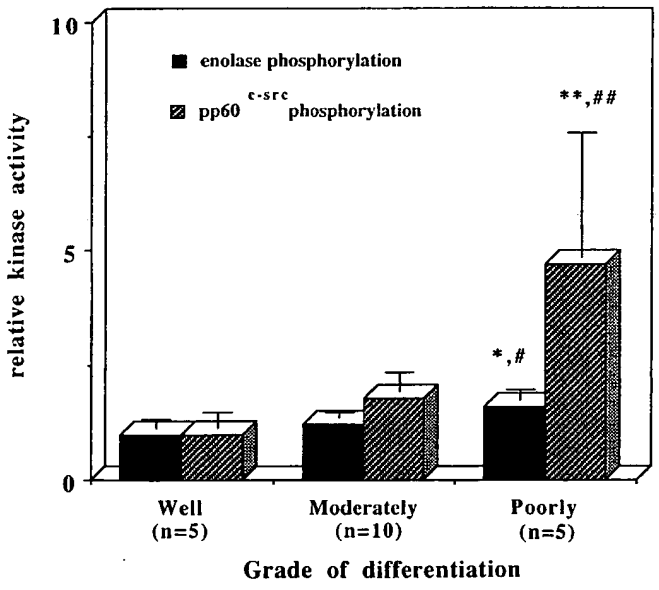

FIG. 5. Relationship between *in vitro* pp60$^{c\text{-}src}$ kinase activity and histopathological differentiation of HCC. Values were averaged for poorly (n = 5) and moderately differentiated HCC (n = 10) and expressed relative to the activity of pp60$^{c\text{-}src}$ in well-differentiated HCC (n = 5). Values shown represent the mean ± SEM of pp60$^{c\text{-}src}$ activity for each group. $^{*}P < .05$; and $^{**}P < .001$ vs. well-differentiated HCC. $^{\#}P < .01$; and $^{\#\#}P < .001$ vs. moderately differentiated HCC.

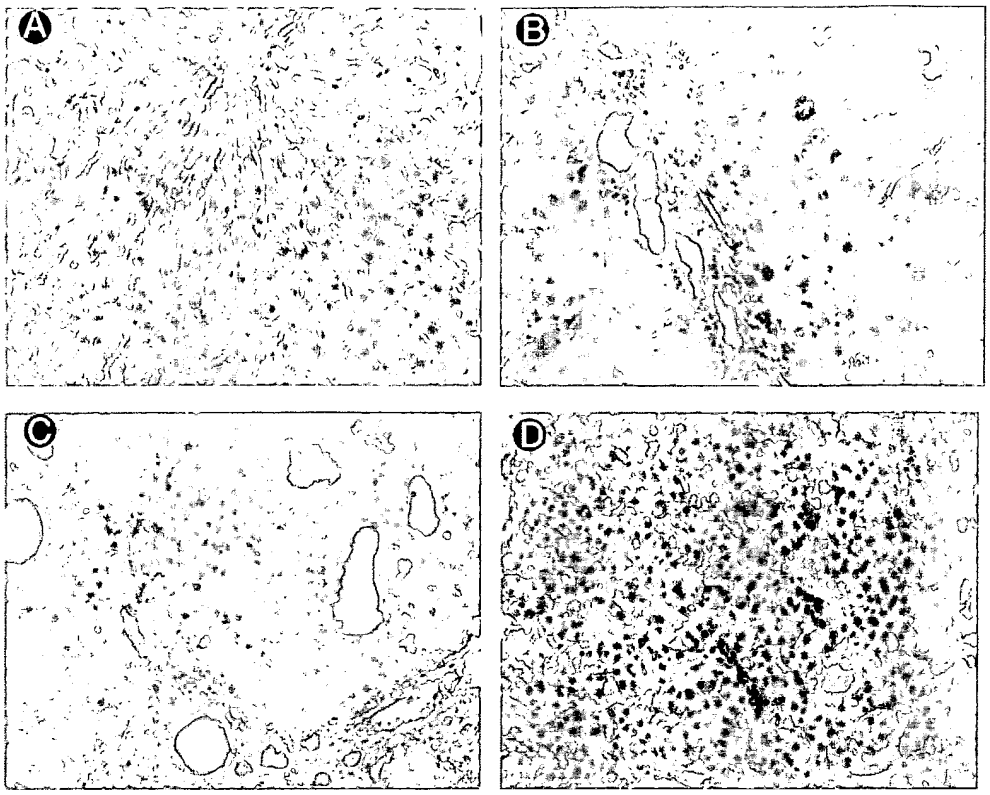

FIG. 6. Hematoxylin-eosin-stained sections from 2-, 6-, and 12-month-old LEC rat liver tissue. (A) Two-month-old LEC rat. (Original magnification ×200.) (B) Six-month-old LEC rat. (Original magnification ×200.) (C) N tissue in 12-month-old LEC rat liver. (Original magnification ×200.) (D) T tissue in 12-month-old LEC rat liver. (Original magnification ×200.) The histopathological findings in 2-, 6-, and 12-month-old LEC rat liver tissues were those of (A) NL, (B) CH, and (D) HCC, respectively. The change of the hepatocytes with nuclear enlargement is a characteristic histopathological feature of chronic hepatitis in 6-month-old LEC rats. (C) The histological finding in the N tissue of 12-month-old LEC rats was CH with preneoplastic lesions.

higher as measured by autophosphorylation, compared with that in 12-month-old Wistar rats, respectively (Fig. 8). The reproducibility of these findings was confirmed in three different experiments. These data suggest that the level of enzymatic activity is highest in the T part of 12-month-old LEC rat liver tissues. The protein levels of pp60$^{c\text{-}src}$ were also determined in these groups of rats by Western blot analysis (Fig. 9). Three bands were detected in each lane, including a top band of pp60$^{c\text{-}src}$, a middle band of heavy-chain immunoglobulin, and another band of light-chain immunoglobulin.[14-17] The amount of pp60$^{c\text{-}src}$ protein in liver tissues of 2- and 6-month-old LEC rat tissues, and in N and T portions

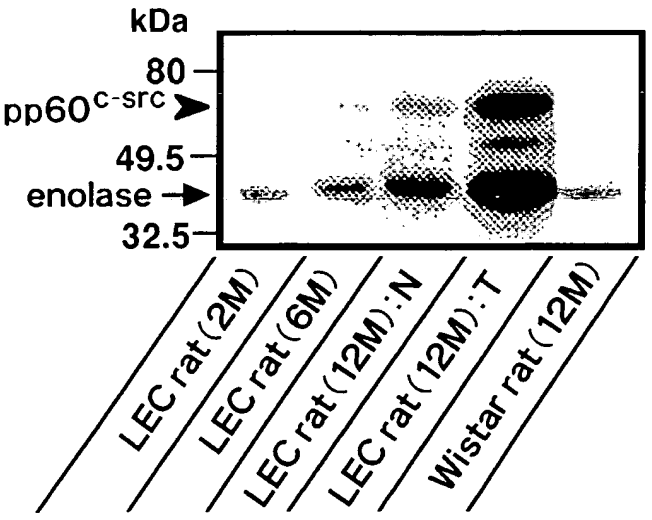

FIG. 7. Tyrosine kinase activity of pp60$^{c\text{-}src}$ in liver tissues of 12-month-old Wistar rats and 2- and 6-month-old LEC rats, and N and T portions of liver tissue in 12-month-old LEC rats. Lysates containing 100 g of total cellular protein were prepared as described in Materials and Methods. The protein was precipitated with excess pp60$^{c\text{-}src}$ antibody, incubated for 10 minutes at 30°C with [γ-^{32}P]-adenosine triphosphate and acid-denatured rabbit muscle enolase, and resolved on 10% SDS-polyacrylamide gels. *Arrowheads*, bands corresponding to pp60$^{c\text{-}src}$ tyrosine phosphorylation, and *arrows*, bands corresponding to enolase.

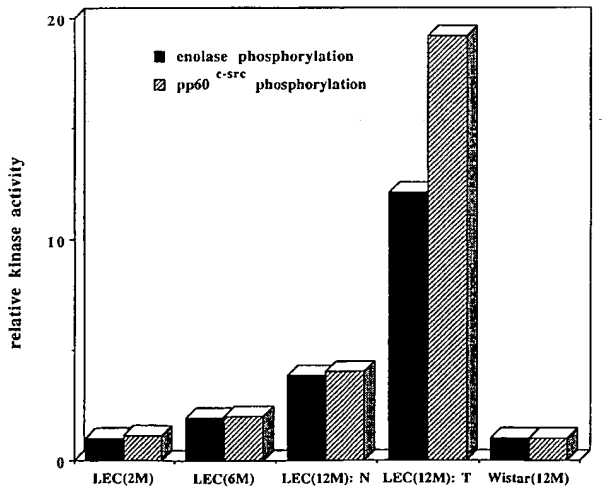

FIG. 8. Relative levels of total kinase activity of pp60$^{c\text{-}src}$ tyrosine kinase. The kinase activity of pp60$^{c\text{-}src}$ in liver tissues of 2- and 6-month-old LEC rats, and in N and T portions of liver tissues of 12-month-old LEC rats was higher than that in liver tissues of 12-month-old Wistar rats, as measured by enolase phosphorylation (■) or autophosphorylation (▨). Note that the enzymatic activity was highest in T parts of liver tissue of 12-month-old LEC rats.

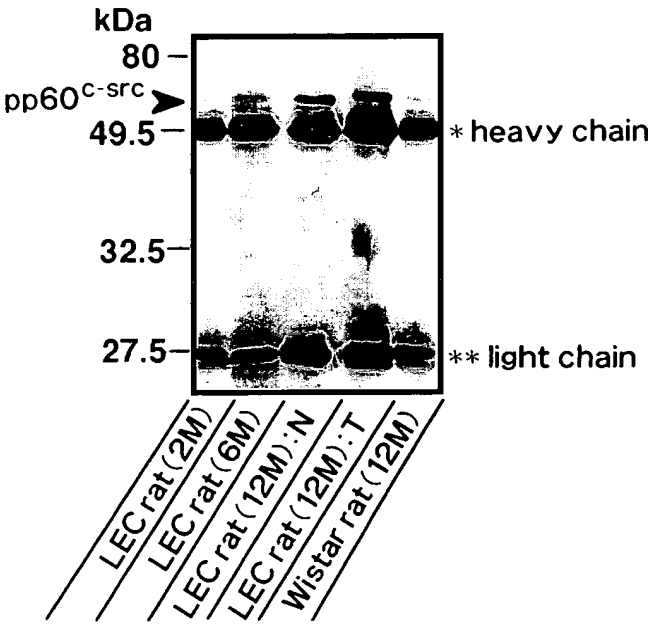

FIG. 9. Protein levels of pp60$^{c\text{-}src}$ in liver tissues of 12-month-old Wistar rat and 2- and 6-month-old LEC rats, and N and T portions of liver tissues of 12-month-old LEC rats. For Western blot analysis, pp60$^{c\text{-}src}$-antibody precipitates prepared from the same lysates as those used for the kinase assays shown in Fig. 6 were resolved by SDS-PAGE and transferred to nitrocellulose. Membranes were incubated with excess mAb 327 and washed, then immunoreactive proteins were visualized with an enhanced chemiluminescence detection system on radiographic films. Lysates containing 50 g of total cellular protein were prepared as described in Materials and Methods. *Arrowheads*, bands corresponding to pp60$^{c\text{-}src}$; * a band representing heavy-chain immunoglobulin; and ** a band representing light-chain immunoglobulin.

of 12-month-old LEC rat tissues was 1.1, 2.1, 6.0, and 6.5 times higher than that in the liver tissue of 12-month-old Wistar rat, respectively. These data suggest that the level of pp60$^{c\text{-}src}$ protein correlated with pp60$^{c\text{-}src}$ kinase activity and increased with the development of HCC. Estimates of pp60$^{c\text{-}src}$-specific kinase activity also seemed to be elevated in HCC in the liver of LEC rats. Thus, as in human HCC, the increased total kinase activity of pp60$^{c\text{-}src}$ in HCC in LEC rats seemed to be caused by an increased amount of pp60$^{c\text{-}src}$ protein and the specific activity of the kinase.

DISCUSSION

Aberrant expression of individual protooncogene has been detected in several kinds of human tumors.[10-17] Although little is known about the biochemical function of most protooncogene products, several are known to possess tyrosine-specific protein kinase activity. The most extensively studied protein kinase is pp60$^{c\text{-}src}$.[37] Rosen et al.[11] demonstrated that pp60$^{c\text{-}src}$ kinase activity is significantly elevated in several apparently related human cancers. However, the activity of pp60$^{c\text{-}src}$ protein kinase has not been previously studied in HCC.

The major finding of the present study was the elevated activity of pp60$^{c\text{-}src}$ tyrosine kinase in T tissues compared with N cirrhotic portions of human HCC (Figs. 1 and 2). However, the level of pp60$^{c\text{-}src}$ protein synthesis judging from Western blot analysis was similar in T and N tissues in cases 5 through 11 and 14. Thus, the enhanced activity in T tissues in these cases was probably caused by a high specific activity of the pp60$^{c\text{-}src}$ kinase. These results strongly suggest that the transformation of liver cirrhosis (LC) to HCC is not critically dependent on the level of pp60$^{c\text{-}src}$ protein synthesis, but rather on the activity of pp60$^{c\text{-}src}$ protein tyrosine kinase. Our results also showed a low pp60$^{c\text{-}src}$ kinase activity in NL (Fig. 1, case 16) and CH (Fig. 1, case 15). pp60$^{c\text{-}src}$ was not detected by Western blot analysis in NL and CH as shown in Fig. 3 (although very weak immunostaining of pp60$^{c\text{-}src}$ may be detected using other methods). The low level of activity may be caused by low levels of the protein in NL and CH tissue. Furthermore, because pp60$^{c\text{-}src}$ activation occurs in LC before the development of HCC, it appears to be an early event in tumorigenesis. However, because pp60$^{c\text{-}src}$ activation does not occur in CH, such a process is not the initial event in tumor formation.

Protein tyrosine kinase of pp60$^{c\text{-}src}$ is known to play an essential role in signal transduction pathways involved in the regulation of cell differentiation.[38] Therefore, to investigate its role in the differentiation of HCC, we analyzed the relationship between the level of pp60$^{c\text{-}src}$ kinase activity and the histopathological grade of HCC. Our results demonstrated that the level of pp60$^{c\text{-}src}$ activity was higher in poorly differentiated HCC than in well-differentiated HCC. These data suggest that pp60$^{c\text{-}src}$ is not only important in the malignant transformation process leading to HCC, it is also closely related to the differentiation of HCC. However, our results could not establish a role for the high level of pp60$^{c\text{-}src}$ kinase in promoting or inhibiting differentiation of hepatic cancer cells.

The inbred strain of LEC rats was established from a closed colony of Long–Evans rats. Severe acute liver injury with jaundice develops spontaneously in these rats 4 to 5 months after birth,[18,19] causing death from fulminant hepatic failure in more than half of the rats. Those rats that survive usually develop chronic hepatitis within a year and invariably develop cholangiofibrosis and HCC.[20] The natural history of liver disease in LEC rats may closely resemble that of human liver disease, in which HCC follows persistent liver disease. Thus, the LEC rat is a useful model for studying the mechanisms of hepatocarcinogenesis induced by nonviral factors.[21-25]

These rats serve as a useful tool for investigating the multistep oncogenic changes occurring at a molecular level. In the present study, we found increased pp60$^{c\text{-}src}$ kinase activity with the development of HCC in LEC rats (Figs. 7 and 8). In particular, the enzymatic activity was highest in T parts of the liver in 12-month-old LEC rats. In contrast, the activity was low and only a very weak pp60$^{c\text{-}src}$ band was detected in the control Wistar rats and 2-month-old LEC rats (Figs. 7 and 8). The low level of activity in the control Wistar and 2-month-old LEC rats probably was caused by low pp60$^{c\text{-}src}$ protein levels in the liver. Using Western blot analysis, we also noted a lack of difference in pp60$^{c\text{-}src}$ protein levels between N and T tissues in 12-month-old LEC rat liver (Fig. 9). Our results suggest that the protein level is not important in the progression of CH to HCC in LEC rats, but rather that the activity of pp60$^{c\text{-}src}$ kinase is more likely to be involved in the transformation of CH to HCC.

What are the mechanisms that activate pp60$^{c\text{-}src}$ in HCC? The activity of pp60$^{c\text{-}src}$ kinase may increase following mutations or deregulation of upstream regulators of pp60$^{c\text{-}src}$ activity, including activated receptor tyrosine kinases, loss of

inhibitory activates such as those of C-terminal Src kinase (Csk) or phosphatase, or other yet undefined, allosteric mechanisms.[39] In particular, Csk is a novel cytoplasmic protein tyrosine kinase that has been shown to inactivate members of the Src family protein tyrosine kinase *in vitro*.[40-41] Preliminary results from our laboratory showed a significant decrease in the levels of tyrosine kinase activity of Csk in T tissues compared with N tissues of human HCC (unpublished results). Thus, reduced levels of Csk activity may be one of the several factors that contribute to the rise in pp60$^{c\text{-}src}$–specific kinase activity in HCC.

In conclusion, activation of the protooncogene product pp60$^{c\text{-}src}$ may play an important role in the malignant transformation of hepatocytes in human and LEC rats and is closely related to the histopathological differentiation of human HCC. Therefore, HCC is a novel model for studying the function of pp60$^{c\text{-}src}$ in malignant transformation. In addition, the suppression of pp60$^{c\text{-}src}$ kinase activity may offer a novel strategy in overcoming the development and invasion of HCC. Further studies are necessary to investigate such processes.

REFERENCES

1. Sugimura T. Multistep carcinogenesis: a 1992 prospective. Science 1992;258:603-607.
2. Hsu TY, Moroy T, Etiemble J, Louise A, Trepo C, Tiollasis P, Buedia MA. Activation of c-myc by woodchuck hepatitis virus insertion in hepatocellular carcinoma. Cell 1988;55:627-635.
3. Fourel G, Trepo C, Bougueleret L, Hengliein B, Ponzetto A, Tiollais P, Buendia MA. Frequent activation of N-myc genes by hepadnavirus insertion in woodchuck liver tumors. Nature 1990;294-298.
4. Courtneidge SA. Activation of pp60$^{c\text{-}src}$ kinase by middle T antigen binding or dephosphorylation. EMBO J 1985;4:1471-1477.
5. Piwnica-Worms H, Saunders KB, Roberts TM, Smith AE, Cheng SH. Tyrosine phosphorylation regulates the biochemical and biological properties of pp60$^{c\text{-}src}$. Cell 1987;49:75-82.
6. Cartwright CA, Eckhalt W, Simon S, Kaplan PL. Cell transforming by pp60$^{c\text{-}src}$ mutated in the carboxyl-terminal regulatory domain. Cell 1987;49:83-91.
7. Kmiecik TE, Shalloway D. Activation and suppression of pp60$^{c\text{-}src}$ transforming ability phosphorylation. Cell 1987;49:65-73.
8. Reynolds AB, Rosel DJ, Kanner SB, Parsons JT. Transformation-specific tyrosine phosphorylation of a novel cellular protein in chicken cells expressing oncogenic variants of the avian cellular *src* gene. Mol Cell Biol 1989;9:629-638.
9. Bolen JB. Nonreceptor tyrosine kinase. Oncogene 1993;8:2025-2031.
10. Bolen JB, Rosen N, Israel MA. Increased pp60$^{c\text{-}src}$ tyrosine kinase activity in human neuroblastoma is associated with amino-terminal tyrosine phosphorylation of the gene product. Proc Natl Acad Sci U S A 1985;82:7275-7279.
11. Rosen N, Bolen JB, Schwartz AM, Cohen P, Desean V, Israel MA. Analysis of pp60$^{c\text{-}src}$ protein kinase activity in human tumor cell lines and tissues. J Biol Chem 1986;261:13754-13759.
12. Bolen JB, Veillette A, Schwartz AM, Desau V, Rosen N. Activation of pp60$^{c\text{-}src}$ protein kinase activity in human colon carcinoma. Proc Natl Acad Sci U S A 1987;84:2251-2255.
13. Barnekow A, Paul E, Schartl M. Expression of the pp60$^{c\text{-}src}$ protooncogene in human skin tumors. Cancer Res 1987;47:235-240.
14. Cartwright CA, Kamps MP, Meisler AI, Pipas JM, Eckhart W. pp60$^{c\text{-}src}$ activation in human colon carcinoma. J Clin Invest 1989;83:2025-2033.
15. Cartwright CA, Meisler AI, Eckhalt W. Activation of the pp60$^{c\text{-}src}$ protein kinase is an early event in colonic carcinogenesis. Proc Natl Acad Sci U S A 1990;87:558-562.
16. Ottenhoff-Kalff AE, Rijksen G, van-Beurden EACM, Hennipman A, Michels AA, Steal GE. Characterization of protein kinase from human breast cancer: involvement of the c-*src* oncogene product. Cancer Res 1992;52:4773-4778.
17. Cartwright CA, Coad CA, Egbert BM. Elevated c-*src* tyrosine kinase activity in premalignant epithelia of ulcerative colitis. J Clin Invest 1994;93:509-515.
18. Sasaki M, Yoshida MC, Kagami K, Takeuchi N, Kobayashi H, Dempo K, Mori M. Spontaneous hepatitis in an inbred strain of Long-Evans rats. Rat News Lett 1985;14:4-6.
19. Yoshida MC, Masuda R, Sasaki M, Takeichi N, Kobayashi H, Dempo K, Mori M. New mutation causing heredity hepatitis in the laboratory rat. J Hepatol 1987;78:361-365.
20. Takeichi N, Kobayashi H, Yoshida MC, Sasaki M, Dempo K, Mori M. Spontaneous hepatitis in Long-Evans rats: a potential animal model for fulminant hepatitis in man. Acta Pathol Jpn 1988;38:1369-1375.
21. Okuda K. A rat strain that spontaneously develops severe hepatic necrosis and later hepatocellular carcinoma. HEPATOLOGY 1988;38:1369-1375.
22. Okuda K. Hepatocellular carcinoma: recent progress. HEPATOLOGY 1992; 15:948-963.
23. Li Y, Togashi Y, Sato S, Emoto T, Kang JH, Takeichi N, Kobayashi H, et al. Spontaneous hepatic copper accumulation in Long-Evans cinnamon rats with hereditary hepatitis. J Clin Invest 1991;87:1858-1861.
24. Togashi Y, Li Y, Kang J-H, Takeichi N, Fujioka Y, Nagashima K, Kobayashi H. D-penicillamine prevents the development of hepatitis in Long-Evans cinnamon rats with abnormal copper metabolism. HEPATOLOGY 1992;15:82-87.
25. Kang J-H, Togashi Y, Kasai H, Hosokawa M, Takeichi N. Prevention of spontaneous hepatocellular carcinoma in Long-Evans cinnamon rats with hereditary hepatitis by the administration of D-penicillamine. HEPATOLOGY 1993;18:614-620.
26. Lipsich LA, Lewis AJ, Brugge JS. Isolation of monoclonal antibodies that recognize the transforming proteins of avian sarcoma viruses. J Virol 1983;48:352-360.
27. Wiestler OD, Walter G. Developmental expression of two forms of pp60$^{c\text{-}src}$ in mouse brain. Mol Cell Biol 1988;8:502-504.
28. Laemmli UK. Cleavage of structural proteins during the assembly of the head of bacteriophage T4. Nature 1970;227:680-685.
29. Towbin H, Stadhelin T, Gordon J. Electrophoretic transfer of protein from polyacrylamide gel to nitrocellulose sheets: procedure and some applications. Proc Natl Acad Sci U S A 1979;76:4350-4354.
30. Eckhart W, Hutchinson MA, Hunter T. An activity phosphorylating tyrosine in polyoma T antigen immunoprecipitates. Cell 1979;18:925-934.
31. Hutchinson MA, Hunter T, Eckhart W. Characterization of T antigens in polyoma-infected and transformed cells. Cell 1978;15:65-77.
32. Cooper JA, Esch FS, Taylor SS, Hunter T. Phosphorylation site in enolase and lactate dehydrogenase utilized by tyrosine protein kinase in vivo and in vitro. J Biol Chem 1984;259:7835-7841.
33. Cartwright CA, Hutchinson MA, Eckhart W. Structural and functional modification of pp60$^{c\text{-}src}$ associated with polyoma middle tumor antigen. Mol Cell Biol 1986;6:1562-1570.
34. Liver Cancer Study Group of Japan. The general rules for the clinical and pathological study of primary liver cancer. 3rd ed. Kyoto: Kimbara, 1992:34-35.
35. Edmondson HA, Steiner PE. Primary carcinoma of the liver. A study of 100 cases among 48,900 necropsies. Cancer 1954;7:462-503.
36. Copper JA, Esch FS, Taylor S, Hunter T. Phosphorylation sites in enolase and lactate dehydrogenase utilized by tyrosine protein kinases in vivo and in vitro. J Biol Chem 1984;259:7835-7841.
37. Cooper JA, Howell B. The when and how of Src regulation. Cell 1993;73:1051-1054.
38. Cantlecy LC, Auger KR, Karpenter C, Duckworth B, Graziani A, Kapeller R, Soiloff S. Oncogene and signal transduction. Cell 1991;64:281-302.
39. Okada M, Nakagawa H. A protein tyrosine kinase involved in regulation of pp60$^{c\text{-}src}$ function. J Biol Chem 1989;264:20887-20893.
40. Okada M, Nada S, Yamanashi Y, Yamamoto T, Nakagawa H. CSK: a protein-tyrosine kinase involved in regulation of *src* family kinase. J Biol Chem 1991;266:24249-24252.
41. Nada S, Okada M, MacAuley A, Cooper JA, Nakagawa H. Cloning of a complementary DNA for a protein-tyrosine kinase that specifically phosphorylates a negative regulatory site of pp60$^{c\text{-}src}$. Nature 1991;351: 69-72.

Decreased Src Tyrosine Kinase Activity Inhibits Malignant Human Ovarian Cancer Tumor Growth in a Nude Mouse Model[1]

Jon R. Wiener,[2] Kayo Nakano, Russell P. Kruzelock,[3] Corazon D. Bucana, Robert C. Bast, Jr., and Gary E. Gallick

Departments of Molecular Oncology [J. R. W., R. P. K.], Cancer Biology [K. N., C. D. B., G. E. G.], and Clinical Investigation [R. C. B.], University of Texas, M. D. Anderson Cancer Center, Houston, Texas 77030

ABSTRACT

The Src protein tyrosine kinase is overexpressed and activated in a number of human cancers, including some human ovarian cancers. To determine whether Src activity plays a role in ovarian tumor growth, stable derivatives of the SKOv-3 human ovarian cancer cell line that exhibited reduced Src tyrosine kinase activity were generated by transfection with an antisense c-*src* construct. Comparison of these cell lines with parental SKOv-3 cells and stable sense c-*src* vector-transfected control lines revealed no phenotypic alterations in anchorage-dependent proliferation, adherence, density saturation, or wound migration. However, reduction in Src activity was associated with altered cellular morphology, dramatically reduced anchorage-independent growth, and, when assessed for tumor development in a xenograft nude mouse model, diminished tumor growth. Furthermore, reduction of Src activity in the antisense c-*src* cell lines was associated with reduced vascular endothelial growth factor mRNA expression *in vitro*, and tumors derived from these cell lines displayed a phenotype indicative of abortive microvessel vascularization. These results strongly suggest that Src is involved in critical oncogenic pathways that modulate tumor growth from this ovarian cell line. Furthermore, this evidence suggests that as in other tumor systems, Src activity is required for vascular endothelial growth factor induction and angiogenic development.

INTRODUCTION

Aberrant signal transduction, particularly inappropriate signaling mediated by unregulated tyrosine phosphorylation, is commonly observed in human tumors. For example, in a significant fraction of human ovarian cancers, the inappropriate expression of the epidermal growth factor receptor PTK[4] HER-2/*neu* receptor PTK and the macrophage colony-stimulating factor receptor (c-fms) PTK forms the basis for their use as prognostic indicators (reviewed in Ref. 1). Alterations in cellular tyrosine phosphorylation-mediated signaling, resulting in unbalanced total protein phosphotyrosine content, may occur via the overexpression or up-regulation of nonreceptor PTKs as well. The role of nonreceptor PTKs in the development of ovarian tumors remains largely unknown.

The M_r 60,000 $pp60^{c\text{-}src}$ nonreceptor PTK (Src) is the prototype member of the Src family of PTKs, all of which are M_r 56,000–62,000 phosphoproteins with intrinsic PTK activity. All nine members of the Src PTK family discovered to date, namely Src, Yes, Fyn, Fgr, Blk, Lck, Lyn, Hck, and Yrk, participate in cell signaling, although the expression and activity of all but Src, Yes, and Fyn are limited primarily to cells of hematopoietic lineage (2). Src is normally involved in cellular functions as diverse as the response to mitogen stimulation, cell cycle control, and cell-cell communication (3). One major function of the Src PTK family is to associate with receptor and nonreceptor PTKs, resulting in the stimulation of tyrosine kinase activity and increased phosphorylation of downstream substrates involved in signaling pathways (4). Indeed, Src activity is required for mitogenesis initiated by the epidermal growth factor receptor and platelet-derived growth factor, two receptor PTKs linked to oncogenic transformation in human tissues (5).

The $pp60^{c\text{-}src}$ PTK is expressed in normal ovarian epithelium at relatively low levels. However, we have recently reported that both the expression of the Src protein and intrinsic Src tyrosine kinase activity are significantly increased in human ovarian tumors as well as in cultured human malignant ovarian cancer cell lines.[5] These results suggest that aberrant Src protein expression and/or kinase activity may also be involved in ovarian tumor development, maintenance, or metastasis. Increased Src protein level and kinase activity are known to be significant contributing factors to early tumor growth in human colon adenocarcinoma (6, 7) and are up-regulated in breast (8, 9) and pancreatic (10) tumors as well. Thus it was of interest to determine whether the up-regulation of Src played a primary role in regulating human ovarian growth, or whether it was an epiphenomenon associated with more fundamental genetic changes that drive the transition to a malignant phenotype. To

Received 2/11/99; revised 5/12/99; accepted 5/17/99.
The costs of publication of this article were defrayed in part by the payment of page charges. This article must therefore be hereby marked *advertisement* in accordance with 18 U.S.C. Section 1734 solely to indicate this fact.
[1] Supported by NIH-National Cancer Institute Grants CA65527 and CA63617 (to G. E. G.), and CA39930 (to R. C. B.).
[2] To whom requests for reprints should be addressed, at Department of Molecular Oncology, Box 317, University of Texas, M. D. Anderson Cancer Center, 1515 Holcombe Boulevard, Houston, TX 77030. Phone: (713) 792-3790; Fax: (713) 794-1807.
[3] Present address: Department of Molecular and Human Genetics, Baylor College of Medicine, 1 Baylor Plaza, Houston, TX 77030.

[4] The abbreviations used are: PTK, protein tyrosine kinase; VPF, vascular permeability factor; VEGF, vascular endothelial growth factor; FBS, fetal bovine serum; ICKA, immune complex kinase assay; mAb, monoclonal antibody; PECAM, platelet endothelial cell adhesion molecule; TCM, tissue culture medium.
[5] J. R. Wiener, T. C. Windham, V. C. Estrella, P. Thall, L-W. Ang, R. C. Bast, Jr., G. B. Mills, and G. E. Gallick. Activated Src protein tyrosine kinase is overexpressed in late stage human ovarian cancer: relationship with Her-2/neu expression, manuscript in preparation.

determine the potential role of Src in ovarian cancer tumor growth, we reduced Src expression and activity in the SKOv-3 human ovarian cancer cell line via antisense technology, using an antisense expression vector construct characterized previously (11). This cell line has been well characterized with regard to its use as a model of late-stage human cancer (12, 13) and is representative of ovarian cancer cells that overexpress the HER-2/*neu* PTK (13). In this study, we report that antisense-mediated reduction of Src PTK activity in SKOv-3 malignant human ovarian cancer cells resulted in significantly decreased tumor growth in nude mice, without affecting cellular proliferation. Reduced xenograft tumor growth was accompanied by decreased vascularization of tumor tissues via abortive vessel development. In combination with results that demonstrate that reduction of Src activity resulted in a marked reduction in the expression of VEGF/VPF mRNA levels, our data suggest that Src activity modulates ovarian tumor growth in part by regulating an oncogenic mechanism exclusive of angiogenesis and in part by modulating angiogenic development.

MATERIALS AND METHODS

Reagents. The liposomal transfection reagent LipofectAMINE was obtained from Life Technologies, Inc. (Gaithersburg, MD) and used as directed by the manufacturer. The c-*src* antisense and sense eukaryotic expression vectors used to generate SKOv-3 stable transfectants have been described previously (11). mAb clone 327, which recognizes amino acids 90–120 of *Src*, was obtained from Oncogene Research Products (Cambridge, MA). mAb clone 1B7 to *Yes* was obtained from Wako, Inc. (Richmond, VA). The 204-bp cDNA probe for VEGF was obtained as a gift from Dr. Lee Ellis (M. D. Anderson Cancer Center, Houston, TX). [γ-^{32}P]ATP (3000 Ci/mmol), [α-^{32}P]dCTP (3000 Ci/mmol), and the RediPrime random prime DNA labeling system were obtained from Amersham (Chicago, IL). Rat antimouse CD31 antibody (clone MEC 13.3) against PECAM was obtained from PharMingen (San Diego, CA).

Cell Culture and Transfection. The SKOv-3 human ovarian cancer cell line was obtained from the American Type Culture Collection (Manassas, VA) and maintained in TCM comprised of McCoy5A medium containing 10% heat-inactivated FBS (Sigma, St. Louis, MO), 2 mM L-glutamine (Life Technologies, Inc.), and 20 μg/ml gentamicin (Life Technologies, Inc.).

Preliminary experiments to determine whether Src expression and activity could be reduced using antisense c-*src* oligonucleotides clearly demonstrated the efficacy of this methodology (data not shown). However, for long-term biological studies, the generation of stable antisense transfectants was deemed to be the most suitable method for specifically reducing Src function. Thus, oligonucleotide linkers encoding either the sense or antisense 40-mer of the c-*src* mRNA sequence enclosing the ATG start codon were cloned into the pcDNA1 vector (11) and used to generate G418/neomycin-resistant SKOv-3 monoclones. For transfection, SKOv-3 parental cells were plated in 100-mm dishes at a density of 1.8×10^4 cells/cm^2 and, after attachment for 24 h, transfected with 6 μg of plasmid DNA and 80 μg of LipofectAMINE, as described by the manufacturer. G418-resistant colonies were selected in 400 μg/ml G418 (Life Technologies, Inc.), isolated, expanded, and assessed for Src protein expression and intrinsic kinase activity as described below.

Immunoblotting. Immunoblot analysis of prepared cell lysates was performed exactly as described previously (11), using 250 μg of total cell protein/lane). Membranes were probed with anti-Src (mAb 327) antibody or anti-Yes (mAb 1B7) and then incubated with horseradish peroxidase-conjugated rabbit antimouse IgG secondary antibodies. Specific binding of the antibody was determined using the enhanced chemiluminescence detection system (Amersham).

ICKA. Monolayer cells in the logarithmic phase of growth were rinsed twice with ice-cold PBS before detergent lysis in modified radioimmunoprecipitation assay buffer containing 20 mM phosphate (pH 7.4), 1% Triton X-100, 150 mM NaCl, 5 mM EDTA, 50 mM NaF, protease inhibitors, and 2 mM sodium orthovanadate. Lysates prepared from solid tumors were homogenized in modified radioimmunoprecipitation assay buffer using a Polytron tissue disrupter (Brinkmann, Inc., Westbury, NY). Clarified lysates (250 μg of total protein) were reacted with 4 μg of either mAb 327 for Src immunoprecipitation or mAb 1B7 for Yes immunoprecipitation, and the immune complexes were used in ICKAs as described previously (14). Labeled proteins were separated by electrophoresis on 10% SDS-polyacrylamide gels and detected by autoradiography.

Anchorage-dependent Proliferation Assays. Determination of cell doubling time was performed by plating 6×10^5 cells/60-mm dish in TCM and counting the representative dishes at days 0, 3, and 5. Each time point/cell line was performed in triplicate. Doubling time was calculated using the formula $D_t = (0.69)(t)/\ln M_f - \ln M_i$, where t is time in hours between plating and counting, M_f is the cell number at time t, and M_i is the cell number at time 0. Anchorage-dependent cell proliferation was assessed using the fluorescent CyQuant GR method exactly as described by the manufacturer (Molecular Probes, Junction City, OR). In brief, 5×10^3 cells were plated/well in 96-well tissue culture plates (Nunc, Napierville, IL; eight wells/condition/cell line) and incubated in medium containing the appropriate concentrations of FBS for 24, 48, and 72 h. Quantitation of cell proliferation was performed by measuring fluorescence emission at 520 nm after excitation at 480 nm using a Beckman fluorescent ELISA reader (Beckman, Los Angeles, CA).

Adherence Assay. To measure adherence to the extracellular matrix, collagen IV (Sigma) was plated as described by the manufacturer in 24-well plates (Nunc) and allowed to attach for 1 h at 22°C. The wells were then washed extensively, blocked with 0.2% FBS, and UV sterilized for 10 min. Attachment was initiated by adding 2.5×10^5 cells in 0.5 ml/well and allowed to continue for 3 h at 37°C before staining with PhastGel Blue (Pharmacia, Piscataway, NJ). Quantitative differences in attachment were estimated by visual examination. To measure adherence to plastic surfaces, 2.5×10^4 cells in 0.2 ml of TCM containing either 10% or 0.2% FBS were added per well of 96-well plates (Nunc; four wells/condition/cell line) and allowed to attach for 3 h at 37°C. The medium was then discarded, the wells were washed gently with PBS, and attachment was assessed using CyQuant GR as described by the manufacturer.

Migration Wound Assay. Assessment of wound migration was performed as described previously (15). Briefly, 4×10^5 cells were plated per 35-mm dish (Nunc) and grown to >80% confluence. Wounding of the monolayer was performed by scraping with a sterile tissue scraper, followed by incubation in TCM containing either 10 or 0.5% FBS. After an additional 48 h of incubation, the monolayers were stained with PhastGel Blue and examined visually.

Saturation Density Assay. Determination of cell number at saturation density was performed by plating 2×10^4 cells

in 200 μl of TCM per well of a 96-well tissue culture plate (Nunc). Cells were allowed to grow to complete confluence and then incubated for an additional 24 h before staining with PhastGel Blue. After extensive washing with PBS, cell density was determined by measuring the proportional stain intensity using absorbance at 490 nm. The mean density for each cell line test group was determined from eight well replicates.

Anchorage-independent Growth Assay. Anchorage-independent (soft agar) cell growth was assessed by planting 2.5×10^4 cells/35-mm tissue culture dish with 2-mm grids (Nunc) in TCM as described previously (16). Each experimental condition was performed in triplicate. Cells were incubated at 37°C in a humidified atmosphere containing 5% CO_2 for 14 days. Colonies that contained ≥30 cells were scored.

Xenograft Tumor Growth Assay in Nude Mice. The tumorigenic capability of the antisense and sense c-*src* transfectants was assessed in *nu/nu* mice as described previously (11), with some modification. Briefly, cells were grown to 80% confluence in TCM, harvested by trypsinization, washed twice in HBSS (Life Technologies, Inc.), and resuspended to a final concentration of 2×10^7 cells/ml in sterile PBS containing 33% (v/v) Matrigel (Becton Dickinson). Cell suspensions (0.15 ml) were injected s.c. into the left flank of 6-week-old female *nu/nu* mice. Five mice were inoculated per test group. Tumor volume (in mm^3) was calculated using the formula for the volume of a prolate ellipsoid, $(w^2/2)(l)$, in which w and l are the width and length of the tumor in millimeters, respectively. Tumors were harvested from exsanguinated mice after 40 days of growth and snap-frozen in OCT compound before CD31/PECAM immunohistochemical staining (see below).

Northern Analysis. Northern analysis for the quantitation of VEGF-specific mRNA was performed as described previously (17). Briefly, the total RNA isolated was electrophoresed (15 μg/lane) through 1% agarose gels containing 0.22 M formaldehyde. Membranes were probed with radiolabeled VEGF probe in 50% formamide, 5× Denhardt's solution, 0.5% SDS, 50 mM Hepes (pH 7.0), 4.8× SSC, and 100 μg/ml salmon sperm single-strand DNA (Sigma) at 42°C for 18 h. Blots were washed in 1× SSC containing 0.5% SDS at 22°C and 0.1× SSC containing 0.1% SDS at 50°C before autoradiography at −80°C for 3 days with one screen.

Immunohistochemistry. Tumor microvasculature was evaluated immunohistochemically using tumor tissue thin sections harvested from nude mouse xenografts (see above). Tissue sections were fixed sequentially in acetone, acetone/chloroform, and acetone; rinsed in PBS; and endogenous peroxidase-blocked by treating the sections with 3% H_2O_2 in methanol. The sections were then incubated for 20 min at 22°C with a nonspecific protein blocking solution consisting of PBS containing 1% normal goat serum and 1% horse serum. The sections were then incubated with 1:100 primary rat antimouse CD31 antibody at 4°C for 18 h, washed in PBS, and incubated with secondary mAb (peroxidase-labeled mouse antirat antibody; 1:200 dilution; Boehringer Mannheim, Indianapolis, IN) for 1 h at 22°C. After washing, the sections were incubated with stable diaminobenzidine (Research Genetics, Huntsville, AL) for 20 min to develop the peroxidase signal and counterstained with Mayer's hematoxylin (Sigma). Sections were washed and mounted with Universal Mount (Research Genetics) and dried on a hot plate at 60°C before examination.

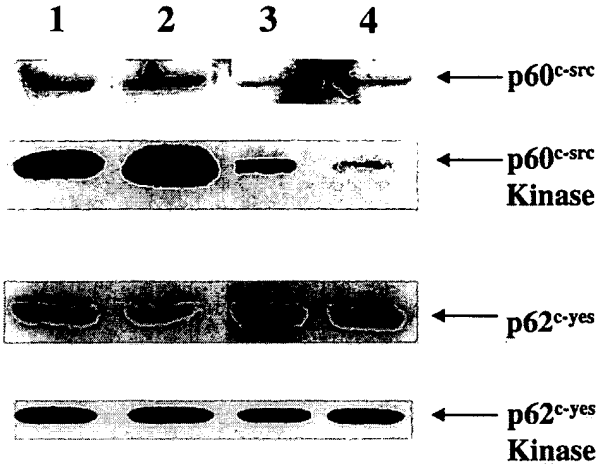

Fig. 1 Western immunoblot analysis and ICKA characterization of c-*src* antisense clones. Immunoblot and immune complex kinase analyses were performed as described in "Materials and Methods." *Lane 1*, parental SKOv-3 human ovarian cancer cell line; *Lane 2*, sense c-*src* clone S20; *Lane 3*, antisense c-*src* clone 2AS4; *Lane 4*, antisense c-*src* clone AS16.

RESULTS

Phenotypic Characterization of SKOv-3 Transfectants with Reduced Src Activity. Assessment of >50 expanded independent clones by immunoblot assay and ICKA yielded a number of antisense clones that possessed reduced Src tyrosine kinase expression and activity. In particular, the AS16 and 2AS4 antisense clones consistently displayed reduced Src expression or activity (Fig. 1) and were chosen for subsequent study.

The Yes PTK is a member of the Src PTK family that is highly homologous to Src, and it is also expressed at low levels in normal ovarian epithelium relative to the observed overexpression in ovarian cancer cells.[5] Assessment of the AS16 and 2AS4 monoclones by ICKA for Yes tyrosine kinase activity demonstrated no change in Yes protein expression or intrinsic kinase activity when compared to the parental cell line (Fig. 1) and verified the specificity of the antisense method.

To further characterize the phenotype of the sense and antisense transfectants, cell doubling, wound migration, adherence to plastic or collagen IV, and saturation density were measured. Although the antisense Src transfectants did display altered gross cellular morphology (Fig. 2), no significant difference was observed for any of the other phenotypic properties among the parental SKOv-3 cells and the S20, AS16, or 2AS4 cell lines (Fig. 3*A*; Table 1).

Reduction of Src Activity Abrogates SKOv-3 Anchorage-independent Growth. The SKOv-3 parental ovarian cancer cell line divides under anchorage-independent conditions to form large colonies (>30 cells) that can be observed visually. A comparison of anchorage-independent growth for the Src transfectants revealed ≈700 colonies/35-mm dish for the parental SKOv-3 and sense S20 cells, whereas the two antisense cell lines exhibited diminished capability to grow in soft agar (<35 colonies/dish; Fig. 3*B*). To address the possibility that the observed reduction in anchorage-independent growth was due merely to clonal variation in the parental SKOv-3 cell line, we isolated single-cell clones of the SKOv-3 parental cell line and performed assays for anchorage-dependent growth and anchor-

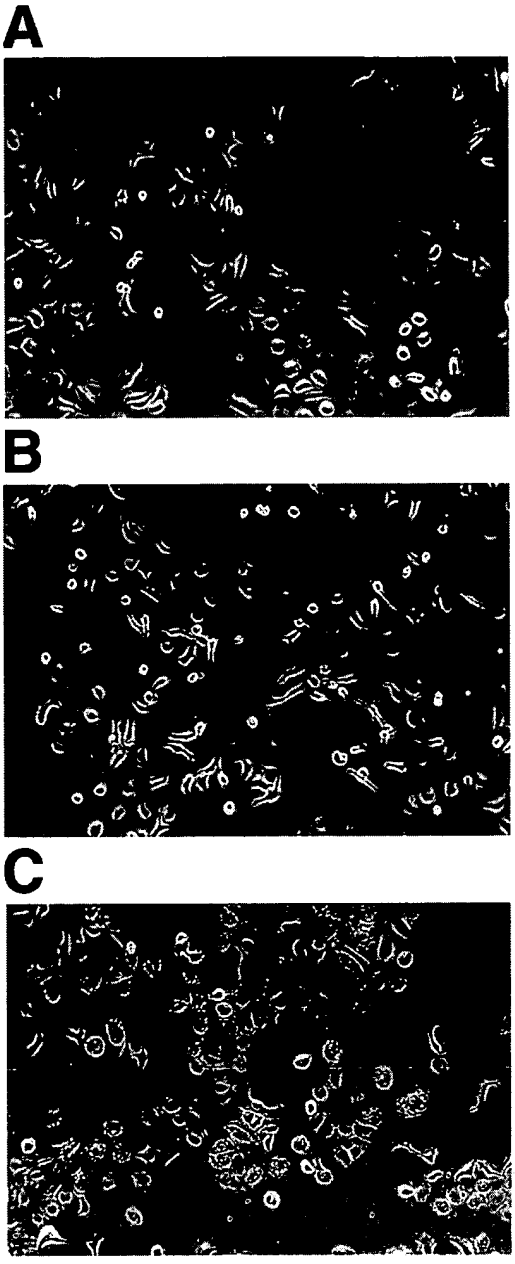

Fig. 2 Gross cellular morphology of c-*src* antisense clone AS16. Photomicroscopy of parental SKOv-3 cells (*A*), sense c-*src* clone S20 (*B*), and antisense c-*src* clone AS16 (*C*). Magnification, ×100.

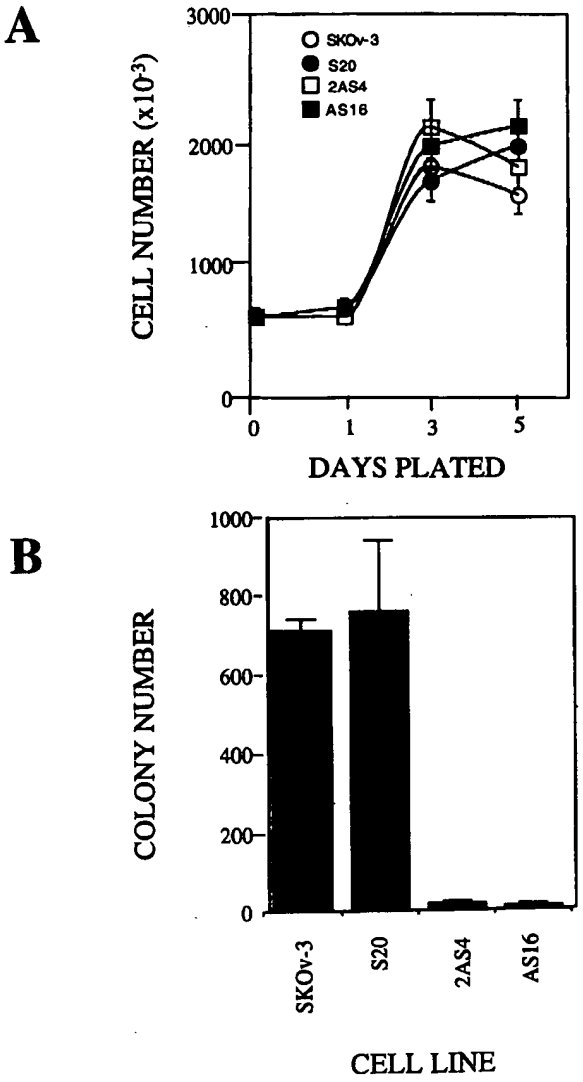

Fig. 3 Analysis of *in vitro* anchorage-dependent and anchorage-independent growth of c-*src* antisense clones. Assays were performed as described in "Materials and Methods." *A*, anchorage-dependent growth assay; 6×10^5 cells were plated on day 0, and replicate dishes were counted on the days shown. Data from the growth curves were used to calculate doubling times (see Table 1). *B*, anchorage-independent growth assay; 2.5×10^4 cells were plated, and replicate dishes were examined 14 days after plating for colonies of ≥30 cells. *Abscissa*, mean colony number/35-mm dish.

age-independent growth. Clonal isolates of the parental cell line showed variation in the ability to form colonies in soft agar, ranging between 600 and 1700 colonies/dish; none of the clones displayed the diminished anchorage-independent growth observed in the Src antisense clones (data not shown).

Ovarian Tumor Growth Is Regulated by Src Activity. To assess directly whether Src activity is involved in *in vivo* tumorigenic growth, the Src transfectants described were used to generate tumors in a nude mouse xenograft model. These stable cell lines were inoculated s.c. into the flanks of 6-week-old female nude mice, and the tumors were monitored for growth volume as described in "Materials and Methods." Rapid tumor growth was observed for the parental SKOv-3 cells and the sense S20 cells (Fig. 4); by day 32, tumors were large (500–600 mm^3) and were beginning to display central necrosis. In contrast, tumors derived from both the 2AS4 and AS16 antisense Src cell lines displayed slower growth kinetics, achieving tumor volumes of only 90–180 mm^3 by day 32 (Fig. 4). To assess whether SKOv-3 clonal variation could account for the diminished tumor growth, SKOv-3 clonal isolates of the parental cell line were assessed for tumor growth in the same nude mouse model. All SKOv-3 subclones formed s.c. tumors with a size

Table 1 Phenotypic characterization of SKOv-3 c-*src* transfectants

Cell line	Doubling time (h/days)[a]	Adherence to plastic[b]	Adherence to collagen IV	Saturation density[c]
SKOv-3 (parental cells)	32.2/1.34	45,000 ± 2,600	NOD[d]	0.606 ± 0.074
S20 (sense)	36.4/1.52	36,000 ± 3,500	NOD	0.700 ± 0.061
AS16 (antisense)	34.4/1.43	37,000 ± 1,600	NOD	0.750 ± 0.060
2AS4 (antisense)	26.3/1.10	43,000 ± 2,900	NOD	0.726 ± 0.103

[a] Doubling time was calculated using the formula $D_t = (0.69)(t)/\ln M_f - \ln M_i$, where t is time in hours between plating and counting, M_f is the cell number at time t, and M_i is the cell number at time 0.

[b] Adherence assays were performed as described in "Materials and Methods." Values shown represent mean fluorescence ± SD, with four replicates/sample. Values shown are in growth medium containing 10% FCS. Similar values were obtained in 0.2% FCS.

[c] Saturation density assay was performed as described in "Materials and Methods." Values shown represent mean absorbance ± SD, with eight replicates/sample.

[d] NOD, no observable difference between sample groups.

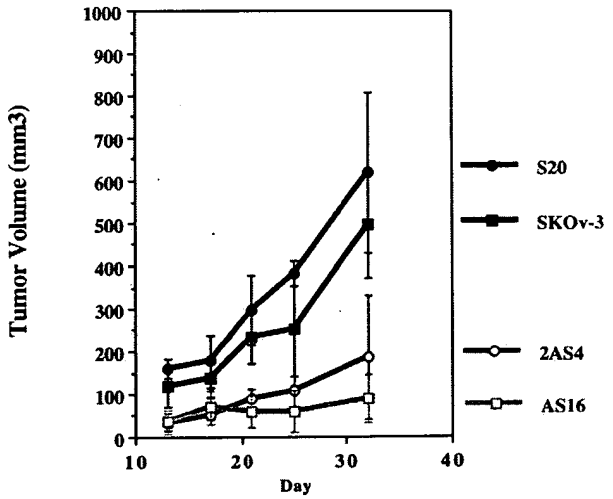

Fig. 4 *In vivo* xenograft tumor growth of c-*src* antisense clones. *In vivo* tumorigenic growth was assessed as described in "Materials and Methods." Replicate groups 6-week-old female nude mice (five mice/group) were inoculated s.c. with 3×10^6 cells in Matrigel in the left rear flank. Tumor growth was monitored by direct measurement, and the volumes (mm^3) were calculated as described in "Materials and Methods."

and growth pattern similar to that of the parental population (data not shown); none displayed the reduced tumor growth observed in the Src antisense clones (data not shown). These data suggest that Src modulates the rate of SKOv-3 ovarian tumor growth *in vivo*.

Analysis of Src kinase activity directly from the mouse tumors verified that the activity was decreased in antisense AS16 and 2AS4 tumors, but not in the parental SKOv-3 or S20 tumor cells. Indeed, the S20 cell line, which generated 17% larger tumors than the SKOv-3 cell line, also displayed a somewhat higher Src activity than the parental cell line (data not shown).

Src Regulates Angiogenic Development in Tumors by Altering VEGF Expression. Src has previously been shown to regulate the expression of the angiogenic factor VEGF/vascular permeability factor in NIH3T3 mouse fibroblasts, 293 kidney cells, and U87 human glioma cells (18) and in colon cancer cells (19, 20). Indeed, Src is required for the hypoxic induction of VEGF (18). In addition, analysis of human ovarian tumors has revealed that high VEGF expression is associated with increased microvessel density and poor overall survival (21, 22). To assess whether a similar mechanism could at least partially explain the reduced ovarian tumor growth in the antisense c-*src* tumors, we first analyzed VEGF steady-state mRNA expression in the antisense cell lines used for mouse inoculation by Northern blot analysis. Expression of the prominent 3.7-kb VEGF/VPF mRNA was observed to be reduced in the AS16 cell line, as compared to the SKOv-3 parental cell line and the S20 sense control cell line (Fig. 5). These data suggested that Src activity directly regulated VEGF/VPF expression in ovarian cancer cells *in vitro* and suggested further examination of the xenograft tumors for the extent of microvessel development. To this end, the tumors were examined immunohisto- chemically for CD31/PECAM expression, a marker for endothelial vasculature (20, 23). Visual examination of stained tumor sections from the growing edge revealed that the endothelial vessels in the AS16 tumors displayed diminished branching and decreased vessel thickness (Fig. 6). Numerical counting of endothelial vessels in multiple planes of the tumors revealed that the total number of stained vessels did not differ significantly among the parental, S20, and AS16 tumors (data not shown). These results suggest that reduction of Src expression and activity decreased endothelial vascularization in ovarian tumors, possibly by causing abortive vascular development.

DISCUSSION

Inappropriate activation of the Src PTK has been observed in human carcinomas of colonic (6, 7), breast (8, 9), and pancreatic (10) origin. Indeed, we have recently reported increased Src activity in late-stage human tumors and in a panel of ovarian cancer cell lines.[5] However, the determination of whether increased Src activity is involved in the regulation of the oncogenic capability of tumor cells must be predicated on a demonstration of diminished tumor growth after the reduction of Src protein kinase activity. In the example presented in this study, we have specifically down-regulated Src kinase activity in the SKOv-3 malignant human ovarian cancer cell line by generating stable transfectants with an antisense c-*src* construct. When compared to the parental cells or to stable sense transfectants, antisense c-*src* transfectants displayed altered morphology, but no significant changes were observed in cellular assays for proliferation, adherence, wound migration, or saturation density. However, the reduction of Src activity in the antisense clones decreased the steady-state expression of VEGF mRNA, dramatically reduced anchorage-independent growth, and sharply curtailed tumor growth in a xenograft mouse model. Finally, reduced tumor growth was coincident with abortive vascular development.

These results strongly suggest that tumor growth in this

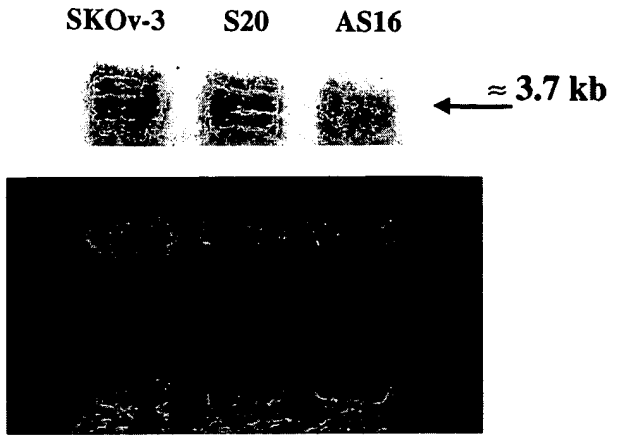

Fig. 5 Northern analysis of steady-state VEGF mRNA expression in c-*src* antisense clone AS16. Analysis of VEGF mRNA expression was performed as described in "Materials and Methods." *Top panel*, autoradiography of membrane probed with ^{32}P-labeled VEGF probe; *bottom panel*, ethidium bromide staining of 1% agarose/formaldehyde gel illustrating equal loading per lane.

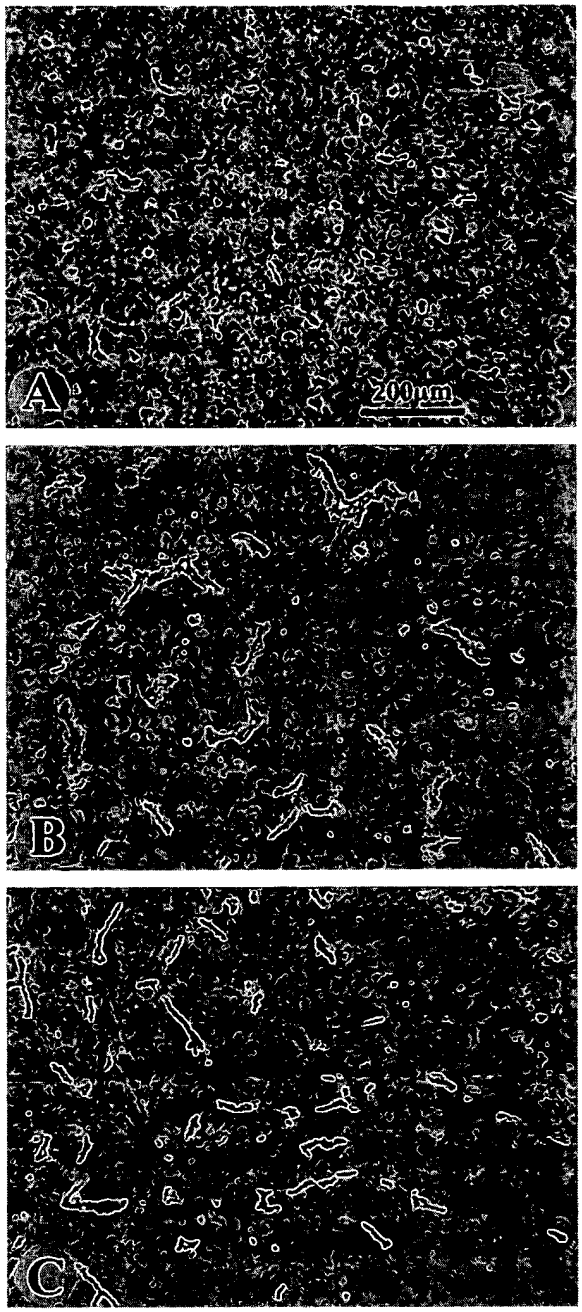

Fig. 6 Immunohistochemical analysis of CD31/PECAM expression in nude mouse tumors from c-*src* antisense clone AS16. Analysis of endothelial vasculature staining in thin sections from mouse tumors was performed as described in "Materials and Methods." Staining was performed on thin sections of tumors derived from c-*src* antisense clone AS16 (*A*), c-*src* sense clone S20 (*B*), and parental SKOv-3 ovarian cancer cells (*C*).

model system is at least partially dependent on Src function. Combined with our previous result that Src is overexpressed and activated in human ovarian tumors and cell lines *in vivo*,[5] our results suggest the possibility that Src has an important, physiologically relevant role in the growth of human ovarian tumors. The mechanism(s) by which Src modulates tumor growth is uncertain at present. Although the reduction in Src did not completely abrogate tumor growth, the dramatic reduction in anchorage-independent growth *in vitro* and the diminished tumor growth *in vivo*, combined with our data showing no observable alteration in anchorage-dependent proliferation *in vitro*, suggest that: (*a*) Src activity is not essential for normal proliferative functions. This conclusion is in agreement with previous studies using c-*src* knockout mice, in which elimination of functional Src resulted in osteopetrosis but no perinatal lethality, implying that Src is not required for general cell viability due to redundant functional overlap with other Src family PTKs (24); (*b*) Src activation is vital for the modulation of anchorage-independent growth of human ovarian cancer cells *in vitro*, in agreement with previous studies of colon epithelium (25) or in studies using the activated viral form of Src (26). The dramatic abrogation of anchorage-independent growth in the *in vitro* environment suggests that the activation of Src is essential for oncogenic transformation, although the molecular mechanism(s) that modulates tumor growth and requires Src remains unclear; and (*c*) Src appears to be involved in the reduced vascularity observed in tumors. The latter phenomenon has been observed in other model tumor systems. Indeed, studies in glioma cells and fibroblasts have revealed that hypoxia induces Tyr^{416} phosphorylation and increased Src activity but does not alter Fyn or Yes activity. Furthermore, VEGF induction by hypoxia is significantly impaired by overexpression of dominant-negative c-*src* and in Src− fibroblasts derived from c-*src* knockout mice (18). Whereas these studies remain to be performed in ovarian cancer cells, they strongly suggest that VEGF production, and thus the stimulation of vascular development, is at least partly dependent on Src activation. However, at the present time, we cannot completely eliminate the alternative possibility that decreased microvessel development is independent of Src activation.

Increased expression and activation of Src in late-stage ovarian tumors and cell lines suggest that Src activation is a frequent event, albeit following the multiple genetic events that are required for the complex transition from normal ovarian

epithelium to malignant ovarian cancer. Indeed, our observations of normal levels of Src activation in SV40 large T-induced immortalized ovarian surface epithelium[5] as well as in normal ovarian epithelium support the concept that Src activation is required to advance ovarian tumor growth after initial genetic events predispose the cell to transformation. However, because we do not have Src activation data on various early stages of ovarian cancers at the present time, it is unclear when Src activation occurs in ovarian cancer development.

In summary, we have used antisense methodology to stably reduce Src expression and activity in human ovarian cancer cells and show that reduced Src activity is associated with diminished anchorage-independent growth and reduced tumor growth in a xenograft nude mouse model. Furthermore, reduced Src activity and tumor growth are coincident with reduced microvessel development. Because this methodology is specific for Src and does not alter Yes activity, redundancy in the Src PTK family precludes affecting normal cellular functions and, at the same time, allows a more detailed investigation of Src-specific functions. Finally, based on the results of this study, it will be of interest to investigate the utilization of small molecule Src-specific inhibitors as a potential therapeutic reagent in ovarian cancers because they should have limited normal cell toxicity. These studies are currently underway.

ACKNOWLEDGMENTS

We thank James Lemoine for expert technical photographic assistance.

REFERENCES

1. Bast, R. C., Jr., Xu, F., Yu, Y., Fang, X. J., Wiener, J., and Mills, G. B. Overview: the molecular biology of ovarian cancer. *In:* F. Sharp, T. Blackett, J. Berek, and R. Bast (eds.), Ovarian Cancer, Vol. 5, pp. 87–97. Oxford, United Kingdom: Isis Medical Media Publishers, 1998.

2. Brickell, P. M. The $p60^{c\text{-}src}$ family of protein-tyrosine kinases: structure, regulation, and function. Crit. Rev. Oncogen., *3:* 401–446, 1992.

3. Brown, M. T., and Cooper, J. A. Regulation, substrates and functions of src. Biochim. Biophys. Acta, *1287:* 121–149, 1996.

4. Erpel, T., and Courtneidge, S. A. Src family protein tyrosine kinases and cellular signal transduction pathways. Curr. Opin. Cell Biol., *7:* 176–182, 1995.

5. Parsons, J. T., and Parsons, S. J. Src family protein tyrosine kinases: cooperating with growth factor and adhesion signaling pathways. Curr. Opin. Cell Biol., *9:* 187–192, 1997.

6. Bolen, J. B., Veillette, A., Schwartz, A. M., DeSeau, V., and Rosen, N. Activation of $pp60^{c\text{-}src}$ protein kinase activity in human colon carcinoma. Proc. Natl. Acad. Sci. USA, *84:* 2251–2255, 1987.

7. Cartwright, C. A., Meisler, A. I., and Eckhart, W. Activation of the $pp60^{c\text{-}src}$ protein kinase is an early event in colonic carcinogenesis. Proc. Natl. Acad. Sci. USA, *87:* 558–562, 1990.

8. Muthuswamy, S. K., Siegel, P. M., Dankort, D. L., Webster, M. A., and Muller, W. J. Mammary tumors expressing the neu proto-oncogene possess elevated c-*src* tyrosine kinase activity. Mol. Cell. Biol., *14:* 735–743, 1994.

9. Verbeek, B. S., Vroom, T. M., Adriaansen-Slot, S. S., Ottenhoff-Kalff, A. E., Geertzema, J. G. N., Hennipman, A., and Rijksen, G. c-*src* protein expression is increased in human breast cancer. An immunohistochemical and biochemical analysis. J. Pathol., *180:* 383–388, 1996.

10. Lutz, M. P., Silke Eber, I. B., Flossmann-Kast, B. B. M., Vogelmann, R., Luhrs, H., Friess, H., Buchler, M. W., and Adler, G. Overexpression and activation of the tyrosine kinase *src* in human pancreatic carcinoma. Biochem. Biophys. Res. Commun., *243:* 503–508, 1998.

11. Staley, C. A., Parikh, N. U., and Gallick, G. E. Decreased tumorigenicity of a human colon adenocarcinoma cell line by an antisense expression vector specific for c-*src*. Cell Growth Differ., *8:* 269–274, 1997.

12. Yu, D., Matin, A., Xia, W., Sorgi, F., Huang, L., and Hung, M-C. Liposome-mediated *in vivo* E1A gene transfer suppressed dissemination of ovarian cancer cells that overexpress HER-2/*neu*. Oncogene, *11:* 1383–1388, 1995.

13. Yoneda, J., Kuniyasu, H., Crispens, M. A., Price, J. A., Bucana, C. D., and Fidler, I. J. Expression of angiogenesis-related genes and progression of human ovarian carcinomas in nude mice. J. Natl. Cancer Inst., *90:* 447–454, 1998.

14. Garcia, R. A., Saya, H., and Gallick, G. E. The ansimycin antibiotic herbimycin A inhibits colon tumor cell lines by interaction with $pp60^{c\text{-}src}$. Oncogene, *6:* 1983–1989, 1991.

15. Lee, J. H., and Welch, D. R. Suppression of metastasis in human breast carcinoma MDA-MB-435 cells after transfection with the metastasis suppressor gene, KiSS-1. Cancer Res., *57:* 2384–2387, 1997.

16. Xu, F. J., Boyer, C. M., Bae, D. S., Wu, S., Greenwald, M., O'Briant, K., Yu, Y. H., Mills, G. B., and Bast, R. C., Jr. The tyrosine kinase activity of the c-erb-B-2 gene product (p185) is required for growth inhibition by anti-p185 antibodies but not for the cytotoxicity of an anti-p185-ricin-a chain immunotoxin. Int. J. Cancer, *59:* 242–247, 1994.

17. Wiener, J. R., Kerns, B-J. M., Harvey, E. L., Conaway, M. R., Iglehart, J. D., Berchuck, A., and Bast, R. C., Jr. Overexpression of the protein tyrosine phosphatase PTP1B in human breast cancer: association with $p185^{c\text{-}erbB\text{-}2}$ protein expression. J. Natl. Cancer Inst., *86:* 372–378, 1994.

18. Mukhopadhyay, D., Tsiokas, L., Zhou, X.-M., Foster, D., Brugge, J. S., and Sukhatme, V. P. Hypoxic induction of human vascular endothelial growth factor expression through c-*src* activation. Nature (Lond.), *375:* 577–581, 1995.

19. Fleming, R. Y. D., Ellis, L. M., Parikh, N. U., Liu, W., Staley, C. A., and Gallick, G. E. Regulation of vascular endothelial growth factor expression in human colon carcinoma cells by activity of *src* kinase. Surgery, *122:* 501–507, 1997.

20. Ellis, L. M., Staley, C. A., Liu, W., Fleming, R. Y. D., Parikh, N. U., Bucana, C. D., and Gallick, G. E. Down-regulation of vascular endothelial growth factor in a human colon carcinoma cell line transfected with an antisense expression vector specific for c-*src*. J. Biol. Chem., *273:* 1052–1057, 1998.

21. Nakanishi, Y., Kodama, J., Yoshinouchi, M., Tokumo, K., Kamimura, S., Okuda, H., and Kudo, T. The expression of vascular endothelial growth factor and transforming growth factor-β associates with angiogenesis in epithelial ovarian cancer. Int. J. Gynecol. Pathol., *16:* 256–262, 1997.

22. Hartenbach, E. M., Olso, T. A., Goswitz, J. J., Mohanraj, D., Twiggs, L. B., Carson, L. F., and Ramakrishnan, S. Vascular endothelial growth factor (VEGF) expression and survival in human epithelial ovarian carcinomas. Cancer Lett., *121:* 169–175, 1997.

23. Vecchi, A., Garlanda, C., Lampugnani, M. G., Resnati, M., Matteucci, C., Stoppacciaro, A., Schnurch, H., Risau, W., Ruco, L., Mantovani, A., and Dejana, E. Monoclonal antibodies specific for endothelial cells of mouse blood vessels. Their application in the identification of adult and embryonic endothelium. Eur. J. Cell Biol., *63:* 247–254, 1994.

24. Soriano, P., Montgomery, C., Geske, R., and Bradley, A. Targeted disruption of the c-*src* proto-oncogene leads to osteopetrosis in mice. Cell, *64:* 693–702, 1991.

25. Pories, S. E., Hess, D. T., Swenson, K., Lotz, M., Moussa, R., Steele, G., Jr., Shibata, D., Rieger-Christ, K. M., and Summerhayes, C. Overexpression of $pp60^{c\text{-}src}$ elicits invasive behavior in rat colon epithelial cells. Gastroenterology, *114:* 1287–1295, 1998.

26. Kato, J. Y., Takeya, T., Grandor, C., Iba, H., Levy, J. B., and Hanafusa, H. Amino acid substitutions sufficient to convert the nontransforming $p60^{c\text{-}src}$ protein to a transforming protein. Mol. Cell. Biol., *6:* 4155–4160, 1986.

Decreased Tumorigenicity of a Human Colon Adenocarcinoma Cell Line by an Antisense Expression Vector Specific for c-*Src*[1]

Charles A. Staley,[2] Nila U. Parikh, and Gary E. Gallick[3]

Department of Tumor Biology, The University of Texas M. D. Anderson Cancer Center, Houston, Texas 77030

Abstract

In greater than 80% of colon tumors and established cell lines, the specific activities of the protein tyrosine kinases $pp60^{c\text{-}src}$ and $pp62^{c\text{-}yes}$ are increased with respect to normal colonic epithelial cells. However, no mutations in either gene have been identified in colon tumors. Therefore, the possible biological consequences of activations of these protein tyrosine kinases in colon tumors have been unclear. To determine if $pp60^{c\text{-}src}$ activation affects growth and tumorigenicity of established colon tumor cell lines, an antisense expression vector that specifically reduces $pp60^{c\text{-}src}$ expression was constructed. The vector was transfected into HT 29 cells, an established colon tumor cell line in which both $pp60^{c\text{-}src}$ and $pp62^{c\text{-}yes}$ are activated. Two stable subclones were isolated in which $pp60^{c\text{-}src}$ but not $pp62^{c\text{-}yes}$ expression and activity were reduced. These established cell lines proliferated more slowly than parental cells proportionately to reduction in $pp60^{c\text{-}src}$ expression. When injected into nude mice, antisense transfected cells formed slow-growing tumors; however, the rate of tumor growth was reduced far greater than would be predicted from decreased proliferation rates in tissue culture. In contrast, stable subclones transfected with a comparable "sense" expression vector were unaltered in growth rates in tissue culture and in nude mice with respect to parental HT 29 cells. These data demonstrate that the activation of $pp60^{c\text{-}src}$ alone contributes to the tumorigenicity of HT 29 cells, a cell line widely used as a model for biological properties of colon carcinoma. Furthermore, because $pp60^{c\text{-}src}$ and $pp62^{c\text{-}yes}$ appear redundant to the growth regulation of normal colonic epithelial cells, the data suggest that src-specific inhibitors might be of therapeutic value for colon cancer.

Received 10/9/96; revised 12/20/96; accepted 12/23/96.
The costs of publication of this article were defrayed in part by the payment of page charges. This article must therefore be hereby marked *advertisement* in accordance with 18 U.S.C. Section 1734 solely to indicate this fact.
[1] Supported by the NIH Grants CA63617 and CA65527.
[2] Present address: Department of Surgical Oncology, Emory University School of Medicine, Atlanta, GA 30322.
[3] To whom requests for reprints should be addressed. Phone: (713) 792-3657; Fax: (713) 794-4784.

Introduction

In the past few years, significant advances have been made toward understanding the molecular basis for the development of colorectal cancer. In both sporadic and familial colon cancers, mutations in specific oncogenes, such as c-*ras*, in tumor suppressor genes, such as *APC*, *MCC*, and *p53*, and in DNA repair genes, such as *MSH 2*, have all been implicated as important to the development of a majority of tumors (1). However, considerably less is known about the cumulative effects of mutations in these genes on growth-regulatory signal transduction pathways of colonic epithelial cells. One family of signal transduction enzymes, the nonreceptor PTKs[4] of which *src* is the prototype, is activated in nearly every human colon tumor, resulting in specific activities of the enzymes equivalent to the cognate retroviral oncogene products (2–4). For $pp60^{c\text{-}src}$, activation is first observed in an early stage of tumorigenesis, beginning with polyps of high malignant potential (5) and persisting through subsequent stages of tumor progression. Furthermore, additional increases in enzymatic activity occur during the development of distant metastases (4–6). Similar activations of $pp62^{c\text{-}yes}$ have been observed in colonic polyps and primary tumors (7, 8). Sporadic activation of $p62^{c\text{-}lck}$ has also been reported in some colon tumor cell lines (9).

The mechanism for the observed alterations of enzymatic activity of *src* family PTKs in colon tumors is unknown but would appear to result from altered posttranslational regulation of the PTK activity, because mutations in the *src* family genes are not found in colon tumors (10). Several growth-regulatory pathways in which $pp60^{c\text{-}src}$ kinase activity is increased have been identified. For example, in fibroblasts, regulatory signals that increase the PTK activity of *src* family kinases include aggregation of integrins (11) and possibly other extracellular matrix components and the addition of several mitogenic peptides (12). Additionally in the cell cycle, *src* family activity is required in G_2 phase for fibroblast cell division (13) and is activated during M phase (14). Thus, activation of *src* family PTKs during tumorigenesis of colonic epithelial cells may be the result of primary genetic changes in genes other than c-*src* that lead to constitutive deregulation of one of the pathways in which c-*src* participates.

Regulation of *src* family PTKs appears to be important in normal colonic epithelial cell growth and differentiation. Normal colonic epithelial cells express both $pp60^{c\text{-}src}$ and $pp62^{c\text{-}yes}$ (15), and the activity of these enzymes is higher in actively dividing crypt cells than in more differentiated cells (16). Thus, high specific activity of *src* family tyrosine kinases may be a marker of proliferation. However, hyperproliferation

[4] The abbreviation used is: PTK, protein tyrosine kinase.

alone is insufficient to explain increased pp60$^{c\text{-}src}$ activity in malignant and premalignant colon epithelial cells, because the enzymatic activity is increased in ulcerative colitis as opposed to inflammation (17) and in polyps of high malignant potential as opposed to more "benign" polyps (5). Activity remains high in primary tumor and in metastases. Additionally, PTK inhibitors greatly reduce the growth of colon tumor cell lines with activated pp60$^{c\text{-}src}$ (18). These results suggest that *src* family activation may contribute to the altered growth regulation of colon tumor cells. Whether these changes are important to tumorigenesis of colonic epithelial cells or are only the result of malignant transformation was examined in this study by specifically inhibiting the expression of pp60$^{c\text{-}src}$ in a well-characterized human colon adenocarcinoma cell line, HT 29.

Results

To accomplish inhibition of pp60$^{c\text{-}src}$ expression, we used antisense oligonucleotides and expression vectors directed against the translation start site of pp60$^{c\text{-}src}$. As a model cell line, HT 29 human colon adenocarcinoma was used because both pp60$^{c\text{-}src}$ and pp62$^{c\text{-}yes}$ have high specific activities in these cells. Twenty-two base sense and antisense unmodified oligonucleotides were synthesized, beginning five bases upstream of the ATG translation start site of c-*src*. This region has only 43% homology with c-*yes*. Increasing concentrations of each purified oligonucleotide were added to HT 29 human colon adenocarcinoma cell cultures in serum-free medium. After a 16-h incubation, the cells were harvested and lysed, and kinase activity and protein levels were determined. As shown in Fig. 1, dose-dependent decreases in pp60$^{c\text{-}src}$ kinase level (*A*) and kinase activity (*B*) were observed in HT 29 cells treated with antisense oligonucleotides to a maximum concentration of 75 μM. No further inhibition was observed at 100 μM. No changes in either c-*src* protein level (Fig. 1*A*) or activity (Fig. 1*B*) were observed in the cells treated with the sense oligonucleotide compared to the control HT 29 cells. No inhibition of c-*yes* expression or kinase activity was observed (data not shown). These results demonstrate that the c-*src* antisense oligonucleotide specifically inhibits c-*src* kinase activity and protein expression.

To evaluate potential alterations in proliferation and tumorigenicity resulting from reduction of c-*src* expression and activity, the antisense and sense oligonucleotides were incorporated into a pcDNA I/Neo plasmid vector under the control of the cytomegalovirus promoter and transfected into HT 29 cells; clones were selected in G418. The kinase activities and protein levels of pp60$^{c\text{-}src}$ and pp62$^{c\text{-}yes}$ were determined in antibiotic-resistant clones, as described in "Materials and Methods." Fig. 2 compares the results from parental HT 29 cells (*Lanes 1*), two antisense transfectants termed AS15 (*Lanes 2*) and AS33 (*Lanes 3*), and a "sense" transfectant, termed S20 (*Lanes 4*) for kinase activity by autophosphorylation of pp60$^{c\text{-}src}$ or pp62$^{c\text{-}yes}$ (Fig. 2*A*), phosphorylation of an exogenous substrate, enolase (Fig. 2*B*), as well as relative protein levels by immunoblotting (Fig. 2*C*). No differences in expression or activity of pp60$^{c\text{-}src}$ or pp62$^{c\text{-}yes}$ were observed between parental HT 29 cells and the "sense" transfectant S20. However, clone AS15 was

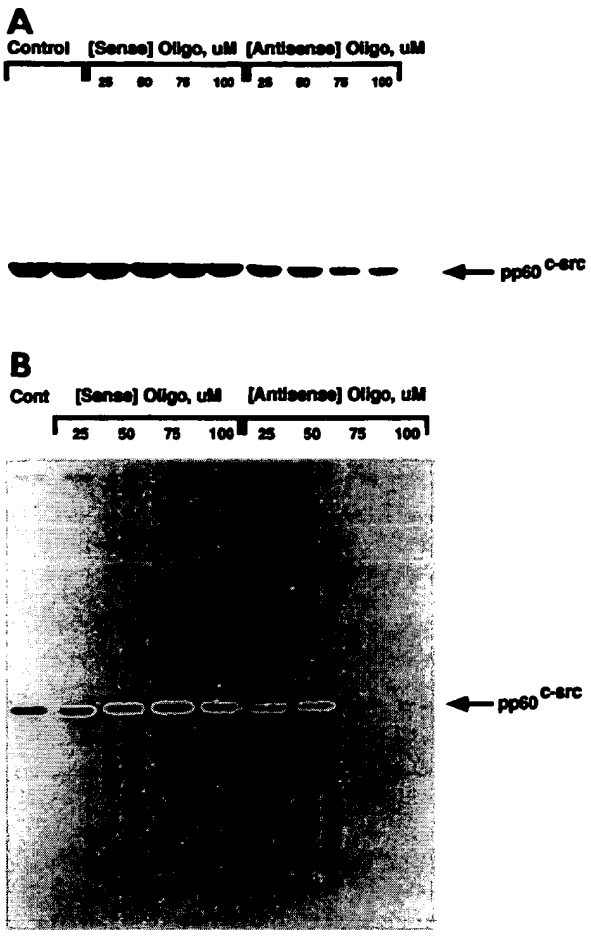

Fig. 1. Expression and activity of pp60$^{c\text{-}src}$ in HT 29 colon adenocarcinoma cells treated with c-src sense and antisense oligonucleotides. Twenty-two base sense (5'-GGACCATGGGTAGCAACAAGAG-3') and antisense (5'-CTCCTTGTTGCTACCCATGGTCC-3') unmodified oligonucleotides were synthesized as described in "Materials and Methods." Concentrations of each oligonucleotide indicated in the figure were added to subconfluent HT 29 cultures (5×10^6 cells) in serum-free medium. After a 16-h incubation, detergent lysates were made in a standard radioimmunoprecipitation assay buffer and subjected to immunoblotting (*A*) or immunoprecipitation and immune complex kinase assay (*B*) for pp60$^{c\text{-}src}$ as described.

reduced 4.5-fold in pp60$^{c\text{-}src}$ activity and level with respect to parental HT 29 cells (compare *Lanes 1* and *2*), and clone AS33 was reduced 2–2.5-fold in pp60$^{c\text{-}src}$ kinase and 2-fold in protein level (compare *Lanes 1* and *3*). To determine the specificity of inhibition of pp60$^{c\text{-}src}$ reduction, the expression and activity of the related *src*-family member pp62$^{c\text{-}yes}$ was assessed. As shown in Fig. 2, the expression and activity of pp62$^{c\text{-}yes}$ in all transfectants were comparable to parental HT 29 cells.

The morphology of AS15 cells in comparison to parental cells is shown in Fig. 3. Subtle morphological differences from parental cells are noted, with AS15 cells growing in a more elongated, organized pattern. Cells at the edge of colonies have a more serrated, villus-like appearance. However, these changes did not correlate with increased expres-

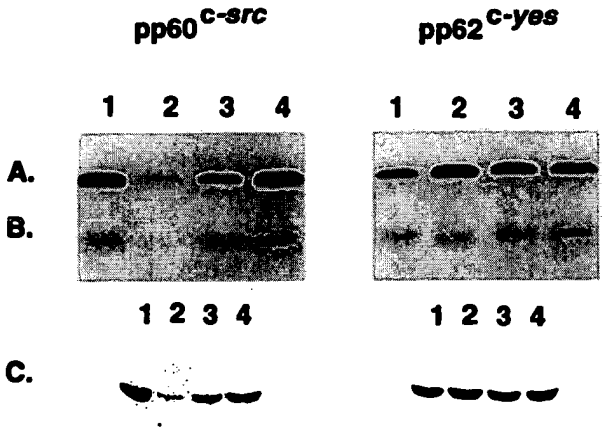

Fig. 2. Expression and activity of pp60$^{c\text{-}src}$ and pp62$^{c\text{-}yes}$ in parental HT 29 cells (*Lanes 1*), "antisense" transfected clones AS15 (*Lanes 2*) and AS33 (*Lanes 3*), and a "sense" transfected clone, S20 (*Lanes 4*). Stable HT 29 subclones were isolated, and cell lysates were subjected to immunoblotting and immune complex kinase assays for pp60$^{c\text{-}src}$ and pp62$^{c\text{-}yes}$ as described in "Materials and Methods." *A*, autophosphorylation of pp60$^{c\text{-}src}$ or pp62$^{c\text{-}yes}$; *B*, phosphorylation of the exogenous substrate enolase; *C*, relative levels of pp60$^{c\text{-}src}$ and pp62$^{c\text{-}yes}$.

sion or altered distribution of villin (data not shown). By electron microscopy, the number of microvilli was unaltered, and no evidence for mucin granules was observed. Thus, AS15 cells lack classic hallmarks of differentiation of HT 29 cells. No morphological changes were observed in AS33 cells or in any clones derived from "sense" transfectants.

Proliferation rates of the clonal cell lines in tissue culture are shown in Fig. 4*A*. HT 29 and S20 cells had doubling times of 23 h, as compared to 28 and 36 h for AS33 and AS15 cells, respectively. To examine anchorage-independent growth, soft agar colony formation was assessed as described in "Materials and Methods." No difference in ability to form soft agar colonies was observed between parental HT 29 cells and S20 "sense" transfectants. AS15 cells were 5-fold reduced in number of colonies, and AS33 cells were 2-fold reduced. The number of cells/colony were also fewer for the antisense transfectants; however, longer growth periods did not significantly increase the number of colonies formed by these cells.

To determine if reduced pp60$^{c\text{-}src}$ level and activity affected tumorigenicity and growth in nude mice, two clones, AS15 (antisense transfected), and S20 (sense transfected) were injected in equal numbers (10^6 viable cells) into the flanks of nude mice. Growth of tumors induced by these cell lines in nude mice is shown in Fig. 4*B*. In three separate trials of 5, 8, and 8 mice per cell type, 100% of mice inoculated with either parental HT 29 or "sense" transfectants developed tumors. In contrast, only 70% of mice inoculated with the reduced *src* clone, AS15, developed viable tumors. AS15-inoculated mice had a significant lag period in tumor development compared to parental and sense clones, with clearly visible tumors not appearing before 30 days after injection. After 50 days, tumor volume resulting from growth of antisense transfectants was approximately 1000-fold less

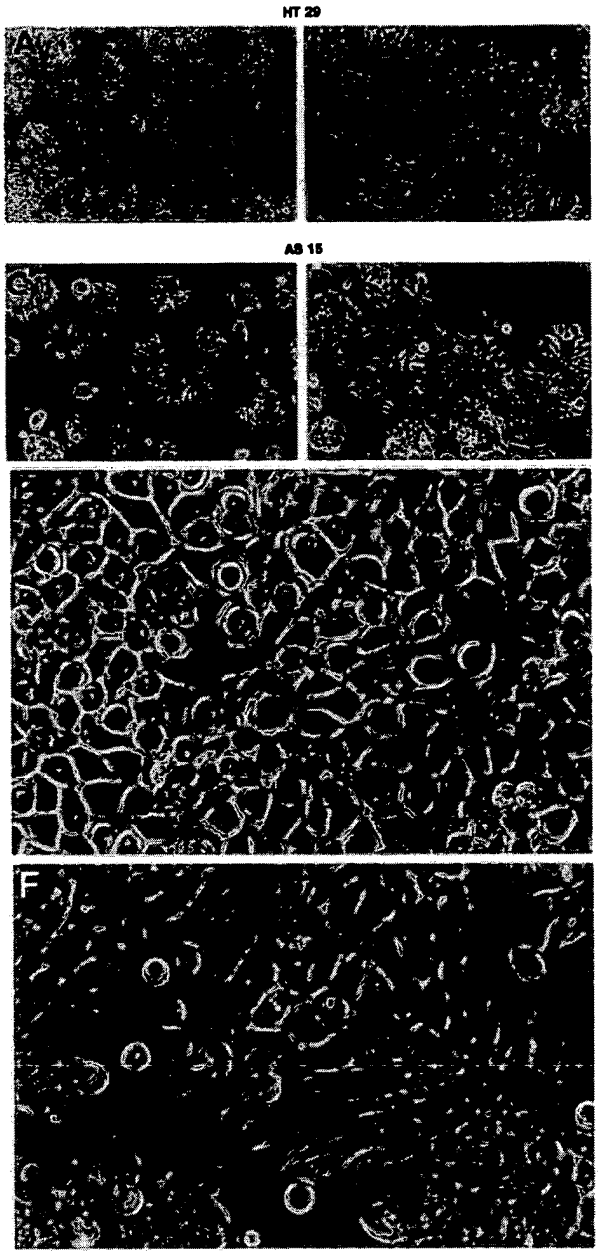

Fig. 3. Morphology of AS15 and parental HT 29 cells. Photomicrographs of cell cultures were taken 3 days after seeding 2×10^6 cells in tissue culture medium. *A* and *C*, ×150; *B* and *D*, ×300. *E*, HT 29, ×400; *F*, AS15, ×400.

than that of the "sense" transfected clone, S20 and parental HT 29 cells. Growth of AS33 tumors was intermediate to that of parental and AS15 clones, in accord with the intermediate steady-state levels of pp60$^{c\text{-}src}$ expressed in this clone. Thus, reduction of pp60$^{c\text{-}src}$ expression corresponds directly with decreased tumorigenicity. Furthermore, the decreased proliferation rate of these in tissue culture is insufficient to account completely for the reduction in growth rate in nude mice.

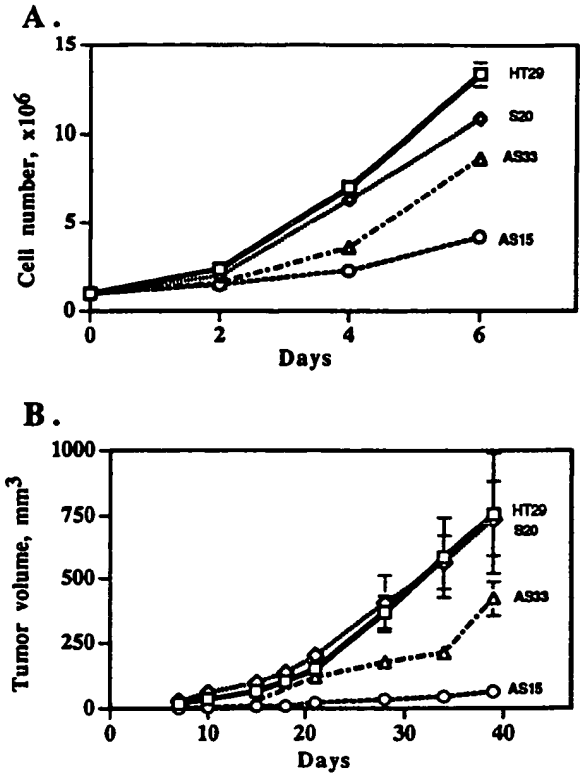

Fig. 4. Growth of parental HT 29 cells and clones AS15 and S20 cells *in vitro* and in nude mice. For *in vitro* growth (*A*), 1×10^6 cells were seeded in 60-mm tissue culture dishes with DMEM, supplemented with 10% fetal bovine serum. Viable cells were counted every second day. For *in vivo* growth (*B*), 1×10^6 cells of each clone were injected s.c. in the flank of eight nude mice/cell type. Tumor diameters were measured biweekly with calipers, and tumor volume was calculated. *Bars*, SE.

Discussion

These findings support an important role for $pp60^{c\text{-}src}$ in the tumorigenicity of a colon adenocarcinoma cell line. Given the frequency of increased specific activity of this PTK in human colon tumors and cell lines, the results suggest that activation of $pp60^{c\text{-}src}$ is a common downstream event following genetic alterations leading to colon cancer. The close association of c-*src* activation with critical early events in malignancy, *i.e.*, activation in polyps of high malignant potential but not in "benign" polyps (5), in ulcerative colitis but not inflammation (17), demonstrates that increased enzymatic activity is likely an important common event in the development of colon cancer. Similar increases in c-*yes* activity have also been observed in early stages of colon tumor development (19, 20). Although the role of c-*yes* activation in early events in colon tumorigenesis is as yet unknown, the results of this study imply that activation of $pp60^{c\text{-}src}$ alone may be critical to sustained tumorigenicity and tumor cell growth.

In two human leukemia cell lines, U937 from a histiocytic lymphoma (21) and K562 from a chronic myelogenous leukemia (22), c-*src* expression has also been implicated as important for proliferation and differentiation by a strategy in which the complete v-*src* gene was expressed in the antisense orientation. These results may suggest a wider role for c-*src* expression in the growth of tumor cells. Alternatively, because the ability of the v-*src* antisense expressed in this vector to inhibit other members of the *src* family was not assessed, inhibition may result from normal functions of the *src* family in growth-regulation pathways.

In the experiments presented in this report, biological effects occurred without c-*yes* inhibition. This result is somewhat surprising, because *src* "knock-out" mice suffer no apparent defects in development or function of the colon (23), suggesting that another family member (presumably c-*yes*) is redundant for c-*src* signaling functions in these processes. However, recent evidence has demonstrated that c-*src* is more important than c-*yes* in the production of vascular endothelial growth factor induced by hypoxia (24). In accord with this result, we have demonstrated that the antisense transfectants are reduced in vascular endothelial growth factor relative to parental cells, proportionately to reduction in steady-state $pp60^{c\text{-}src}$ levels.[5] Thus, decreased vascular endothelial growth factor production might explain the differences in the proliferation rates of antisense transfectants in tissue culture relative to their ability to grow in nude mice. Indeed, mice with AS15-induced tumors have survived for more than 1 year, with tumor burdens no larger than those induced by HT 29 cells in 60 days.

In other model systems in which *src* family activation is required for tumor development, c-*src* and c-*yes* are also not redundant in tumorigenic function. In transgenic mice expressing the polyoma virus-encoded middle T oncogene in mammary epithelium, mammary tumors universally develop (25). When these mice are crossed with "*src*less" mice, the progeny do not develop mammary tumors (26). In contrast, when the mice are crossed with mice in which c-*yes* has been functionally deleted, mammary tumors develop consistently, although $pp62^{c\text{-}yes}$, like $pp60^{c\text{-}src}$, is capable of associating with polyoma middle T antigen, an association which increases the specific activities of either *src* family member [reviewed by Courtneidge *et al.* (27)]. Thus, in several tumor systems, activation of $pp60^{c\text{-}src}$ in the absence of mutation may be critical to tumor development. However, to eliminate any potential role for c-*yes* in colon cancer, further experiments will be required.

The mechanism by which increased specific activity of $pp60^{c\text{-}src}$ kinase occurs in colon cancer remains unknown. However, recent data have demonstrated that cytoskeletal and extracellular matrix proteins may induce signaling through *src* [reviewed by Erpel *et al.* (28)]. Because several of the genetic mutations that commonly occur in colon cancer development involve proteins of the cytoskeleton (APC, DCC, and MCC), an obvious possibility is that these proteins play a role in normal regulation of $pp60^{c\text{-}src}$ activity, which is higher in actively dividing crypt cells than in differentiated, nonproliferative colon epithelial cells. The strategy used here, *i.e.*, specific reduction of expression through the use of a small antisense transcript, may provide further insight into the signaling pathways in colon epithelial cells that involve $pp60^{c\text{-}src}$ regulation and the relative roles of *src* family mem-

[5] L. Ellis and G. Gallick, unpublished data.

bers in colon tumorigenesis and progression. Furthermore, the differences between the enzymes may be exploited in the design of PTK inhibitors. A *src*-specific inhibitor would be expected to have limited toxicity but effectively and specifically reduce the growth rate of colon tumor cells.

Materials and Methods

Cell Culture. HT 29 cells were maintained in DMEM with Earle's salts and 2 mM glutamine (Life Technologies, Inc., Grand Island, NY) supplemented with 10% fetal bovine serum (Hyclone Laboratories, Inc., Logan, UT). For studies with antisense oligonucleotides, cells were transferred to serum-free media 12 h prior to the addition of the oligonucleotide.

Immunoprecipitation and Immune Complex Kinase Assays. Prior to lysis, cells were rinsed twice with ice-cold PBS. Detergent lysates were made in a standard radioimmunoprecipitation assay buffer. Cells were homogenized and clarified by centrifugation at 10,000 × *g*. Cell lysates (250 μg protein) were reacted for 2 h with either monoclonal antibody 327 (Oncogene Sciences) for immunoprecipitation of $pp60^{c\text{-}src}$ or 1B7 (Wako, Inc., Richmond, VA) for immunoprecipitation of $pp62^{c\text{-}yes}$. Immune complexes were formed by the addition of 6 μg of rabbit anti-mouse IgG (Organon Teknika, Durham, NC) for 1 h, followed by 50 μl of 10% (v/v) formalin-fixed Pansorbin (*Staphylococcus aureus*, Cowan strain; Calbiochem, La Jolla, CA) for 30 min. Pellets were washed three times in a buffer consisting of 0.1% Triton X-100, 150 mM NaCl, and 10 mM sodium phosphate. Immune complex kinases assays were performed by standard procedures as described previously (16). Briefly, reactions were initiated at 4°C by the addition to each sample of 10 μCi of [γ^{32}P]ATP, 10 mM Mg^{2+}, and 100 μM sodium orthovanadate in 20 mM HEPES buffer. After 10 min, reactions were terminated by the addition of SDS sample buffer. Proteins were separated by SDS-PAGE on 10% polyacrylamide gels, and radioactive proteins were detected by autoradiography. Quantitation of differences in activity was determined by densitometry.

Immunoblotting. Clarified cell lysates (250 μg/lane) were separated by SDS-PAGE on 10% gels and electroblotted onto polyvinylidene difluoride membranes (Amersham Corp., Chicago, IL) using standard procedures (16). Membranes were blocked with 15% skimmed milk in PBS, then incubated with anti-src or anti-yes antibodies at 1:1000 dilution, followed by horseradish peroxidase-conjugated rabbit anti-mouse IgG. Specific binding of antibody was determined using the ECL detection system (Amersham).

Oligonucleotide Synthesis. Twenty-two base sense (5'-GGACCATGGGTAGCAACAAGAG3') and antisense (5'-CTCCTTGTTGCTACCCATGGTCC3') unmodified oligonucleotides were synthesized by standard protocols (Millipore Cyclone plus DNA synthesizer), deprotected with 30% NH_4OH, and extracted with 1-butanol (29).

Construction of c-src Expression Vectors and Transfection. A construct spanning the translation start site of $pp60^{c\text{-}src}$ was generated by annealing two primers (5'-AGCTTGGACCATGGGTAGCAACAAGAGCAAGCCCAAGGAT-3') and (5'-CTAGATCCTTGGGCTTGCTCTTGTTGCTACCCATGGTCCA-3'). The antisense construct was synthesized in a similar manner with the two primers (5'-AGCTATCCTTGGGCTTGCTCTTGTTGCTACCCATGGTCCT-3') and 5'-CTAGAGGACCATGGGTAGCAACAAGAGCAAGCCCAAGGAT-3'). The pcDNAI plasmid (InVitrogen) was then digested with *Hin*dIII and *Xba*I, and a ligation reaction was performed to insert the sense and antisense constructs. *Escherichia coli* was transformed by the plasmids, selected clones were harvested, the bacteria were lysed by alkali treatment, and plasmids were purified. Confirmation of the correct insert was determined by PCR followed by DNA sequencing.

Transfection. HT 29 cells were grown to 70% confluency. Cells were transfected in serum-free media for 6 h with the aid of Lipofectamine (Life Sciences) at a ratio of 100 μg of lipofectamine/16 μg of plasmid DNA. G418-resistant colonies were expanded, and the resulting clones were screened for expression and activity of $pp60^{c\text{-}src}$, as described above.

Tumorigenicity Assays. Cells from clones to be tested were grown in tissue culture to log phase (~70% confluent), trypsinized, and counted with the aid of a hemacytometer. Cells (1×10^6) of each clone were injected s.c. in the flank of eight nude mice/cell type. After tumors were detected by visual observation, tumor diameters were measured biweekly with calipers. In animals in which tumors formed, the average tumor volume was calculated.

Acknowledgments

We thank Dr. Hideyuki Saya for advice in constructing the plasmids and Dr. R. B. Arlinghaus for careful reading of the manuscript.

References

1. Vogelstein, B., and Kinzler, K. W. Colorectal cancer and the intersection between basic and clinical research. Cold Spring Harbor Symp. Quant. Mol. Biol., *59:* 517–521, 1994.

2. Bolen, J. B., Veillette, A., Schwartz, A. M., Deseau, V., and Rosen, N. Activation of $pp60^{c\text{-}src}$ protein tyrosine kinase activity in human colon carcinoma. Proc. Natl. Acad. Sci. USA, *84:* 2251–2255, 1987.

3. Cartwright, C. A., Kamps, M. P., Meisler, A. I., Pipas, J. M., and Eckhart, W. $pp60^{c\text{-}src}$ activation in human colon carcinoma. J. Clin. Invest., *83:* 2025–2033, 1989.

4. Talamonti, M. S., Roh, M. S., Curley, S. A., and Gallick, G. E. Increase in level and activity of $pp60^{c\text{-}src}$ in progressive stages of human colorectal cancer. J. Clin. Invest., *91:* 53–60, 1993.

5. Cartwright, C. A., Meisler, A. I., and Eckhart, W. Activation of the $pp60^{c\text{-}src}$ protein kinase is an early event in colonic carcinogenesis. Proc. Natl. Acad. Sci. USA, *87.* 558–562, 1990.

6. Termuhlen, P. M., Curley, S. A., Talamonti, M. S., Saboorian, M. H., and Gallick, G. A. Site-specific differences in $pp60^{c\text{-}src}$ activity in human colorectal metastases. J. Surg. Res., *54:* 293–298, 1993.

7. Park, J., Meisler, A. I., and Cartwright, C. A. c-Yes tyrosine kinase activity in human colon carcinoma. Oncogene, *8:* 2627–2635, 1993.

8. Park, J., and Cartwright, C. A. Src activity increases and Yes activity decreases during mitosis of human colon carcinoma cells. Mol. Cell. Biol., *15:* 2374–2382, 1995.

9. Veillette, A., Foss, F. M., Sausville, E. A., Bolen, J. B., and Rosen, N. Expression of the *lck* tyrosine kinase gene in human colon cancer and other non-lymphoid tumor cell lines. Oncogene Res., *1:* 357–374, 1987.

10. Wang, P., Fromowitz, F., Koslow, M., Hagag, N., Johnson, B., and Viola, M. c-*src* structure in human cancers with elevated $pp60^{c\text{-}src}$ activity. Br. J. Cancer, *64:* 531–533, 1991.

11. Schlaepfer, D. D., Hanks, S. K., Hunter, T., and van der Geer, P. Integrin-mediated signal transduction linked to Ras pathway by GRB2 binding to focal adhesion kinase. Nature (Lond.), *372:* 786–791, 1994.

12. Roche, S., Koegl, M., Barone, M. V., Roussel, M. F., and Courtneidge, S. A. DNA synthesis induced by some but not all growth factors requires Src family protein tyrosine kinases. Mol. Cell. Biol., *15:* 1102–1109, 1995.

13. Roche, S., Fumagalli, S., and Courtneidge, S. A. Requirement for Src family protein tyrosine kinases in G2 for fibroblast cell division. Science (Washington DC), *269:* 1567–1569, 1995.

14. Chackalaparampil, I., and Shalloway, D. Altered phosphorylation and activation of $pp60^{c\text{-}src}$ during fibroblast mitosis. Cell, *52:* 801–810, 1988.

15. Zhao, Y., Krueger, J. G., and Sudol, M. Expression of cellular yes protein in mammalian tissues. Oncogene, *5:* 1629–1635, 1990.

16. Cartwright, C. A., Mamajiwalla, S. A., Skolnick, S. A., Eckhart, W., and Burgess, D. R. Intestinal crypt cells contain higher levels of cytoskeletal-associated $pp60^{c\text{-}src}$ protein tyrosine kinase activity than do differentiated enterocytes. Oncogene, *8:* 1033–1039, 1993.

17. Cartwright, C. A., Coad, C. A., and Egbert, B. M. Elevated c-Src tyrosine kinase activity in premalignant epithelia of ulcerative colitis. J. Clin. Invest., *93:* 509–515, 1994.

18. Garcia, R., Parikh, N. U., Saya, H., and Gallick, G. E. Effect of herbimycin A on growth and $pp60^{c\text{-}src}$ activity in human colon tumor cell lines. Oncogene, *6:* 1983–1989, 1991.

19. Pena, S. V., Melhem, M. F., Meisler, A. I. and Cartwright, C. A. Elevated c-Yes activity in premalignant lesions of the colon. Gastroenterology, *108:* 117–124, 1995.

20. Han, N. M., Curley, S. A., and Gallick, G. E. Differential activation of $pp60^{c\text{-}src}$ and $pp62^{c\text{-}yes}$ in human colorectal liver metastases. Clin. Cancer Res., *2:* 1397–1404, 1996.

21. Waki, M., Kitanaka, A., Kamano, H., Tanaka, T., Kubota, Y., Ohnishi, H., Takahara, J., and Irino, S. Antisense src expression inhibits U937 human leukemia cell proliferation in conjunction with reduction of c-myb expression. Biochem. Biophys. Res. Commun., *201:* 1001–1007, 1994.

22. Kitanaka, A., Waki, M., Kamano, H., Tanaka, T., Kubota, Y., Ohnishi, H., Takahara, J., and Irino, S. Antisense src expression inhibits proliferation and erythropoietin-induced erythroid differentiation of K562 human leukemia cells. Biochem. Biophys. Res. Commun., *201:* 1534–1540, 1994.

23. Soriano, P., Montgomery, C., Geske, R., and Bradley, A. Targeted disruption of the c-*src* proto-oncogene leads to osteopetrosis in mice. Cell, *64:* 693–702, 1991.

24. Mukhopadhyay, D., Tsiokas, L., Zhou, X. M., Foster, D., Brugge, J. S., and Sukhatme, V. P. Hypoxic induction of human vascular endothelial factor expression through c-*src* activation. Nature (Lond.), *375:* 577–581, 1995.

25. Guy, C. T., Cardiff, R. D., and Muller, W. J. Induction of mammary tumors by expression of polyomavirus middle T oncogene: a transgenic model for metastatic disease. Mol. Cell. Biol., *12:* 954–961, 1992.

26. Guy, C. T., Muthuswamy, S. K., Cardiff, R. D., Soriano, P., and Muller, J. W. Activation pf the c-Src tyrosine kinase is required for the induction of mammary tumors in transgenic mice. Genes Dev., *8:* 23–32, 1994.

27. Courtneidge, S. A., Fumagalli, S., Koegl, M., Superti-Furga, G., and Twamley-Stein, G. M. The Src family of protein tyrosine kinases: regulation and functions. Development (Camb.) (Suppl.): 57–64, 1993.

28. Erpel, T., and Courtneidge, S. A. Src family protein tyrosine kinases and cellular signal transduction pathways. Curr. Opin. Cell Biol., *7:* 176–182, 1995.

29. Sawadago, M., and Van Dyke, M. A rapid method for the purification of oligodeoxynucleotides. Nucleic Acids Res., *19:* 674, 1991.

THE JOURNAL OF BIOLOGICAL CHEMISTRY
Vol. 266, No. 14, Issue of May 15, pp. 8667-8670, 1991

The Tyrosine Kinase *lck* Is Critically Involved in the Growth Transformation of Human B Lymphocytes*

(Received for publication, October 31, 1990)

Roy K. Cheung and Hans-Michael Dosch‡

From the Departments of Pediatrics and Immunology, University of Toronto and The Research Institute, Hospital for Sick Children, Toronto, Ontario M5G 1X8, Canada

Epstein-Barr virus (EBV) exposure of human B lymphocytes induces rapid, Ca^{2+}-dependent tyrosine phosphorylation of two cytosolic proteins, one likely the CD21 EBV receptor and another unknown species of 55–60 kDa. We now identify the latter protein as the tyrosine kinase *lck* ($p56^{lck}$). In T cells many activation events *reduce* the high constitutive $p56^{lck}$ expression levels typical for that lineage, and they induce the appearance of a 60-kDa *lck* species. We now demonstrate that in B cells exposed to EBV the at best low constitutive $p56^{lck}$ expression levels are rapidly and transiently up-regulated without generation of 60-kDa *lck*. *lck*-specific antisense oligonucleotides block $p56^{lck}$ induction and prevent subsequent B cell activation and immortalization whereas B cell activation by nononcogenic agents was unaffected. We propose that $p56^{lck}$ superinduction is a transformation prerequisite which signals entry into the oncogenic growth transformation process.

Protein modification by phosphorylation is the post-translational motor for a wide range of cellular functions and usually involves serine- or threonine phosphokinases. Tyrosine kinases provide <1% of cytosolic phosphorylation and have specifically been associated with cell activation and growth control (1, 2). The lymphoid cell lineage-specific tyrosine kinase $p56^{lck}$, a relative of the viral oncogene v-*src*, is overexpressed in several T-lymphomas/leukemias (3–5). Human $p56^{lck}$ transcripts are abundant in thymus, common in $CD4^+$ and $CD8^+$ T cells, and present in at least some B cells and some but not all EBV[1]-transformed B cell lines (6, 7).

EBV is a ubiquitous, usually latent human herpes virus closely associated with several malignancies (8–12). *In vitro*, EBV transforms human B lymphocytes into immortal cell lines; latently infected B cells, transformed lines, or injected virus produce high grade lymphomas in susceptible hosts (9, 12–15).[2] Transition to the transformed phenotype is of considerable clinical relevance but poorly understood (9–11). A recent series of experiments delineated cytosolic events triggered in target B cells within minutes following EBV infection (16). These events include activation of the Na^+/H^+ antiporter, uniquely shaped transmembrane Ca^{2+} fluxes, induction of several heat shock proteins (hsp), as well as tyrosine phosphorylation of an unknown 55–60 kDa protein and of (likely) the 145-kDa EBV receptor (CD21). Several of these events are unique for EBV and critical for successful B cell transformation, suggesting that the oncogenic transformation process differs from nononcogenic B cell activation pathways already very early (16). In this report, we identify $p56^{lck}$ as an enzyme critically associated with this process.

MATERIALS AND METHODS

Cell and Virus Preparations—Mononuclear cells were obtained by Ficoll-Hypaque density centrifugation from tonsils of children undergoing tonsillectomy, and B lymphocytes were purified by E-rosette depletion of mononuclear tonsil cells (17). Growth-transforming EBV was obtained from the B95–8 marmoset line (18). Cell-free supernatants were concentrated 10-fold by ultracentrifugation and stored in liquid nitrogen (19).

Western Blots—Purified B cells (10^6) were incubated (10 min–24 h, 37 °C) with 10^5 B95–8 EBV particles (16). EBV-treated or untreated B cells were spun through oil (3 parts corn oil and 10 parts dibutyl phthalate) and washed twice with phosphate-buffered saline. Cells were solubilized in 10 μl sample buffer (5 ml of 10% SDS, 2.5 ml of 1.5 M Tris, pH 8.8, 2.5 ml of glycerol, 0.25 ml of 2-mercaptoethanol, 0.2 ml of 5% bromphenol blue, and 5 ml of dH_2O) and boiled (10 min), chilled, cleared, and separated on 10% SDS-polyacrylamide gels followed by electroblotting onto nitrocellulose membranes. Membranes were blocked (2 h) with 5% skim milk, followed by 1-h exposure to monoclonal antibody against phosphotyrosine (1/500, Amersham, Mississauga, Ontario), human CD20 (1/1000, Coulter Diagnostics, Hialeah, FL), or human *lck* (1/10, gift from Dr. T. Mak, Ontario Cancer Institute, Toronto, Ontario). Membranes were washed with TBS/Tween (10 mM Tris, 150 mM NaCl, 0.5% Tween), and biotinylated anti-mouse Ig (1/500, Amersham) was added for 20 min. Membranes were washed with TBS/Tween, and streptavidin-alkaline phosphatase complex (1/3000) (Amersham) was added for 20 min, washed, and exposed to substrate (nitroblue tetrazolium/BCIP in diethanolamine buffer, Amersham) until visible bands developed (16).

Polymerase Chain Reaction—Purified B lymphocytes were treated with EBV as before, and Jurkat (T-) cells provided *lck*-positive control cells (5). Extracted cytosolic RNA (10 ng) was reverse-transcribed to cDNA and amplified by PCR in a single tube reaction as described (20). Oligonucleotide primers (100 nM) lck^{121} (5′-CGCCAGAAGCCATTAACTA-3′) and lck^{601} (5′-GACAATGTGCAGAGTCCAC-3′) used published sequences from the positions indicated (6, 21). Following an initial denaturation step, samples were cycled through 1 min/51 °C, 2 min/72 °C, and 1 min/94 °C in a Thermocycler (Ericomp Inc., San Diego, CA). After 28 cycles, 10 μl of the PCR-amplified product was size-fractionated by gel electrophoresis, blotted onto nylon membranes, and probed with a γ-^{32}P-end-labeled, internal oligonucleotide probe lck^{481} (5′-GCACAAGAACTCCATTCTCC-3′). Control samples where the reverse transcriptase-mediated cDNA synthetic step was omitted never showed PCR product that hybridized with the reporter oligonucleotide.

Uptake of Oligonucleotides into B Cells—γ-^{32}P-End-labeled oligonucleotide (2 μM) was incubated with B cells (10^6) at 37 °C for 30 min–8 h until cells were separated from supernatant by centrifugation through oil (3 parts corn oil and 10 parts dibutyl phthalate). Cells and aliquots of supernatant were counted.

Measurement of B Cell Activation and Transformation—EBV-

* This work was supported by grants from the Medical Research Council and National Cancer Institute of Canada as well as a URIF Program Grant from the Province of Ontario. The costs of publication of this article were defrayed in part by the payment of page charges. This article must therefore be hereby marked "*advertisement*" in accordance with 18 U.S.C. Section 1734 solely to indicate this fact.

‡ To whom correspondence should be addressed: The Hospital for Sick Children, 555 University Ave., Toronto, Ontario M5G 1X8, Canada. Fax: 416-598-6897.

[1] The abbreviations used are: EBV, Epstein-Barr virus; SDS, sodium dodecyl sulfate; PCR, polymerase chain reaction; BCECF, 2′,7′-biscarboxyethyl-5[6]-carboxyfluorescein; BCIP, 5-bromo-4-chloro-3indoyl phosphate.

[2] Dosch, H.-M., D. M. G. Cochrane, V. A. Cook, S. L. Leeder, and R. K. Cheung (1991) *Int. Immunol.*, in press.

induced growth transformation was measured by two closely linked parameters: Ig production and actual cell growth as described (16, 17). Purified B lymphocytes (5×10^4) were incubated (30 min, 2 μM in 96-well round bottom plates) with one of the following oligonucleotides: *lck*^{121}, *lck*^{481}, *lck*^{601} (see above), or *lck*^{580} (5′-CTCAAGGAAATGGGAGAGC-3′). EBV (10^5 particles) was then added, and cells were cultured in RPMI 1640 containing 10% fetal calf serum at 37 °C for 14 days. Ig secretion was measured by automated particle concentration fluorescence immunoassay procedures using a Baxter-Pandex ScreenMachine (Baxter-Pandex, Mundelein, IL) as described (16, 22, 23). Briefly, affinity-purified goat antibodies to a given Ig isotype (BioCan Scientific, Mississauga, Ontario) were covalently conjugated onto 0.9-μm polystyrene particles, and 20 μl of a 0.15% suspension were added to 96-well unidirectional flow vacuum filtration plates, followed by 5–20 μl of culture supernatant, phase separation, and 10 ng of fluorescein isothiocyanate-conjugated, affinity-purified goat anti-human Ig antibodies. Additions, incubation, phase separation, washing steps, and fluorescence reading were done automatically by the instrument, and data were transmitted to and analyzed with MacPlate Macintosh software (HSC, Toronto, Ontario). EBV-induced cell growth was measured in a ScreenMachine by an automated fluorescence technique with the fluorescent dye 2′,7′-biscarboxyethyl-5[6]-carboxyfluorescein (BCECF) (22). Briefly, cells were dye-loaded (30 min) with 1 μg/ml BCECF-acetoxy methyl ester, and aliquots were transferred to 96-well vacuum filtration plates, washed by the ScreenMachine. The fluorescence emission (493/540 nm excitation/emission) of intracellular dye was measured together with that of standard purple dye particles (540/640 nm). Cell numbers were extrapolated using as a reference dilutions of dye-loaded transformed lymphoblasts generated in our laboratory (22).

RESULTS AND DISCUSSION

Rosette-purified human B cells (<1% T cells) were exposed (5 min–24 h, 37 °C) to EBV, washed twice, spun through oil, and lysed (Fig. 1). Lysates were separated on SDS-polyacrylamide gels and Western-transferred to nitrocellulose membranes for probing with monoclonal anti-phosphotyrosine antibody (16). Tyrosine phosphorylation of a ~56-kDa protein appeared rapidly within 10 min of virus exposure, reaching a maximum at 3–6 h and declining to control levels by 24 h. We previously found no such phosphorylation following activation of B cells with mitogen, phorbol myristate acetate, or ionomycin (16). Control blots, probed with anti-CD20 (23), confirmed that similar amounts of lysate had been analyzed (*panel B*).

Parallel blots were probed with anti-*lck* antibody (*panel C*) (24). A single species of p56^{lck} protein was positively identified as a faint but definitive band before and 5 min after EBV exposure. After 15 min (total processing time, 23 min) p56^{lck} was superinduced, reaching maximum levels by 3–6 h and declining to control levels by 24 h (*panel A*). Sequential immune precipitation (not shown) demonstrated that prior precipitation with anti-p56^{lck} removed the tyrosine-phosphorylated 56-kDa species, confirming that it represents autophosphorylated p56^{lck}. In neither untreated nor EBV-infected samples did we find a protein species with slower mobility (60 kDa) that was detected by either anti-phosphotyrosine or by anti-*lck* antibodies.

Exposure of purified T cells to EBV had no effects on p56^{lck} (not shown) or ion fluxes (16). T cell activation reduces p56^{lck} and generates a modified 60-kDa *lck* protein (25, 26). Our observation of increased p56^{lck} and absent p60^{lck} (Fig. 1) suggests either different processing pathways in T and B cells, or differences among nononcogenic and oncogenic transformation processes. As murine lymphoma lines (*e.g.* LSTRA (27)) express the p56^{lck} but not p60^{lck} at high levels, the latter may be more likely.

The rapid onset of tyrosine phosphorylation placed the kinase and its substrate as normal, low level constituents of the cytosol in resting B cells. To understand the further rise in expression, levels of p56^{lck} mRNA were compared in EBV-exposed B lymphocytes as described (16, 20). To reduce cell and virus requirements, PCR was used to establish time kinetics of post-EBV *lck* expression; results were confirmed by Northern blots for zero and 3-h exposure times. For PCR, primer pairs were constructed to flank a 500-base pair *lck* gene region (positions 100–600 (21)), *lck* cDNA was reverse-transcribed from cytoplasmic RNA as described (20), and cDNA was amplified in a standard, 28-cycle PCR reaction (28). PCR product was gel-separated, blotted, and probed with an internal ^{32}P-end-labeled reporter probe (positions 461–481).

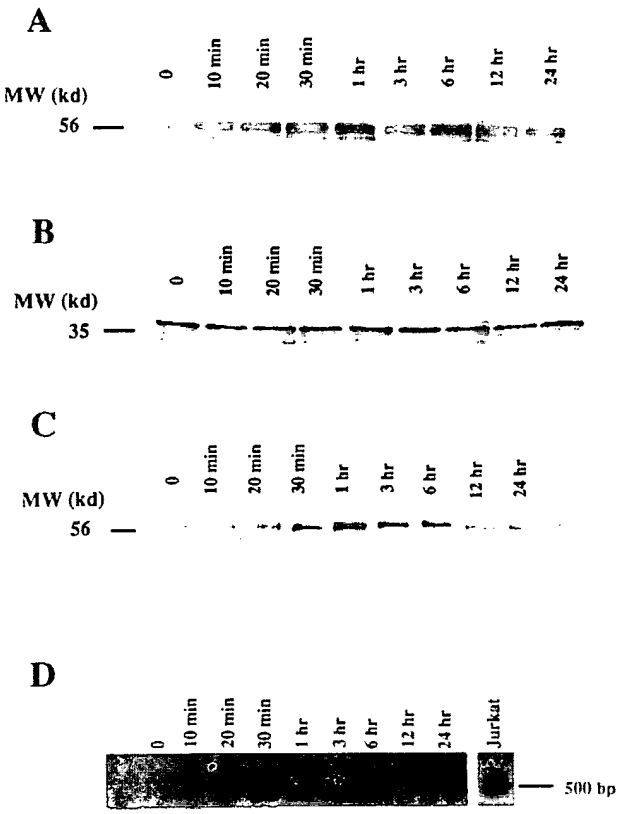

FIG. 1. **Induction kinetics of tyrosine phosphorylation, p56^{lck}, and *lck* mRNA in B lymphocytes exposed to EBV.** Purified B cells (10^6) were incubated with 10^6 B95-8 EBV particles for the periods indicated (10 min–24 h, 37 °C). Cell lysates were then size-fractionated by SDS-polyacrylamide gel electrophoresis and blotted onto nitrocellulose membrane. Monoclonal anti-phosphotyrosine antibodies (*A*), anti-CD20 antibodies (*B*), and anti-*lck* antibodies (*C*) were used to probe parallel blots. *D*, induction of *lck* mRNA by EBV in human B cells. Purified B lymphocytes were treated with EBV as in *A–C*. Jurkat (T-) cells provided *lck*-positive control cells. Extracted cytosolic RNA (10 ng) was reverse-transcribed to cDNA and amplified by standard, 28-cycle PCR. PCR product was size-fractionated by gel electrophoresis, blotted onto nylon membranes, and probed with a γ-^{32}P-end-labeled, internal oligonucleotide probe *lck*^{481} (5′-GCACAAGAACTCCATTCTCC-3′). In control samples where the reverse transcriptase-mediated cDNA synthetic step was omitted no DNA was found hybridizing with the reporter oligonucleotide. *bp*, base pairs.

lck message could barely be amplified and detected in untreated B cells (Fig. 1*D*). Upon EBV exposure, there was a rapid induction of *lck* mRNA, demonstrable by 10-min (total processing time, 15 min) and maximal 3 h after EBV exposure. This mRNA was consumed to control levels 12 h after stimulation. In agreement with findings elsewhere (7), *lck* message was very faint in Northern blots of untreated cells even after several weeks of film exposure, but it was easily detectable 3

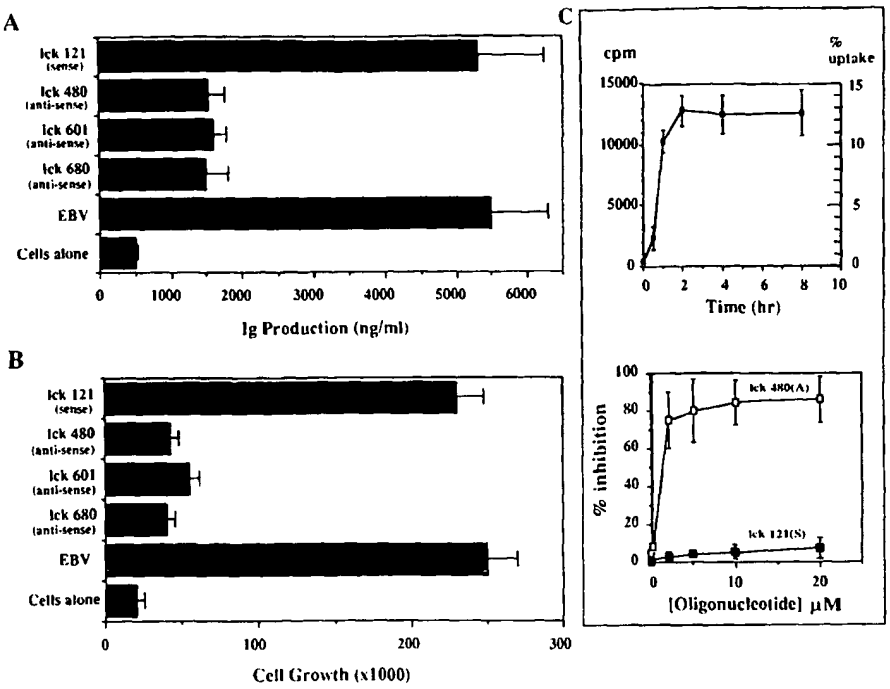

FIG. 2. **Effects of *lck* sense- and antisense oligonucleotides on EBV-induced growth transformation.** Purified B lymphocytes (5×10^4) were incubated (30 min, 2 μM) with oligonucleotides lck^{121}, lck^{481}, lck^{601}, or lck^{680} (see "Materials and Methods"). EBV (10^5 particles) was then added, and cells were cultured in RPMI 1640 containing 10% fetal calf serum for 14 days. Ig secretion (*A*) was measured by automated particle concentration fluorescence immunoassay procedures. EBV-induced cell growth (*B*) was measured in the same instrument using an automated fluorescence technique with the fluorescent dye BCECF for automated counts of viable cells generated. Data represent the mean ± 1 S.D. of three experiments. *C*: *top panel*, uptake of oligonucleotide into B cells. γ^{32}-P-End-labeled oligonucleotide (2 μM) was incubated with B cells (10^6, 30 min–8 h, 37 °C) until cells were spun through oil. Cells and aliquots of supernatant were counted and plotted as absolute uptake and proportional (%) uptake over time. Data represent the mean ± 1 S.D. of three experiments for the oligonucleotide lck^{481}. Other oligonucleotides including both sense and antisense oligonucleotides show similar uptake kinetics. *Bottom panel*, dose dependence of *lck* antisense oligonucleotide effects on EBV-induced Ig secretion. B cells (5×10^4) were incubated with the respective oligonucleotide at the doses shown, infected with EBV as before, cultured (14 days), and analyzed for EBV-induced Ig secretion. Results are expressed as % inhibition of oligonculeotide-free control *versus* concentrations of oligonucleotide. Data (mean ± 1 S.D. of three experiments) are shown for lck^{481} (antisense) and lck^{121} (sense) sequences; results were similar for cell growth measurements with BCECF.

h after EBV infection. EBV induced no changes of *lck* message levels in T cells (not shown). The *lck* primer pairs chosen consistently amplified two sequence species of slightly (<100 base pairs) different size. We are presently cloning these fragments to determine if alternative RNA splicing accounts for these two products.

The induction of tyrosine kinase by EBV is dependent on a transmembrane Ca^{2+} flux and activation of the Na^+/H^+ antiport. Blockade of either event reversibly prevents tyrosine phosphorylation and generates nontransforming cells which do, however, contain competent virus and viral transcripts (16). To evaluate whether the induction of $p56^{lck}$ is a by-product or an essential, consecutive step after the initial ionic activation events, we used *lck* sense/antisense oligonucleotides to manipulate its expression levels in a sequence-specific fashion, likely through RNase H-mediated destruction of mRNA (29–31).

Human B cells take up 8–15% of ~20-mer oligonucleotides with cytosolic plateau concentrations of 1–3 μM reached with 2 h of exposure to such concentrations (Fig. 2). B lymphocytes were exposed to EBV in the presence of the above sense or antisense *lck* oligonucleotides and cultured for 14 days. We then measured two closely linked (16) indicators of transformation: absolute cell growth and Ig production (17, 22, 23).

EBV-induced cell growth and Ig production were inhibited (>70%) by *lck* antisense but not sense oligonucleotides (Fig. 2, *A* and *B*). This antisense effect was dose-dependent and followed the cellular uptake curve closely (Fig. 2*C*). B cells escaping antisense inhibition proceeded normally toward immortalization, perhaps due to low level expression of the DNA receptor mediating oligonucleotide uptake (33). Control cultures were stimulated with pokeweed mitogen in the presence of T cell help (32) and oligonucleotides. Neither oligonucleotide affected the mitogen response, indicating that treated B cells were functionally unimpaired (not shown).

Taken together, our observations delineate a critical role for $p56^{lck}$ in the EBV-directed B cell transformation into oncogenic (9, 12–14), immortalized lines. Its timing, and calcium- and Na^+/H^+-antiport dependence make *lck* superinduction perhaps the earliest *structural* signal for cell entry into a growth transformation process that is even early on quite distinct from activation pathways utilized by nontransforming agents (16). The nature and target of the $p56^{lck}$ signal remain to be delineated. Since only some but not all EBV-transformed lines express $p56^{lck}$ (6, 7),[3] it appears that its functions are not necessary to sustain the transformed phe-

[3] R. K. Cheung and H.-M. Dosch, unpublished observations.

notype once appropriate changes have occurred under *lck* influence.

Acknowledgments—We wish to thank Dr. Tak Mak (Toronto) for his kind gift of anti-*lck* antibody and Drs. Cohen, Doherty, and Mak (Toronto) for helpful suggestions and critical review.

REFERENCES

1. Ullrich, A., and Schlessinger, J. (1990) *Cell* **61,** 203–212
2. Ralph, R. K., Darkin R. S., and Schofield, P. (1990) *Bioessays* **12,** 121–124
3. Garvin, A. M., Pawar, S., Marth, J. D., and Perlmutter, R. J. (1988) *Mol. Cell. Biol.* **8,** 3058–3064
4. Marth, J. D., Cooper, J. A., King, C. S., Ziegler, S. F., Tinker, D. A., Overell, R. W., Krebs, E. G., and Perlmutter, R. M. (1988) *Mol. Cell Biol.,* **8,** 540–550
5. Koga, Y., Kimura, N., Minowada, J., and Mak, T. W. (1988) *Cancer Res.* **48,** 856–859
6. Perlmutter, R. M., Marth, J. D., Lewis, D. B., Peet, R., Ziegler, S. F., and Wilson, C. B. (1988) *J. Cell. Biochem.* **38,** 117–126
7. Koga, Y., Caccia, C., Toyonaga, B., Spolski, R., Yanagi, Y., Yoshikai, Y., and Mak, T. W. (1986) *Eur. J. Immunol.* **16,** 1643–1650
8. Baer, R., Bankier, A., Biggin, M., Deininger, P., Farrel, P., Gibson, T., Hatful, G., Hudson, G., Stachwell, S., Sequin, P., and Barrell, B. (1984) *Nature* **310,** 207–211
9. Brusamolino, E., Pagnucco, G., and Bernasconi, C. (1989) *Haematologica* **74,** 605–622
10. Cleary, M. L., Nalesnik, M. A., Shearer, W. T., and Sklar, J. (1988) *Blood* **72,** 349–352
11. Nalesnik, M. A., Jaffe, R., Starzl, T. E., Demetris, A. J., Porter, K., Burnham, J. A., Makowka, L., Ho, M., and Locker, J. (1988) *Am. J. Pathol.* **133,** 173–192
12. Purtilo, D. T., Manolov, G., Manolova, Y., Harada, S., Lipscomb, H., and Tatsumi, E. (1985) *IARC Sci. Publ.* **198,** 231–247
13. Cannon, M. J., Pisa, P., Fox, R. I., and Cooper, N. R. (1990) *J. Clin. Invest.* **85,** 1333–1337
14. Mosier, D. E., Gulizia, R. J., Baird, S. M., Spector, S., Spector, D., Kipps, T. J., Fox, R. I., Carson, D. A., Cooper, N., Richman, D. D., *et al.* (1989) *Curr. Top. Microbiol. Immunol.* **152,** 195–199
15. EMBO Workshop (1989) *Curr. Top. Microbiol. Immunol.* **152,** 1–263
16. Dosch, H.-M., Lam, P., Hui, M. F., Hibi, T., and Cheung, R. K. (1990) *Int. Immunol.* **2,** 833–848
17. MacKenzie, T., and Dosch, H. M. (1989) *J. Exp. Med.* **169,** 407–430
18. Hibi, T., Chan, M. A., Petsche, D., and Dosch, H. M. (1986) *J. Immunol.* **136,** 3211–3218
19. Hibi, T., and Dosch, H. M. (1986) *Eur. J. Immunol.* **16,** 139–145
20. Doherty, P. J., Huesca, M., Dosch, H. M., and Pan, S. (1989) *Anal. Biochem.* **177,** 7–10
21. Veillette, A., Foss, F. M., Sausville, E. A., Bolen, J. B., and Rosen, N. (1987) *Oncogene Res.* **1,** 357–374
22. Leeder, J. S., Dosch, H. M., Harper, P. A., Lam, P., and Spielberg, S. P. (1989) *Anal. Biochem.* **177,** 364–372
23. Hui, M. F., Lam, P., and Dosch, H. M. (1989) *J. Immunol.* **143,** 2470–2479
24. Takadera, T., Leung, S., Gernone, A., Koga, Y., Takihara, Y., Miyamoto, N. G., and Mak, T. W. (1989) *Mol. Cell. Biol.* **9,** 2173–2180
25. Veillette, A., Horak, I. D., Horak, E. M., Bookman, M. A., and Bolen, J. B. (1988) *Mol. Cell. Biol.* **8,** 4353–4361
26. Marth, J. D., Lewis, D. B., Cooke, M. P., Mellins, E. D., Gearn, M. E., Samelson, L. E., Wilson, C. B., Miller, A. D., and Perlmutter, R. M. (1989) *J. Immunol.* **142,** 2430–2437
27. Voronova, A. F., Adler, H. T., and Sefton, B. M. (1987) *Mol. Cell. Biol.* **7,** 4407–4413
28. Saiki, R. K., Gelfand, D. H., Stoffel, S., Scharf, S. J., Higuchi, R., Horn, G. T., Mullis, K. B., and Erlich, H. A. (1988) *Science* **239,** 487–491
29. Stein, C. A., and Cohen, J. S. (1988) *Cancer Res.* **48,** 2659–2668
30. Marcus, C., and Sekura, J. (1988) *Anal. Biochem.* **172,** 289–295
31. Shuttleworth, J., and Colman, A. (1988) *EMBO J.* **7,** 427–434
32. Dosch, H. M., Lam, P., and Guerin, D. (1985) *J. Immunol.* **135,** 3808–3816
33. Loke, S. L., Stein, C. A., Zhang, X. H., Mori, K., Nakanishi, M., Subasinghe, C., Cohen, J., and Neckers, L. M. (1989) *Proc. Natl. Acad. Sci. U. S. A.* **86,** 3474–3478

25 Roy, J.B. *et al.* (1990) A clinical trial of intracavernous vasoactive intestinal peptide to induce penile erection. *J. Urol.* 143, 302–304
26 McMahon, C.G. (1996) A pilot study of the role of intracavernous injection of vasoactive intestinal peptide (VIP) and phentolamine mesylate in the treatment of erectile dysfunction. *Int. J. Impot. Res.* 8, 233–236
27 Montorsi, F. *et al.* (1995) Pharmacological management of erectile dysfunction. *Drugs* 50, 465–479
28 Mulhall, J.P. *et al.* (1997) Intracavernosal forskolin: role in management of vasculogenic impotence resistant to standard 3-agent pharmacotherapy. *J. Urol.* 158, 1752–1758
29 Burnett, A.L. (1997) Nitric oxide in the penis: physiology and pathology. *J. Urol.* 157, 320–324
30 Gupta, S. *et al.* (1995) Possible role of Na^+–K^+-ATPase in the regulation of human corpus cavernosum smooth muscle contractility by nitric oxide. *Br. J. Pharmacol.* 116, 2201–2206
31 Nathan, C. and Xie, Q.W. (1994) Nitric oxide synthases: roles, tolls, and controls. *Cell* 78, 915–918
32 Stief, C.G. *et al.* (1992) Preliminary results with the nitric oxide donor linsidomine chlorhydrate in the treatment of human erectile dysfunction. *J. Urol.* 148, 1437–1440
33 Porst, H. (1993) Prostaglandin E_1 and the nitric oxide donor linsidomine for erectile failure: a diagnostic comparative study of 40 patients. *J. Urol.* 149, 1280–1283
34 Hatzichristou, D. (1998) Current treatment and future perspectives for erectile dysfunction. *Int. J. Impot. Res.* 10, S3–S13
35 Dousa, T.P. (1999) Cyclic-3′,5′-nucleotide phosphodiesterase isozymes in cell biology and pathophysiology of the kidney. *Kidney Int.* 55, 29–62
36 Taher, A. *et al.* (1997) Cyclic nucleotide phosphodiesterase in human cavernous smooth muscles. *World J. Urol.* 15, 32–35
37 Ballard, S.A. *et al.* (1998) Effects of sildenafil on the relaxation of human corpus cavernosum tissue *in vitro* and on the activities of cyclic nucleotide phosphodiesterase isozymes. *J. Urol.* 159, 2165–2171
38 Goldstein, I. *et al.* (1998) Oral sildenafil in the treatment of erectile dysfunction. *New Engl. J. Med.* 338, 1397–1404
39 Bivalacqua, T.J. *et al.* (1999) Potentiation of erectile response and cAMP accumulation by combination of prostaglandin E_1 and rolipram, a selective inhibitor of the type 4 phosphodiesterase (PDE 4). *J. Urol.* 162, 1848-1855
40 Traish, A.M. *et al.* (1999) α-Adrenergic receptors in the penis: identification, characterization, and physiological function. *J. Androl.* 20, 671–682
41 Kunelius, P. *et al.* (1997) Is high-dose yohimbine hydrochloride effective in the treatment of mixed-type impotence? A prospective, randomized, controlled double-blind crossover study. *Urology* 49, 441–444
42 Zorgniotti, A.W. (1993) On demand oral drug for erection on impotent men. *J. Urol.* 147, 308A
43 Moncada Iribarren, I. and Saenz de Tejada, I. (1999) Pharmacological treatment of erectile dysfunction. *Curr. Opin. Urol.* 9, 547–551
44 Padma-Nathan, H. *et al.* (1999) Efficacy and safety of apomorphine sl vs placebo for male erectile dysfunction. *J. Urol.* 161, 821A
45 Christ, G.J. and Melman, A. (1998) The application of gene therapy to the treatment of erectile dysfunction. *Int. J. Impot. Res.* 10, 111–112
46 Garban, H. *et al.* (1997) Cloning of rat and human inducible penile nitric oxide synthase. Application for gene therapy of erectile dysfunction. *Biol. Reprod.* 56, 954–963
47 Christ, G.J. *et al.* (1998) Intracorporal injection of hSlo cDNA in rats produces physiologically relevant alterations in penile function. *Am. J. Physiol.* 275, H600–H608
48 Champion, H.C. *et al.* (1999) Gene transfer of endothelial nitric oxide synthase to the penis augments erectile responses in the aged rat. *Proc. Natl. Acad. Sci. U. S. A.* 96, 11648–11652
49 Bivalacqua, T.J. *et al.* (2000) Adenoviral gene transfer of endothelial nitric oxide synthase (eNOS) to the penis improves age-related erectile dysfunction in the rat. *Int. J. Impot. Res.* 12, S8–S17

Src inhibitors: drugs for the treatment of osteoporosis, cancer or both?

Mira Šuša, Martin Missbach and Jonathan Green

Src was one of the first proto-oncogenes to be identified and is a prototype of non-receptor type tyrosine kinases. The role of Src in bone metabolism first became apparent in Src-deficient mice and has been confirmed using low-molecular-weight Src inhibitors in animal models of osteoporosis. At the cellular level, it is well established that Src plays an important role in proliferation, and adhesion and motility. In addition, recent data indicate an involvement of Src in cell survival and intracellular trafficking in various specialized cell types. These new findings suggest that Src inhibitors might have therapeutic value in the suppression of tumor growth, tumor angiogenesis and bone resorption.

The protein tyrosine kinase Src is the prototype of a kinase family that comprises eight members in vertebrates, namely: Src, Fyn, Yes, Fgr, Hck, Lyn, Lck and Blk. In contrast to receptor tyrosine kinases, which are integral plasma membrane proteins, Src belongs to the non-receptor class of tyrosine kinases[1]. Src associates with various intracellular membranes, where it catalyzes the transfer of phosphate from ATP to a tyrosine residue within proteins. Src, the first tyrosine kinase to be characterized, was initially identified in the late 1970s in its viral form (v-Src) as a protein encoded by chicken Rous sarcoma virus. The cellular counterpart of v-Src, c-Src, is widely expressed in mammalian cells, with particularly high concentrations in brain, platelets and bone-resorbing osteoclasts.

The structure of Src and its regulation are well understood as a result of both mutational studies and structural models derived from X-ray crystallography data[2]. The N-terminus has a unique sequence but its three-dimensional structure and function are poorly defined. Two globular domains, Src homology domains 2 and 3 (SH2 and SH3), are adjacent to the N-terminus, and are involved in protein–protein interactions. The SH1 domain has tyrosine kinase functionality within a two-lobe structure (corresponding to an ATP- and substrate-binding site) that is common to other protein kinases. Within the catalytic SH1 domain, Tyr416 (in chicken c-Src) must be autophosphorylated for maximal activity, whereas the C-terminus (tail) can be phosphorylated (Tyr527 in chicken c-Src) and folded back onto the SH2 domain to produce an inactive conformation.

M. Šuša, Program Head, E-mail: mira.susa_spring@pharma.novartis.com
M. Missbach, Head of Bone Metabolism Chemistry, E-mail: martin.missbach@pharma.novartis.com and
J. Green, Head of the Src Program, Arthritis and Bone Metabolism Therapeutic Area, Novartis Pharma Research, WKL-125.9.12, CH-4002 Basel, Switzerland. E-mail: jonathan.green@pharma.novartis.com

0165-6147/00/$ – see front matter PII: S0165-6147(00)01567-4

Box 1. Cellular functions of Src

Many of the known and putative functions of Src (Fig. I) were first elucidated in a fibroblast cell culture, which is a generic *in vitro* cellular system. In fibroblasts, a role of Src became apparent in both receptor-tyrosine-kinase-mediated proliferation and transformation of the cell to a tumor phenotype[a]. For example, after binding directly to the cytoplasmic part of platelet-derived growth factor (PDGF) receptor, Src is phosphorylated and activated. Activated Src transduces a signal via phosphorylation of the adaptor protein Shc to the cascade that involves Ras and the mitogen-activated protein kinase (MAPK) family member, extracellular regulated kinase (Erk). This induces transcription of the early gene *c-myc* and increases DNA synthesis. In human tumors, Src probably contributes to tumor growth in synergy with receptor tyrosine kinases, such as c-Met and those of the ErbB family[b,c]. ErbB receptors (in breast cancer) or interleukin 6 (IL-6) receptors (in multiple myeloma) can activate signal transducer and activator of transcription 3 (STAT3) via Src and Etk kinase and induce cell transformation, whereas Src inhibitors can reverse the transformed cell phenotype[d–f].

The roles of Src in integrin signaling, cell migration and internalization (endocytosis) of tyrosine kinase receptors were first elucidated in fibroblasts and tumor cell lines[g,h]. Integrin signaling involves Src in a complex interplay between Fak and Pyk2 (both of these tyrosine kinases are related and also substrates for Src), p130 Cas (an adaptor protein) and Src substrate, all of which regulate the formation of actin stress fibers[i]. The small GTP-binding protein Rho modulates this process and can activate Src (Ref. j). In bone-resorbing osteoclasts, Src probably has a role in cell motility (via integrins) and, via Pyk2, in the formation of the sealing zone, which is a ring of polymerized actin that separates the bone-resorbing ruffled membrane from the extracellular surroundings[j] (M. Šuša *et al.*, unpublished). Through vesicular trafficking on the microtubular network[k], Src might also influence the exocytosis of proteases that are required for bone resorption.

Furthermore, Src could mediate the survival signal that is induced by receptor activator of nuclear factor κB (RANK) and involves the adaptor molecule tumor necrosis factor receptor-associated factor 6 (TRAF6) and protein kinase B (PKB)[l]. This probably results in the inhibition of apoptosis via downstream proteases, such as caspase-3.

Finally, Src is involved in macrophage colony stimulating factor (M-CSF)-receptor-mediated proliferation of osteoclast precursors and osteoclast spreading[m,n]. In vascular endothelial cells, Src is required for both vascular endothelial growth factor (VEGF)-mediated vascular permeability, possibly via vesiculo–vacuolar organelles (VVOs)[o], and VEGF-induced cell survival[p].

References

a Thomas, S.M. and Brugge, J.S. (1997) Cellular functions regulated by Src family kinases. *Annu. Rev. Cell. Dev. Biol.* 13, 513–609

b Biscardi, J.S. *et al.* (1999) c-Src, receptor tyrosine kinases and human cancer. *Adv. Cancer Res.* 76, 61–119

c Mao, W. *et al.* (1997) Activation of c-Src by receptor tyrosine kinases in human colon cancer cells with high metastatic potential. *Oncogene* 15, 3083–3090

d Turkson, J. *et al.* (1998) STAT3 activation by Src induces specific gene regulation and is required for cell transformation. *Mol. Cell. Biol.* 18, 2545–2552

e Karni, R. *et al.* (1999) Inhibition of pp60c-Src reduces Bcl-XL expression and reverses the transformed phenotype of cells overexpressing EGF and HER-2 receptors. *Oncogene* 18, 4654–4662

f Tsai, Y. *et al.* (2000) Etk, a Btk family tyrosine kinase, mediates cellular transformation by linking Src to STAT3 activation. *Mol. Cell. Biol.* 20, 2043–2054

g Fincham, V.J. and Frame, M.C. (1998) The catalytic activity of Src is dispensable for translocation to focal adhesions but controls the turnover of these structures during cell motility. *EMBO J.* 17, 81–92

h Wilde, A. *et al.* (1999) EGF receptor signaling stimulates Src kinase phosphorylation of clathrin, influencing clathrin redistribution and EGF uptake. *Cell* 96, 677–687

i O'Neill, G.M. *et al.* (2000) Integrin signalling: a new Cas(t) of characters enters the stage. *Trends Cell Biol.* 10, 111–119

j Chellaiah, M. *et al.* (2000) Rho-A is critical for osteoclast podosome organization, motility, and bone resorption. *J. Biol. Chem.* 275, 11993–12002

k Abu-Amer, Y. *et al.* (1997) Substrate recognition by osteoclast precursors induces c-Src/microtubule association. *J. Cell Biol.* 137, 247–258

l Wong, B.R. *et al.* (1999) TRANCE, a TNF family member, activates Akt/PKB through a signaling complex involving TRAF6 and c-Src. *Mol. Cell.* 4, 1041–1049

m Arai, F. *et al.* (1999) Commitment and differentiation of osteoclast precursor cells by the sequential expression of c-Fms and receptor activator of nuclear factor κB (RANK) receptors. *J. Exp. Med.* 190, 1741–1754

n Insogna, K.L. *et al.* (1997) Colony-stimulating factor-1 induces cytoskeletal reorganization and c-Src-dependent tyrosine phosphorylation of selected cellular proteins in rodent osteoclasts. *J. Clin. Invest.* 100, 2476–2485

o Dvorak, A.M. *et al.* (1996) The vesiculo–vacuolar organelle (VVO): a distinct endothelial cell structure that provides a transcellular pathway for macromolecular extravasation. *J. Leukoc. Biol.* 59, 100–115

p Eliceiri, B.P. *et al.* (1999) Selective requirement for Src kinases during VEGF-induced angiogenesis and vascular permeability. *Mol. Cell.* 4, 915–924

Despite the high level of expression of Src in brain and platelets, mice that are deficient in Src do not show any abnormalities in brain function and blood clotting[3]. Instead, the phenotype of these animals is restricted to defective bone resorption, which results in excessive bone mass and osteopetrosis. Therefore, interest arose in the potential use of Src inhibitors as therapeutic agents for the treatment of osteoporosis, a widespread disease of low bone mass that particularly affects post-menopausal women[4]. In addition, the fact that Src was discovered as an oncogene suggests that Src inhibitors could be used as anti-cancer agents[5].

Cellular functions of Src

Cell proliferation and transformation

Normal growing cells have a tightly regulated cell cycle so that proliferation only occurs in response to various growth factors. By contrast, many transformed cancer cells have a deregulated cell cycle that prevents them from exiting into the G0 (resting) phase, which results in proliferation occurring independently of growth factors. Src associates with several growth factor receptor tyrosine kinases and mediates some of the signal transduction pathways that lead to cell proliferation. One of the best-studied receptor signal transduction pathways is that of the platelet-derived growth factor (PDGF) receptor[3] (Box 1).

Activation of Src by growth factor receptors might contribute to the transformation of the cell to a tumor phenotype (for proposed mechanisms, see Refs 3,5–8). Although activation of the PDGF receptor is not strongly linked to activation of Src in human tumors, there is a good correlation between the activation of c-Met and ErbB tyrosine kinase receptors and the activation of Src in human tumors[5,6].

that are related to cancer and bone

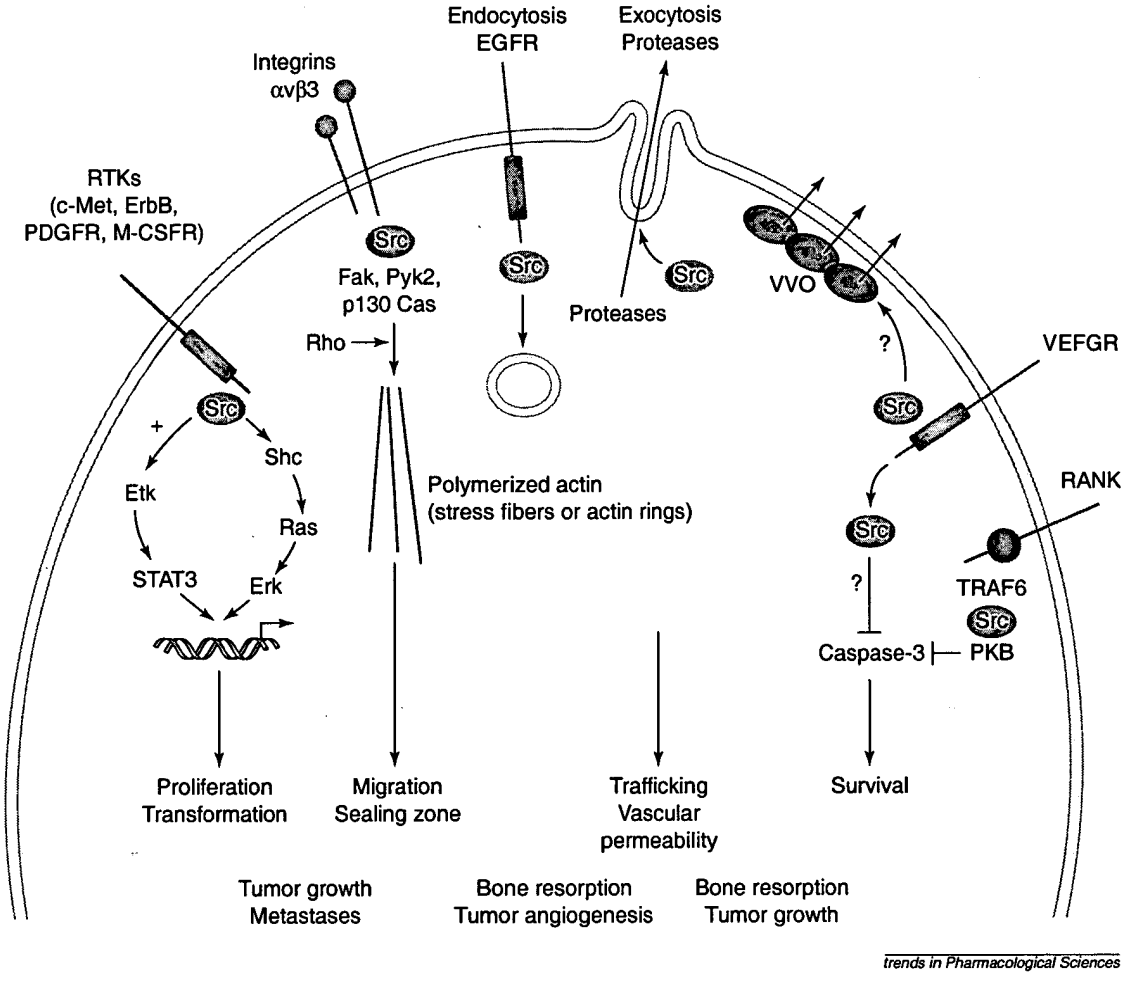

Fig. I. The known and putative functions of Src in various cell types. Abbreviations: EGFR, epidermal growth factor receptor; Erk, extracellular regulated kinase; M-CSFR, macrophage colony stimulating factor receptor; PDGFR, platelet-derived growth factor receptor; PKB, protein kinase B; RANK, receptor activating nuclear factor κB; RTKs, receptor tyrosine kinases; STAT3, signal transducer and activator of transcription 3; TRAF6, tumor necrosis factor receptor-associated factor 6; VEGFR, vascular endothelial growth factor receptor; VVO, vesiculo–vacuolar organelles.

Furthermore, Src has also been implicated in the estrogen-receptor-dependent proliferation of breast cancer cells[9], although the significance of this finding is unclear at present.

Cell adhesion, migration and chemotaxis

Cell adhesion and motility in response to specific extracellular cues are essential events in many physiological and pathological processes, such as angiogenesis, inflammation and bone resorption. An abundance of data supports a role for Src in signal transduction via cell-adhesion receptors (integrins), and their molecular mechanisms have been elucidated (Box 1)[3]. Nevertheless, the precise biological role of Src in cell adhesion remains elusive. Recent reports[10,11] have highlighted the crucial requirement of Src, Fyn, Yes and, in particular, Src kinase in cell motility but not in adhesion or growth-factor responsiveness, as had been proposed previously. Src-dependent cell migration is important for the function of many cell types and, within the scope of this review, is of particular interest for the motility of osteoclasts (during bone resorption) and metastasizing cancer cells[12,13]. In addition, Src-dependent cell migration might be important for the recruitment of vascular smooth muscle cell precursors in response to PDGF produced by endothelial cells during blood vessel formation[14].

Intracellular trafficking

Endocytosis is the process by which cells take up extracellular molecules, microorganisms or activated receptors from the cell surface, whereas exocytosis is the reverse process. Transcytosis refers to transport across a polarized cell, such as occurs in osteoclasts[15]. Consistent with its association with endocytic membranes, Src assists endocytosis of epidermal

Table 1. The properties of representative Src inhibitors[a,b]

Mode of action or name	Chemical class	Src IC_{50} (μM)		Selectivity (Src versus other)	Effect *in vivo*	Refs
		Enzyme	Cell			
Irreversible kinase inhibition and protein degradation						
Herbimycin A	Macrocyclic ansamycin	12.00	NR	−, =Yes, Fps, Abl, EGFR, ErbB2, IGF1R, InsR +PKA, PKC, Raf-1	Decreased IL-1-induced hypercalcemia	22 44
SH2 binding inhibition						
AP22161	Non-peptidic	0.24	70.0	+Yes, ZAP-70	NR	23
Urea 5	Non-peptidic	7.00	NR	NR	NR	25
Kinase inhibition (substrate binding)						
Peptide 29	Peptidic	0.13	NR	+Lck, Lyn	NR	27
Kinase inhibition (ATP binding)						
PP1	Pyrazolopyrimidine	0.17	2.0	−Lck, Fyn, Hck =PDGFR +ZAP-70, JAK2 +EGFR, KDR, FGFR, IGF1R	NR	28 32 45
PD166285	Pyridopyrimidine	0.01	NR	=FGFR, PDGFR, EGFR +InsR +PKC, cdk-4	Decreased tumor growth	29
CGP77675	Pyrrolopyrimidine	0.02	0.2	=Yes, PDGFR +Lck, Abl, Fak, Csk +EGFR, FGFR, IGF1R, KDR, Flt-1 +cdc2, Erk	Decreased IL-1-induced hypercalcemia Decreased bone loss Decreased loss of trabecular bone architecture	32 46

[a]This table is not a comprehensive list of all Src inhibitors but preferentially includes compounds that fulfill at least one of the following criteria: they are often used, they are well characterized and reported in a peer-reviewed journal; they have a novel mechanism of action; or they possess a known *in vivo* action. Only one representative compound for each chemical class is included. The inhibition of Src kinase or SH2 binding with purified reagents or under cell-free conditions are shown under the subheading 'Enzyme' and the inhibition of Src activity (substrate phosphorylation) or SH2 binding in cells is shown under the subheading 'Cell'. Selectivity against other kinases comprises both activities in enzymatic and cellular assays.

[b]Abbreviations: EGFR, epidermal growth factor receptor; Erk, extracellular regulated kinase; FGFR, fibroblast growth factor receptor; Flt-1, fms-like tyrosine kinase (vascular endothelial growth factor receptor 1); IGF1R, insulin-like growth factor 1 receptor; InsR, insulin receptor; IL-1, interleukin 1; JAK2, Janus kinase 2; KDR, kinase domain-containing region (vascular endothelial growth factor receptor 2); NR, not reported; PDGFR, platelet-derived growth factor receptor; PKA, protein kinase A; PKC, protein kinase C; −, higher potency than on Src; =, equal potency as on Src; +, lower potency than on Src.

growth factor (EGF) receptors in the A431 cancer cell line via clathrin-coated vesicles (Box 1)[16]. Because Src is highly expressed in those cell types that specialize in regulated exocytosis (e.g. neurons, platelets and osteoclasts) and associates with proteins from exocytic vesicles, such as dynamin and synapsin[17], Src probably also influences exocytosis. However, the role of Src in transcytosis remains to be determined. Another process that is related to trafficking and depends on Src is blood vessel hyperpermeability that is induced by vascular endothelial growth factor (VEGF)[18]. This process occurs in tumor vessels partly through the formation of vesiculo–vacuolar organelles (VVOs) in endothelial cells (Box 1)[19].

Cell survival

Factors that stimulate cell survival do so mostly by inhibiting the process of apoptosis. A role for Src in promoting cell survival in a factor- and cell-specific manner became apparent only recently[20]. Two processes that are affected by Src, VEGF-induced survival of endothelial cells[18] and the survival of osteoclast precursors in response to the ligand of receptor activating nuclear factor κB (RANKL)[21], are related to tumor-induced angiogenesis and the formation of osteoclasts (Box 1).

Src inhibitors as research tools and therapeutic agents

Inhibition of the cellular functions of Src by low-molecular-weight compounds can be achieved at several sites within the Src protein, including: (1) protein–protein interactions between the Src SH2 and SH3 domains and their substrates, adaptor proteins or proteins that determine the subcellular localization of Src; (2) interaction between protein substrates and the substrate-binding site; and (3) ATP binding to the ATP-binding site within the tyrosine kinase domain of Src. Another approach to inhibiting Src is to modulate the synthesis or degradation of Src protein.

Natural products

Several classes of Src inhibitors have been identified from natural products. However, Src inhibitors are often not selective against other kinases and some act irreversibly. One such compound, the macrocyclic ansamycin herbimycin A, has been used extensively *in vitro* and *in vivo* as a Src inhibitor. Herbimycin A is not a potent inhibitor of Src kinase activity (Table 1) but can initiate ubiquitin-mediated degradation of Src protein in cells, as has been demonstrated for EGF and insulin receptor tyrosine kinases[22] (Table 1). The non-selectivity of herbimycin A makes such a class of inhibitors unsuitable for development as therapeutic agents.

SH2 and substrate-binding inhibitors

Potent ligands for the Src SH2 domain that inhibit the *in vitro* interaction between the SH2 domain and peptides have been described[4]. Two such compounds (AP22161 and AP22408) that contain a peptide bond that connects unnatural amino acids or other non-amino acid templates have been profiled in cellular systems[23,24], where they showed a marked reduction in potency (Table 1). This finding needs to be investigated further and might be related to compound stability, cellular penetration or cellular mechanism of action. The latter compound (AP22408) accumulated at the site of action by binding to the bone mineral and was active in an *in vivo* model of hypercalcemia, albeit only following intravenous administration[24]. Src SH2 ligands that contain a urea bond instead of a peptide bond are less potent[25] (Table 1). These compounds might be more stable *in vivo* but their potential as an effective therapy is currently limited by their relatively low potency and the lack of data on their selectivity and activity in cells *in vivo* (Table 1). The inhibition of SH3–protein interaction appears to be difficult to achieve owing to the shallow, hydrophobic binding surface[26]. To date, no non-peptide inhibitors have been reported.

Protein substrate-based inhibitors have the potential for high specificity because protein substrates are divergent and need not compete with high intracellular ATP concentrations. Such inhibitors have been reported recently but no data are available relating to their activity in either cells or animal models (Table 1)[27].

Kinase inhibitors

In terms of selectivity, cellular potency and possible therapeutic application, Src kinase inhibitors have emerged as the most successful therapeutic agents to date. Several classes of low-molecular-weight compounds that are ATP-competitive inhibitors of Src-mediated tyrosine phosphorylation have been reported[4,13,28–30] (Tables 1,2). Some Src kinase inhibitors even achieve a moderate to high selectivity within the Src family[28,31,32] (Table 2). Selectivity within the Src family is important because this avoids possible interference with immune responses (Lck, Lyn, Hck, Fgr and Blk are preferentially expressed in hematopoietic cells[1]) and proliferation in general (Src, Fyn and Yes share a role in proliferation[3]). Unfortunately, there are no data yet available on the cellular activity and selectivity against kinases that are not within the Src family for Src inhibitors that are highly selective against Fyn, Lyn and Lck (Ref. 31). The IC_{50} values for the inhibition of Src and other kinases by Src kinase inhibitors are shown in Table 2. The efficacy of these compounds *in vitro* depends not only on their selectivity, but also on the degree of cell penetration. *In vivo*, their pharmacokinetics and toxicity will undoubtedly be

Table 2. *In vitro* selectivity of most potent Src kinase inhibitors[a]

Compound	IC_{50} values (μM) for various protein kinase classes[b]						Refs
	Src	Src family	Non-receptor PTK	Receptor PTK	Ser/Thr kinase	Cellular Src	
PP1	0.17	Lck, 0.01 Fyn, 0.01 Hck, 0.02	JAK2, >50 ZAP-70, >100	PDGFR, 0.1 EGFR[c], >10.0 KDR, >10.0 FGFR[c], >10.0 IGFR[c], >10.0[d]	NR	2.0[c]	28,32,45
PD116285	0.01	NR	NR	FGFR, 0.04 EGFR, 0.09 PDGFR, 0.10 InsR, >50.00	PKC, 22.7 cdk-4, >50.0	NR	29
CGP77675	0.02	Yes, 0.01 Lck, 0.29	Abl, 0.31 Fak, >1.00 Csk, 5.70	PDGFR, <0.3 KDR, 1.0 Flt-1, >1.0 EGFR[c], >2.0 FGFR[c], >2.0 IGFR[c], >2.0	Cdc2, >10.0 Erk[c], >2.0	0.2[c]	32,46
[90273, n=2]	0.06	Fyn, 5.0 Lyn, 13.0 Lck, >250.0	NR	NR	NR	NR	31

[a]Abbreviations: EGFR, epidermal growth factor receptor; Erk, extracellular regulated kinase; FGFR, fibroblast growth factor receptor; IGFR, insulin-like growth factor receptor; InsR, insulin receptor; JAK2, Janus kinase 2; KDR, kinase domain-containing region (vascular endothelial growth factor receptor 2); NR, not reported; PDGFR, platelet-derived growth factor receptor; PKC, protein kinase C; PTK, protein tyrosine kinase.

[b]Within each class, the kinases are sorted according to the increasing IC_{50} values. The assays were done in cell-free systems, except when indicated ([c]denotes cellular assays). Where lower than 0.01, the numbers were rounded to two decimal places.

[d]Inhibition at 0.3 μM, stimulation at >1 μM.

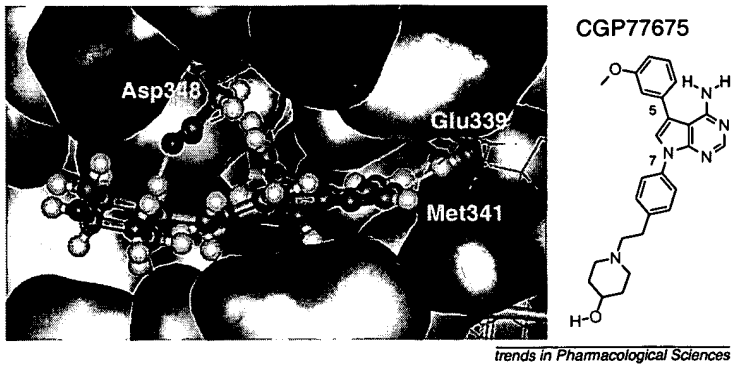

trends in Pharmacological Sciences

Fig. 1. Binding mode for an Src inhibitor at the ATP-binding site within the kinase domain of human Src. The Src kinase domain illustrated was modeled from the Hck structure[33]. This Src inhibitor (CGP77675) belongs to the 5,7-diphenyl-pyrrolo[2,3*d*] pyrimidine series. The compound is shown in ball-and-stick mode, whereas the amino acids surrounding the ATP-binding site are represented in surface mode (red, negative charge; blue, positive charge). The amino acids that contribute to hydrogen bond interactions with the compound are shown in ball-and-stick mode (yellow). CGP77675 exhibits the characteristics of a typical tyrosine kinase inhibitor (e.g. hydrogen bond donor–acceptor pairs to the backbone of the enzyme and an important interaction between the 5-methoxyphenyl substituent and the hydrophobic region not occupied by ATP).

trends in Pharmacological Sciences

Fig. 2. The effect of CGP77675 on bone architecture in rat vertebrae. Ovariectomized rats were treated orally with the Src inhibitor CGP77675 (50 mg kg^{-1} twice a day for six weeks). Vertebral bone was analyzed with high-resolution microtomography and the three-dimensional structure reconstructed. Ovariectomy of rats causes estrogen depletion and induces loss of vertebral trabecular bone, mimicking the hormone changes and bone loss that are observed in post-menopausal women. Treatment with CGP77675 partially preserves bone architecture (as illustrated) and bone mass (not shown). Reproduced, with permission, from Ref. 32.

important. Although Src inhibitors with absolute specificity are not yet available, the compounds that are currently available are useful tools for elucidating the role of Src in cells and whole organisms.

Binding mode

We used the X-ray crystal structures of human Hck (a Src family member)[33] to generate a model of the binding mode of Src and a Src kinase inhibitor from the pyrrolopyrimidine series (Fig. 1). The crystal structure data for Src bound to this inhibitor exhibit a similar binding mode (M. Eck, pers. commun.). These experimental data and further models should facilitate the design of more specific compounds with fewer side-effects *in vivo*.

In conclusion, Src kinase inhibitors from the pyrrolopyrimidine series are currently the only reported compounds that are well characterized, potent, reversible, relatively selective and exhibit sufficient oral bioavailability for application in long-term *in vivo* models[32].

Inhibition of bone resorption

The importance of Src for bone resorption is well recognized. However, the exact molecular mechanisms through which Src regulates osteoclast-mediated bone resorption remain poorly understood. The initial observation that Src-deficient mice developed osteopetrosis generated a new direction for research into bone biology. Subsequently, several studies concluded that the defect in Src-deficient mice is localized to the bone-resorbing cells, called osteoclasts, and is associated with the absence of the 'ruffled border' (the part of the plasma membrane facing the bone surface, which is active in vesicular transport[13]). However, a recent report indicates that bone-forming cells, the osteoblasts, might also be affected because their activity appears to be increased in Src-deficient mice[34].

At the molecular level, the function of Src in osteoclasts has been studied using several approaches, including biochemical (the search for relevant substrates), genetic (transgenic and knockout mice) and cell biology (role in osteoclast adhesion) methods. To date, two Src substrates appear to be relevant to osteoclasts, namely c-Cbl, an adaptor protein that is thought to negatively regulate signaling by tyrosine kinases[35] and Pyk2, a tyrosine kinase that is upregulated during osteoclast differentiation, is involved in osteoclast adhesion and can be indirectly inhibited by a Src inhibitor[36,37] (M. Šuša *et al.*, unpublished). A role for Pyk2 in osteoclasts is supported by recent observations that Pyk2-deficient mice exhibit mild osteopetrosis[38]. In contrast to these findings, which indicate a role for the kinase activity of Src, a study of transgenic mice with inactive Src kinase crossed with Src-deficient mice suggested that the kinase activity of Src plays a minor role in osteoclast resorption[13]. However, a major role of the kinase domain *in vitro* and *in vivo* is again reinforced by a study in which a Src inhibitor from the pyrrolopyrimidine series was used[32]. Moreover, this study indicated that inhibition of Src with a low-molecular-weight compound in an animal model of osteoporosis is a feasible therapeutic principle for treating this disease (Fig. 2).

Thus, the above-mentioned studies identified reduced osteoclastic activity as the mechanism of action of Src inhibitors. However, recent data indicate that Src inhibitors might also affect RANKL-mediated osteoclast survival[21] and osteoclast formation (A. Teti, pers. commun.).

Inhibition of tumor growth and metastases

Both the involvement of Src in human cancers and the possible sites for therapeutic intervention have been reviewed in detail elsewhere[3,5,13] and are briefly summarized below. Src has been implicated in the growth and proliferation of cells that can be induced by several receptor tyrosine kinases[3]. The correlation between elevated Src expression (or activity) and tumor growth is greatest for ErbB2 and c-Met receptors and for colon, breast and lung cancers[5,6,39,40]. In addition, several other types of tumor (e.g. pancreas, liver, esophagus and bladder) might involve Src and a Src mutation has been identified in human colon cancer[41].

Lung, liver and bone are the three most frequent sites for cancer metastases. For metastases to occur, tumor cells need to dissociate from one another, migrate from the site of the primary tumor, penetrate the vasculature and attach to and grow in a distant metastatic site. Once a metastatic site is established,

angiogenesis is essential for tumor growth. One or more of these processes could be suppressed by Src inhibitors[13]. Indeed, substantial evidence supports the involvement of Src in these processes. (1) The phosphorylation of the Src substrate Fak correlates with invasiveness of a prostate carcinoma cell line[13]. (2) The abnormal expression of the cadherin-/Src-associated substrate of 120 kDa (p120 Cas) correlates with poor survival in patients with colon and bladder cancer[42,43]. (3) Src might be involved in VEGF-induced angiogenesis[18,40]. Clearly, the picture is far from complete, but the identification of inhibitors of the Src family that are both potent and selective and that have suitable pharmacokinetic properties should enable the role of Src in tumor growth and metastases to be investigated.

Concluding remarks

Although Src has been extensively studied and understood at the molecular level for two decades, Src inhibitors that are potent, selective and bioavailable have only recently been identified. Such Src family inhibitors are effective in reducing bone loss in animal models of osteoporosis and, based on cellular studies, have the potential for the treatment of some cancers, particularly of their bone metastases.

References

1 Neet, K. and Hunter, T. (1996) Vertebrate non-receptor protein-tyrosine kinase families. *Genes Cells* 1, 147–169
2 Xu, W. *et al.* (1999) Crystal structures of c-Src reveal features of its autoinhibitory mechanism. *Mol. Cell.* 3, 629–638
3 Thomas, S.M. and Brugge, J.S. (1997) Cellular functions regulated by Src family kinases. *Annu. Rev. Cell. Dev. Biol.* 13, 513–609
4 Gowen, M. *et al.* (2000) Emerging therapies for osteoporosis. *Emerging Drugs* 5, 1–43
5 Biscardi, J.S. *et al.* (1999) c-Src, receptor tyrosine kinases and human cancer. *Adv. Cancer Res.* 76, 61–119
6 Mao, W. *et al.* (1997) Activation of c-Src by receptor tyrosine kinases in human colon cancer cells with high metastatic potential. *Oncogene* 15, 3083–3090
7 Turkson, J. *et al.* (1998) STAT3 activation by Src induces specific gene regulation and is required for cell transformation. *Mol. Cell. Biol.* 18, 2545–2552
8 Tsai, Y. *et al.* (2000) Etk, a Btk family tyrosine kinase, mediates cellular transformation by linking Src to STAT3 activation. *Mol. Cell. Biol.* 20, 2043–2054
9 Castoria, G. *et al.* (1999) Non-transcriptional action of oestradiol and progestin triggers DNA synthesis. *EMBO J.* 18, 2500–2510
10 Klinghoffer, R.A. *et al.* (1999) Src family kinases are required for integrin but not PDGF signal transduction. *EMBO J.* 18, 2459–2471
11 Fincham, V.J. and Frame, M.C. (1998) The catalytic activity of Src is dispensable for translocation to focal adhesions but controls the turnover of these structures during cell motility. *EMBO J.* 17, 81–92
12 Chellaiah, M. *et al.* (2000) Rho-A is critical for osteoclast podosome organization, motility, and bone resorption. *J. Biol. Chem.* 275, 11993–12002
13 Šuša, M. and Teti, A. (2000) Tyrosine kinase Src inhibitors: Mechanisms of action in potential therapeutic applications. *Drug News Perspect.* 13, 169–175
14 Hirschi, K.K. *et al.* (1998) PDGF, TGF-β and heterotypic cell-cell interactions mediate endothelial cell-induced recruitment of 10T1/2 cells and their differentiation to a smooth muscle fate. *J. Cell. Biol.* 141, 805–814
15 Nesbitt, S.A. and Horton, M.A. (1997) Trafficking of matrix collagens through bone-resorbing osteoclasts. *Science* 276, 266–269
16 Wilde, A. *et al.* (1999) EGF receptor signaling stimulates Src kinase phosphorylation of clathrin, influencing clathrin redistribution and EGF uptake. *Cell* 96, 677–687
17 Foster-Barber, A. and Bishop, J.M. (1998) Src interacts with dynamin and synapsin in neuronal cells. *Proc. Natl. Acad. Sci. U. S. A.* 95, 4673–4677
18 Eliceiri, B.P. *et al.* (1999) Selective requirement for Src kinases during VEGF-induced angiogenesis and vascular permeability. *Mol. Cell.* 4, 915–924
19 Dvorak, A.M. *et al.* (1996) The vesiculo–vacuolar organelle (VVO): a distinct endothelial cell structure that provides a transcellular pathway for macromolecular extravasation. *J. Leukoc. Biol.* 59, 100–115
20 Schlessinger, J. (2000) New roles for Src kinases in control of cell survival and angiogenesis. *Cell* 100, 293–296
21 Wong, B.R. *et al.* (1999) TRANCE, a TNF family member, activates Akt/PKB through a signaling complex involving TRAF6 and c-Src. *Mol. Cell* 4, 1041–1049
22 Sepp-Lorenzino, L. *et al.* (1995) Herbimycin A induces the 20 S proteasome- and ubiquitin-dependent degradation of receptor tyrosine kinases. *J. Biol. Chem.* 270, 16580–16587
23 Violette, S.M. *et al.* (2000) A Src SH2 selective binding compound inhibits osteoclast-mediated resorption. *Chem. Biol.* 7, 225–235
24 Shakespeare, W. *et al.* (2000) Structure-based design of an osteoclast-selective, nonpeptide src homology 2 inhibitor with *in vivo* anti-resorptive activity. *Proc. Natl. Acad. Sci. U. S. A.* 97, 9373–9478
25 Plummer, M.S. *et al.* (1997) Design, synthesis and cocrystal structure of a nonpeptide Src SH2 domain ligand. *J. Med. Chem.* 40, 3719–3725
26 Morken, J.P. *et al.* (1998) Exploring the leucine–proline binding pocket of the Src SH3 domain. *J. Am. Chem. Soc.* 120, 30–36
27 Alfaro-Lopez, J. *et al.* (1998) Discovery of a novel series of potent and selective substrate-based inhibitors of $p60^{c\text{-}Src}$ protein tyrosine kinase: conformational and topographical constraints in peptide design. *J. Med. Chem.* 41, 2252–2260
28 Hanke, J.H. *et al.* (1996) Discovery of a novel, potent and Src family selective tyrosine kinase inhibitor. *J. Biol. Chem.* 271, 695–701
29 Klutchko, S.R. *et al.* (1998) 2-Substituted aminopyrido[2,3d]pyrimidin-7(OH)ones. Structure–activity relationships against selected tyrosine kinases and *in vitro* and *in vivo* anticancer activity. *J. Med. Chem.* 41, 3276–3292
30 Missbach, M. *et al.* (2000) Substituted 5,7-diphenyl-pyrrolo(2, 3d)pyrimidines: potent inhibitors of the tyrosine kinase pp60 c-Src. *Biorg. Med. Chem. Lett.* 10, 945–949
31 Maly, D.J. *et al.* (2000) Combinatorial target-guided ligand assembly: identification of potent subtype-selective c-Src inhibitors. *Proc. Natl. Acad. Sci. U. S. A.* 97, 2419–2424
32 Missbach, M. *et al.* (1999). A novel inhibitor of the tyrosine kinase Src suppresses phosphorylation of its major cellular substrates and reduces bone resorption *in vitro* and in rodent models *in vivo*. *Bone* 24, 437–449
33 Sicheri, F. *et al.* (1997) Crystal structure of the Src family tyrosine kinase Hck. *Nature* 385, 602–609
34 Marzia, M. *et al.* (2000) Decreased c-Src expression enhances osteoblast differentiation and bone formation. *J. Cell Biol.* 151, 311-320
35 Tanaka, S. *et al.* (1996) c-Cbl is downstream of c-Src in a signalling pathway necessary for bone resorption. *Nature* 383, 528–531
36 Jeschke, M. *et al.* (1998) Expression of Src family kinases and their putative substrates in the human preosteoclastic cell line FLG 29.1. *J. Bone Miner. Res.* 13, 1880–1889
37 Duong, L.T. *et al.* (1998) Pyk2 in osteoclasts is an adhesion kinase, localized in the sealing zone, activated by ligation of αvβ3 integrin and phosphorylated by Src kinase. *J. Clin. Invest.* 102, 881–892
38 Sims, N.A. *et al.* (1999) Impaired osteoclast function in Pyk2 knockout mice and cumulative effects in Pyk2/Src double knockout. *J. Bone Miner. Res.* 14: S183
39 Staley, C.A. *et al.* (1997) Decreased tumorigenicity of a human colon adenocarcinoma cell line by an antisense expression vector specific for c-Src. *Cell Growth Differ.* 8, 269–274
40 Ellis, L.M. *et al.* (1998) Downregulation of vascular endothelial growth factor in a human colon carcinoma cell line transfected with an antisense expression vector specific for c-Src. *J. Biol. Chem.* 273, 1052–1057
41 Irby, R.B. *et al.* (1999) Activating SRC mutation in a subset of advanced human colon cancers. *Nat. Genet.* 21, 187–190
42 Gold, J.S. *et al.* (1998) Loss of p120ctn in human colorectal cancer predicts metastasis and poor survival. *Cancer Lett.* 132, 193–201
43 Syrigos, K.N. *et al.* (1998) Abnormal expression of p120 correlates with poor survival in patients with bladder cancer. *Eur. J. Cancer* 34, 2037–2040
44 Yoneda, T. *et al.* (1993) Herbimycin A, a pp60c-Src tyrosine kinase inhibitor, inhibits osteoclastic bone resorption *in vitro* and hypercalcemia *in vivo*. *J. Clin. Invest.* 91, 2791–2795
45 Waltenberger, J. *et al.* (1999) A dual inhibitor of platelet-derived growth factor β-receptor and Src kinase activity potently interferes with motogenic and mitogenic responses to PDGF in vascular smooth muscle cells. A novel candidate for prevention of vascular remodeling. *Circ. Res.* 85, 12–22
46 Šuša, M. *et al.* (2000) Active recombinant human tyrosine kinase c-Yes: expression in baculovirus system, purification, comparison to c-Src, and inhibition by a c-Src inhibitor. *Protein Expr. Purif.* 19, 99–106

Chemical names

AP22161: 4-[(*S*)-2-acetylamino-2-(3-carbamoyl-2-cyclohexyl-methoxy-6,7,8,9-tetrahydro-5*H*-benzocyclohepten-5-ylcar-bamoyl)-ethyl]-2-formyl-benzoic acid

AP22408: {4-[(*S*)-2-acetylamino-2-(3-carbamoyl-2-cyclohexyl-methoxy-6,7,8,9-tetrahydro-5*H*-benzocyclohepten-5-ylcar-bamoyl)-ethyl]-2-phosphono-phenyl}-phosphonic acid

CGP77675: 1-(2-{4-[4-amino-5-(3-methoxy-phenyl)-pyrrolo[2,3-*d*]pyrimidin-7-yl]-phenyl}-ethyl)-piperidin-4-ol

PD116285: 6-(2,6-dichloro-phenyl)-2-[4-(2-diethylamino-ethoxy)-phenylamino]-8-methyl-8*H*-pyrido[2,3-*d*]pyrimidin-7-one

Acknowledgements
We thank A. Teti (University of L'Aquila, L'Aquila, Italy) and M. Eck (Dana-Farber Cancer Institute, Boston, USA) for communicating unpublished data. The authors are indebted to R. Gamse and R. Beerli (Novartis Pharma Research) for critical reading of the manuscript. Due to the limits in reference numbers, not all relevant work deserving acknowledgement could be cited.

st 15, 2003]

nase Activity Is Associated with Tumor Colonization in Bone and Lung in an Animal Model of Human Breast Cancer Metastasis[1]

Akira Myoui, Riko Nishimura, Paul J. Williams, Toru Hiraga, Daisuke Tamura, Toshimi Michigami, Gregory R. Mundy, and Toshiyuki Yoneda[2]

Osaka University, Graduate School of Medicine, Department of Orthopaedics [A. M., D. T.], Graduate School of Dentistry, Department of Biochemistry [R. N., T. H., D. T., T. Y.], Suita, Osaka 565-0871, Japan; Department of Environmental Medicine, Osaka Medical Center and Institute for Maternal and Child Health, Izumi, Osaka 594-1101, Japan [T. M.]; and The University of Texas Health Science Center at San Antonio, Department of Medicine, Division of Endocrinology and Metabolism, San Antonio, Texas 78229-3900 [P. J. W., G. R. M., T. Y.]

ABSTRACT

The proto-oncogene, c-src, has been implicated in the tumorigenesis in breast cancer. However, the relationship of c-src with distant metastasis is unclear. Moreover, the role of c-src in organ-preferential metastasis of breast cancer is unknown. Because breast cancer has a strong predilection for metastasizing to bone, we examined the role of c-src in bone metastases using an animal model in which inoculation of the MDA-231 human breast cancer cells into the left cardiac ventricle preferentially developed osteolytic bone metastases in female nude mice. A clone of the MDA-231 with the increased capacity of bone metastasis exhibited elevated c-src tyrosine kinase (TK) activity compared with parental cells. MDAsrc527 cells caused significantly increased size of the osteolytic bone metastases with increased number of osteoclasts and mitotic cancer cells compared with MDA-231EV or MDAsrcWT. In contrast, MDAsrc295 cells caused impaired metastases to bone. Of note, mice inoculated with MDAsrc295 cells via tail vein developed reduced lung metastases and prolonged survival compared with mice with MDA-231EV cells, suggesting that c-src TK is unlikely to play a specific role in bone metastases. The growth *in vitro* and *in vivo* and production of parathyroid hormone-related protein, a key cytokine in the pathogenesis of osteolytic bone metastases in breast cancer, were promoted in MDAsrc527 and diminished in MDAsrc295. These results suggest that c-src TK is associated with the capacity of breast cancer to metastasize to bone through regulating cell growth and parathyroid hormone-related protein production. Our results together with the fact that c-src is an essential molecule for bone resorption by osteoclasts, which are central players in osteolytic bone metastases, support the notion that c-src TK is a potential target molecule for designing novel therapeutic interventions, especially for bone metastases in breast cancer.

INTRODUCTION

The proto-oncogene c-src is the cellular homologue of v-src that was initially found in the Rous sarcoma virus that induces tumors in chickens and transformation in a variety of mammalian cells (1, 2). c-src encodes an M_r 60,000 cytoplasmic protein with intrinsic TK[3] activity. It consists of an NH_2 terminus-containing myristylation site for the binding to inner cell membrane, nonconserved unique domain for each src family member, a SH3 domain that binds to proline-rich sequences, a SH2 domain that binds to phosphotyrosine, a TK domain, and a short COOH-terminal tail in its primary structure (1, 3, 4). In chicken c-src, there are one lysine residue at 295, one tyrosine residue at 416 in the kinase domain, and one tyrosine residue at 527 in the COOH-terminal tail, all of which play critical roles in the regulation of c-src TK activity. Lysine 295 is the binding site for ATP that is the source of phosphates necessary for phosphorylation of c-src, tyrosine 416 is the autophosphorylation site, and tyrosine 527 is the negatively regulatory phosphorylation site of c-src TK activity (1, 3, 4). Point mutation of these sites markedly changes c-src TK activity.

Recent human and animal studies suggest the association between c-src TK and the development, progression, and metastasis of breast cancer (5–11). It is demonstrated that c-src TK activity is profoundly increased in human breast cancer tissues compared with benign breast tumors or adjacent normal breast tissues (5–7, 11) and that elevated c-src TK activity is correlated with poor metastasis-free survival (8). Transgenic mice with polyoma middle T antigen under the control of mouse mammary tumor virus promoter were found to develop highly metastatic mammary tumors with increased c-src TK activity (9). Moreover, when these mice were cross-bred with c-src-deficient mice, the resulting chimeric mice no longer developed mammary tumors (9). In addition, it is described that mice overexpressing the *neu* oncogene develop highly metastatic mammary tumors with elevated c-src TK activity (10). Taken together, these results strongly indicate that the c-src TK plays an important role in the development and progression of breast cancer. However, the relationship of c-src TK in distant metastasis of breast cancer is still largely unknown. In addition, whether c-src TK contributes to the organ preference of breast cancer metastasis is unknown. It has been long and widely recognized that breast cancer has a strong predilection for metastasizing to bone (12). Here, we investigated the role of c-src TK in the development of bone metastases in breast cancer using a well-characterized animal model of experimental bone metastasis (13–17). We introduced WT chicken c-src and its mutants that exhibit different levels of TK activity into the MDA-231 human breast cancer cells and examined the ability of these transfected MDA-231 cells to develop bone metastases. We also examined whether the manipulation of c-src TK activity affects lung metastasis of MDA-231 cells using a different animal model. Our results show that MDA-231 cells overexpressing a constitutively active c-src TK develop increased osteolytic bone metastases. In contrast, MDA-231 cells with a kinase-dead c-src TK caused reduced bone metastases compared with control MDA-231 cells. Furthermore, mice inoculated with MDA-231 cells with a kinase-dead c-src developed diminished lung metastases and exhibited prolonged survival. These results demonstrate that the c-src TK activity modulates the capacity of MDA-231 cells to spread to distant organs, including bone and lung.

MATERIALS AND METHODS

Antibodies and TK Inhibitors. Antibodies to v-src were purchased from Upstate Biotechnology (Lake Placid, NY), Quality Biotech (Camden, NJ; residues 2–17), and Calbiochem (San Diego, CA; Ab-1, clone 327). Anti-β-actin antibody was purchased from Santa Cruz Biotechnology (Santa Cruz,

Received 9/19/02; revised 5/29/03; accepted 6/10/03.

The costs of publication of this article were defrayed in part by the payment of page charges. This article must therefore be hereby marked *advertisement* in accordance with 18 U.S.C. Section 1734 solely to indicate this fact.

[1] Supported by NIH Grants PO1-CA40035, RO1-AR28149, and RO1-DK45229 and grants from the Ministry of Health, Labour and Welfare and Ministry of Education, Culture, Sports, Science and Technology, Japan.

[2] To whom requests for reprints should be addressed, at The University of Texas Health Science Center at San Antonio, Department of Medicine, Division of Endocrinology and Metabolism, 7703 Floyd Curl Drive, San Antonio, TX 78229-3900. Phone: (210) 567-4900; Fax: (210) 567-6693; E-mail: yoneda@uthscsa.edu.

[3] The abbreviations used are: TK, tyrosine kinase; EV, empty vector; WT, wild-type; TBS, Tris-buffered saline; PTH-rP, parathyroid hormone-related protein; IRMA, immunoradiometric assay; MAP, mitogen-activated protein.

CA). Antiphosphotyrosine antibody was described previously (18). Herbimycin A and tyrphostin were purchased from Life Technologies, Inc. (Rockville, MD).

MDA-MB-231 Human Breast Cancer Cells. The estrogen-independent human breast cancer cell line MDA-231 (American Type Culture Collection, Rockville, MD) was cultured in DMEM (Life Technologies, Inc.) supplemented with 10% fetal bovine serum (Hyclone Laboratories, Logan, UT). A bone-seeking clone of MDA-231 cells (MDA-231BO cells) was established as described (19). All cells were routinely tested for *Mycoplasma* contamination.

c-src Plasmids. Plasmids containing chicken c-src gene and its mutants were kind gifts from Dr. David Shalloway (20, 21). It is shown that chicken c-src is >95% homologous to human c-src at amino acid levels, that the 295 ATP-binding site and 527 tyrosine phosphorylation site are well conserved between chicken and human, and that an introduction of chicken c-src into human cells causes expected effects (1–4). The plasmid pM5HHB5 encoding the c-DNA for WT chicken c-src was inserted into an expression vector pEVX. The plasmid, pcR295, has the cDNA encoding the c-src with a point mutation at the ATP-binding site (lys295 to Arg295). This mutation was shown to cause complete loss of c-src TK activity and inhibit endogenous c-src TK in a dominant-negative fashion in chicken embryo fibroblasts (22). The plasmid pcsrc527 contains the c-src gene with a point mutation at the COOH-terminal inhibitory residue (Tyr527 to Phe527), resulting in a constitutive activation of c-src TK (18, 23, 24) by causing a conformational change (25–27).

Transfection. Transfection of MDA-231 cells was performed using LipofectAMINE (Life Technologies, Inc.) with cotransfection of pSVneo2 vector containing the neomycin resistant gene in the presence of G-418 (0.75 mg/ml).

Immunoblotting and Immunoprecipitation. Cell lysates were prepared, and immunoblotting and immunoprecipitation were performed as described (18). In brief, the lysates were separated on 7.5% SDS-polyacrylamide gel and transferred onto nitrocellulose membrane. The membranes were blocked with 50 mg/ml BSA (Sigma, St. Louis, MO) in TBS (pH 7.4, 10 mM Tris·Cl and 150 mM NaCl) for 2 h at room temperature, incubated with a primary antibody in BSA-TBS for 2 h, washed with TBS containing 0.1% Triton X-100, and incubated with horse radish peroxidase-conjugated antimouse IgG (Cappel, Durham, NC) or horse radish peroxidase-conjugated protein A (Kirkegaard & Perry Laboratories, Gaithersburg, MD) in 50 mg/ml dry milk-TBS for 1 h. The signals were visualized with enhanced chemiluminescence detection system (DuPont NEN, Boston, MA).

For immunoprecipitation, the cell lysates were incubated with antibodies for 4 h at 4°C, precipitated with protein G-agarose (Boehringer Mannheim, Indianapolis, IN), separated by SDS-PAGE, transferred to nitrocellulose membrane, and immunoblotted with corresponding antibodies.

***In Vitro* Kinase Assay.** c-src protein in the cell lysates was immunoprecipitated using anti-src antibody (residues 2–17) and protein G agarose (Boehringer Mannheim). Because the expression level of the c-src protein varied in each clone, the starting amounts of the cell lysates were adjusted according to the expression level of the c-src protein to include the same amounts of the c-src protein in the reaction mixture. The immunocomplexes were incubated with 5 μg of acid-denatured rabbit muscle enolase (Boehringer Mannheim) and 1 μl of 1.7 μM [γ-^{32}P]ATP (6000 Ci/mmol; DuPont NEN) for 5 min at 30°C in kinase reaction buffer containing 10 mM Tris (pH 7.4), 5 mM $MnCl_2$, 100 μM sodium orthovanadate, and 1 μM unlabeled ATP as described (28). Samples were separated by SDS-PAGE and visualized by autoradiography. Radioactivity of [^{32}P]enolase in excised bands was determined by scintillation counting. Data were expressed as proportions to the radioactivity of [^{32}P]enolase for MDA-231EV cells, which represent relative activities of c-src TK per unit c-src protein.

Anchorage-independent Growth in Soft Agar. Anchorage-independent growth of the transfectants was determined by colony formation in soft agar as described (14). Colonies > 200 μm in diameter were manually counted under an inverted microscope.

PTH-rP Assay. PTH-rP concentration in the serum-free, 48-h conditioned media of MDA-231 cells was measured using a two-site IRMA (Nichols Institute, San Juan Capistrano, CA) that uses two polyclonal antibodies specific for the NH_2-terminal-(1–40) and -(60–72) portions of PTH-rP. Data were normalized for cell number and analyzed using Prism (GraphPAD Software for Science, San Diego, CA) on an IBM-compatible computer.

PTH-rP Promoter Activity. Cells were transiently transfected with a reporter construct consisting of the PTH-rP promoter hooked with the firefly luciferase gene. Luciferase enzymatic activity was measured by Luciferase Assay System (Promega, Madison, WI) using luminometer (Turner Designs Luminometer Model TD-20/20; Promega). Data were corrected with cell number at the end of culture period or protein concentration of the lysates.

Orthotopic Tumor Formation. MDA-231 cells (3×10^6 cells) in 0.1 ml of 50% Matrigel (Collaborative Research, Bedford, MA) in PBS were inoculated into the mammary fat pad of 5-week-old female Fox CHASE C.B-17/Icr-scid Jcl mice (Clea Japan, Tokyo, Japan). Tumors formed were excised and weighed at 3 weeks.

Bone Metastasis. Intracardiac injection was performed according to the technique described previously (13–17). Quantitative assessment for osteolytic bone metastases was described previously (13–17). Radiographs were carefully evaluated for the area of osteolytic bone metastases in long bones of hindlimbs by three individuals (P. J. W., T. Y., Mark Dallas) who had no information about the experimental design using a computer-assisted Jandal Video Analysis image analysis system (Jandal Scientific, Corte Madera, CA) as described (15).

The experiment was conducted twice using a different transfectant in each of the experiments (6 mice for each group/experiment for MDAsrcWT, 8 mice for each group/experiment for MDAsrc527, and 9 mice for each group/experiment for MDAsrc295). Total animal numbers for each group for MDAsrcWT, MDAsrc527, and MDAsrc295 were 6 mice × two transfectants = 12 mice, 8 mice × two transfectants = 16 mice, and 9 mice × two transfectants = 18 mice, respectively.

Lung Metastasis. MDA-231 cells (1×10^6 cells/mouse) were inoculated via the lateral tail vein of 5-week-old, female Fox CHASE C.B-17/Icr-scid Jcl mice (Clea Japan). Lungs were harvested 7 weeks after tumor cell inoculation, fixed, and stained with Bouin's solution, and the number of metastatic foci was counted as described previously (29).

Histology and Determination of Mitotic Index. Hindlimbs were fixed with 10% natural buffered formalin for 48 h, decalcified in EDTA (pH 7.2) for 2 weeks, and processed for conventional paraffin-embedded H&E staining. Mitotic index was determined by manually counting mitotic figures in 10 randomly selected high-power fields of the metastatic tumors in bone on histological sections.

Statistical Analysis. All results are expressed as the mean ± SE. Data were analyzed by Student's *t* test or repeated measures ANOVA followed by Tukey-Kramer post test. Survival curves were estimated by Kaplan–Meier method, and the difference was analyzed by generalized Wilcoxon test. *P*s of <0.05 were considered significant.

RESULTS

Relationship between the Capacity of Bone Metastasis and c-src TK Activity in MDA-231 Cells. To examine the relationship between c-src TK activity and the capacity of bone metastasis, we compared c-src TK activity between parental MDA-231 cells (MDA-231P) and a clone of MDA-231 cells, which show increased capacity of bone metastasis (MDA-231BO; Ref. 19). Western analysis demonstrated that the MDA-231BO cells expressed elevated c-src protein (Fig. 1*a*) and tyrosine phosphorylation of c-src (Fig. 1*b*, *bottom*) and several unidentified cellular proteins (Fig. 1*b*, *top*) compared with MDA-231P cells. Moreover, c-src kinase activity was also higher in MDA-231BO than MDA-231P cells (Fig. 1*c*). These results suggest that c-src TK activity correlates with the capacity of bone metastasis of MDA-231 cells.

c-src TK Activity and Bone Metastasis in MDA-231 Cells. To investigate the effects of c-src TK activity on the development of bone metastases in MDA-231 cells, we examined the capacity bone metastasis of MDA-231 cells that were stably transfected with EV, WT c-src (pM5HHB5), kinase-dead c-src (pcR295), and constitutively active c-src (pcsrc527). These transfectants were found to stably overexpress WT, kinase-dead, and constitutively active c-src, respectively (Fig. 2*a*) and designated as MDAsrcWT, MDAsrc295, and MDAsrc527, respectively. *In vitro* kinase assays demonstrated that kinase activity in MDAsrcWT was higher than MDA-231EV (Fig. 2,

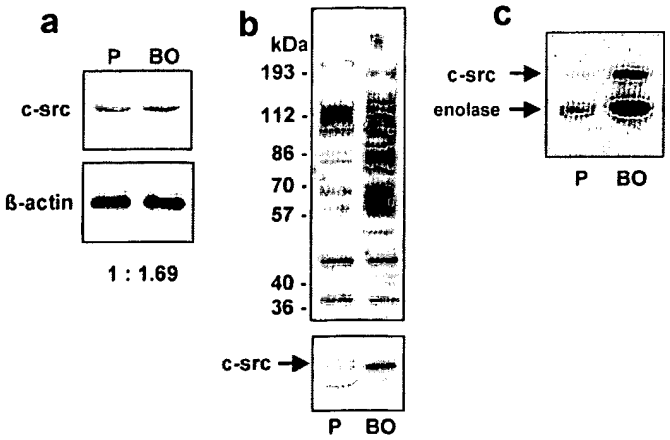

Fig. 1. c-src TK activity in parental MDA-231 cells (MDA-231P cells) and a MDA-231 clone with increased capacity of bone metastasis (MDA-231BO cells). *a*, Western blot analysis on whole cell lysates of MDA-231P and MDA-231BO cells using anti-v-src antibody (clone 327, *top*) and anti-β-actin antibody (*bottom*). Expression levels of c-src and β-actin protein were semiquantified using an image analyzer, and the ratio of c-src:β-actin was calculated. The number shown is calculated by dividing c-src (*BO*) by c-src (*P*). *b*, tyrosine-phosphorylation of cellular proteins in whole cell lysates (*top*) and auto-phosphorylation of immunoprecipitated c-src (*bottom*) in MDA-231P and MDA-231BO cells using antiphosphotyrosine antibody. *c*, *in vitro* kinase assay. Immunoprecipitated endogenous c-src from lysates of MDA-231 cells and enolase was used as a source of c-Src TK and a substrate, respectively. *Top band*, auto-phosphorylation of c-src; *bottom band*, TK activity of c-src on enolase.

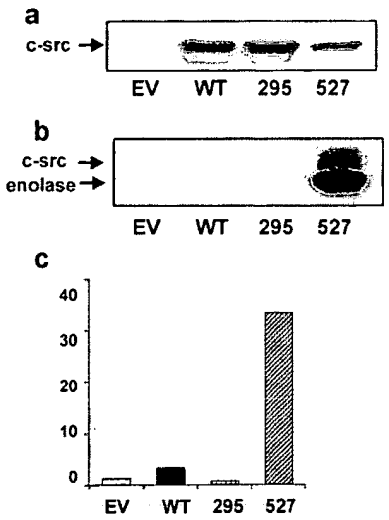

Fig. 2. Establishment of MDA-231 cells overexpressing c-src with different kinase activity. *a*, Western blotting for c-src using an anti-v-src antibody (clone 327, 1:400 dilution) in the cell lysates of MDA-231EV, MDAsrcWT, MDAsrc295, or MDAsrc527. *b*, *in vitro* kinase assay. The lysates of c-src-transfected MDA-231 cells immunoprecipitated with an anti-v-src antibody (residues 2–17) and enolase were used as a source of c-Src TK and a substrate, respectively. *Top band*, auto-phosphorylation of c-src; *bottom band*, TK activity of c-src on enolase. *c*, specific activity of c-src kinase. The *bottom bands* shown in *b* were excised and measured for their radioactivity in a scintillation counter. Values on *Y* axis are relative radioactivity to that of MDA-231EV cells.

b and *c*). On the other hand, MDAsrc527 showed markedly higher kinase activity than others, and kinase activity in MDAsrc295 was abolished (Fig. 2, *b* and *c*).

We then studied MDA-231EV, two clones of MDAsrcWT (A and B), two clones of MDAsrc527 (A and B), and two clones of MDAsrc295 (A and B) for the capacity to develop bone metastases using a well-characterized animal model (13–17). As shown in Fig. 3, *a* and *b*, MDAsrc527 (A) developed increased size of osteolytic bone metastases compared with MDA-231EV cells and MDAsrcWT (A) cells on radiographs. Quantification of these osteolytic lesions using computerized image analysis system revealed that the area of osteolytic lesion was significantly greater in mice inoculated with MDAsrc527 (A) cells than mice inoculated with MDA-231EV or MDAsrcWT (A) and (B) cells (Fig. 3*b*). MDAsrc527 (B) also developed larger bone metastases. In contrast, mice inoculated with MDAsrc295 (A and B) cells developed significantly smaller osteolytic bone metastases than mice inoculated with MDA-231EV cells (Fig. 3, *a* and *b*).

Histological examination revealed MDAsrcWT colonization in bone with osteoclastic bone resorption (Fig. 4, *a* and *d*). MDA-src295 developed markedly reduced tumor in bone (Fig. 4, *b* and *e*). In contrast, MDAsrc527 caused profoundly increased bone metastases with increased number and size of osteoclasts (Fig. 4, *c* and *f*). MDA-231EV developed equivalent bone metastases to MDAsrcWT (data not shown). These data demonstrate that elevated c-src TK activity promotes the development of osteolytic bone metastases of MDA-231 cells and that decreased c-src TK activity impairs bone metastases of MDA-231 cells. The results are consistent with a notion that c-src TK modulates the capacity of breast cancer colonization in bone.

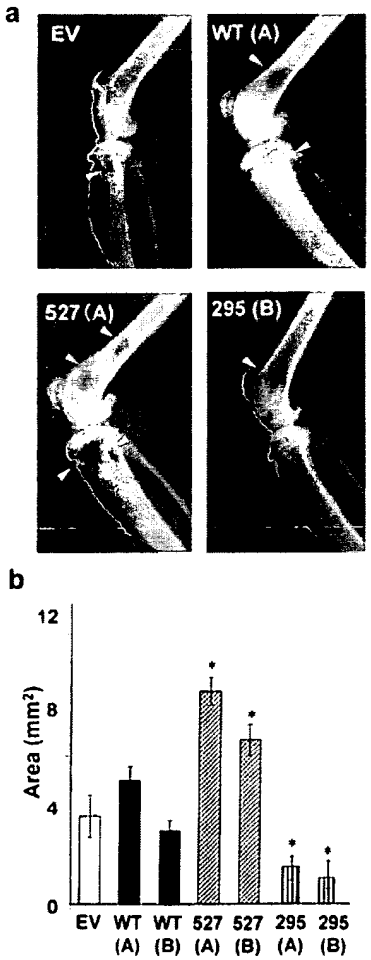

Fig. 3. c-src TK activity and osteolytic bone metastases. *a*, radiographs of hindlimbs of mice bearing MDA-231EV, MDAsrcWT, MDAsrc527, and MDAsrc295 tumors that were taken 28 days after intracardiac inoculation of 1×10^5 tumor cells. Osteolytic metastases are indicated by *arrowheads*. *b*, quantitative measurement of the area of the osteolytic lesions on radiographs shown in *a* using a computerized image analyzer. Two different transfectants (*A* and *B*) from each group were tested. The experiment was conducted twice, and the results of two experiments were combined. The numbers of animals were 20, 6, 6, 8, 8, 9, and 9 for MDA-231EV, MDAsrcWT (*A*), MDAsrcWT (*B*), MDAsrc527 (*A*), MDAsrc527 (*B*), MDAsrc295 (*A*), and MDAsrc295 (*B*), respectively. Values represent mean ± SE. *, $P < 0.05$ *versus* other groups.

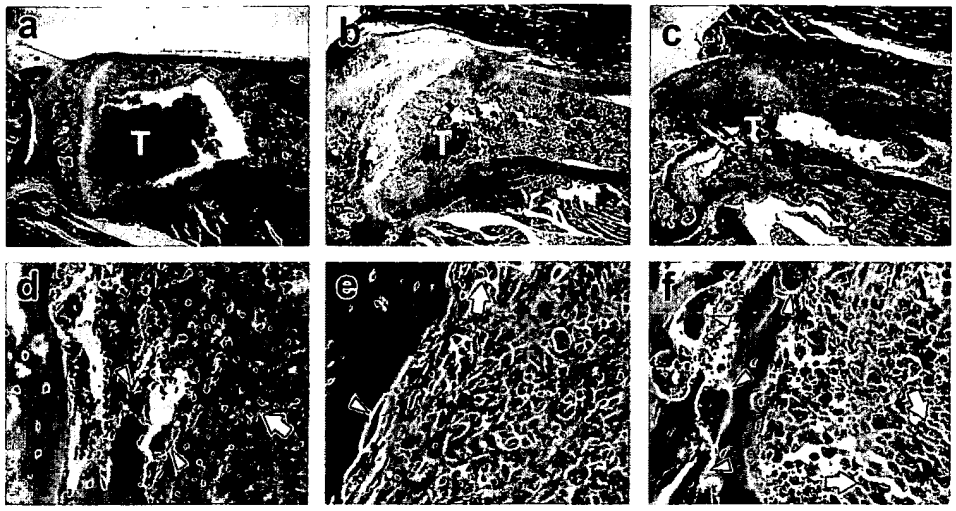

Fig. 4. Histological pictures of bone metastases. Histological sections were made using proximal tibial midsection of mice bearing MDAsrcWT (*a* and *d*), MDAsrc295 (*b* and *e*), and MDAsrc527 (*c* and *f*) tumors. Lower (*a–c*) and higher (*d–f*) magnification. Tumor (*T*) occupies the marrow cavity and replaces normal cellular elements and bone trabeculae of metaphysis with osteoclastic bone resorption in mouse bearing MDAsrcWT (*a* and *d*). Note the destruction of cortical wall and extraskeletal extension of the tumor (*c*). On the tumor bone interface in the mouse bearing MDAsrc527 (*f*), numerous large bone-resorbing osteoclasts (*arrowheads*) are seen. *Arrows*, mitotic cells.

c-src TK Activity and Lung Metastasis. To examine whether c-src TK specifically affects bone metastases, the capacity of MDAsrc295 cells to spread to lung after tail vein inoculation was assessed compared with MDA-231EV cells. We found that lung metastases of MDAsrc295 were significantly decreased (Fig. 5*a*). As a consequence of this, survival of mice bearing MDAsrc295 cells was significantly prolonged (Fig. 5*b*). Thus, c-src TK affects not only bone metastases but also lung metastases.

Effects of c-src TK on MDA-231 Cell Growth *in Vivo* and *in Vitro*. Because c-src plays a critical role in cell growth (30), we next examined the effects of c-src TK on the growth of MDA-231 cells metastasized in bone by manually counting the number of mitotic cells on the histological sections. Mitotic index in MDAsrc527 cells in bone was significantly greater than MDA-231EV, MDAsrcWT, and MDAsrc295 cells (Fig. 6*a*). Consistent with these results, MDAsrc527 cells exhibited larger tumor formation than MDAsrcEV in the orthotopic mammary fat pad (Fig. 6*b*).

We subsequently determined the relationship between the c-src TK activity and anchorage-independent growth in MDA-231 cells by assessing for the colony formation in soft agar. Colony formation of MDAsrc527 cells was significantly greater than other src-transfected MDA-231 cells (Fig. 6*c*). Collectively, these data show that elevated c-src TK activity promotes MDA-231 cell growth *in vitro* and *in vivo*.

PTH-rP Production in c-src-transfected MDA-231 Cells. We have reported that overexpression of PTH-rP cDNA increased osteolytic bone metastases and a neutralizing antibody against PTH-rP-inhibited bone metastases in MDA-231 cells in the same animal model of metastasis as described here (15, 17). In addition, it was also reported that v-src-transfected fibroblasts produced increased levels of

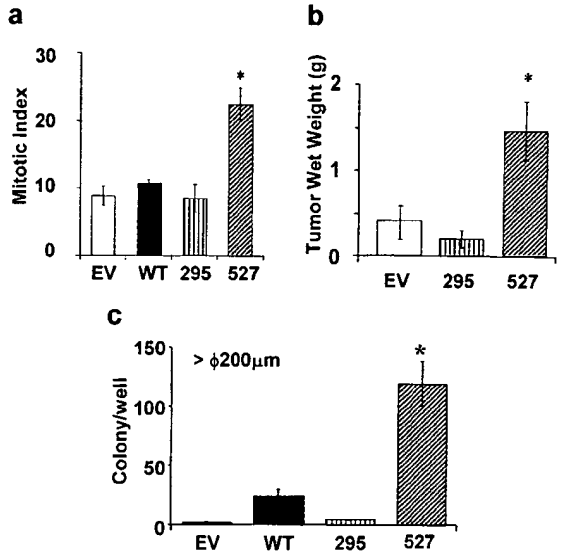

Fig. 6. c-src TK activity and MDA-231 cell growth. *a*, mitotic index in metastatic MDA-231 cells in bone. There are numeral mitotic cells in metastatic tumors in bone (Fig. 4, *arrows*). Mitotic indices were measured by counting mitotic figures in 10 high-power (×400) fields in respective tumors. Data represent mean ± SE (n = 5). *, $P < 0.001$ *versus* other groups. *b*, tumorigenicity of MDA-231 cells in the mammary fat pad. MDA-231 cells (3×10^6) in 0.1 ml of 50% Matrigel were inoculated into the mammary fat pad in 5-week-old female C.B-17/Icr-*scid*/Icl mice. Three weeks after cell inoculation, tumors formed were excised and weighed. Data represent the mean ± SE (n = 3). *, $P < 0.05$ *versus* MDAsrc295. *c*, anchorage-independent growth of MDA-231 cells. Five-hundred MDA-231 cells suspended in 0.45% agarose gel were inoculated onto 35-mm dishes and grown for 2 weeks. Colonies > 200 μm in diameter were manually counted under an inverted microscope. Data represent the mean ± SE (n = 6) from two separate experiments using different transfectants. *, $P < 0.001$ *versus* other groups.

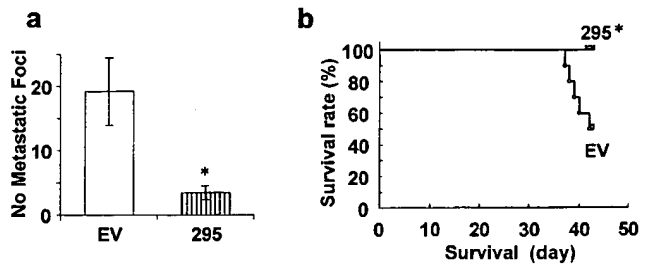

Fig. 5. c-src TK and lung metastasis. *a*, number of metastatic foci in lung 7 weeks after i.v. inoculation of MDA-231 cells (1×10^6 cells in 0.1 ml of PBS). The experiment was conducted twice using 10 mice for each group. Values represent mean ± SE. *, $P < 0.001$ *versus* MDA-231EV. *b*, overall survival curves estimated by Kaplan-Meier method for the mice inoculated with MDA-231 cells via tail vein. *, $P < 0.05$ *versus* MDA-231EV.

PTH-rP (31). We, therefore, determined the effects of c-src TK on the PTH-rP production in MDA-231 cells. As demonstrated in Fig. 7*a*, MDAsrc527 cells produced significantly greater amounts of PTH-rP than MDA-231EV cells. On the other hand, MDAsrc295 showed significantly reduced PTH-rP production compared with MDA-231EV cells. It is likely that this decrease in PTH-rP production, in part, contributes to the reduced bone metastases in MDAsrc295 despite that the mitosis (Fig. 6*a*) and anchorage-independent growth (Fig. 6*c*) of MDAsrc295 were equivalent to MDA-231EV. In addition, herbimycin A, an inhibitor of c-src TK (32), significantly reduced elevated PTH-rP production in MDAsrc527 cells (Fig. 7*b*), suggesting an involvement of c-src TK in the regulation of PTH-rP production.

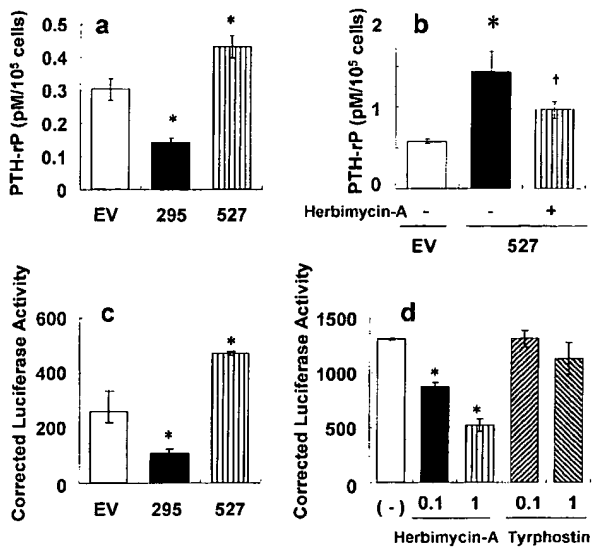

Fig. 7. Effects of c-src TK activity on PTH-rP production (*a* and *b*) and PTH-rP promoter activity (*c* and *d*) in MDA-231 cells. *a*, c-src-transfected MDA-231 cells were cultured in serum-free medium for 48 h. PTH-rP concentration in the conditioned media was measured by IRMA and normalized for cell number. Values represent mean ± SE ($n = 6$). *, $P < 0.001$ *versus* MDA-231EV. In *b*, MDAsrc527 cells were treated with a c-src TK selective inhibitor, herbimycin A at 1 μg/ml as described in the text, and PTH-rP concentration of the conditioned media was determined by IRMA. Values represent mean ± SE ($n = 3$). *, $P < 0.05$ *versus* MDA-231EV. †, $P < 0.05$ *versus* MDAsrc527 without Herbimycin A. In *c*, PTH-rP promoter hooked with luciferase gene was transiently transfected into MDA-231EV, MDAsrc295, and MDAsrc527 cells. Twenty-four h after transfection, luciferase activity of the cell lysates was determined. Values represent mean ± SE of luciferase activity corrected by cell number at the end of the culture period ($n = 4$). *, $P < 0.001$ *versus* MDA-231EV. In *d*, MDA-231 cells stably transfected with luciferase gene driven by PTH-rP promoter were cultured in serum-free media for 18 h and treated with TK inhibitors at indicated concentrations (μg/ml) for 6 h. Data represent mean ± SE of luciferase activity corrected by protein concentration ($n = 3$). *, $P < 0.001$ *versus* untreated.

Finally, we examined whether c-src TK regulated PTH-rP gene transcription using the reporter construct described in "Materials and Methods." Transactivation of PTH-rP promoter was significantly less in MDAsrc295 cells than MDA-231EV cells (Fig. 7*c*). In contrast, MDAsrc527 cells showed up-regulated PTH-rP promoter activity. Furthermore, herbimycin A suppressed PTH-rP promoter activity in a dose-dependent manner (Fig. 7*d*), whereas tyrphostin, an inhibitor of epidermal growth factor receptor TK, showed no effect. These data suggest that c-src TK regulates PTH-rP production in MDA-231 cells at transcriptional levels.

DISCUSSION

Bone is one of the commonest target sites of distant metastasis in breast cancer (12). However, the molecular mechanism by which breast cancer preferentially spreads to bone is poorly understood. In the present study, we examined whether c-src TK plays a specific role in bone metastasis in breast cancer. Our results demonstrate that the mutant c-src with constitutively active TK (src527) enhances and the mutant c-src with little TK activity (src295) decreases the development of osteolytic bone metastases in MDA-231 cells, respectively. Furthermore, we also found that a clone of MDA-231 cells that exclusively and aggressively metastasized to bone (MDA-231BO cells) exhibited increased c-src TK activity compared with parental MDA-231 cells. These results suggest that c-src TK activity is positively correlated with the capacity to develop bone metastases in the MDA-231 human breast cancer cells. However, because our data also show that MDAsrc295 cells develop reduced lung metastases compared with MDAsrcEV cells, it is likely that c-src TK activity does not play a specific role in bone metastases but affects nonbone metastases as well.

Modulation of distant metastases of MDA-231 cells by c-src TK activity is largely attributable to changes in the cell growth. Histological examination revealed increased mitosis in MDAsrc527 cells compared with MDA-231EV, MDAsrcWT, and MDAsrc295 cells in bone metastases. MDAsrc527 cells formed much larger tumors than MDAsrc295 in the orthotopic mammary fat pad. Furthermore, MDAsrc527 cells showed increased anchorage-independent growth compared with other MDA-231 cells in soft agar. Consistent with our data, previous studies have reported that microinjection of a neutralizing anti-Src/Fyn/Yes antibody into mouse fibroblasts at G_2 phase blocks subsequent cell division (30) and that the expression of antisense cDNA for c-src decreases the growth of colon cancer cells *in vitro* and *in vivo* (33). Chk, which down-regulates c-src TK activity, has been shown to inhibit the growth of the human breast cancer cell line MCF-7 *in vivo* and *in vitro* (34). Taken together, it is suggested that increased osteolytic bone metastases of MDAsrc527 cells are attributable to the stimulation of cell proliferation in bone. Conversely, reduced lung metastases in MDAsrc295 cells are likely attributable to decreased cell proliferation.

Elevated production of PTH-rP, which is a powerful stimulator of osteoclastic bone resorption, also significantly contributes to increased bone metastases in MDAsrc 527 cells. Accumulating clinical (35–37) and experimental data, including ours (15, 17, 38), has shown that PTH-rP plays an important role in the development of osteolytic bone metastases in breast cancer. Our results show increased PTH-rP production in MDA-231src 527 cells and reduced PTH-rP production in MDAsrc295 cells. Furthermore, our data also demonstrate that activation of PTH-rP gene promoter is controlled with c-src TK activity, which is consistent with an earlier report (31). Taken together, it is suggested that c-src TK stimulates PTH-rP production at transcriptional levels in MDA-231 breast cancer cells, which in turn activates osteoclastic bone resorption, leading to the progression of osteolytic bone metastases.

The mechanism by which c-src TK promotes PTH-rP production is currently unknown. Recent studies have reported that PTH-rP production in MDA-231 cells is increased by transforming growth factor-β through an activation of cytoplasmic signaling pathways, including Smad and MAP kinases (39), and that there is a cross-talk between c-src and MAP kinase (40). It is, therefore, possible that c-src TK stimulates PTH-rP production in MDA-231 cells through establishing interactions with MAP kinase signaling pathways.

The substrates for c-src TK that are involved in bone metastasis of MDA-231 cells were not determined in this study. It is notable that amplified expression of a cytoskeletal protein cortactin/EMS1, which is a relatively specific substrate for c-src TK (41–43), has been reported to be correlated with increased metastases (44) and poor survival in breast cancer patients (45, 46). Moreover, cortactin has been recently found to increase bone metastasis of MDA-231 cells in the same animal model as described here (47). Thus, cortactin/EMS1 is a likely candidate for a substrate for c-src TK that plays a role in bone metastasis in breast cancer.

It should be noted that c-src TK is known to be essential for osteoclasts to resorb bone (48, 49). Osteoclasts play a central role in the development and progression of osteolytic bone metastases. These facts and our result that c-src TK activity is critical to bone metastasis in breast cancer cells collectively raise the possibility that inhibition of c-src TK in both osteoclasts and breast cancer cells suppresses bone metastases in an additive fashion (32, 50). Our results provide a support for this notion.

In conclusion, we have shown that c-src TK activity modulates the capacity of MDA-231 human breast cancer cells to colonize in bone

and lung. Although extensive clinical studies are needed to clarify whether this is also the case in metastases in breast cancer patients, our results suggest that c-src TK is a potential molecular target for designing specific therapeutic interventions for the treatment of distant metastases, particularly bone metastases, in breast cancer.

ACKNOWLEDGMENTS

We thank Dr. David Shalloway for kindly providing us plasmids. We also thank Mark Dallas, Maryla Niewolna, and Mina Okamoto for expert technical assistance and Hisako Takeuchi for her excellent secretarial assistance.

REFERENCES

1. Jove, R., and Hanafusa, H. Cell transformation by the viral src oncogene. Annu. Rev. Cell Biol., *3:* 31–56, 1987.
2. Irby, R. B., and Yeatman, T. J. Role of Src expression and activation in human cancer. Oncogene, *19:* 5636–5642, 2000.
3. Thomas, S. M., and Brugge, J. S. Cellular functions regulated by Src family kinases. Annu. Rev. Cell Dev. Biol., *13:* 513–609, 1997.
4. Abram, C. L., and Courtneidge, S. A. Src family tyrosine kinases and growth factor signaling. Exp. Cell Res., *254:* 1–13, 2000.
5. Jacobs, C., and Rübsamen, H. Expression of $pp60^{c\text{-}src}$ protein kinase in adult and fetal human tissue: high activities in some sarcomas and mammary carcinomas. Cancer Res., *43:* 1696–1702, 1983.
6. Hennipman, A., van Oirschot, B. A., Smits, J., Rijksen, G., and Staal, G. E. J. Tyrosine kinase activity in breast cancer, benign breast disease, and normal breast tissue. Cancer Res., *49:* 516–521, 1989.
7. Lehrer, S., O'Shaughnessy, J., Song, H. K., Levine, E., Savoretti, P., Dalton, J., Lipsztein, R., Kalnicki, S., and Bloomer, W. D. Activity of $pp60^{c\text{-}src}$ protein kinase in human breast cancer. Mt. Sinai J. Med., *56:* 83–85, 1989.
8. Ottenhoff-Kalff, A. E., Rijksen, G., van Beurden, E. A. C. M., Hennipman, A., Michels, A. A., and Staal, G. E. J. Characterization of protein kinases from human breast cancer: Involvement of the c-src oncogene product. Cancer Res., *52:* 4773–4778, 1992.
9. Guy, C. T., Muthuswamy, S. K., Cardiff, R. D., Soriano, P., and Muller, W. J. Activation of the c-Src tyrosine kinase is required for the induction of mammary tumors in transgenic mice. Gene Dev., *8:* 23–32, 1994.
10. Muthuswamy, S. K., Siegel, P. M., Dankort, D. L., Webster, M. A., and Muller, W. J. Mammary tumors expressing the neu proto-oncogene possess elevated c-Src tyrosine kinase activity. Mol. Cell. Biol., *14:* 735–743, 1994.
11. Verbeek, B. S., Vroom, T. M., Adriaansen-Slot, S. S., Ottenhoff-Kalff, A. E., Geertzema, J. G., Hennipman, A., and Rijksen, G. c-Src protein expression is increased in human breast cancer. An immunohistochemical and biochemical analysis. J. Pathol., *180:* 383–388, 1996.
12. Coleman, R. E., and Rubens, R. D. The clinical course of bone metastases from breast cancer. Br. J. Cancer, *55:* 61–66, 1987.
13. Sasaki, A., Boyce, B. F., Story, B., Wright, K. R., Chapman, M., Boyce, R., Mundy, G. R., and Yoneda, T. Bisphosphonate risedronate reduces metastatic human breast cancer burden in bone in nude mice. Cancer Res., *55:* 3551–3557, 1995.
14. Mbalaviele, G., Dunstan, C. R., Sasaki, A., Williams, P. J., Mundy, G. R., and Yoneda, T. E-cadherin expression in human breast cancer cells suppresses the development of osteolytic bone metastases in an experimental metastasis model. Cancer Res., *56:* 4063–4070, 1996.
15. Guise, T. A., Yin, J. J., Taylor, S. D., Kumagai, Y., Dallas, M., Boyce, B. F., Yoneda, T., and Mundy, G. R. Evidence for a causal role of parathyroid hormone-related protein in the pathogenesis of human breast cancer-mediated osteolysis. J. Clin. Investig., *98:* 1544–1549, 1996.
16. Yoneda, T., Sasaki, A., Dunstan, C., Williams, P. J., Bauss, F., De Clerck, Y. A., and Mundy, G. R. Inhibition of osteolytic bone metastasis of breast cancer by combined treatment with the bisphosphonate ibandronate and tissue inhibitor of the matrix metalloproteinase-2. J. Clin. Investig., *99:* 2509–2517, 1997.
17. Yin, J. J., Selander, K., Chirgwin, J. M., Dallas, M., Grubbs, B. G., Wieser, R., Massague, J., Mundy, G. R., and Guise, T. A. TGF-beta signaling blockade inhibits PTHrP secretion by breast cancer cells and bone metastases development. J. Clin. Investig., *103:* 197–206, 1999.
18. Nishimura, R., Li, W., Kashishian, A., Mondino, A., Zhou, M., Cooper, J., and Schlessinger, J. Two signaling molecules share a phosphotyrosine-containing binding site in the platelet-derived growth factor receptor. Mol. Cell. Biol., *13:* 6889–6896, 1993.
19. Yoneda, T., Williams, P. J., Hiraga, T., Niewolna, M., and Nishimura, R. A bone-seeking clone exhibits different biological properties from the MDA-MB-231 parental human breast cancer cells and a brain-seeking clone in vivo and in vitro. J. Bone Miner. Res., *16:* 1486–1495, 2001.
20. Kmiecik, T. E., and Shalloway, D. Activation and suppression of $pp60^{c\text{-}src}$ transforming ability by mutation of its primary sites of tyrosine phosphorylation. Cell, *49:* 65–73, 1987.
21. Bagrodia, S., Chackalaparampil, I., Kmiecik, T. E., and Shalloway, D. Altered tyrosine 527 phosphorylation and mitotic activation of $p60^{c\text{-}src}$. Nature (Lond.), *349:* 172–175, 1991.
22. Kamps, M. P., and Sefton, B. M. Neither arginine nor histidine can carry out the function of lysine-295 in the ATP-binding site of $p60^{src}$. Mol. Cell. Biol., *6:* 751–757, 1986.
23. Cartwright, C. A., Eckhart, W., Simon, S., and Kaplan, P. L. Cell transformation by $pp60^{c\text{-}src}$ mutated in the carboxy-terminal regulatory domain. Cell, *49:* 83–91, 1987.
24. Reynolds, A. B., Vila, J., Lansing, T. J., Potts, W. M., Weber, M. J., and Parsons, J. T. Activation of the oncogenic potential of the avian cellular src protein by specific structural alteration of the carboxy terminus. EMBO J., *6:* 2359–2364, 1987.
25. Matsuda, M., Mayer, B. J., Fukui, Y., and Hanafusa, H. Binding of transforming protein, $P47^{gag\text{-}crk}$, to a broad range of phosphotyrosine-containing proteins. Science (Wash. DC), *248:* 1537–1539, 1990.
26. Roussel, R. R., Brodeur, S. R., Shalloway, D., and Laudano, A. P. Selective binding of activated $pp60^{c\text{-}src}$ by an immobilized synthetic phosphopeptide modeled on the carboxyl terminus of $pp60^{c\text{-}src}$. Proc. Natl. Acad. Sci. USA, *88:* 10696–10700, 1991.
27. Xu, W., Harrison, S. C., and Eck, M. J. Three-dimensional structure of the tyrosine kinase c-Src. Nature (Lond.), *385:* 595–602, 1997.
28. Clark, E. A., and Brugge, J. S. Redistribution of activated pp60c-src to integrin-dependent cytoskeletal complexes in thrombin-stimulated platelets. Mol. Cell. Biol., *13:* 1863–1871, 1993.
29. Abdel-Ghany, M., Cheng, H-C., Elble, R. C., and Pauli, B. U. The breast cancer beta 4 integrin and endothelial human CLCA2 mediate lung metastasis. J. Biol. Chem., *276:* 25438–25446, 2001.
30. Roche, S., Fumagalli, S., and Courtneidge, S. A. Requirement for Src family protein tyrosine kinases in G2 for fibroblast cell division. Science (Wash. DC), *269:* 1567–1569, 1995.
31. Li, X., and Drucker, D. J. Parathyroid hormone-related peptide is a downstream target for ras and src activation. J. Biol. Chem., *269:* 6263–6266, 1994.
32. Susa, M., Missbach, M., and Green, J. Src inhibitors: drugs for the treatment of osteoporosis, cancer or both. Trend Pharmacol. Sci., *21:* 489–495, 2000.
33. Staley, C. A., Parikh, N. U., and Gallick, G. E. Decreased tumorigenicity of a human colon adenocarcinoma cell line by an antisense expression vector specific for c-Src. Cell Growth Differ., *8:* 269–274, 1997.
34. Bougeret, C., Jiang, S., Keydar, I., and Avraham, H. Functional analysis of Csk and CHK kinase in breast cancer cells. J. Biol. Chem., *276:* 33711–33720, 2001.
35. Bundred, N. J., Ratcliffe, W. A., Walker, R. A., Coley, S., Morrison, J. M., and Ratcliffe, J. G. Parathyroid hormone related protein and hypercalcaemia in breast cancer. Br. Med. J., *303:* 1506–1509, 1991.
36. Powell, G. J., Southby, J., Danks, J. A., Stillwell, R. G., Hayman, J. A., Henderson, M. A., Bennett, R. C., and Martin, T. J. Localization of parathyroid hormone-related protein in breast cancer metastases: increased incidence in bone compared with other sites. Cancer Res., *51:* 3059–3061, 1991.
37. Southby, J., Kissin, M. W., Danks, J. A., Hayman, J. A., Moseley, J. M., Henderson, M. A., Bennett, R. C., and Martin, T. J. Immunohistochemical localization of parathyroid hormone-related protein in human breast cancer. Cancer Res., *50:* 7710–7716, 1990.
38. Mundy, G. R., and Yoneda, T. Bisphosphonates as anticancer drugs. N. Engl. J. Med., *339:* 398–400, 1998.
39. Kakonen, S. M., Selander, K. S., Chirgwin, J. M., Yin, J. J., Burns, S., Rankin, W. A., Grubbs, B. G., Dallas, M., Cui, Y., and Guise, T. A. Transforming growth factor-beta stimulates parathyroid hormone-related protein and osteolytic metastases via Smad and mitogen-activated protein kinase signaling pathways. J. Biol. Chem., *277:* 24571–24578, 2002.
40. Boney, C. M., Sekimoto, H., Gruppuso, P. A., and Frackelton, A. R., Jr. Src family tyrosine kinases participate in insulin-like growth factor I mitogenic signaling in 3T3-L1 cells. Cell Growth Differ., *12:* 379–386, 2001.
41. Wu, H., Reynolds, A. B., Kanner, S. B., Vines, R. R., and Parsons, J. T. Identification and characterization of a novel cytoskeleton-associated $pp60^{src}$ substrate. Mol. Cell. Biol., *11:* 5113–5124, 1991.
42. Nada, S., Okada, M., Aizawa, S., and Nakagawa, H. Identification of major tyrosine-phosphorylated proteins in Csk-deficient cells. Oncogene, *9:* 3571–3578, 1994.
43. Thomas, S. M., Soriano, P., and Imamoto, A. Specific and redundant roles of Src and Fyn in organizing the cytoskeleton. Nature (Lond.), *376:* 267–271, 1995.
44. Cuny, M., Kramar, A., Courjal, F., Johannsdottir, V., Iacopetta, B., Fontaine, H., Grenier, J., Culine, S., and Theillet, C. Relating genotype and phenotype in breast cancer: an analysis of the prognostic significance of amplification at eight different genes or loci and of p53 mutations. Cancer Res., *60:* 1077–1083, 2000.
45. Schuuring, E., Verhoeven, E., van Tinteren, H., Peterse, J. L., Nunnink, B., Thunnissen, F. B. J. M., Devilee, P., Cornelisse, C. J., van de Vijver, M. J., Mooi, W. J., and Michalides, R. J. A. M. Amplification of genes within the chromosome 11q13 region is indicative of poor prognosis in patients with operable breast cancer. Cancer Res., *52:* 5229–5234, 1992.
46. Hui, R., Ball, J. R., Macmillan, R. D., Kenny, F. S., Prall, O. W., Campbell, D. H., Cornish, A. L., McClelland, R. A., Daly, R. J., Forbes, J. F., Blamey, R. W., Musgrove, E. A., Robertson, J. F., Nicholson, R. I., and Sutherland, R. L. EMS1 gene expression in primary breast cancer: relationship to cyclin D1 and oestrogen receptor expression and patient survival. Oncogene, *17:* 1053–1059, 1998.
47. Li, Y., Tondravi, M., Liu, J., Smith, E., Haudenschild, C. C., Kaczmarek, M., and Zhan, X. Cortactin potentiates bone metastasis of breast cancer cells. Cancer Res., *61:* 6906–6911, 2001.
48. Soriano, P., Montgomery, C., Geske, R., and Bradley, A. Targeted disruption of the c-src proto-oncogene leads to osteopetrosis in mice. Cell, *64:* 693–702, 1991.
49. Lowe, C., Yoneda, T., Boyce, B. F., Chen, H., Mundy, G. R., and Soriano, P. Osteopetrosis in Src-deficient mice is due to an autonomous defect of osteoclasts. Proc. Natl. Acad. Sci. USA, *90:* 4485–4489, 1993.
50. Missbach, M., Jeschke, M., Feyen, J., Muller, K., Glatt, M., Green, J., and Susa, M. A novel inhibitor of the tyrosine kinase Src suppresses phosphorylation of its major cellular substrates and reduces bone resorption in vitro and in rodent models in vivo. Bone, *24:* 437–449, 1999.

Exhibit L

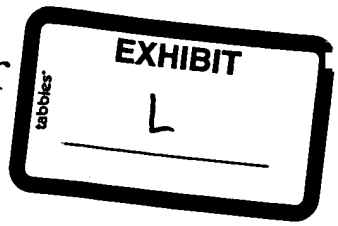

Activation of pp60$^{c\text{-}src}$ is necessary for human vascular smooth muscle cell migration

Leila Mureebe, MD, Peter R. Nelson, MD, Shinji Yamamura, MD, Joel Lawitts, PhD, *and* **K. Craig Kent, MD,** *Boston, Mass.*

Background. *The most widely distributed nonreceptor tyrosine kinase is pp60$^{c\text{-}src}$ (src), yet the role of this intracellular signaling protein in cell migration has not been defined. Given that smooth muscle cell (SMC) migration is essential for the development of intimal hyperplasia, we investigated the importance of src in locomotion of human vascular SMC.*

Methods. *SMC migration was evaluated using a microchemotaxis chamber assay and videomicroscopy. Src kinase activity was determined by measuring phosphorylation of a synthetic derivative of p34^{cdc2}, a specific substrate for src. Blocking antibodies to src were introduced using a cytoplasmic microinjection technique.*

Results. *Stimulation of SMC with platelet-derived growth factor (PDGF)–BB and AB resulted in an increase in src activation, whereas PDGF-AA did not consistently enhance src activity. These findings correlated with the ability of the PDGF isotypes to stimulate SMC chemotaxis; PDGF-BB and AB produced 7.4 ± 0.3- and 5.3 ± 0.5-fold increases in SMC chemotaxis, whereas PDGF-AA inhibited chemotaxis. SMC migration in response to PDGF-BB and serum was significantly inhibited by intracellular injection of a blocking antibody.*

Conclusions. *Our findings reveal an association between agonist-induced src activation and chemotaxis. Moreover, an antibody that inhibits src activation dramatically inhibits migration of individual SMC. We conclude that activation of src is necessary for SMC migration. Because of its importance in SMC migration, either molecular or pharmacologic inhibitors of src may be useful in the control of intimal hyperplasia. (Surgery 1997;122:138-45.)*

From the Department of Surgery, Division of Vascular Surgery, Beth Israel Deaconess Medical Center and Harvard Medical School, Boston, Mass.

ALTHOUGH ARTERIAL RECONSTRUCTION is often successful in improving the quality of life in patients with peripheral vascular disease, at least 20% to 25% of these reconstructions will fail or require revision within 5 years. Graft failures between 1 month and 2 years are often related to hyperplastic lesions that develop within a graft or at its anastomosis with the native artery.[1] Prerequisite for the development of intimal plaque is the migration into the intima of vascular smooth muscle cells (SMCs) that normally reside in the medial layer of a vessel.[2,3] Although several agonists of SMC migration have been defined, the intracellular pathways that are activated by these agonists have not been well elucidated.

The protein pp60$^{c\text{-}src}$ (src) is one of a few protein tyrosine kinases that lacks an extracellular domain. This ubiquitous protein is the prototype and most widely distributed member of the src family of tyrosine kinases. Other family members include blk, fgr, fyn, hck, lck, lyn, yes, and yrk, although only src, fyn, and yes are widely expressed. The remaining proteins in this family are found mainly in cells of hematopoietic lineage.[4] The activity of this family of proteins is regulated by "src homology" domains, which are peptide sequences that modulate attachment of src to other proteins. The SH2 domain regulates binding of src to phosphorylated tyrosine residues including the autophosphorylated platelet-derived growth factor (PDGF) and epidermal growth factor receptors. SH3 domains of src recognize proline-rich domains in other proteins.

Supported by National Institute of Health grants HL55465 (K.C.K.) and 5T32-HL07734-04 (L.M.).

Presented at the Fifty-eighth Annual Meeting of the Society of University Surgeons, Tampa, Fla., Feb. 13-15, 1997.

Reprint requests: K. Craig Kent, MD, Division of Vascular Surgery, Cornell Medical Center/New York Hospital (F-1909), 525 E. 68th St., New York, NY 10021.

0039-6060/97/$5.00 + 0 11/6/82484

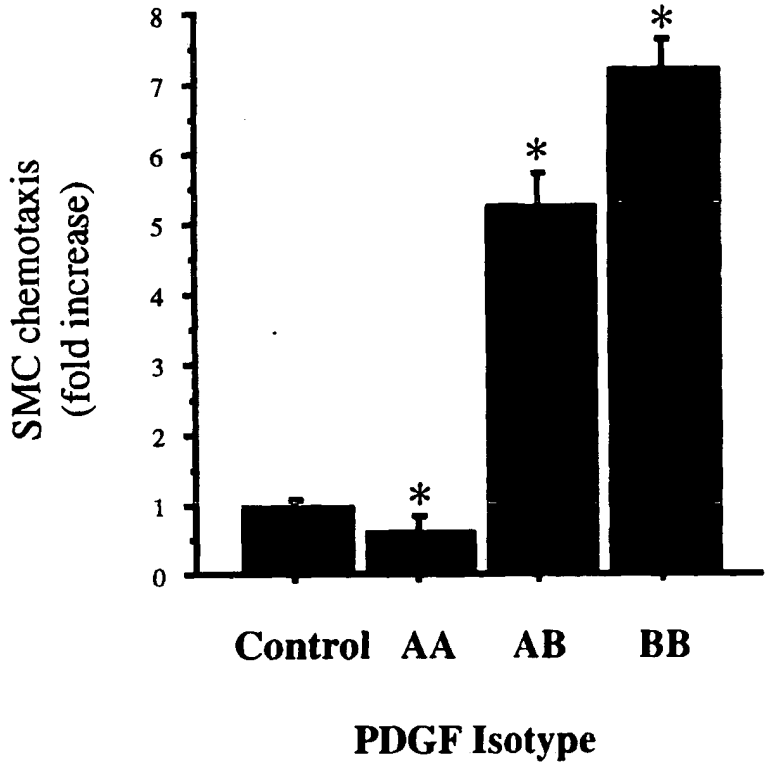

Fig. 1. SMC chemotaxis in response to PDGF isotypes. SMC chemotaxis was measured in response to PDGF-AA, -AB, and -BB (5 ng/ml). Results are expressed as fold-increase over unstimulated control ± SD. Experiments were performed in triplicate and repeated multiple times with cells from different lines. Data from a representative experiment are shown. $*p \leq 0.05$ from control.

Table I. Effect of IgG and anti-src microinjection on human SMC migration

Stimulus	*Injectate*	*Total distance*	*Net distance*	*% Motile cells*
PDGF-BB	IgG	243.68 ± 231.71*	192.38 ± 155.05*	88
	anti-src	27.69 ± 52.60	24.43 ± 43.66	29
10% Serum	IgG	146.78 ± 138.88*	106.88 ± 89.75*	80
	anti-src	11.40 ± 21.97	11.40 ± 21.97	43
Unstimulated	IgG	106.02 ± 106.68*	68.02 ± 64.80*	90
	anti-src	14.82 ± 32.37	14.82 ± 32.27	20

Net migration, total migration, and percent motility were calculated for each experiment. Representative data are shown. Values are expressed in micrometers as average ± SD. Experiments were repeated using multiple cell lines with similar findings. $*p \leq 0.05$ from anti-src injected cells.

Thus far, src has been implicated convincingly in the signaling pathway leading to cellular proliferation. Src family kinases are required for the mitogenic response to PDGF. The kinase activity of src has been shown to increase during mitosis,[5] and absence of kinase activity has been shown to block PDGF-mediated entry of cells into the S phase of the cell cycle.[6] A dominant-negative form of src (structurally similar, but lacking kinase activity) associated with the PDGF receptor, but did not lead to mitosis in cells stimulated with PDGF.[7] Moreover, an antibody that inhibited the kinase activity of src prevented mitosis in response to PDGF.[7]

Several observations suggest that there may be an association between src and migration. Src has been localized to focal adhesions, which are membrane-associated complexes of proteins that bind actin filaments and are essential for cell migration. Various members of the focal adhesion complex are activated by phosphorylation on tyrosine residues, and several of these proteins—cortactin, paxillin, and $p125^{FAK}$—have been identified as substrates for src. Moreover, PDGF-BB, which is known to activate src in addition to being a potent SMC mitogen, also promotes SMC migration.

We therefore postulated that src activation

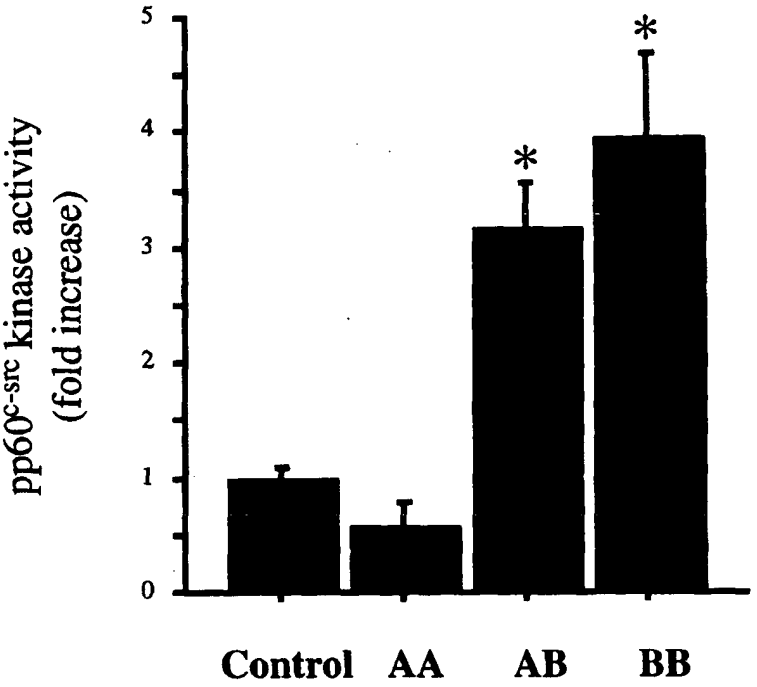

Fig. 2. The pp60$^{c\text{-}src}$ kinase activity in response to PDGF isotypes. Results are expressed as fold-increase compared to unstimulated control ± SD. Experiments were performed in duplicate and repeated multiple times. Data from a representative experiment are shown. *$p \leq 0.05$ from control.

might facilitate or be required for SMC migration. To further explore this hypothesis, we evaluated whether SMC agonists stimulate src activity in a manner that parallels their ability to stimulate SMC chemotaxis. We then evaluated the effect of cytoplasmic injection of an antibody known to block src activity on SMC migration. Our findings delineate a role for src in the signaling pathways leading to SMC migration and consequently in the development of intimal hyperplasia.

MATERIAL AND METHODS

General material. Dulbecco's modified Eagle's medium (DMEM), phosphate-buffered saline (PBS), fetal bovine serum, trypsin–ethylenediaminetetraacetic acid (EDTA), penicillin/streptomycin/fungizone solution, L-glutamine, and HEPES were obtained from Gibco BRL Life technologies (Gaithersburg, Md.). Smooth muscle specific actin staining kit was purchased from Sigma Chemical Company (St. Louis, Mo.). Polycarbonate 8 mm-pore membranes were from Poretics Corporation (Livermore, Calif.). Human recombinant PDGF-AA, -AB, -BB, antibody against pp60$^{c\text{-}src}$, src kinase substrate (residues 6-20 of p34^{cdc2}), and rabbit immunoglobulin G were obtained from Upstate Biotechnology (Lake Placid, N.Y.). Inhibitory antibody to pp60$^{c\text{-}src}$ used for microinjection was obtained from Santa Cruz Biotechnologies (Santa Cruz, Calif.).[8] Protein A-Sepharose (PAS) was obtained from Pharmacia Biotech (Uppsala, Sweden). γ-^{32}P-ATP (6000 Ci/mmol) was obtained from DuPont-New England Nuclear (Boston, Mass.).

Cell culture. Human SMCs were harvested from explants of remnant portions of saphenous veins intended for aortocoronary or peripheral bypass as previously described.[9] Sections of saphenous vein were opened lengthwise, and the endothelial and adventitial layers were gently removed. Fragments of the medial layer were placed into tissue culture dishes, and outward-growing SMCs were harvested and subcultured. Cells were maintained at 37° C and 5% CO_2 in DMEM supplemented with 10% FBS, 25 mmol/L HEPES, 40 units/ml penicillin G, 40 mg/ml streptomycin, 100 ng/ml amphotericin B, and 4.8 mmol/L L-glutamine. Cells in passages 2 through 5 were used for all experiments. SMC identity was confirmed by immunostaining with anti-human α-actin antibody and by observing the characteristic hill and valley growth pattern.

Measurement of chemotaxis. SMCs were grown to confluence and then made quiescent in serum-free media for 72 hours. Cells were washed in PBS and harvested using 0.05% trypsin-EDTA and resuspended in serum-free DMEM. Migration was assayed for 4

hours at 37° C in a 48-well microchemotaxis chamber (Neuroprobe, Cabin John, Md.), with upper and lower wells separated by polycarbonate 8 mm-pore membranes. SMCs were seeded at a density of 50,000 cells/well (6000 cells/mm^2) in the upper wells of the chamber. The appropriate soluble agonists diluted in DMEM were added to the lower wells. The vehicle for PDGF in serum-free DMEM was used as control.

Microinjection. Confluent SMCs were seeded onto 60 mm culture dishes marked with a 2 × 2 mm grid (Corning Glass Works, Corning, N.Y.) and allowed to grow to confluence. Cells were placed in serum-free media for 12 hours before injection. Borosilicate capillary tubes (IMCS; outer diameter, 1 mm) (Narishige, Tokyo, Japan) were sized for injection using a programmable model P-87 Flaming/Brown micropipette puller (Sutter Instrument Company, Novato, Calif.) and beveled to 25 to 30 degrees.[10] Pipette tips were individually calibrated to a threshold pressure of 120 to 140 kPa, which correlates to an inner diameter of 0.6 to 0.8 μm. Cytoplasmic injections were performed under 400× magnification using an IM 300 microinjection/manipulation system (Narishige, Tokyo, Japan) on a Diaphot 300 inverted microscope equipped with Hoffman modulation optics (Nikon Corporation, Tokyo, Japan). Two adjacent grids were selected, and all cells within these grids were injected, one with the anti-src antibody, and the other with immunoglobulin G (IgG). Injection success was determined by the presence of a "flow wave" within the cytoplasm, extending from the site of injection to the periphery of the cell.

Videomicroscopy. After injection of two adjacent grids, one with anti-src and one with IgG, a razor blade was used to create a linear injury through both grids. Videomicroscopy was accomplished through use of a Diaphot inverted phase-contrast microscope (Nikon Corporation) coupled to a high resolution black and white CCD camera (model CV-252; Aims Technology, Bronx, N.Y.), a 12-inch monitor (model BWM12A; Javelin Electronics, Torrance, Calif.), and a time-lapse video recorder (model TLC1400; GYYR, Anaheim, Calif.). Temperature was maintained at 37° C by a heated stage insert (model A-50; Fryer Company, Carpentersville, Ill.). CO_2 was maintained by covering the medium with a thin layer of sterile mineral oil and sealing the culture plate with parafilm immediately after injection. Images were recorded at 7.2 frames per minute for 24 hours. Migration distance was measured using NIH-Image version 1.60 (public domain software, available via anonymous file transfer protocol at ftp://zippy.nimh.gov/pub/image/) after acquiring images through a scientific frame grabber board (Scion LG3; Scion Corporation, Frederick, Md.) on a Power Macintosh 7500/100 (Apple Computer Corporation, Cupertino, Calif.).

Src kinase assay

Immunoprecipitation. Confluent cultures of human vascular SMCs were stimulated with agonists as indicated and reactions halted by twice rinsing with iced PBS. Cells were incubated in modified radioimmunoprecipitation assay buffer (150 mmol/L NaCl, 50 mmol/L Tris-HCl pH 7.5, 1% NP-40, 0.25% sodium deoxycholate, 1 mmol/L phenylmethylsulfonyl fluoride, 2 mmol/L EGTA, 50 mg/ml leupeptin, 0.5% aprotinin) for 20 minutes at 4° C. Cell lysates were collected into microcentrifuge tubes, vortexed, and centrifuged at 4° C for 20 minutes. Protein concentration was measured and equalized for all samples. Cell lysates were coincubated with src antibody (1 μg antibody/100 mg protein) overnight, with shaking followed by the addition of PAS for 2 hours. The PAS-antibody-src conjugate was washed three times in modified radioimmunoprecipitation assay buffer and twice in 150 mM NaCl, 50 mmol/L Tris-HCl and then used in the immunocomplex kinase assay.

Immunocomplex kinase assay. Samples of immunoprecipitated src were used for in vitro kinase assays. This assay measures the ability of src to catalyze the phosphorylation of a synthetic derivative of $p34^{cdc2}$, which has been shown to be an efficient substrate for human platelet $pp60^{c\text{-}src}$.[11] The immunoprecipitated pellet was resuspended in an equal volume of kinase buffer (Tris-HCl 100 mmol/L, pH 7.0, EGTA 0.4 mmol/L, Na_3VO_4 0.4 mmol/L, magnesium acetate 40 mmol/L), src kinase substrate (residues 6-20 of $p34^{cdc2}$, 1.5 mmol/L final concentration), and a 9:1 ratio of 0.5 mmol/L ATP, 40 mmol/L manganese chloride to γ-^{32}P ATP. After 10 minutes, this reaction was terminated with 40% trichloroacetic acid. The reaction mixture was blotted onto phosphocellulose and counted in a scintillation counter. Differences were expressed as fold-increase over control (unstimulated) values.

RESULTS

Effect of PDGF isotypes on SMC chemotaxis. To investigate a possible association between src activation and SMC migration, we stimulated SMCs with agonists that have a differential effect on SMC chemotaxis and then searched for a similar differential in the ability of these agonists to stimulate src activity. We used as agonists for these studies the three isotypes of PDGF because of their known potential to differentially stimulate SMC chemotaxis.[12] A 4-hour microchemotaxis chamber assay

revealed that 5 ng/ml of PDGF-BB and AB stimulated, respectively, a 7.4 ± 0.3- and 5.3 ± 0.5-fold increase in SMC chemotaxis (Fig. 1). This difference was statistically significant. PDGF-AA diminished chemotaxis to levels below control (0.64 ± 0.3-fold decrease, $p \leq 0.05$). Thus, there exists a hierarchy in the ability of the PDGF isotypes to stimulate SMC locomotion (PDGF-BB > AB > AA).

Effect of PDGF isotypes on activation of $pp60^{c\text{-}src}$. We evaluated the potential for the three isotypes of PDGF to stimulate activation of src as measured by their ability to promote phosphorylation of a peptide sequence of $p34^{cdc2}$. Both PDGF-BB and AB increased src activity in SMCs (Fig. 2). PDGF-BB increased src activity to the greatest degree (3.97 ± 0.71-fold), followed by PDGF-AB (3.17 ± 0.4-fold) (representative data). In some experiments this difference was statistically significant and in others it was not. PDGF-AA either did not stimulate src activity or stimulated src to a minor degree (0.56 ± 0.21-fold) (representative data). Thus, we found a gross correlation between src activation and the ability of SMC agonists to stimulate chemotaxis.

Effect of blocking $pp60^{c\text{-}src}$ antibodies on SMC migration. An antibody against the carboxy terminal portion of src was introduced into SMCs using the microinjection technique as described in Material and Methods. After injection and injury, SMCs were stimulated with PDGF-BB (5 ng/ml) for 24 hours and cell movement was constantly monitored with videomicroscopy. Several different parameters of migration were measured including (1) the *total* distance migrated, calculated by measuring the actual course of each cell; (2) the *net* distance migrated, calculated by drawing and measuring a straight line between the origin and terminal location of each migrating cell; and (3) the *percent motility*, the percentage of cells that moved during the 24-hour period of study. After stimulation with PDGF-BB, there was significantly greater migration in cells injected with IgG than in those injected with anti-src antibody, as assessed by all three parameters (Table I). These differences were dramatic and consistent in experiments using cells derived from multiple saphenous veins. Injection with the anti-src antibody diminished migration below control levels in unstimulated SMCs. Anti-src antibody also inhibited migration of cells stimulated by 10% serum (Table I).

DISCUSSION

In these studies, we have explored a potential relationship between the nonreceptor tyrosine kinase src and migration of human vascular SMC. Using the isotypes of the PDGF as agonists, we first evaluated whether there might be a parallel between src activity and the ability of SMCs to migrate. We and others have shown that the isotypes of PDGF have a differential ability to stimulate SMC chemotaxis.[12] As demonstrated in Fig. 1, PDGF-BB and AB both stimulate chemotaxis; the effect of PDGF-BB was consistently greater than that of AB. PDGF-AA, however, inhibited SMC chemotaxis to levels below baseline. Using a synthetic fragment of $p34^{cdc2}$ as a substrate, we measured src activation in response to these same isotypes.[11] PDGF-BB stimulated src-kinase to levels fourfold greater than control. The activity of src after stimulation with PDGF-AB was usually somewhat less than that of BB, although this difference was not always statistically significant. PDGF-AA produced either no or a slight increase in src activity. Thus the ability of the PDGF isotypes to stimulate SMC chemotaxis paralleled their ability to activate src, suggesting a possible association between these two events.

To our knowledge, this is the first report of a differential effect of the PDGF isotypes on src activity. The explanation for this varied response is not clear but may be related to interaction of these isotypes with the PDGF receptor. The PDGF receptor is an α/β dimer of which there are three possible combinations—αα, αβ, or ββ. The interaction between the three PDGF ligands and these dimers is specific in that PDGF-BB binds to all three receptors, PDGF-AB binds to the αα and αβ dimers, and PDGF-AA binds only to the αα receptor. Our previous findings that PDGF-AA is a potent agonist of human vascular SMC proliferation verify that the αα receptor is present on these cells.

Other investigatiors have shown that the β subunit of the PDGF receptor binds and activates src.[13-15] However, it is not known whether the α component of this receptor interacts with src. Because PDGF-AA activates only the αα receptor and we have found that PDGF-AA has little or no potential to activate src, it can be surmised that either the α subunit of the PDGF receptor does not bind or activate src or the degree of activation of src by the α subunit is significantly less than that of the β subunit. Specific binding studies will be necessary to verify this hypothesis.

To measure more directly the effect of src on the migration of human SMCs, an inhibitory anti-src antibody was microinjected into human vascular SMCs. Individual cells were then observed using a videomigration assay. Introduction of this antibody consistently led to a decrease in the migration of SMCs as measured by a variety of different parameters. Injection of nonspecific IgG did not inhibit

migration; thus this effect was related to the specificity of the antibody to src. We can conclude from these observations that activation of src is necessary for SMC migration.

The role of src in cell migration has been previously investigated in other vascular cells. Garfinkel et al.[19] found that senescent human umbilical vein endothelial cells (ECs) had diminished ability to proliferate and migrate in response to fibroblast growth factor as compared to their younger counterparts. These investigators also found that both tyrosine phosphorylation and the kinase activity of src were diminished in senescent versus earlier passage cells. They proposed that these two events were related and that the decreased migratory and proliferative response of senescent ECs to fibroblast growth factor may in part be due to decreased activity of src.[19] Bell et al.[20] found that angiotensin inhibited SMC migration and postulated that this effect might be mediated through suppression of src. Inhibitors of angiotensin simultaneously increased src activation and EC migration. Moreover, overexpression of src in EC enhanced the ability of cells to migrate. These authors also observed increased levels of urokinase-like plasminogen activator (u-PA) in ECs overexpressing src. Plasminogen, which is produced in response to u-PA, is believed to regulate SMC migration by lysing the extracellular matrix, thereby creating a pathway through which the cell can move. Their data suggest that src overexpression might increase cellular migration by increasing the expression and/or production of u-PA.

The interaction of src with the focal adhesion might offer an alternative "intracellular" hypothesis for its effect on SMC migration. Focal adhesion contacts are regions adjacent to the cell membrane in which actin filaments, cytoskeletal proteins, integrins, and the extracellular matrix proteins interact. These focal contacts are necessary for maintenance of the structure of the cell, as well as for cell attachment. Migration is cyclic process in which forward movement of a cell requires detachment and reattachment of the basal surface of a cell to the extracellular matrix. Detachment requires disassembly and attachment requires assembly of focal adhesion contacts. Thus reorganization of the focal adhesion complex is necessary for cell migration. Src appears to be integrally involved with focal adhesions. After platelet stimulation by thrombin, src undergoes redistribution from the membrane to the cytoskeleton.[21] Src also associates with the cytoskeleton in a glioblastoma cell line after PDGF stimulation.[15] Moreover, src induces cytoskeletal reorganization in epithelial cells.[22] The focal adhesion complex is composed of multiple proteins, many of which are also tyrosine kinases. Src has been found to associate with and phosphorylate at least three of these proteins—the focal adhesion kinase ($p125^{FAK}$),[23] cortactin,[24] and paxillin.[25] Thus, src activation may influence migration by aiding the dissolution and reformation of focal adhesion complexes.

We have demonstrated the necessity of src in SMC migration using a cytoplasmic microinjection technique. This is an attractive method for investigating signal transduction pathways involved in SMC migration because the behavior of single cells can be altered, and the pattern and course of migration of these individual cells can subsequently be monitored. The injection technique that we used is minimally injurious to human SMCs and allows for rapid simultaneous exposure of multiple cells to inhibitors or agonists of intracellular processes. Cytoplasmic injection bypasses the need to permeabilize cells, a process that can be injurious to cells and alter their behavior. The addition of continuous videomicroscopy allows for direct visualization of physiologic processes such as migration and proliferation.

In conclusion, we have found a strong correlation between src activation and SMC chemotaxis. The isotypes of PDGF stimulate chemotaxis in a pattern similar to their effect on src activation. We have additionally demonstrated that src activity is necessary for SMC migration. The exact position of src in the signaling pathway that mediates migration is still unclear. However, because src appears to be necessary for cellular migration and proliferation, both of which are prerequisite to the development of intimal hyperplasia, this signaling protein may be a useful and specific target for inhibitors of this process.

REFERENCES

1. Donaldson MC, Mannick JA, Whittemore AD. Causes of primary graft failure after in situ saphenous vein bypass grafting. J Vasc Surg 1992;15:113-20.
2. Chervu A, Moore WS. An overview of intimal hyperplasia. Surg Gynecol Obstet 1990:433-40.
3. Ross R. The pathogenesis of atherosclerosis: a perspective for the 1990s. Nature 1993:801-9.
4. Superti-Furga G, Courtneidge SA. Structure-function relationships in src family and related protein tyrosine kinases. Bioassays 1995;17:321-30.
5. Park J, Cartwright CA. Src activity increases and Yes activity decreases during mitosis of human colon carcinoma cells. Mol Cell Biol 1995;15:2374-82.
6. Roche S, Koegl M, Barrone V, Roussel MF, Courtneidge SA. DNA synthesis induced by some but not all growth factors requires src family protein tyrosine kinases. Mol Cell Biol 1995;15:1102-9.
7. Twamley-Stein GM, Pepperkok R, Ansorge W, Courtneidge

SA. The src family tyrosine kinases are required for platelet-derived growth factor-mediated signal transduction in NIH 3T3 cells. Proc Natl Acad Sci U S A 1993;90:696-700.
8. Marrero MB, Schieffer B, Paxton WB, Schieffer E, Bernstein KE. Electrophoration of pp60$^{c\text{-}src}$ antibodies inhibits the angiotensin II activation of phospholipase C-γl in rat aortic smooth muscle cells. J Biol Chem 1995;270:15734-8.
9. Mii S, Khalil RA, Morgan KG, Ware JA, Kent KC. Mitogen-activated protein kinase and proliferation of human vascular smooth muscle cells. Am J Physiol 1996;270:H142-50.
10. Hogan B, Beddington R, Costantini F, Lacy E. Manipulating the mouse embryo: a laboratory manual. 2nd ed. Plainview (NY): Cold Spring Harbor Laboratory Press; 1994.
11. Cheng HC, Nishio H, Hatase O, Ralph S, Wang JH. A synthetic peptide derived from p34^{cdc2} is a specific and efficient substrate of src-family tyrosine kinases. J Biol Chem 1992;267:9248-56.
12. Jiang B, Yamamura S, Nelson PR, Mureebe L, Kent KC. Differential effects of platelet-derived growth factor isotypes on human smooth muscle cell proliferation and migration are mediated by distinct signaling pathways. Surgery 1996;120:427-32.
13. Kypta RM, Goldberg Y, Ulug ET, Courtneidge SA. Association between the PDGF receptor and members of the src family of tyrosine kinases. Cell 1990;62:481-92.
14. Chen YH, Pouyssegur J, Courtneidge SA, Van Obberghen-Schilling E. Activation of Src family kinase activity by the G protein-coupled thrombin receptor in growth-responsive fibroblasts. J Biol Chem 1994;269:27372-7.
15. Weernink PA, Rijksen G. Activation and translocation of c-Src to the cytoskeleton by both platelet-derived growth factor and epidermal growth factor. J Biol Chem 1995;270:2264-7.
16. Heldin CH, Ostman A, Eriksson A, Siegbahn A, Claesson-Welsh L, Westermark B. Platelet-derived growth factor: isoform-specific signalling via heterodimeric or homodimeric receptor complexes. Kidney Int 1992;41:571-4.
17. Ralston R, Bishop JM. The product of the protooncogene c-src is modified during the cellular response to platelet-derived growth factor. Proc Natl Acad Sci U S A 1985;82:7845-9.
18. Gould KL, Hunter T. Platelet-derived growth factor induces multisite phosphorylation of pp60$^{c\text{-}src}$ and increases its protein-tyrosine kinase activity. Mol Cell Biol 1988;8:3345-56.
19. Garfinkel S, Hu X, Prudovsky IA, McMahon GA, Kapnik EM, McDowell SD, et al. FGF-1-dependent proliferative and migratory responses are impaired in senescent human umbilical vein endothelial cells and correlate with the inability to signal tyrosine phosphorylation of fibroblast growth factor receptor-1 substrates. J Cell Biol 1996;134:783-91.
20. Bell L, Luthringer DJ, Madri JA, Warren SL. Autocrine angiotensin system regulation of bovine aortic endothelial cell migration and plasminogen activator involves modulation of proto-oncogene pp60$^{c\text{-}src}$ expression. J Clin Invest 1992;89:315-20.
21. Walker F, deBlaquiere J, Burgess AW. Translocation of pp60$^{c\text{-}src}$ from the plasma membrane to the cytosol after stimulation by platelet-derived growth factor. J Biol Chem 1993;268:19552-8.
22. Warren SL, Handel LM, Nelson WJ. Elevated expression of pp60$^{c\text{-}src}$ alters a selective morphogenetic property of epithelial cells in vitro without a mitogenic effect. Mol Cell Biol 1988;8:632-46.
23. Calalb MB, Polte TR, Hanks SK. Tyrosine phosphorylation of focal adhesion kinase at sites in the catalytic domain regulates kinase activity: a role for Src family kinases. Mol Cell Biol 1995;15:954-63.
24. Thomas SM, Soriano P, Imamoto A. Specific and redundant roles of Src and Fyn in organizing the cytoskeleton. Nature 1995;376:267-71.
25. Erpel T, Courtneidge SA. Src family protein tyrosine kinases and cellular signal transduction pathways. Curr Opin Cell Biol 1995;7:176-82.

DISCUSSION

Dr. Colleen M. Brophy (Augusta, Ga.). I have a few specific questions for the investigators. First, can you provide us with any information about the temporal associations between PDGF stimulation, src kinase activation, and chemotaxis? Is src kinase activation a transient or sustained event after PDGF activation, and/or does it require persistence of the PDGF stimulation to maintain activation? Second, I have some concerns about using antibodies to block specific intracellular events. Have you tried any control antibodies other than nonspecific IgGs? For example, have you tried blocking with other antibodies against different types of tyrosine kinases so that you can specifically implicate src kinase? Is the antibody actually blocking the kinase activity, or is it blocking kinase movement within the cell or some other effect of the kinase? Have you been able to show that that antibody blocks kinase activity in your in vitro kinase activity studies? Finally, have you been able to identify any specific substrates of src kinase that may be implicated in the chemotactic process? I agree with your conclusion that the focal point for cellular movement or migration is at the focal adhesion bodies. Is p125^{FAK} or paxillin the specific substrate that is actually modulating this process?

Dr. Mureebe. In answer to the first question about the timing of src activation in SMC migration, from our studies we cannot determine this. We used 10 minutes of PDGF stimulation for our kinase assays. It has been shown in other cell types that PDGF-induced stimulation of src is transitory. Activity peaks at about 5 to 10 minutes. This is followed by a plateau of activity that is significantly less than the twofold to fourfold increase found after 10 minutes of stimulation. In response to the question regarding the actual function of the antibody we have used, we are confident that this is an antibody that is specifically against src. Whether it actually affects the kinase activity or the trafficking of src is still unclear. In response to your final question regarding the substrates of src, we currently have not looked at any downstream substrates of src. Other groups have shown that src is partly responsible for the hyperphosphorylation of paxillin in cells transformed with the viral homologue, v-*src*.

Dr. Timothy J. Yeatman (Tampa, Fla.). I was intrigued by the slide that showed that after PDGF stimulation, there was perinuclear association of src. That seems to contradict what I know about it. Have you investigated whether the antibody blocked src association with the plasma membrane? In other words, did it

block the myristoylation site in association with the plasma membrane and therefore block its activity?

Dr. Mureebe. We have not looked at whether the antibody used for microinjection blocks the myristoylation site of src. The antibody binds near the carboxyl terminus, not at the N-terminal myristoylation site, which is where src attaches to the cell membrane. However, we are planning to evaluate whether the antibody will block the nuclear translocation of src.

Dr. J. Jeffrey Alexander (Cleveland, Ohio). I was interested in your selection of SMCs from saphenous vein. Could these same results be expected from arterial SMCs, which may be a more clinically relevant cell type?

Dr. Mureebe. We chose saphenous vein SMCs because of the frequent use of saphenous vein as bypass conduit. Other groups have used bovine aortic ECs in studies that implicate src in the signaling pathways, leading to migration. We have not yet looked at arterial SMCs.

Surgery is abstracted and/or indexed in *Index Medicus, Science Citation Index, Current Contents/ Clinical Medicine, Current Contents/Life Sciences, Excerpta Medica,* and MEDLINE.